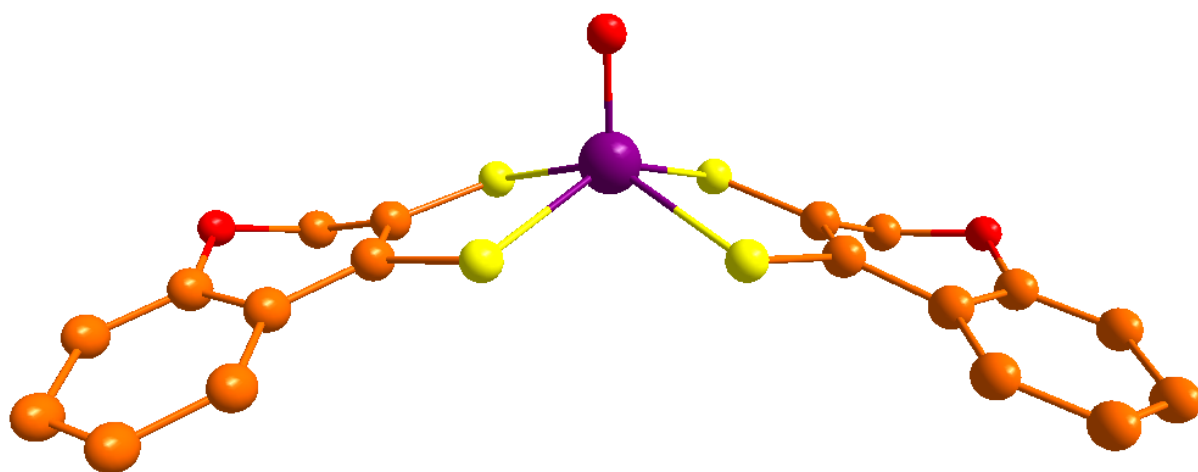**Prinson P. Samuel**

# *Molybdenum and tungsten compounds with dithiolene ligands inspired by molybdopterin as models for the molybdenum and tungsten cofactors*

**Göttingen 2011**

# *Molybdenum and tungsten compounds with dithiolene ligands inspired by molybdopterin as models for the molybdenum and tungsten cofactors*

Dissertation

zur Erlangung des Doktorgrades

der Mathematisch–Naturwissenschaftlichen Fakultäten

der Georg–August–Universität zu Göttingen

vorgelegt von

**Prinson Poikayil Samuel**

aus Vilangara, Kerala

(Indien)

Göttingen 2011

D 7

Referent: Prof. Dr. Carola Schulzke

Korreferent: Prof. George M. Scheldrick, FRSC

Tag der mündlichen Prüfung: 31.01.2011

*Dedicated to my parents, siblings & Shanty*

# Acknowledgement

# CONTENTS

# INTRODUCTION TO MOLYBDOPTERIN BEARING MOLYBDENUM AND TUNGSTEN ENZYMES

## 1.1. Evolutionary development of Mo and W enzymes

Molybdenum and tungsten are the only among the second and third row transition metals, having substantial biological significance and one of both elements is indeed incorporated by almost all organisms ranging from the single celled ancient microorganisms like archaea to the modern human being.[1] Because of their chemical similarity, both metals are found in nearly identical enzymes, with an exception of nitrogenase, for which no tungsten analogue is known.[2] The successive development of molybdenum and tungsten enzymes has proven to be related to the changing bioavailability of both elements during the course of evolution.[3] The geographical conditions of the early earth did not let both metals be equally available to biological system at the same span of time which resulted in an unequal distribution of Mo and W in different microorganisms. It is believed that life arose in hot, sulfur rich anaerobic habitats in which the biochemical availability of molybdenum was extremely low due to the infinitesimal solubility of molybdenum sulfides. Under these

conditions, tungsten was able to stay in the oxidation state six and form *bis*-anionic and consequently soluble $[WO_xS_{x-n}]^{2-}$ (n = 0 − 4) species. As a result tungsten became bio-available to the first evolved living organisms. In addition, it is argued that the higher solubility of the low valent tungsten sulfides, in comparison to molybdenum sulfides in water contributed to making them more available in the hot anaerobic environment of the early earth.[4] When earth's crust became cooler and as the photosynthetic organisms liberated more oxygen, the cooler habitats with lower sulfur concentration in an oxidizing atmosphere, made molybdenum more easily available to biological systems compared to tungsten. Even though, the abundance of molybdenum in earth's crust is rather small, it is the most abundant transition element found in modern oceans.[5] This high abundance is facilitated by the exceptionally good water solubility of molybdate $[MoO_4]^{2-}$ ions, which are being liberated during oxidative weathering of continental crust containing an average of 1 to 2 ppm molybdenum.[6-7] The increasing availability of soluble molybdenum species resulted in its cumulative incorporation into the active sites of several enzymes during the course of evolution, while the ancient organisms, mainly archaea, that live in habitats resembling the conditions of early earth, continued to utilize tungsten. The change from scarcity to availability of molybdenum, which in turn resulted in the evolution from tungsten to molybdenum enzymes, is supported by new findings on the delay in the evolution of eukaryotes from 2.7 to 0.7 billion years ago.[5] Based on experimental results, it has been proposed that the anaerobic environment prevailed in the early earth caused the scarcity of molybdenum in sea water and thereby slowed down the development of nitrogen fixing bacteria. Since eukaryotes cannot fix nitrogen by themselves, the unavailability of nitrogen fixing prokaryotes resulted in the delay of domination of the former during this geological time period. In addition to this, it has been proposed that the change from molybdenum to

tungsten during evolution was based on functionality, mainly related to the redox potential behavior upon temperature change.[8] It seems as if molybdenum provides a functional advantage by being less influenced by temperature fluctuation, further driving evolution to switch from tungsten to molybdenum. However, research in this area is still ongoing, trying to understand this interesting topic in utmost detail.

## 1.2. Mo and W enzymes as oxotransferases

The catalytic centers of Mo and W enzymes are redox active between the oxidation states IV and VI. Oxygen atom transfer (OAT) as a two electron redox process is mediated by an oxidation state V facilitating proton coupled electron transfer (PCET) as part of the enzyme's regeneration. With exception of nitrogenase, in general, molybdenum and tungsten enzymes catalyze reactions of the type:

$$X + H_2O \leftrightarrows XO + 2H^+ + 2e^- \quad ............................(1)$$
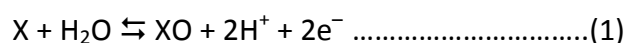
X acts as the accepter of oxygen and XO as the donor. In most cases water acts as either a source or sink of oxygen.[9] The chemical identity of X varies from enzyme to enzyme depending on which reaction they catalyze. Since the substrate and product in this reaction (X and XO) differ only by an oxygen atom, it has been termed oxygen atom transfer reaction and the enzymes catalyzing this type of reactions are called oxotransferases. All molybdenum and tungsten enzymes except nitrogenase belong to this broad class. Due to this, in all the following discussions, nitrogenase is excluded from the general phrase 'Mo enzyme', wherever it is mentioned. The term oxotransferase is often misleading as it does not bear a mechanistic implication in every case, even though there are examples like the reduction of DMSO to DMS and oxidation of sulfite to sulfate which can be viewed as actual oxygen atom transfer reactions. In addition as mentioned above these reactions involve

proton coupled electron transfer [10] allowing a net redox change between substrates and products and a stepwise recovery of the enzyme's active state. Therefore the terms oxotransfer and oxotransferase used throughout this chapter have broad meanings apart from their direct implications. These enzymes are usually named after the specific reactions they catalyze and some representative examples are summarized in table 1.

**Table 1. Reactions catalyzed by some of the Mo/W enzymes.**

| Enzyme | Reaction |
|---|---|
| Aldehyde oxidoreductase | $RCHO + H_2O \rightleftharpoons RCO_2H + 2H^+ + 2e^-$ |
| Arsenite oxidase | $H_2AsO_3^- + H_2O \rightleftharpoons HAsO_4^{2-} + 3H^+ + 2e^-$ |
| Carbon monoxide oxidoreductase | $CO + H_2O \rightleftharpoons CO_2 + 2H^+ + 2e^-$ |
| Dimethyl sulfoxide reductase | $Me_2SO + 2H^+ + 2e^- \rightleftharpoons Me_2S + H_2O$ |
| Nitrate reductase | $NO_3^- + 2H^+ + 2e^- \rightleftharpoons NO2^- + H_2O$ |
| Sulfite oxidase | $SO_3^{2-} + H_2O \rightleftharpoons SO_4^{2-} + 2H^+ + 2e^-$ |
| Xanthine oxidase | $xanthine + H_2O \rightleftharpoons uric\ acid + 2H^+ + 2e^-$ |

## 1.3. Active sites of oxotransferases

Attempts to investigate the active site structures of oxotransferases commenced more than three decades ago. Before this period sulfur co-ordination to the molybdenum centers was known to chemists but it was believed that solely responsible for this was the presence of a sulfur-cysteinate in the coordination sphere of molybdenum. This prevailed as a notion in the scientific community for many years until Rajagopalan and co-workers proposed in 1982 that the sulfur atoms are part of a specific ligand system which they called molybdopterin (MPT).[11] In their remarkable work they isolated the di(carboxamidomethyl)

derivatives of molydbdopterin and then characterized them by fluorescence and mass spectrometry. Based on first results, the first structure of the active site was proposed as having a pterin dithiolene chelation to molybdenum as shown in figure 1.a. There was an unidentified group at the sixth position of the pterin nucleus. This first proposed structure of molybdopterin consists of a bi-cyclic pterin ring with a side chain carrying an ene-dithiol group and a phosphate group with the dithiolene part being coordinated to molybdenum. The first proposed structure for the molybdenum cofactor was refined later in 1987 by the same authors and in this model molybdopterin is a 6-alkylpterin with a 4-carbon side chain containing an enedithiol on C- 1' and C-2', a secondary alcohol on C-3', and a phosphorylated primary alcohol on C-4' (figure 1.b).[12] Yet, the speculation about structural characteristics of the molybdopterin cofactor remained hot in scientific circles and the ambiguity was removed only after Chan et al. published the crystal structure of the tungsten containing aldehyde ferredoxin oxidoreductase (AOR) from *Pyrococcus furiosus*, a hyperthermophilic archaeon in 1995.[13] The active site structure of this enzyme (figure 1.c) revealed the
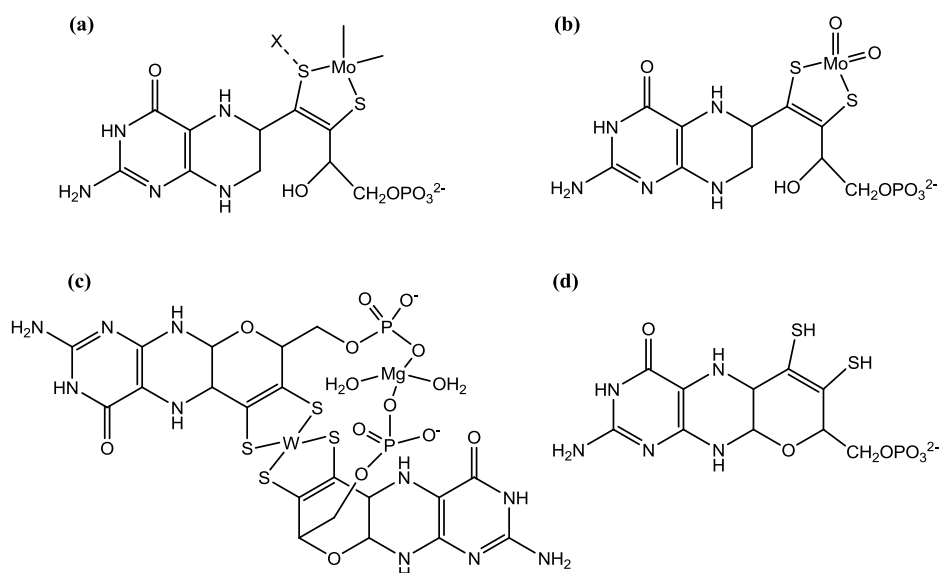


**Figure 1. The development of insights into the structure of molybdopterin (MPT). (a) the structure first proposed in 1982, (b) the refined structure proposed in 1987, (c) structure of a MPT containing active site established by crystallographic means in 1995, (d) today's commonly accepted structure of MPT.**

molybdopterin being bound to the metal via dithiolene sulfurs, exactly as proposed by Rajagopalan et al. much earlier. The now commonly accepted chemical structure of molybdopterin based on various crystallographic studies is shown in figure 1.d.

## 1.4. Mo and W enzymes: Current state of art

More than fifty molybdenum and tungsten enzymes are known today. Of all the enzymes carrying molybdenum, nitrogenase can be considered as an exceptional case. This is the only enzyme in which Mo does not bind to MPT but to an iron sulfur cluster, histidine and homocitrate.[2] All other molybdenum and tungsten enzymes are associated with the above shown unusual ligand system called molybdopterin and all of them are mononuclear. However, at this juncture the term molybdopterin is confusing as it sounds like something incorporating molybdenum. But, "molybdopterin" actually refers only to the organic part of the cofactor and it does not include molybdenum. Consequently, molybdopterin can be associated with both molybdenum and tungsten enzymes. Because all this might be confusing different names have been proposed throughout the literature as pyranopterindithiolate [9], pterin-dithiolene [14], pterin-ene-dithiolate [15] or even tungstopterin when bound to tungsten.[16] As mentioned in the previous section, molybdopterin is coordinated to the metal center (Mo/W) via its dithiolene function. Depending on the type of enzyme, the number of coordinated molybdopterin ligands can be one or two. In eukaryotes, molybdopterin bears a terminal phosphate group at the pyrane ring as shown in figure 1.d. In case of prokaryotes it carries in addition a nucleotide at the end of a phosphate chain, which can be cytosine, guanosine, adenosine or inosine. The later are termed dinucleotide versions of molybdopterin because molybdopterin itself is structurally related to the nucleotides via its pterin part.

Hille has classified molybdenum and tungsten enzymes into different families based on the geometrical and chemical structure of the oxidized active sites and sequence homologies.[4, 17] According to this classification, the molybdenum and tungsten enzymes fall into the following families:

**Molybdenum enzyme families**

- xanthine oxidase

- sulfite oxidase

- DMSO reductase

**Tungsten enzyme families**

- aldehyde ferredoxin oxido reductase

- formate dehydrogenase

- acetylene hydratase

Each family is named after their most prominent or sole member. The active site structures of each family of enzymes are depicted in figure 2. The xanthine oxidase family of enzymes has an $(MPT)Mo^{VI}OS(OH)$ core (figure 2.a) in the oxidized state whereas the structurally somehow similar sulfite oxidase family has an $(MPT)Mo^{VI}O_2(S\text{-Cys})$ core (figure 2.c). While both afore mentioned classes of molybdenum enzymes carry only one MPT equivalent in their active sites, the DMSO reductase family is an exception with its $(MPT)_2MO^{VI}O(X)$ core possessing two MPT ligands (figures 2.f-2.h). The group X most often is an amino acid moiety like serine, aspartate, cysteine or selenocysteine. Arsenite oxidase (AO) classified under the DMSOR family, has a different active site structure so that its oxidized state bears a dioxomolybdenum center, $(MPT)_2MO^{VI}O_2$. This different structure of arsenite oxidase from other members of the DMSOR family can be taken as a reason for considering AO to represent a fourth family of Mo enzymes. Among the tungsten enzymes, the aldehyde ferredoxin oxidorecuctase family has the core structure $(MPT)_2W^{VI}O(OH)$ (figure 2.l). The second class of tungsten enzymes, the formate dehydrogenase family carries an oxidized core of the type $(MPT)_2W^{VI}O(X)$ where X= S-Cys or Se-Cys (figure 2.m). Both families show resemblance to the DMSO reductase family of molybdenum enzymes. The third family of

tungsten dependent enzymes comprises only of a single member: the very unusual

acetylene hydratase (figure 2.n), catalyzing the hydration of acetylene to acetaldehyde.[18]
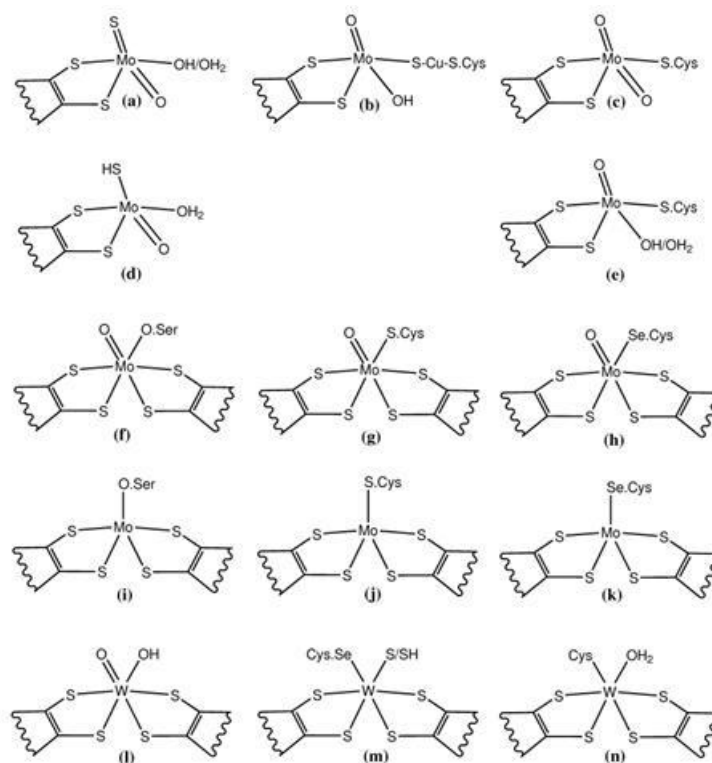


**Figure 2. The active site structures of the different molybdenum and tungsten enzyme families as derived from crystal structures of individual enzymes.** (a) xanthine oxidase family (oxidized); (b) unique active site of *Oligotropha carboxydovorans* CO dehydrogenase; (c) sulfite oxidase family (oxidized); (d) xanthine oxidase family (reduced); (e) sulfite oxidase family (reduced); (f)-(h) DMSO reductase family enzymes with different coordinated amino acids (oxidized) (f): DMSO redcutase, (g): dissimilatory nitrate reductase, (h): formate dehydrogenase; (i)-(k) DMSO reductase family enzymes with different coordinated amino acids (reduced); (l) aldehyde ferredoxin oxido reductase family: (m) formate dehydrogenase family; (n) acetylene hydratase.

## 1.4.1. Structure and function of the sulfite oxidase family of enzymes

The sulfite oxidase (SO) family of enzymes comprises the sulfite oxidases and

assimilatory nitrate reductases. Sulfite oxidases catalyze the transformation of sulfite to

sulfate accompanied by a change of molybdenum's oxidation state from VI to IV in the reductive half reaction of the catalytic cycle. Upon reacting with sulfite, one oxygen atom from the active $Mo^{VI}$ is transferred to sulfite to produce sulfate, and the molybdenum center is reduced by two electrons to $Mo^{IV}$. Water then displaces sulfate, and the removal of two protons ($H^+$) and two electrons ($e^-$) returns the active site to its original state. In fact, the re-oxidation of molybdenum occurs first to $Mo^V$ and then to $Mo^{VI}$, by electron transfer to the physiological oxidant cytochrome *c* mediated by a *b*-type cytochrome site present in the enzyme.[19-22] Figure 3 shows the catalytic cycle in the sulfite oxidase enzyme.
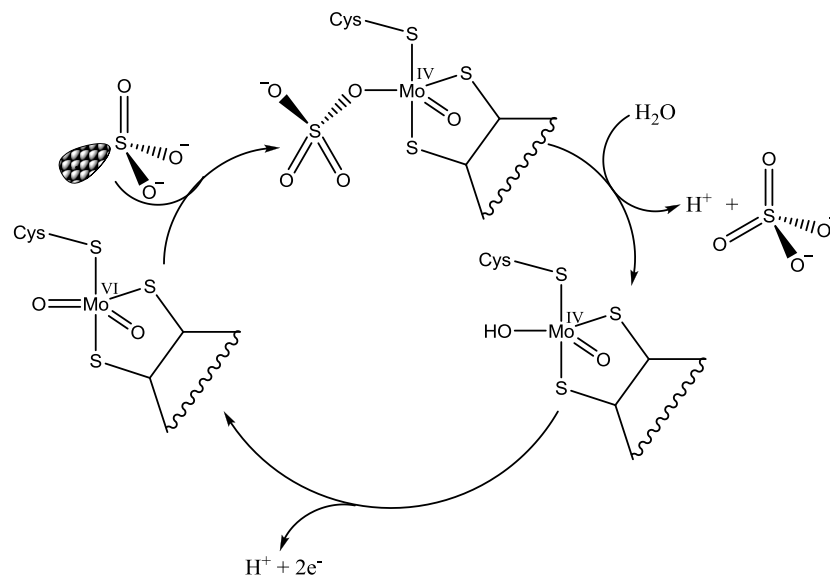


**Fig. 3. Catalytic cycle in sulfite oxidase**

The second member of this enzyme family nitrate reductase is playing a key role in the global denitrification process. Denitrification can be expressed as the redox reaction (2):

$$2NO_3^- + 10\ e^- + 12\ H^+ \rightarrow N_2 + 6H_2O \ \dots\dots\dots\dots\dots\dots\dots\dots\dots \ (2)$$
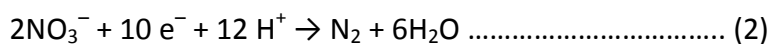
This overall reaction is accomplished by four enzymatic steps 3-6:

$$NO_3^- + 2e^- + 2H^+ \rightarrow NO_2^- + H_2O \ \dots\dots\dots\dots\dots\dots\dots\dots\dots\dots \ (3)$$

9

$$NO_2^- + e^- + 2H^+ \rightarrow NO + H_2O \dots\dots\dots\dots\dots\dots\dots\dots\dots (4)$$

$$2NO + 2e^- + 2H^+ \rightarrow N_2O + H_2O \dots\dots\dots\dots\dots\dots\dots\dots (5)$$

$$N_2O + 2e^- + 2H^+ \rightarrow N_2 + H_2O \dots\dots\dots\dots\dots\dots\dots\dots\dots (6)$$
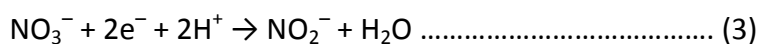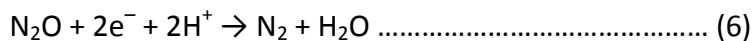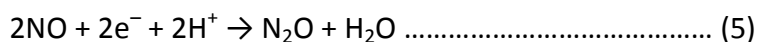
Out of these four reactions, reaction 3 is catalyzed by nitrate reductase. Therefore nitrate reductase is catalyzing a type of reaction electronically reverse to that involved in case of sulfite oxidase discussed above. In executing the reduction of nitrate to nitrite, the formal oxidation state of molybdenum changes from IV to VI in the oxidative half reaction. The earliest attempts to investigate the coordination sphere of molybdenum in sulfite oxidases and nitrate reductases were documented by Cramer et al..[23-24] It was reported that $Mo^{VI}O_2$ and $Mo^{IV}O$ units were present in the oxidized and reduced forms of these enzymes, respectively. For oxidized sulfite oxidase the EXAFS (Extended X-ray Absorption Fine Structure) analysis revealed two oxygen atoms at a distance of 1.68 Å to molybdenum and two or three sulfur atoms at 2.41 Å, changing to only one oxygen at 1.69 Å, and three sulfur atoms at 2.38 Å upon reduction. In case of the oxidized state of the assimilatory nitrate reductase, EXAFS results showed that molybdenum carried two terminal oxygen atoms at 1.71 Å as well as two or three sulfur atoms at 2.44 Å. One single terminal oxygen at 1.67 Å and a set of sulfurs at 2.37 Å were found upon full reduction by NADH. Similar information was obtained by George et al. by X-ray absorption spectroscopy studies of the $Mo^{IV}$, $Mo^{V}$ and $Mo^{VI}$ oxidation states of SO.[25] These studies indicated that the $Mo^{VI}$ oxidation state possesses two terminal oxo (M=O) and approximately three thiolate-like (Mo-S-R) ligands, unaffected by changes in pH and chloride concentration. The $Mo^{IV}$ and $Mo^{V}$ oxidation states were found to carry one oxo ligand, one Mo-OX (most probably Mo-OH) and two to three sulfur ligands. X-ray absorption spectroscopy at the molybdenum and sulfur K-edges was

carried out for the oxidized $Mo^{VI}$ active sites of wild-type and cysteine 207 to serine mutant human sulfite oxidases.[26] The wild-type enzyme was found to possess two terminal oxygen ligands to molybdenum at 1.71 Å and three Mo-S distances of 2.41 Å whereas in the mutant one sulfur ligand was replaced by an oxygen ligand. With this it was proven that the amino acid residue of cysteine 207 was a ligand to molybdenum in the wild type. The crystal structure of chicken liver sulfite oxidase was published by Kisker et al. in 1997.[27] The structure showed that the active site molybdenum is five-fold coordinated by one oxo group, three sulfur ligands (two from the molybdopterin and one from the cysteinate ligand) and one water or hydroxo ligand. A little ambiguity was left in the report since the protein was purified in its fully oxidized form [$Mo^{VI}$/$Fe^{III}$] but molybdenum was found to be a mono oxo species in contrast with the afore mentioned EXAFS results and resonance Raman studies.[28] Nevertheless, subsequent experiments proved beyond doubt that the SO family of enzymes is characterized by a $Mo^{VI}O_2$ group in the oxidized form with a molybdopterin ligand coordinated through its dithiolene function and the chicken liver SO has been characterized to bear one cysteinate ligand at the molybdenum center.[29-31]

## 1.4.2. Structure and function of the xanthine oxidase family of enzymes.

Xanthine oxidase enzymes perform the interconversion of xanthine to uric acid which is the last step of the purine nucleotide catabolism in human beings as well as primates, birds, reptiles, and insects. In fact the overall reaction is performed by two distinct enzymes called xanthine oxidase (XO) and xanthine dehydrogenase (XDH). The name of the enzyme family under discussion was chosen after the former one. The active sites of these enzymes bear a $LMo^{VI}O(S)$ core, where L is the molybdopterin ligand system. L can be the mononucleotide form of molybdopterin, a molybdopterin cytosine dinucleotide, a molybdopterin guanine dinucleotide or a molybdopterin adenine dinucleotide depending on

whether the enzyme is eukaryotic or prokaryotic and which reaction it catalyzes.[16] Although the name xanthine oxidase (XO) is widely used, today's detailed and up-to-date knowledge of structure and function of these enzymes strongly suggests to refer to them by the more accurate name xanthine oxidoreducase (XOR). As indicated previously, the term oxotransferase is not entirely correct in case of the xanthine oxidase family of enzymes. This is because, the reactions they catalyze usually involve cleaving an R-H bond and forming an R-OH moiety according to equation 7

$$RH + H_2O \rightarrow ROH + 2\ H^+ + 2e^- \dots\dots\dots\dots\dots\dots\dots (7)$$
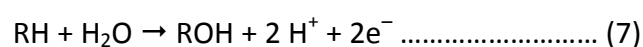
Consequently, they are called hydroxylases acknowledging their function and not oxo transferases. Many attempts have been made to explore the coordination environment of molybdenum in the XO family of enzymes, especially making use of X-ray absorption spectroscopic techniques.[32-35] Aldehyde oxidoreductase from *Desulfovibrio gigas* was the first molybdenum hydroxylase characterized crystallographically.[36-37] These studies suggested an overall square-pyramidal geometry around molybdenum and the composition of the active site to be $LMoO_2(OH_{(2)})$. Of the two terminal oxo groups, one is in the apical position and the other in an equatorial position with a close resemblance to the oxidized SO family structures. However, the enzyme used in this initial crystallographic study was the inactive desulfo form lacking a terminal sulfido ligand. This presented further ambiguity about the position of the terminal sulfido group in the active form of the enzyme. Electron density studies on the activated enzyme obtained by treating the crystals with a resulfurating agent suggested that it was the apical oxo group that was replaced by sulfur to form the Mo=S moiety. This assignment was quite unlikely from the chemical point of view because the single oxo group is supposed to be in the apical position and opposite to the vacant coordination site of a square-pyramidal coordination geometry, owing to its strong

*trans* influence. A freeze–quench magnetic circular dichroism spectroscopic study of the "very rapid" intermediate of xanthine oxidase supported indeed an apical position for the oxo ligand as in common model complexes.[38] Subsequent crystal structures of other enzymes of this family (CO dehydrogenase from the aerobic *Oligotropha carboxydovorans* and quinoline-2-oxidoreductase from *Pseudomonas putida*) also underlined the fact that it is the equatorial position that is sulfurated upon activation in molybdenum hydroxylases.[39-42] A notable and very unusual feature in the coordination sphere of molybdenum in CO dehydrogenase is that the equatorial sulfur is bound to a copper ion, thereby forming a sulfide bridge between Mo and Cu instead of being a terminal sulfido ligand (figure 2.b).

### 1.4.3. Structure and function of the DMSOR family of enzymes

The DMSO reductase (DMSOR) enyzme family is different from the other two families described above since two molecules of MPT in their dinucleotide form are bound to molybdenum. These enzymes have a $L_2Mo^{VI}(O)R$ core in the oxidized state and a $L_2Mo^{IV}(R)$ core in the reduced state (L = MPT and R = ligand most often contributed by the polypeptide). Compared to the other two molybdenum families of enzymes, the DMSOR family is diverse with respect to substrates but restricted to the prokaryotic regime. Crystal structures of several enzymes of the DMSOR family are known today. One of the first was the crystal structure of DMSO reductase from *Rhodobacter sphaeroides*. This oxidized enzyme has a monooxo molybdenum(VI) cofactor containing two molybdopterin guanine dinucleotides (MGD) represented as P-MGD and Q-MGD and one serinate (O-Ser).[43] One of the MGDs exhibits distinct coordination modes to the molybdenum in the oxidized and in the reduced state. The reduced form of DMSO reductase is responsible for binding the substrate DMSO at the beginning of the catalytic cycle. Comparison with the oxidized form reveals no major conformational changes in the protein structure but significant changes at

the active site. This indicates the loss of the oxo ligand (this is expected) and a different coordination of the Mo atom by the molybdopterin S atoms. Only three S ligands remain attached to the molybdenum center, two from P pterin at 2.5 Å and one from the Q pterin at 2.9 Å in addition to the O atom of serinate at 1.8 Å. It was found that the second sulfur of the Q pterin has shifted to a position 3.7 Å from the Mo atom. The structure is consistent with the occurrence of a keto-enol tautomerization after protonation of the thiolate. This change in MGD coordination from the $Mo^{VI}$ species to the $Mo^{IV}$ species is supposed to be crucial in the mechanism for substrate binding and reduction by this enzyme. In fact, a lower coordination number in the reduced form gives room for the oxygen atom of the DMSO to bind to the molybdenum(IV) center and this significantly weakens the S=O bond. A subsequent shift of the sulfur atoms in the Q pterin toward Mo should trigger the liberation of the reaction product DMS by a combination of electronic and steric factors. This leaves the molybdenum in its +VI oxidation state with the formation of the Mo=O bond and the oxidative half cycle is completed. In the reductive half reaction the subsequent transfer of two electrons from a cytochrome and two protons liberates a molecule of water consuming the oxygen atom from the molybdenum center. This brings the molybdenum center back to its active desoxo molybdenum(IV) state. The catalytic cycle of the DMSO reductase as proposed by Rees and Rajagoplan is illustrated in figure 4.

In the crystal structure of oxidized trimethylamine *N*-oxide reductase (TMAOR) from *Shewanella massilia* molybdenum was found to be ligated by four sulfur atoms from the two MGDs, two oxo groups and the oxygen of Ser149 (serine) which would constitute an unfavorable seven-fold coordination.[44] The proposed structure faces several serious limitations such as anomalous bond lengths (e.g. the Mo−O(Ser149) bond length at 1.7 Å is
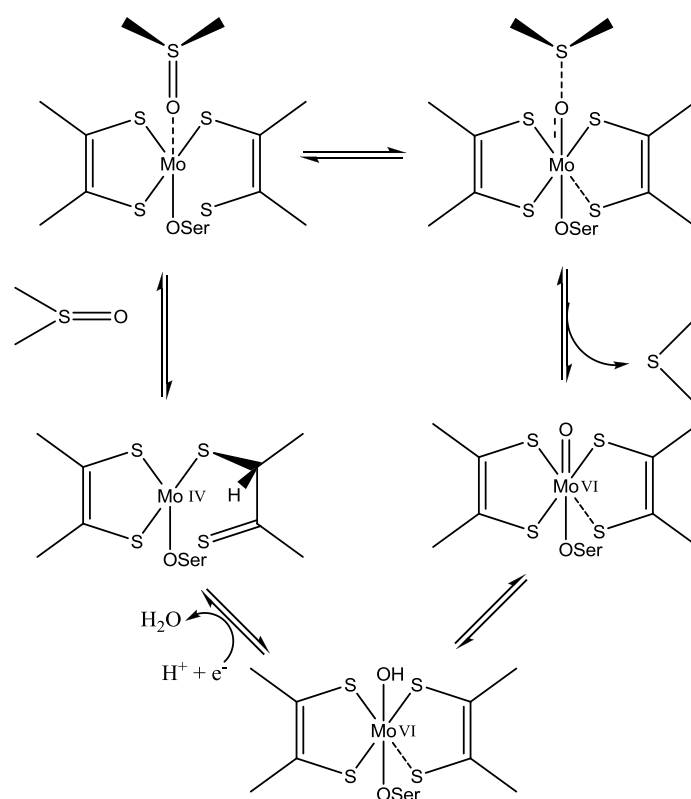
**Fig.4. Catalytic cycle in DMSO reductase**

far too short for an alcoholate coordination to molybdenum and the Mo−S bonds are all suspiciously long, at 2.5, 2.6, 2.7, and 2.8 Å). All this indicates that the postulated molybdenum coordination structure is chemically impossible. A re-examination of the proposed crystal structure by Mo-K edge EXAFS experiments of the molybdenum site of recombinant *Escherichia coli* trimethylamine *N*-Oxide reductase revealed substantial discrepancies between both studies.[45] The EXAFS data of the redox-cycled enzyme (reoxidation of reduced enzyme as part of the purification processes) indicates a single Mo=O ligand at 1.71 Å, four Mo−S ligands (from two MGDs) at 2.43 Å, and one Mo−O-Ser ligand at 1.83 Å just like the oxidized form of DMSO reductase. An explanation for the shortcomings in the crystal structure determination most likely is the presence of the enzyme in more than one oxidation state leading to a superposition of different forms.

A similar ligand environment of the molybdenum center was found in the crystal structure of dissimilatory nitrate reductase (NR) from *Desulfovibrio desulfuricans.* In this case

cysteinate (S-Cys) is the amino acid residue connecting molybdenum and polypeptide. In the oxidized form of the enzyme, $Mo^{VI}$ is coordinated by six ligands in the typical distorted trigonal prismatic geometry. Four coordination sites are occupied by sulfur atoms of each MGD, the fifth position by Cys140 (cysteine) and the sixth is an oxo ligand. The oxidized form will be transferred back to the square pyramidal desoxo $Mo^{IV}$ form through a state of hydroxo/water co-ordination by subsequent proton and electron abstraction processes and elimination of water.[46] The X-ray structure of respiratory nitrate reductase (Nar) from *E. coli* also shows a similar geometry only with aspartate (Asp) as the polypeptide ligand.[47] It should be noted that, in contrast to the co-ordination environment seen in all other enzymes of the DMSOR family, another member of this family, arsenite oxidase, bears a different coordination sphere at the molybdenum center. The crystal structure of arsenite oxidase from *Alcaligenes faecalis* shows a five coordinated $Mo^{IV}$ center with one oxo group and four ene-dithiolate sulfur atoms of two MGDs.[48] The oxidized state is a six coordinate dioxo species. AO has no covalent linkage between the protein and the molybdenum atom. In all other reported enzymes of this family, the molybdenum is coordinated by the side chain of a serine, aspartate, cysteine, or selenocysteine amino acid. In arsenite oxidase, the corresponding residue is an alanine, consequently there is no direct connection between molybdenum and polypeptide through this group. X-ray absorption spectroscopic studies on AO from *Alcaligenes faecalis* indicate that the Mo–S bonds shorten from 2.47 to 2.37 Å upon reduction with the physiological substrate. The studies also confirm that an oxo ligand at 1.70 Å is present in both oxidized and reduced forms of the enzyme and that the oxidized form has an additional Mo–O bond at 1.83 Å which is lost upon reduction.[49] The difference from the typical Mo=O length of 1.70 Å is close to the resolution limit and suggest that this is either an oxo or a hydroxo ligand. Taking into consideration the difference in the

coordination environment in the active center of AO and other members of the DMSOR family, it has been suggested that arsenite oxidase should represent a fourth family of Mo enzymes.[50] Another enzyme, which is assumed to have a bis(MPT)Mo center, is selenate reductase. The active site of this enzyme from *Thauera selenatis* has been characterized by Mo, Se, and Fe K-edge X-ray absorption spectroscopy. It was found that the molybdenum site of the oxidized enzyme carries 3 to 4 sulfur ligands from two molybdopterins at 2.33 Å, one terminal oxo group at 1.68 Å and one Mo−O bond with an intermediate bond length of 1.81 Å. The reduced enzyme has a desoxo Mo center, with four sulfur ligands at 2.32 Å and possibly one Mo-O bond at 2.22 Å.[50] The enzyme was found to contain selenium in a reduced form. However, *T. selenatis* selenate reductase does not contain the SECIS (selenocysteine insertion sequence) and therefore the selenium is unlikely to be part of a selenocysteine. Selenate reductase most probably contains a six co-ordinate $Mo^{VI}O(OH)$ center with two MPTs in the oxidized form and a five co-ordinate $Mo^{IV}(OH)$ with two MPTs in the reduced form. It is therefore analogous to the active site structures that are characteristic for the DMSO reductase family of molybdenum enzymes without the molybdenum peptide bond.

### 1.4.4. Structure and function of the AOR family of enzymes

The function of the AOR enzymes is to convert aldehydes to carboxylic acids according to equation 8.[4]

$RCHO + H_2O + 2$ oxidized ferredoxin $\rightarrow RCOOH + 2H^+ + 2$ reduced ferredoxin. ………….(8)

It can be seen that the majority of tungsten enzymes belong to the AOR family. It was already stated in chapter 1.3. that the first enzyme with the molybdopterin ligand that has been structurally characterized by X-ray diffraction was aldehye oxidoreductase from

*Pyrococcus furiosus* (*P*[f] AOR)*,* a hyperthermophilic archaeon.[13] The crystal structure showed the presence of two molybdopterin ligands bound to tungsten through the sulfur atoms as in case of DMSOR enzymes. The tungsten atom and the two pairs of dithiolene sulfurs are arranged in a distorted square pyramid and the angle between the planes of the molybdopterin ligands was found to be ca. 97°. As shown in figure 1.c the two MPTs do not only bind to the tungsten but are also linked together through their phosphate functions, which coordinate axial sites of the same magnesium ion. In this study, no coordinating protein ligands were found at tungsten, but the electron density studies indicated the presence of two additional coordination sites at the W center. Chan et al. proposed that an additional coordination site would be occupied by either glycerol or oxo ligands (or both) in a distorted trigonal prismatic geometry. Later on it was suggested that the observed glycerol stems from a protein storage buffer and may represent a substrate analogue.[51] Despite considerable ambiguity about the additional coordination sites, it is likely that the oxidized enzyme has a $(MPT)_2W^{VI}O(OH)$ core and the reduced enzyme has a $(MPT)_2W^{IV}(OH)$ core.[4] An EXAFS study by George et al. on *P. furiosus* AOR indicated the presence of an oxo group at 1.7 Å coordinated to the tungsten atom and an additional O or N atom possibly present at 2.1 Å.[52] Another enzyme of this family which was crystallographically characterized is *P. furiosus* formaldehyde ferredoxin oxidoreductase (*P*[f] FOR).[53] As in the case of AOR, the tungsten atom is coordinated by four dithiolene sulfur atoms from two molybdopterins with an average W-S distance of 2.49 Å. There is no protein side-chain coordination to the tungsten atom and the two pterin molecules are linked to each other by a magnesium ion. Besides the four sulfur atoms, an additional ligand was found to bind to tungsten in *Pf* FOR, and it is assumed to be an oxygen atom. The potential difficulty in identifying additional coordination sites on the very heavy tungsten is supposed to be due to the heterogeneous

nature (mainly the simultaneous occurrence of different oxidation states) of the tungsten site itself.

### 1.4.5. Structure and function of the FDH family of enzymes

The two prominent members of the formate dehydrogenase (FDH) family are formate dehydrogenase and N-formylmethanofuran dehydrogenase. The former catalyzes conversion of formate to $CO_2$ and the later catalyzes conversion of N-formylmethanofuran to $CO_2$. The crystal structure of *Desulfovibrio gigas* formate dehydrogenase has been measured to a resolution of 1.8 Å by Raajimakers et al.[54] In this enzyme four sulfur atoms from two MGDs coordinate to tungsten in addition to the selenium atom of a SeCys and one hydroxyl or sulfide ligand. Although X-ray absorption spectroscopy of the similar molybdenum site of *Escherichia coli* formate dehydrogenase seems to favor the OH ligand rather than sulfur [55] this observation is not transferable to tungsten FDH. The structural data by Raajimakers favor a sulfur atom for the sixth ligand, although the resolution of the data is not sufficient to unambiguously distinguish between O and S. Interestingly, in a recent re-evaluation of the crystallographic data of the molybdenum-containing *E. coli* formate dehydrogenase originally recorded by Boyington et al..[56], Romão and co-workers found that the apical ligand was better refined as a sulfur atom (=S or –SH, not $H_2O$ or –OH) at the molybdenum site.[57] This would actually be analogous to the W-FDH from *D. gigas.* Yet the available resolution is not high enough to reach a conclusion based on structural data to judge between O and S for the apical occupation. However, there is chemical evidence for the presence of a sulfur ligand. In the inactivation experiment of formate dehydrogenase from *Methanobacterium formicicum* using cyanide, it was observed that the incubation of the oxidized form of formate dehydrogenase with cyanide resulted in the release of equimolar amounts of thiocyanate and the subsequent deactivation of the enzyme.[58] This

observation strongly suggests the presence of a sulfur ligand (most probably –SH) at the sixth coordination site in W-FDH.[16]

### 1.4.6. Structure and function of the AH family of enzyme

The structure of acetylene hydratase was not known at the time when Hille first classified the enzymes and therefore only two tungsten families were proposed. Acetylene hydratase is different from these two families of tungsten enzymes and the MPT dependent enzymes in general as it does not catalyze a redox reaction. Instead it catalyzes the conversion of acetylene to acetaldehyde which is the net addition of water to acetylene. Interestingly, tungsten is not even believed to change its oxidation state during the catalytic turn over. In 2007 Seiffert et al. published the crystal structure of acetylene hydratase from *P. acetylenicus*.[18] The structure shows a distorted octahedral geometry of the tungsten site. Four coordination sites are occupied by the sulfur atoms from the dithiolene groups of two MGDs, the fifth site by a sulfur atom of a cysteine residue and the sixth by a water molecule.

## 1.5. Why synthetic models?

A synthetic model of an enzyme is a chemical compound synthesized in the laboratory which mimics the structure and/or function of the enzymatic center. The structural information about active sites of enzymes obtained by advanced analytical and theoretical means together with the acquired knowledge on their biological functions have fueled the interest of bioinorganic chemists to synthesize such model complexes and explore their chemical and electronic behavior. In that respect, the area of molybdenum and tungsten dithiolene chemistry was well documented in the last two decades as these compounds serve as model complexes for the molybdenum and tungsten cofactors in the

oxotransferases. The description under chapter 1.4 clearly underlines the plurality in the active site structures and substrate specificity of the individual enzymes and it poses a great challenge to the bioinorganic community to develop the respective model systems as accurately as possible. The importance of model chemistry lies in the possibility of fine-tuning the ligand structure and coordination environment and by this directly paving the way for a trial and error approach towards understanding the logic behind the nature's choices with respect to coordination environment, ligand systems and active site metal. Another important aspect of model chemistry is the overcoming of analytical limitations associated with the complicated natural systems comprising the molybdenum and tungsten cofactors. The characterization limitations associated with the natural enzymes are due to the presence of heavy Mo and W centers which complicate EXAFS investigations and the accompanying Fe-S cluster, heme or flavin having strong absorbing chromophores obscuring electronic transitions of the metal reaction centers.[59] The EXAFS studies are in addition limited in the determination of exact M-S bond length due to their multiple presence in the same coordination sphere. The smallest resolvable difference by EXAFS for metal-ligand bonds involving similar ligands is >0.1 Å and by this equal to the uncertainty associated with data obtained from protein crystallography of most of the molybdenum and tungsten centers.[60-61] Above all, the instability of the isolated cofactors further presents a substantial difficulty for understanding its nature by analytical means. Considering all these factors, the development of apt synthetic models mimicking the structural and functional features of molybdenum and tungsten cofactors are highly demanding to both chemists and biologists. Bioinorganic chemists' attempts in this respect have afforded so far numerous complex structures of molybdenum and tungsten, either with or without the ene-1,2-dithiolate (= dithiolene) function. Those compounds with one or two dithiolate ligands are

commonly known as ligand environment analogues and they have close similarity to the natural enzyme centers. The other class of complexes called co-ordination analogues have no dithiolene ligands. Such complexes are prepared to mimic the co-ordination environment of the enzyme center in terms of geometry and binding atoms neglecting the physical and biochemical importance of the unique structure of molybdopterin. Complimented by advances in the analytical and theoretical fields, several enzymes containing molybdenum or tungsten in their active sites have been discovered recently. This new information coined with their catalytic functions continue to present inorganic chemists several synthetic challenges to create exact mimics in order to unveil their structure activity relationships.

Several unusual coordination features of the active sites of enzymes are still not known in synthetic chemistry. The chemistry of bisdithiolene complexes of $M^{IV}O$ and $M^{VI}O_2$ (M = Mo, W) cores have been thoroughly studied by inorganic chemists but the bisdithiolene complexes of desoxo $M^{IV}$ and $M^{VI}O$ are rare. In addition, monodithiolene complexes of molybdenum and tungsten also are very rare in literature. The most important and still elusive coordination features in the focus of bioinorganic chemists working in this field include bis(dithiolene) complexes of the $Mo^{VI}O(OH)/Mo^{IV}(OH)$ couple relevant for the selenate reductase active site, monodithiolene complexes of the $Mo^{VI}O(S)X/Mo^{IV}O(SH)X$ couple(X= OH, $H_2O$ or N) relevant for the xanthine oxidase family of enzymes, bis(dithiolene) complexes of $Mo^{VI}S(SeS)$ relevant for the Mo-FDH active site, monodithiolene complexes of the $Mo^{VI}O(OH)(\mu\text{-}S)Cu^{I}/Mo^{IV}O(OH_2)(\mu\text{-}S)Cu^{I}$ couple relevant for CODH and finally bis(dithiolene) complexes of $W^{VI}(OH_2)(SR)$ relevant for the W-AH active site. $(Et_4N)[W^{VI}S(SeAd)(S_2C_2Me_2)]$ has already been synthesized as a structural analogue of the active site of FMDH, but a crystal structure could not be obtained and therefore the important structural information remains elusive.[62] In addition to provide complexes

mimicking the coordination environments of active sites of enzymes, a serious focus on modelling the molybdopterin structure is also important.

## 1.6. Objectives of this thesis

The above description clearly indicates the need of developing new synthetic analogues of molybdenum and tungsten enzymes. This thesis mainly focuses on the development of rare model systems. First of all, the main focus is the synthesis and characterization of molybdenum and tungsten dithiolene complexes having a pyrane ring attached to the dithiolene moiety and understanding their structure and function. This is important because such a complex is a better mimic of the molybdenum and tungsten cofactors with respect to the structure of molybdopterin than the large majority of available models. Since the bioinorganic chemistry of molybdenum and tungsten developed mainly based on conventional ligands, not enough attention was paid to study the influence of the pyrane ring in the structure on the function of model complexes. In the following part of this thesis, chapter 2 describes the development of molybdenum and tungsten complexes with two chromandithiolene (cdt) ligands. The cdt ligand has a pyrane ring adjacent to dithiolene as seen in natural molybdopterin. The prepared complexes with the cdt ligand have been extensively studied using advanced analytical methods including single crystal XRD and EXAFS. In chapter 3, the developed synthetic models using cdt ligands have been screened for their catalytic activity in the model oxotransfer reaction between DMSO and PPh$_3$. In addition to this a comparative study has been made between different model complexes in order to understand the role of the heteroatom (oxygen atom in molybdopterin as well as cdt). The obtained results have been correlated with the electrochemical behavior of all the compounds under study. The second main focus of the thesis is to develop new and economic synthetic routes to synthesize monodithiolene complexes. In order to achieve this

goal, molybdenum oxochlorides have been supported on various ligands like N-heterocyclic carbenes, bipyridines and β-diketiminate and further treated with dithiolenes. Chapter 4 is dedicated to carbene complexes of molybdenum in different oxidation states and emphasizes their potential utility for synthesizing monodithiolene complexes of molybdenum. Chapter 5 describes the synthesis of bipyridine and β-diketiminate complexes of MoOCl$_3$ and their use as templates for preparing both mono and bis dithiolene complexes. As a third focus, dithiolene ligand transfer chemistry of tungsten has been explored. Chapter 6 presents the unprecedented chemistry of the dithiolene ligand transfer between tungsten and the alkaline earth metal strontium. The thesis ends with chapter 7 with a short summary of results and an outlook.

## References

[1]    Samuel. P. P.; Schulzke, C. Handbook of Inorgnaic Chemisry, Chapter 3. Nova Sci.Publ., 2010 (In press)

[2]    Einsle, O.; Tezcan, F.A.; Andrade, S. L .A.; Schmid, B.; Yoshida, M.; Howard, J.B.; Rees, D.C. *Science*  297 (2002) 1696

[3]    Kletzin, A.; Adams, M. W. W. *FEMS Microbiol. Rev.* 18 (1996) 5

[4]    Hille, R. *Trend. Biochem. Sci.* 27 (2002) 360

[5]    Scott, C.; Lyons, T. W.; Bekker, A.; Shen, Y.; Poulton, S. W.; Chu, X.; Anbar, A. D. *Nature* 452 (2008) 456

[6]    Bertine, K. K.; Turekian, K. K. *Geochim. Cosmochim. Acta* 37 (1973) 1415

[7]    Taylor, S. R.; McLennan, S. M. Rev. *Geophys.* 33 (1995) 241

[8]    Schulzke, C. *Dalton Trans*. (2005) 713

[9]    Enemark, J. H.; Cooney, J. J. A.; Wang, J.J.; Holm, R. H. *Chem. Rev.* 104 (2004) 1175

[10]  Huynh, M. H. V.; Meyer T. J. *Chem. Rev.* 107 (2007) 5004

[11]  Johnson, J. L.; Rajagopalan, K. V. *Proc. Nat. Acad. Sci. USA.* 79 (1982) 6856

[12]  Kramer, S. P.; Johnson, J. L.; Ribeiro, A. A.; Millington, D. S.; Rajagopalan, K. V. *J. Biol. Chem.* 262 (1987) 16357

[13]  Chan, M. K.; Mukund, S.; Kletzin, A.; Adams, M. W. W.; Rees, D. C. *Science* 267 (1995) 1463

[14]  Lorber, C.; Donahue, J. P.; Goddard, C. A.; Nordlander, E.; Holm, R. H. *J. Am. Chem. Soc*. 120 (1998)  8102

[15]  Stiefel, E. I. *Dalton Trans.* (1997) 3915

[16]  Bevers, L. E.; Hagedoorn P.-L., Hagen, W. R. *Coord. Chem. Rev.* 2009, 253, 269-290

[17]  Hille R. *Chem. Rev.* 96 (1996) 2757

[18]  Seiffert, G. B.; Ullmann, G. M; Messerschmidt, A.; Schink, B.; Kroneck, P. M. H.; Einsle O. *Proc. Nat. Acad. Sci. USA* 104 (2007) 3073

[19]  Johnson, J.; Rajagopalan, K.V. *J Biol. Chem.* 252 (1977) 2017

[20]  Kipke, C. A., Cusanovich, M.A.; Tollin, G. ; Sunde, R. A.; Enemark, J.A. *Biochemistry* 27 (1988) 2918

[21]  Sullivan Jr., E. P.; Hazzard, J. T.; Tollin, G.; Enemark, J.H. *Biochemistry* 32 (1993) 12465

[22]  Rajagopalan, K. V. In *Molybdenum and Molybdenum Containing Enzymes*; Coughlan, M.; Ed.; Pergamon: Oxford (1980) 241

[23]  Cramer, S. P.; Wahl, R.; Rajagopalan, K.V. *J. Am. Chem. Soc.* 103 (1981)  7721

[24]  Cramer, S. P.; Solomonson, L. P.; Adams, M. W. W.; Mortenson, L. E. *J. Am. Chem. Soc.* 106 (1984) 1467

[25]  George, G. N.; Kipke, C.A.; Prince, R. C.; Sunde, R. A.; Enemark, J. H.; Cramer, S. P. *Biochemistry* 28 (1989) 5075

[26] George, G. N.; Garrett, R. M., Prince, R.C.; Rajagopalan, K.V. *J. Am. Chem. Soc.* 118 (1996) 8588

[27] Kisker, C.; Schindelin, H.; Pacheco, A.; Wehbi, W. A.; Garrett, R.M.; Rajagopalan, K.V.; Enemark, J. H.; Rees, D.C. *Cell* 91 (1997) 973

[28] Garton, S. D.; Garrett, R.M.; Rajagopalan, K.V.; Johnson, M.K. *J. Am. Chem. Soc.* 119 (1997) 2590

[29] George, G. N.; Pickering, I. J; Kisker, C. *Inorg. Chem.* 38 (1999) 2539

[30] Hille, R. *J. Biol. Inorg. Chem.* 2 (1997) 804

[31] Fischer, B.; Enemark, J. H.; Basu, P. *J. Inorg. Biochem.* 72 (1998) 13

[32] Lim, B. S.; Willer, M. W.; Miao, M. Holm, R. H. *J. Am. Chem. Soc.* 123 (2001) 8343

[33] Bray, B .J.; Garner, R. C.; Gutteridge, C. D.; Hasnain, S. S. *J. Biochem* 191 (1980) 499

[34] Cramer, S. P., Hille, R. *J. Am. Chem. Soc.* 107 (1985) 8164

[35] Turner, N. A.; Bray, R.C.; Diakun, G.P. *Biochem. J.* 260 (1989) 563

[36] Romão, M. J.; Archer, M.; Moura, I; Moura, J. J. G.; LeGall, Jean; Engh, R.; Schneider, M.; Hof, P.; Huber, R. *Science* 270 (1995) 1170

[37] Huber, R.; Hof, P.; Duarte, R.O; Moura, J.J.G., Moura, I., Liu, M.Y., LeGall, J., Hille, R., Romão, M.J *Proc. Nat. Ac. Sci USA* 93 (1996) 8846

[38] Jones, R. M.; Inscore, Frank E.; Hille, R.; Kirk, M. L. *Inorg. Chem.* 38 (1999) 4963

[39] Ragsdale, S.W. *Critical Reviews in Biochemistry and Molecular Biology* 39 (2004) 165

[40] Gremer, D. H.; Kiefersauer, L.; Huber, R.; Meyer, O. *Proc. Nat. Ac. Sci. USA* 99 (2002) 15971

[41] Gnida, M.; Ferner, R.; Gremer, L.; Meyer, O.; Meyer-Klaucke, W. *Biochemistry* 42 (2003) 222

[42] Bonin, I.; Martins, B. M.; Purvanov, V.; Fetzner, S.; Huber, R. Dobbek, H. *Structure* 12 (2004) 1425

[43] Schindelin, H.; Kisker, C. ; Hilton, J.; Rajagopalan K. V.; Rees, D. C. *Science* 272 (1996) 1615

[44] Czjzek, M.; Dos Santos, J.-P.; Pommier, J.; Giordano, G.; Méjean, V.; Haser, R. *J. Mol. Biol.* 284 (1998)  435

[45] Zhang, L.; Nelson, K.J.; Rajagopalan, K.V.; George, G.N. *Inorg. Chem*. 47 (2008) 1074

[46] Dias, J.M.; Than, M. E.; Humm, A.; Huber, R.; Bourenkov, G. P.; Bartunik, H. D.; Bursakov, S.; Calvete, J.; Caldeira, J.; Carneiro, C.; Moura, J.J.; Moura, I.; Romão, M. J. *Structure* 7 (1999) 65

[47] Jormakka, M.; Richardson, D; Byrne, B.; Iwata, S. *Structure* 12 (2004) 95

[48] Ellis, P. J.; Conrads, T.; Hille, R.; Kuhn, P. *Structure* 9 (2001) 125

[49] Conrads, T.; Hemann, C.; George, G. N.; Pickering, I.J.; Prince, R. C.; Hille, R. *J. Am. Chem. Soc.* 124 (2002) 11276

[50] Maher, M. J.; Santini, J.; Pickering, I. J.; Prince, R.C.; Macy, J. M.; George, G. N. *Inorg. Chem.* 43 (2004) 402

[51] Johnson, M. K.; Rees, D. C.; Adams**,** M. W. W. *Chem. Rev.* 96 (1996) 2817

[52] George, G. N.; Prince, R. C.; Mukund, S.; Adams, M. W. W. *J. Am. Chem. Soc.* 114 (1992) 3521

[53] Hu, Y.; Faham, S.; Roy, R.; Adams, M. W. W.; Rees, D. C. *J. Mol. Biol.* 286 (1999) 899

[54] Raaijmakers, H.; Macieira, S.; Dias, J.M.; Teixeira, S.; Bursakov, S.; Huber, R.; Moura, J. J.G; Moura, I.; Romão, M. J. *Structure* 10 (2002) 1261

[55] George, G.N.; Colangelo, C. M.; Dong, J.; Scott, R. A.; Khangulov, S. V.; Gladyshev V. N.; Stadtman T. C. *J. Am. Chem. Soc.* 120 (1998) 1267

[56] Boyington J. C.; Gladyshev V. N.; Khangulov S. V.; Stadtman T. C.; Sun P. D. *Science* 275 (1997) 1305

[57] Raaijmakers, H. C. A.; Romão, M. J. *J. Inorg. Biochem.* 11 (2006) 849

[58] Barber, M. J. *Biochemistry* 25 (1986) 150

[59] Sugimoto, H; Tsukube, H. *Chem. Soc. Rev.* 37 (2008) 2609

[60] Enemark, J.H.; Garner, C.D. *J .Bio. Inorg. Chem.* 2 (1997) 817

[61] George, G.N. *J. Bio. Inog. Chem.* 2 (1997) 790

[62] Groysman, S.; Holm, R. H. *Inorg. Chem.* 46 (2007) 4090

# MONOOXO BISDITHIOLENE MOLYBDENUM AND TUNGSTEN COMPLEXES: SYNTHETIC ANALOGUES OF ARSENITE OXIDASE

## 2.1. Modeling chemistry of bis(MPT)Mo enzymes

As mentioned in the previous chapter, the bis(MPT)Mo enzymes are classified as members of the DMSO reductase family by Hille. Throughout the literature, the model chemistry of the DMSO reductase family of enzymes has taken two courses: firstly, modeling the $Mo^{IV}S_4R/Mo^{VI}(O)S_4R$ (R = Amino acid analogue) couple as in the case of structurally characterized DMSOR, TMAOR and NR enzymes and secondly modeling the $Mo^{IV}(O)S_4/Mo^{VI}(O)_2S_4$ couple as in the case of AO. Most of the early developed model complexes come under the second class, even though at the time of their development the structure of AO was unknown. Bearing in mind the active site structures of the large majority of the DMSOR family enzymes it is clear that rather monooxo six co-ordinate $Mo^{VI}$ compounds are required when modeling enzymes of this family but such complexes are rarely reported. The most frequently reported form in the early synthetic model chemistry was the *cis*-dioxo moiety $MoO_2^{2+}$.[1] At the same time, of the early monooxo $Mo^{VI}$

29

compounds a large number was even seven-fold coordinated.[2-4] In 1988, Mondal et al. reported MoO(cat)(Sap) complexes (cat = catecholate ($Cat^{2-}$), naphthalene-2,3-diolate ($Naphcat^{2-}$), or 3,5-di-*tert*-butylcatecholate ($DTBcat^{2-}$) and Sap = the Schiff base dianion N-salicylidene-2-aminophenolate) as first examples of mononuclear $MoO^{4+}$ centers with a six-fold coordination (figure 1).[5] Following this, several monooxo $Mo^{VI}$ coordination complexes were reported and some of them were screened for understanding redox potentials and oxotransfer properties.[6-11]
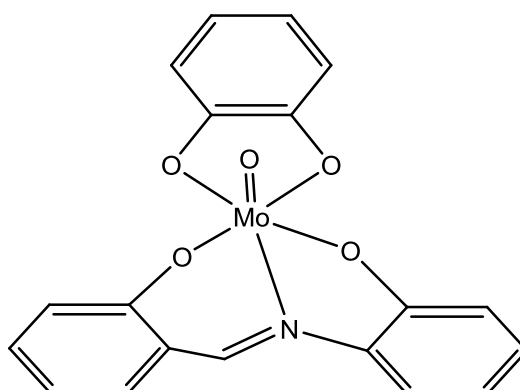


**Fig.1. Chemical structure of MoO(Cat)(Sap)**

The accessible molybdenum oxidation state V is assumed to act as mediator between the obligatory two-electron and one-electron redox systems and a detailed understanding of its properties is equally important as for the more commonly observed enzymatic oxidation states $Mo^{IV}$ and $Mo^{VI}$. Nearly two decades prior to the publication of crystal structures of DMSO family enzymes, Wedd and co-workers synthesized $[Mo^{V}O(SPh)_4]^-$ which can be considered as one of the very early developed model complexes in this series.[12] After that, several complexes having $[Mo^{V}OS_4]^-$ coordination have been synthesized and extensively studied theoretically and experimentally with respect to geometry, electronic structure, redox properties and bonding.[13-16] In an effort to identify the geometric control of the redox potential by serine ligation to the molybdenum center of DMSO reductase, Kirk, Basu

and co-workers synthesized and isolated *cis*-[(L1O)Mo$^V$OCl$_2$] and *trans*-[(L1O)Mo$^V$OCl$_2$] complexes [L1OH = (3-*tert*-butyl-2-hydroxy-5-methylphenyl)bis(3,5-dimethylpyrazolyl) methane] with the *cis* and *trans* notation referring to the position of the phenolato oxygen relative to that of the terminal oxo ligand (figure 2). Cyclic voltammetry experiments were conducted to probe the redox chemistry of the two isomers. Both *trans* and *cis* isomers exhibit well-defined one-electron reductive signals for Mo$^V$ → Mo$^{IV}$ at −940 mV and at −1160 mV respectively. Thus the results show that the *trans* isomer is easier to reduce than the *cis* isomer by about 200 mV provocatively suggesting that the position of the serinate oxygen relative to the terminal oxo ligand at the molybdenum center of DMSOR may play a critical role in gating the electron transfer process of active site regeneration as part of the catalytic cycle.[17] Another monooxo Mo$^V$ complex, Tp*Mo$^V$O(O-*p*-C$_6$H$_4$OEt)$_2$, has been screened for its oxotransfer ability. The electrochemical oxidation of this compound affords [Tp*Mo$^{VI}$O(O-*p*-C$_6$H$_4$OEt)$_2$]$^+$ which reacts with tertiary phosphines (PR$_3$) to generate a phosphineoxide-coordinated adduct, [Tp*Mo$^{IV}$(OPR$_3$)(O-*p*-C$_6$H$_4$−OEt)$_2$]$^+$. This compound subsequently eliminates OPR$_3$ to give the Mo$^{IV}$ desoxo species, [Tp*Mo$^{IV}$(O-*p*-C$_6$H$_4$OEt)$_2$]$^+$. The desoxo species generates Tp*Mo$^V$O(O-*p*-C$_6$H$_4$OEt)$_2$ in the presence of water and an oxidizing agent completing the catalytic cycle, that closely resembles the postulated enzymatic turnover.[18]



L1OH    *cis*-[Mo$^V$OCl$_2$]    *trans*-[Mo$^V$OCl$_2$]
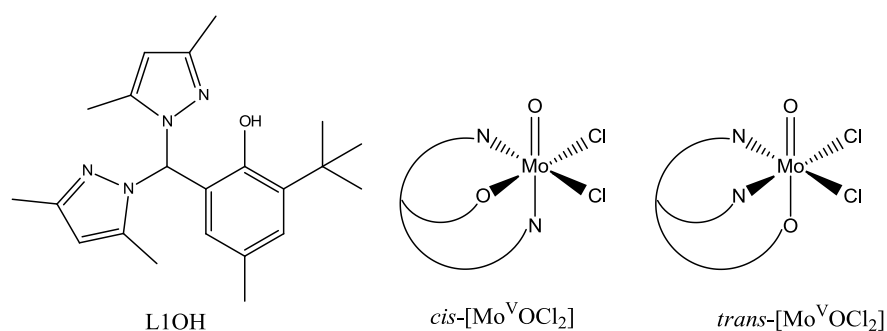
**Fig.2. *cis* and *trans* orientation of the phenolato oxygen of L1OH with respect to the terminal oxo group in MoOCl$_2$**

The first oxobis-(dithiolene)metallate complexes to be characterized by X-ray crystallography were [MoO(bdt)$_2$]$^{2-}$ and [MoO(bdt)$_2$]$^-$ synthesized by the Garner group.[19] Following this, several bisdithiolene Mo$^{IV}$O complexes were synthesized with symmetrical dithiolenes like bdtCl$_2$, mnt (S$_2$C$_2$(CN)$_2$), edt (S$_2$C$_2$H$_2$), S$_2$C$_2$Ph$_2$, S$_2$C$_2$Me$_2$ etc. (figure 3) and unsymmetrical dithiolenes like sdt, 2-pedt, 4-pedt (figure 4).[20-28] The preparation procedures for the bis(dithiolene)Mo(IV)O complexes are versatile and for a majority of these compounds the methods are summarized in the literature.[29]



bdt          bdtCl$_2$          edt          mnt          S$_2$C$_2$Me$_2$          S$_2$C$_2$Ph$_2$
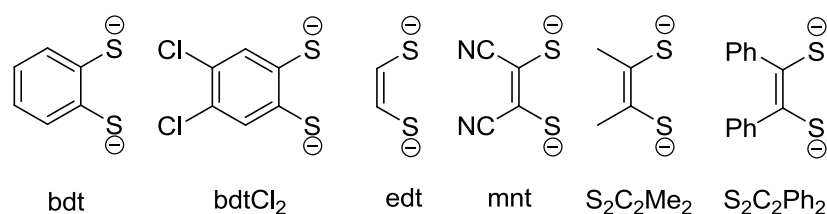
**Fig.3. The symmetrical dithiolene ligands as models for MPT**



sdt          2-pedt          4-pedt
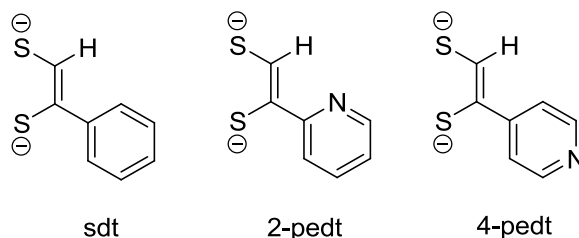
**Fig.4. The unsymmetrical dithiolene ligands as models for MPT**

Bis-(dithiolene)mono-oxo Mo$^{IV}$ complexes can be converted to the corresponding dioxo Mo$^{VI}$ complexes through controlled oxidation by Me$_3$NO making model compounds for both the reduced and the oxidized oxidation state of the enzymes, and especially for AO, easily accessible at least when using plain dithiolene ligands. In recent years, the trend has been diverted from the above mentioned conventional dithiolene ligands to those with a closer resemblance of the molybdopterin structure. In 2005 [MoO(fdt)$_2$]$^{2-}$ (figure 5) was reported from our group as the first molybdenum complex with a ligand system that not

only includes the dithiolene group but also the pyrane feature of the enzymatic molybdopterin.[30] Crystals of these complexes could not be obtained possibly due to the fact that they form *cis-* and *trans-* (ligand orientation) and *R-* and *S-* (position of the phenyl group at the pyran ring) isomers *i.e.* a mixture of diastereomers, which usually results in poor crystallization behavior. Later in the same year, Sugimoto et al. synthesized the complexes [MoO(L$^{CH2}$)$_2$]$^{2-}$, [MoO(L$^S$)$_2$]$^{2-}$ and [MoO(L$^O$)$_2$]$^{2-}$ (figure 5) with the latter again including a pyrane dithiolene molybdenum moiety. The crystal structures of these complexes show that the oxo ligand together with the four sulfur atoms from the dithiolene function constitute a square pyramidal geometry with a weakened Mo=O bond character.[31] The significance of such a weakened Mo=O bond will be described in chapter 2.5.



[MOL$^O$)$_2$]$^{2-}$
M= Mo/W

[MO(fdt)$_2$]$^{2-}$
M = Mo/W
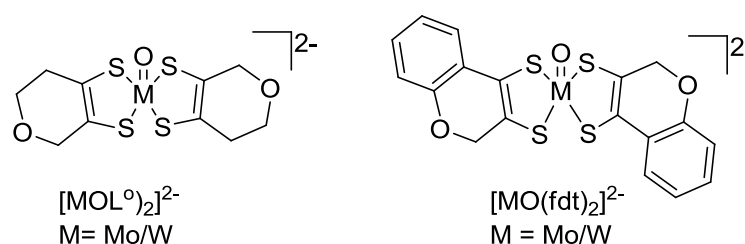
**Fig. 5. Molybdenum and tungsten complexes with pyrane dithiolene co-ordination**

## 2.2. Modelling chemistry of bis(MPT) tungsten enzymes

As in the case of molybdenum model chemistry the W$^{IV}$O(dithiolene)$_2$ and W$^{VI}$O$_2$(dithiolene)$_2$ complexes have been investigated because of their frequent occurrence in inorganic chemistry. In addition bis(dithiolate) and *non*-dithiolene complexes of tungsten relevant for the oxo transfer enzymes have been developed. Many of them have been screened for their oxo transfer ability. Several six-fold coordinated W$^{VI}$O$_2$ complexes have been reported and a lesser number of corresponding W$^{IV}$O complexes. Among those are the tungsten(VI)

dithiocarbamate complexes, $W^{VI}O_2(R_2dtc)_2$ (R=Et, Me, $^nPr$; dtc = dithiocabamate).[32] These compounds were originally prepared by the oxo transfer reaction between $W(CO)_2(PPh_3)(R_2dtc)_2$ and $Mo_2O_3(Et_2dtp)_4$. Other complexes of this class are $(NH_4)_2[W^{VI}O_2(O_2CC(S)PPh_2)_2]$[33] and $W^{VI}O_2(ssp)$ (ssp= 2-(salicylideneamino)benzene-thiolate), a Schiff base complex[34]. The synthesis of monooxo tungsten(IV) analogues of these complexes was found to be almost impossible. But stable bis(dithiolene) $W^{IV}O$, $W^VO$ and $W^{VI}O_2$ complexes with the ligands benzenedithiolene (bdt) and maleonitriledithiolene (mnt), which are much better models for MPT than the dithiocarbamates or Schiff bases, have been reported.[35-36] $(PPh_4)_2[W^{IV}O(bdt)_2]$ and $(NEt_4)_2[W^{IV}O(bdt)_2]$ were synthesized by borohydride reduction of $(PPh_4)[W^VO(bdt)_2]$ or $(NEt_4)[W^VO(bdt)_2]$ which were obtained by a simple ligand exchange reaction between $[WO(SPh)_4]^-$ and two equivalents of bdt-$H_2$. These complexes readily undergo oxidation by triethylamine-N-oxide to give the corresponding dioxo tungsten(VI) complexes. $[Et_4N]_2[W^{IV}O(mnt)_2]$ was prepared by the oxo transfer between $[Et_4N]_2[W^{VI}O_2(mnt)_2]$ and $PPh_3$. Remarkably the mnt complex $[Et_4N]_2[W^{IV}O(mnt)_2]$ was shown to reduce $CO_2/HCO_3^-$ (at pH 7.5) to yield $HCOO^-$ and $[Et_4N]_2[W^{VI}O_2(mnt)_2]$ mimicking tungsten-formate dehydrogenase (W-FDH) activity.[37] A similar redox couple involving $Me_3NO$ as a substrate analogue and $S_2C_2Me_2$ as the MPT analogue has been reported by the Holm group.[38] More recently, other important tungsten compounds with promising ligand systems involving pyrane dithiolene species have been synthesized. $[W^{IV}O(fdt)2]^{2-}$ was the first in this series, but no crystal structure was reported (figure 15).[6] Later, Sugimoto et al. synthesized $[WO(pdt)_2]^{2-}$ and $[WO_2(pdt)_2]^{2-}$ as the first structurally characterized tungsten complexes with pyrane dithiolene ligands (figure 15; $L^o$ = pdt).[39]

A series of various bis(dithiolene)tungsten(IV,VI) complexes with benzenedithiolene was prepared by Holm and co-workers in a synthetic approach to more accurate models for

the active sites of tungstoenzymes.[40] Using $[W^{IV}O(bdt)_2]^{2-}$ as precursor, silylation with $Me_3SiCl$, $^tBuMe_2SiCl$ and $^tBuPh_2SiCl$ transforms the oxo ligand to a silyloxide ligand affording $[W^{IV}(bdt)_2(OSiMe_3)]^{1-}$, $[W^{IV}(bdt)_2(OSi^tBuMe_2)]^{1-}$ and $[W^{IV}(bdt)_2(OSi^tBuPh_2)]^{1-}$ respectively. Oxidation of the desoxo complex, $[W^{IV}(bdt)_2(OSi^tBuPh_2)]^{1-}$ with $Me_3NO$ gives the corresponding monooxo tungsten(VI) complex $[W^{VI}O(bdt)_2(OSi^tBuPh_2)]^{1-}$. Silylation of $[W^{VI}O_2(bdt)_2]^{2-}$ with $^tBuPh_2SiCl$ affords the same complex. Further silylation of $[W^{VI}O(bdt)_2(OSi^tBuPh_2)]^{1-}$ with $Me_3SiCl$ leads to the formation of $[W^{VI}O(bdt)_2Cl]^{1-}$ from which the unstable species $[W^{VI}O(bdt)_2L]^{1-}$ (L = $^tBuO^-$, $PhS^-$) were generated in solution. Interestingly, the reaction of $[W^{VI}O(bdt)_2Cl]^{1-}$ with L' = $P(OEt)_3$ or $^tBuNC$ afforded the reduced products $[W^{IV}(bdt)_2L'_2]$. Complexes $[W^{IV}(bdt)_2(OSiMe_3)]^{1-}$, $[W^{IV}(bdt)_2(OSi^tBuMe_2)]^{1-}$ and $[W^{IV}(bdt)_2(OSi^tBuPh_2)]^{1-}$ are regarded as tungsten analogues of the molybdenum model complexes for the reduced DMSOR family enzymes. However, the elusive $[W^{VI}O(OH)(dt)_2]$ and $[W^{IV}(OH)(dt)_2]$ complexes would be still better mimics of the active sites of tungsten-AOR family enzymes considering the current knowledge of the coordination environment of these enzymes, which was not available at the time of preparation. Further development of this chemistry by the Holm group led to similar models with less unnatural mono-anionic ligands ($[W^{VI}O(L^-)(dt)_2]$ / $[W^{IV}(L^-)(dt)_2]$; LH = PhOH, PhSH, PhSeH, $^iPrOH$).[41-42] The reactions follow the equations 1 and 2 affording $[W(S_2C_2R_2)_2L(CO)_{2-n}]^-$ complexes in analogy to the corresponding molybdenum chemistry. In case of molybdenum complexes, the $L^-$ ligands are considered as the structural analogues of the amino acids present at the molybdenum center of the DMSOR family of enzymes and this applies also to cysteine and selenocysteine at the active sites of the tungsten FDH and AH families. In addition, the coordination environment of the above mentioned complexes $[W^{VI}O(^-OR)(dt)_2]$/ $[W^{IV}(^-OR)(dt)_2]$ can be regarded as analogous to that in the AOR family of enzymes. More recently

the synthesis of $[W^{IV}(OMe)(S_2C_2Me_2)]^-$ was reported.[43] This complex shows a remarkable similarity to the coordination environment of tungsten in the AOR family of enzymes with the anionic oxygen based ligand carrying only a small methyl substituent.

$[M(CO)_3(MeCN)_3] + 2[Ni(S_2C_2R_2)_2] \rightarrow [M(S_2C_2R_2)_2(CO)_2] + [Ni^{II}_2(S_2C_2R_2)_2] + 3MeCN + CO$ ......... (1)

$[M(S_2C_2R_2)_2(CO)_2] + L^- \rightarrow [M(S_2C_2R_2)_2L(CO)_{2-n}]^- + n\,CO$ ..................................................... (2)
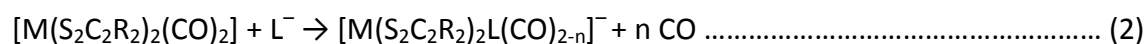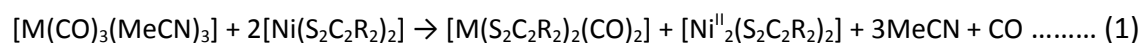
As discussed above, in order to model the FDH family of enzymes a sulfur ligand is required though it is not known with certainty if it is a sulfide or a thiolate that is bound to tungsten at the active site. Not so long ago, the Holm group was successful in synthesizing $(Et_4N)[W^{VI}S(SeAd)(S_2C_2Me_2)_2]$ as the first FDH family analogue with the coordination of a sulfide ligand to tungsten.[44] Unfortunately a crystal structure or a functional oxo transfer study of this complex has not been reported yet. It is obvious that the tungsten model chemistry is still not advanced enough to address all the structural and reactivity issues and remains to pose a challenge to bioinorganic chemists working in this field.

## 2.3. Scope of the present work

One of the most interesting features of the molybdenum and tungsten enzymes (except nitrogenase) is the metal carrying the common and unique ligand molybdopterin. Since MPT binds to the metal by a dithiolene function, the respective *non-innocent* nature of this ligand is supposed to play a significant role in the redox properties of the active site. As a consequence the redox properties of the enzyme's active sites cannot be regarded as strictly metal based. Effectively the metal is part of an electronically delocalized system constituted by the planar $MS_2C_2$ ring. This electron delocalization allows the dithiolene function to be a

mediator for the electronic coupling between the metal center and the pterin nucleus.[45] The coupling will be highly favored if the carbon atom adjacent to the dithiolene group is $sp^2$ hybridized because this allows conjugation between the metal dithiolene system and the pyrazine ring.[46] The entire role of the pterin and pyrane rings in the MPT structure has not been clarified yet even though its participation in fine tuning the redox nature of the active site is beyond doubt. It has to be mentioned here that the bicyclic MPT structure originally proposed by Rajagopalan and the tricyclic form found in X-ray crystal structures of MPTs in the following years is different only by two hydrogens. At the same time, the X-ray crystal structure of molybdenum nitrate reductase showed the presence of two MPTs at the metal center, one with a bicyclic open alcohol structure and the other with a tricyclic closed pyrane ring structure.[47] This indicates the possibility of pyrane ring opening and closing during the catalytic turnover effecting a redox action in the adjacent pterin ring which is conjugated to the metal-dithiolene aromatic system. The pyrazine ring present in the tricyclic form of MPT is in its reduced tetrahydro form as evidenced by crystallographic structures, but the opening of the pyrane ring may result in a dihydropyrazine structure and therefore the loss of two protons coupled to an oxidation of this ring. The reversal of this process is a two proton reduction (addition of protons) combined with the pyrane ring closing and restoration of the reduced tetrahydro pyrazine. A scheme illustrating the opening and closing of the pyrane in the MPT structure is shown in figure 6.[45] Consequently MPT is believed to have a considerable role in handling the two protons involved in the catalytic PCET reaction.

Even if several synthetic analogues for the enzymes in the AO family have been reported, there were no attempts to include the essential pyrane ring close to the dithiolene function as it is seen in the molybdopterin until $[MoO(fdt)_2]^{2-}$ and $[WO(fdt)_2]^{2-}$ were reported

from our group in 2005. Here in I report the second generation of the fdt based complexes in which fdt is replaced by cdt (chromandithiolene). The $[MoO(cdt)_2]^{2-}$ and $[WO(cdt)2]^{2-}$ have been prepared, characterized and screened for their oxotransfer catalytic activity. This chapter describes the preparation and characteristics of the above mentioned complexes. A comparative study on the temperature dependent electrochemistry and the oxotransfer catalytic properties will be described in chapter 3.
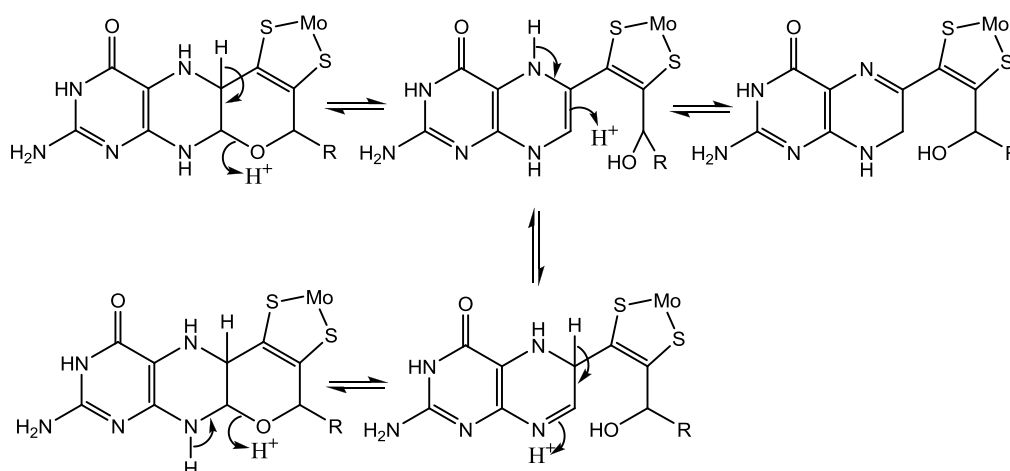


**Fig.6. Opening and closing of the pyrane ring in the MPT structure**

## 2.4. Experimental

### 2.4.1. Materials and methods

Syntheses of molybdenum and tungsten complexes were done using Schlenk line techniques under a pure nitrogen atmosphere and oxygen free solvents were used. The solvents used for crystallization trials were perfectly dry and flushed with nitrogen. The commercially obtained chemicals were used as received. NMR-spectra were recorded on NMR-spectrometers Bruker Avance DRX 500 or Bruker Avance DPX 300. The residual ^{1}H or ^{13}C peak of the deuterated solvent was used as an internal standard and tetramethysilane as external standard for ^{1}H spectra. Infrared spectra were collected on a Mattson Genesis FT-

MIR spectrometer in the range of 4000 - 400 cm$^{-1}$ using KBr pellets. Mass spectra were recorded with a Finnigan MAT System 8200. For FAB spectra, ionization was achieved using 3-nitrobenzylalcohol. Elemental analyses were carried out with a 4.1 Varido EL 3 Analyzer from Elementar. If possible, X-ray crystal analysis was carried out. Suitable crystals were mounted on a glass fiber and data was collected on an IPDS II Stoe image-plate diffractometer (graphite monochromated Mo $K_\alpha$ radiation, $\lambda$=0.71073 Å at 133(2) K. The data was integrated with X-Area. The structures were solved by Direct Methods (SHELXS-97) and refined by full-matrix leastsquares methods against $F^2$ (SHELXL-97). [48] All *non-hydrogen* atoms were refined with anisotropic displacement parameters.

Compound **6** was analyzed at the molybdenum K-edge by X-ray absorption methods. The measured X-Ray spectrum was averaged and normalized using the *Bessy* program and then used for comparison in the simulations. Simulation models were generated using the HyperChem program version 8.0.6. The basic model for the O=Mo-4S geometry was created based on the most likely structure of the compound and then further refined during the simulation process. The measured EXAFS bond lengths were constrained in HyperChem. The FEFF program version 9 was used to create XANES simulations. FEFF was used for a k-range of 6, a FMS (full multiple scattering) calculation range of 6 Å and a SCF (self consistent field) radius of likewise 6 Å. Ionization due to bond partners was estimated as 1.2 for molybdenum (equals +VI) and -0.4 for oxygen and sulfur ligands (equals -II). The simulated ionization feature was found to be depending on the amount of ligands rather than the oxidation state, and was used to remove the shift of the simulated spectrum. The amplitude reduction factor $S_0^2$ was calculated by FEFF. Bond distances were derived from the EXAFS data evaluation.

**2.4.2. Preparation of 3-Bromochroman-4-one; (1):** 4-chromanone (2 g, 13.5 mmol) and K$_2$CO$_3$ (2.1 g, 15 mmol) were stirred in 160 ml CCl$_4$ to which bromine liquid (0.70 ml,

13.6 mmol) was added slowly at room temperature. The reddish brown solution was allowed to stir for an hour which then turned to pale yellow. It was then filtered to remove the precipitated KBr and the solution was concentrated in a rotavapor. The pale yellow oil was then dissolved in 100 ml chloroform and washed three times with distilled water to remove the inorganic salts. Further concentration to dryness affords a very pale yellow solid which was then recrystallized from ethanol. Yield 2.9 g (12.78 mmol, 95%).

Elemental analysis for $C_9H_7BrO_2$ (227.05 g/mol) calcd. (%) C: 47.61; H: 3.11; expt. (%) C: 47.72; H: 3.18. $^1$H NMR (CDCl$_3$-[d$_1$], 300 MHz), 25°C, TMS: δ = 4.69-4.48 (m, 3H), 7.02-6.99 (m, 1H), 7.09-7.03 (m, 1H), 7.93-7.89 (m, 1H, 7.54-7.48 (m, 1H) ppm. $^{13}$C NMR (CDCl$_3$-[d$_1$], 75.47  MHz, 25°C, TMS): δ = 45.33, 71.20, 117.88, 122.26, 128.18, 136.66, 160.59, 185.13 ppm. EI-MS: *m/z* 226 [$C_9H_7BrO_2$]$^+$.

**2.4.3. Preparation of *O*-ethyl *S*-4-oxochroman-3-yl carbanodithioate; (2):** To a solution of 3-bromochroman-4-one (2.5 g, 11 mmol) in 25 ml EtOH, was added a solution of potassium *O*-ethyl carbonodithioate (1.76 g, 11 mmol) in 25 ml EtOH. The mixture was heated at 60$^o$C for one hour and the precipitated KBr was filtered. The collected yellow solution was concentrated in a rotavapor and the yellow oil obtained was dissolved in dichloromethane. The solution was washed three times with water and dichloromethane was evaporated in vacuum. The viscous yellow oil was then dissolved in minimum amount of ethanol and cooled to obtain the yellow solid. Yield 2.5 g (9.31 mmol, 85%).

Elemental analysis for $C_{12}H_{12}O_3S_2$ (268.35 g/mol) calcd (%): C: 53.71; H: 4.51; S: 23.90. expt.: C: 53.67; H: 4.56; S: 23.86. IR (KBr) [cm$^{-1}$]: 409.2 (w), 445.1 (w), 516.9 (w), 584.4 (w), 619.0 (m), 672.9 (w), 750.6 (m), 767.9 (m), 824.9 (m), 837.8 (w), 871.3 (w), 958.4 (m), 1002.5 (m),1043.8 (s), 1115.9 (m), 1146.3 (m), 1176.2 (w), 1208.9 (s), 1232.4 (s), 1278.4 (m),  1307.4

(s), 1325.2 (m), 1376.4 (w), 1391.9 (w), 1461.6 (s), 1474.5 (s), 1576.5 (m), 1603.3 (s), 1692.8 (s), 1798.4(w), 1832.8 (w), 1940.3 (w), 2033.9 (w), 2357.6 (w), 2454.5 (w), 2647.0 (w), 2853.0 (m), 2915.3 (w),2986.5 (w), 3036.7 (w),3062.6 (w), 3366.5 (w); $^1$H-NMR (CDCl$_3$-[d$_1$], 500 MHz, 25°C, TM): δ = 1.41-1.22 (t, 3H), 4.47-4.42 (m, 1H), 4.68-4.62 (q, 2H), 4.75-4.72 (m, 1H), 4.96-4.93 (m, 1H), 7.04-6.95 (m, 2H), 7.50-7.46 (m, 1H), 7.87 (m, 1H). $^{13}$C-NMR (CDCl$_3$-[d$_1$], 125.8 MHz, 25°C, TMS): δ = 13.66, 53.45, 69.65, 70.95, 117.86, 120.43, 121.88, 127.67, 136.49, 161.31, 187.07, 210.94. EI-MS: m/z 268 [C$_{12}$H$_{12}$O$_3$S$_2$]$^+$.

### 2.4.4. Preparation of H-[1,3]dithiolo[4,5-c]chromen-2-one; (3):

35% HBr in acetic acid solution (30 ml) was added to *O*-ethyl *S*-4-oxochroman-3-yl carbanodithioate (1.5 g, 5.6 mmol) and stirred for 15 h at room temperature. The resultant brownish solution was slowly added to excess of ice water while vigorous stirring which affords a highly hydrophobic and soft pale brown solid. It was then filtered in a Buchner funnel and the solid was washed with distilled water. The product was air dried for 1 hr and then in extreme vacuum for another 15 h. A solution of **3** in a mixture of hexane and diethylether (6:4) at -30°C afforded single crystals suitable for X-ray diffraction measurement. Yield 1.27 g (4.72 mmol, 70%).

Elemental analysis for C$_{10}$H$_6$O$_2$S$_2$ (222.28 g/mol)calcd. (%): C: 54.03; H: 2.72; S: 28.85. expt (%).: C: 54.23; H: 2.82; S: 28.76. IR (KBr) [cm$^{-1}$]: 441.5 (m), 509.4 (w), 542.7 (w), 561.6 (w), 584.8 (w), 621.4 (w), 651.0 (m), 746.1 (s), 790.3 (m), 818.3 (m), 854.9 (w), 898.3 (m), 854.9 (w), 898.3 (m), 928.4 (w), 963.1 (w), 1009.0 (s), 1040.8 (m), 1101.4 (m), 1133.8 (w), 1153.9 (w), 1230.6 (s), 1252.4 (w), 1271.1 (w), 1303.0 (w), 1378.2 (w), 1453.8 (m), 1487.2 (s), 1562.1 (w), 1619.9 (s), 1665.5 (s) 1715.2 (s) 1787.1 (w), 1852.0 (w), 1896.3 (w), 1940.9 (w), 2338.8 (w), 2359.2 (w), 2619.8 (w), 3022.1 (w), 3067.8 (w), 3270.3 (w). $^1$H-NMR (CDCl$_3$-[d$_1$],

500 MHz, 25°C, TMS): δ = 5.03 (s, 2H), 6.97-6.90 (m, 3H), 7.21-7.17 (m, 1H). $^{13}$C-NMR (CDCl$_3$-[d$_1$], 500 MHz, 25°C, TMS): δ = 64.00, 116.76, 118.36, 119.55, 122.54, 123.61, 124.50, 129.94, 152.31, 190.04. EI-MS: m/z 222 [C$_{10}$H$_6$O$_2$S$_2$]$^+$.

**2.4.5. Preparation of K$_3$Na[MoO$_2$(CN)$_4$].6H$_2$O; (4):** This complex was prepared by following the reported procedure.[49] Na$_2$MoO$_4$.2H$_2$O (7g, 0.03 mol) , KBH$_4$ (3.0g, 0.063 mol) and KCN (5.0g, 0.077 mol) were dissolved in water and cooled to 5$^o$C, followed by the drop wise addition of acetic acid (5 ml, 0.08 mol) over 10 min. More KCN (5g, 0.077 mol) was then added, followed by the drop wise addition of another aliquot of acetic acid (5 ml, 0.08 mol) over 10 min. A mixture of NaOH (10 g, 0.25 mol) and KOH (14 g, 0.25 mol) was added slowly to the Mo(IV) solution followed by slow addition of ethanol (30 ml). The pink crystals were washed successively, in small portions with an ethanol/water (9:1, 600 ml) mixture. Recrystallisation was performed by dissolving the crystals in a minimum of water, addition of NaOH and KOH (1g of each) and precipitation of K$_3$Na[MoO$_2$(CN)$_4$].6H$_2$O by the slow addition of ethanol.

Elemental analysis: calc (%): C: 10.00; H: 2.52; N: 11.66. expt. (%): C: 10.15; H: 2.64; N: 11.88.

**2.4.6. Preparation of K$_3$Na[WO$_2$(CN)$_4$].6H$_2$O; (5):** This complex was prepared by following the similar procedure adopted for compound 4. Na$_2$WO$_4$.2H$_2$O (9.54g, 0.03 mol) , KBH$_4$ (3.0g, 0.063 mol) and KCN (5.0g, 0.077 mol) were dissolved in water and cooled to 5$^o$C, followed by the drop wise addition of acetic acid (5 ml, 0.08 mol) over 10 min. More KCN (5g, 0.077 mol) was then added, followed by the drop wise addition of another aliquot of acetic acid (5 ml, 0.08 mol) over 10 min. A mixture of NaOH (10 g, 0.25 mol) and KOH (14 g, 0.25 mol) was added slowly to the W(IV) solution followed by slow addition of ethanol (30 ml). The yellowish brown crystals were washed successively, in small portions with an ethanol/water

(9:1, 600 ml) mixture. Recrystallisation was performed by dissolving the crystals in a minimum of water, addition of NaOH and KOH (1g of each) and precipitation of $K_3Na[WO_2(CN)_4].6H_2O$ by the slow addition of ethanol.

Elemental analysis: calc (%): C: 8.45; H: 2.13; N: 9.86. expt. (%): C: 8.63; H: 2.38; N: 9.59.

**2.4.7. Preparation of [MoO(cdt)$_2$](NBu$_4$)$_2$; (6)** 4H-[1,3]dithiolo[4,5-c]chromen-2-one (0.38 g, 1.71 mmol) was dissolved in 12.5 ml of oxygen free methanol and stirred for 45 min with KOH (0.38 g, 6.83 mmol). The solution turned to dark reddish brown and to this a blue solution of $K_3Na[MoO_2(CN)_4].6H_2O$ (0.41 g, 0.85 mmol) in oxygen free water (12.5 ml) was added under nitrogen atmosphere. The reaction mixture was stirred for 3 h at 70°C, cooled and concentrated in vacuum to dryness. It was then dissolved in 10 ml of water and washed three times with oxygen free chloroform to remove the unreacted organic compounds. The aqueous layer was collected, dried, dissolved in oxygen free acetonitrile and filtered. The evaporation of acetonitrile under high vacuum at room temperature affords a red solid. This product was dissolved again in oxygen free water (20 ml) and a solution of NBu$_4$Br (0.55 g, 1.71 mmol) in water (20 ml) was added drop-wise while stirring. The precipitated orange-brown solid compound was filtered, washed with water and dried under extreme vacuum overnight. The single crystals suitable for X-ray diffraction analysis were obtained from a solvent mixture of acetonitrile and hexane (7:3) at -35$^o$C.

Elemental analysis for $C_{50}H_{84}MoN_2O_3S_4$ (986.44 g/mol) calcd. (%) C: 60.94; H: 8.59; N: 2.84; S: 13.02. expt. (%): C: 60.80; H: 8.53; N: 2.88; S: 12.89. IR (KBr) [cm$^{-1}$]: 448.1 (w), 482.1 (w), 519.6 (w), 547.5 (w), 618.2 (w), 643.0 (m), 749.6 (s), 784.0 (m), 904.5 (s), 993.2 (m), 1033.5 (m), 1065.4 (w), 1084.9 (w), 1107.2 (w), 1150.0 (w), 1215.7 (m), 1246.6 (m), 1303.5 (w), 1359.5 (w), 1380.6 (m), 1479.0 (s), 1550.5 (m), 1577.4 (m), 2443.9 (w), 2703.7 (w), 2816.8

(w), 2874.1 (m), 2939.2 (s), 2961.3 (s), 3023.4 (w), 3065.9 (w); $^1$H-NMR (CD$_3$CN-[d$_3$],

500 MHz): 7.86-7.82 (m, 2H), 6.87 (m, 4H), 6.74 (m, 2H), 5.10 (s, 4H), 2.97-2.94 (t, 16H), 1.45-

1.39 (p, 16H), 1.30-1.22 (h, 16H). $^{13}$C-NMR (CD$_3$CN-[d$_3$], 125.8 MHz, 25°C, TMS): 13.89, 20.32,

24.36, 58.97, 74.14, 114.60, 118.254, 121.505, 124.49, 125.76, 152.10. (FAB$^-$, 3-NBA) e/z:

502 [C$_{18}$H$_{12}$MoO$_3$S$_4$]$^-$

**2.4.8. Preparation of [WO(cdt)$_2$](NBu$_4$)$_2$; (7):** 4H-[1,3]dithiolo[4,5-c]chromen-2-one (0.38 g,

1.71 mmol) was dissolved in 12.5 ml of oxygen free methanol and stirred for 45 min with

KOH (0.38 g, 6.83 mmol). The solution turned to dark reddish brown and to this a purple

solution of K$_3$Na[WO$_2$(CN)$_4$].6H$_2$O (0.48 g, 0.85 mmol) in oxygen free water (12.5 ml) was

added under nitrogen atmosphere. The reaction mixture was stirred for 3 h at 70°C, cooled

and concentrated in vacuum to dryness. It was then dissolved in 10 ml of water and washed

three times with oxygen free chloroform to remove the unreacted organic compounds. The

aqueous layer was collected, dried, dissolved in oxygen free acetonitrile and filtered. The

evaporation of acetonitrile under high vacuum at room temperature affords a red solid. This

product was dissolved again in oxygen free water (20 ml) and a solution of NBu$_4$Br (0.55 g,

1.71 mmol) in water (20 ml) was added drop-wise while stirring. The precipitated brick-red

solid compound was filtered, washed with water and dried under extreme vacuum

overnight.

Elemental analysis for C$_{50}$H$_{84}$WN$_2$O$_3$S$_4$ (1073.31 g/mol) calcd. (%) C: 55.95; H: 7.89; N: 2.61; S:

11.95; expt. (%): C: 56.10; H: 8.10; N: 2.55; S: 12.23. IR (KBr) [cm$^{-1}$]: 448.5 (w), 519.0 (w),

546.9 (w), 591.8 (w), 618.3 (w), 642.9 (m), 749.5 (s), 784.1 (m), 904.6 (s), 993.3 (m), 1033.35

(m), 1068.2 (w), 1085.1 (w), 1106.6 (w), 1150.4 (w), 1215.9 (m), 1246.7 (m), 1303.5 (w),

1359.3 (w), 1380.6 (m), 14445.8 (m), 1479.9 (s), 1550.7 (m), 1577.2 (m), 2446.0 (w), 2361.5

(w), 2605.5 (w) 2703.4 (w), 2742.0 (w), 2796.1 (w), 2817.7 (w), 2873.3 (m), 2937.3 (m), 2960.0 (m), 3022.7 (w), 3065.8 (w); $^1$H-NMR (CD$_3$CN-[d$_3$], 500 MHz): 7.88-7.84 (m, 2H), 6.90-6.88 (m, 4H), 6.82-6.80 (m, 2H), 5.20 (s, 4H), 2.98-2.95 (t, 16H), 1.48-1.41 (p, 16H), 1.31-1.23 (h, 16H). $^{13}$C-NMR (CD$_3$CN-[d$_3$], 125.8 MHz, 25°C, TMS): 13.80, 20.26, 24.29, 58.97, 75.16, 114.19, 118.20, 121.51, 124.49, 124.92, 153.64. (FAB$^-$, 3-NBA) e/z : 588 [C$_{18}$H$_{12}$WO$_3$S$_4$]$^-$

## 2.5. Results and Discussion

The overall synthetic route to obtain compound **3** starting from the commercially available chromanone is shown in figure 7. The first reaction is α-halogenation of the carbonyl compound, chromanone. The reaction of chromanone with molecular bromine in the presence of the base potassium carbonate results in the formation of 3-Bromochroman-4-one. The reaction is supposed to be base catalyzed by potassium carbonate in CCl$_4$ solution. The possible mechanism is depicted in figure 8. The first step is supposed to be the base catalyzed enolization to give the enolate ion. The enolate ion then attacks the bromine molecule to give the bromide. The product **1** is not stable enough to be kept for many days but is quite durable for at least three days in a closed bottle at -35$^o$C. Because of this instability, the product was converted to compound **2** within a few hours after its preparation. The bromination of the α-position is clearly visible from the downfield shift of a 2H triplet at 2.8 ppm in 4-chromanone to a single hydrogen peak in the 4.69-4.48 ppm region in compound **1**. Presence of bromine makes the two protons in the adjacent CH2 groups magnetically inequivalent and so the splitting of the peak is expected. However these two peaks appear together with CHBr proton in the same region 4.69-4.48. These peaks are not distinguishable from each other but together account for three protons as expected.

The second reaction is the simple nucleophilic substitution replacing $Br^-$ with the xanthate anion at a saturated carbon atom. This could occur by an $SN^2$ mechanism demanding back side attack, which in general is favored by neither the secondary carbon atoms nor the alicyclic ring systems because of the steric strain. On the other hand, the $SN^1$
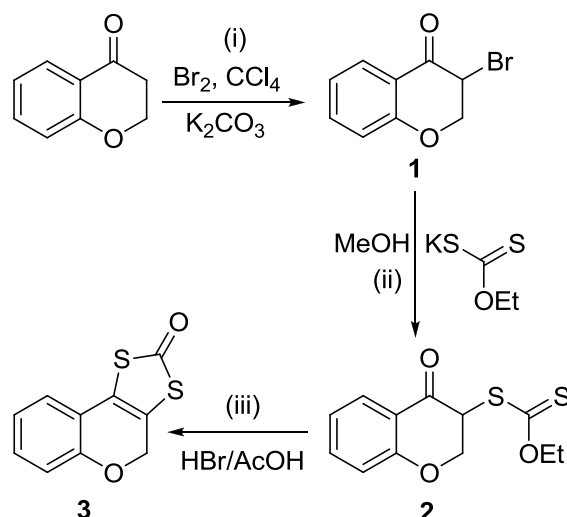


**Fig.7. Synthesis of compound 3 from 4-chromanone**
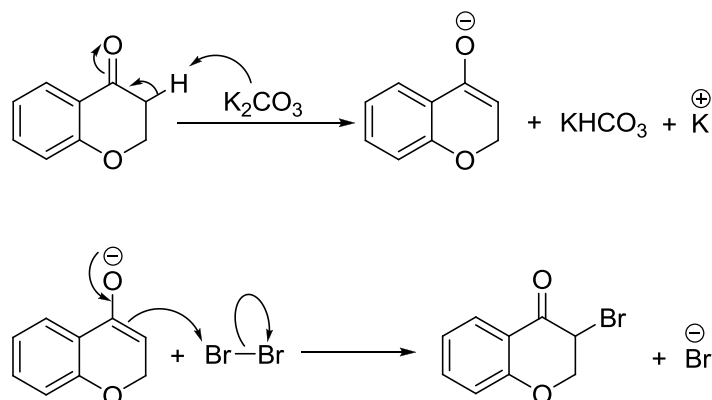


**Fig. 8. Formation of 4-chromanone**

mechanism demands the formation of a carbocation by the elimination of bromide ion, which in our case is stabilized by the status of secondary carbon, but destabilized to some extend by the carbonyl group α to it. Further investigations would be required to decide which is the actual mechanism involved in this reaction. The product after the reaction with

the potassium xanthate is a yellow powder and is quite stable to keep for long time under normal conditions. Replacing Br⁻ by the xanthate anion clarifies the magnetic inequivalency of the $CH_2$ protons near to the pyrane oxygen atom. 4.47-4.42 (m, 1H) belongs to the proton of the CHBr group and the 4.75-4.72 (m, 1H) and 4.96-4.93 (m, 1H) peaks belongs to the magnetically inequivalent $CH_2$ protons. IR spectrum shows weak absorption bands for aromatic C-H stretching frequencies at 3036.7 and 3062.6 $cm^{-1}$. The $(sp^3)$C-H stretching frequencies are observed at 2853 and 2915.3 $cm^{-1}$. The $(sp^3)$C-H bending frequencies are observable at  1391.9 , 1461.6 and 1474.5 $cm^{-1}$. The absorption band at 1376.4 $cm^{-1}$ is originating from the umbrella deformation of the $CH_3$ group.  The C-O stretching frequencies are observed at 1208.9 and 1232.4 $cm^{-1}$ and the C=O stretching frequency is seen at 1692.8 $cm^{-1}$.

The reaction (iii) is following the Tsugaeff reaction in which the net elimination of a molecule of ethylene and water affords the product **3**. The mechanism of the reaction is illustrated in figure 9. The reaction starts with the attack of the proton from the acid on the thioketone, which leads to a ring current resulting in the elimination of an ethylene molecule. This step is perfectly catalytic where the used $H^+$ ion is released during the elimination of ethylene. In the resulting intermediate product, the SH proton is highly acidic which protonates the C=O group in the pyrane ring. This leaves the carbonyl carbon of the pyranone positively charged and the terminal sulfur atom negatively charged. Obviously S- attempts a nucleophilic attack on the positive carbon atom closing the ring. This product is highly vulnerable for water elimination in acidic medium and forms compound **3**. The ring closure removes the magnetic inequality of the CH2 protons and it appears as a 2H singlet at 5.03 ppm in the ¹H-NMR spectrum. IR spectrum shows weak absorption bands for aromatic C-H stretching frequencies at 3022.1 and 3067.8 cm-1. The C-H bending frequencies are

observable at 1378.2 and 1453.8 cm$^{-1}$. The C-O stretching frequency is observed at 1230.6

cm$^{-1}$. The observed frequency at 1715.2 cm$^{-1}$ originates from the C=O stretching.

However, the reaction (iii) is the most difficult step in the whole preparation of

compound **3** from chromanone. The amount of acid used is very crucial and the optimum is

reported in the procedure. The compound **3** is a light weighted material and it is highly

hydrophobic. It is soluble in almost all common organic solvents. A solution of **3** in a mixture

of hexane and diethylether (6:4) at -30$^{o}$C afforded single crystals. Figure 10 shows the

molecular structure of **3** derived from its single crystal X-ray diffraction pattern.
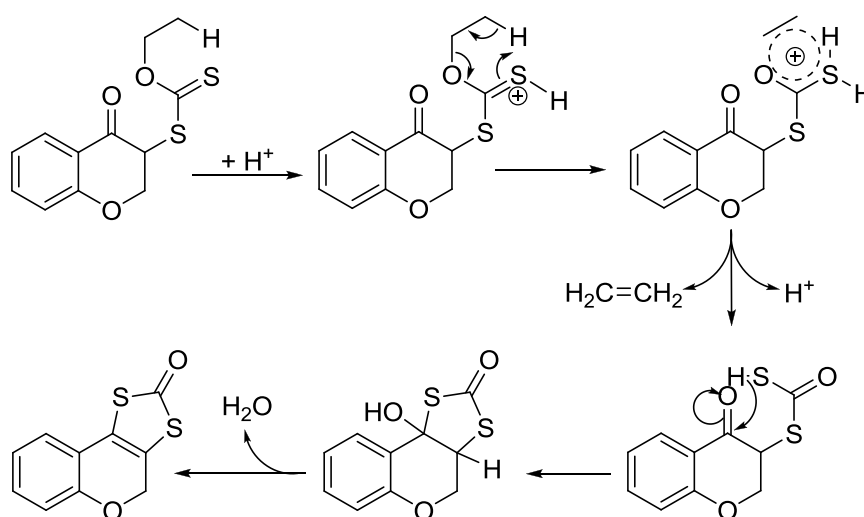


**Fig. 9. Mechanism of formation of compound 3**
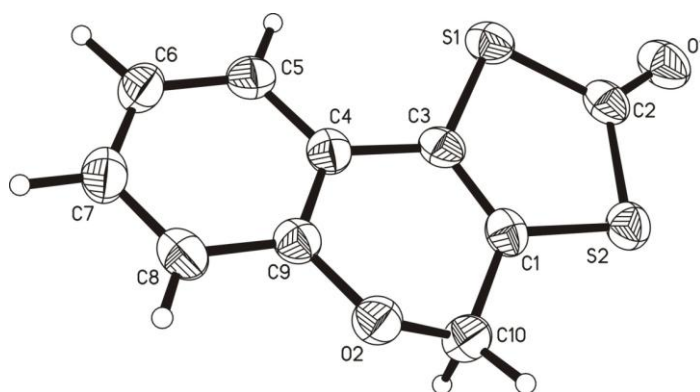


**Fig.10.Molecular structure of compound 3**

The selected bond distances, bond angles and other crystallographic information are furnished in table 1. The oxygen atom, O2, in the pyrane ring is not in the same plane of the benzene ring plane. It makes a dihedral angle of $2.495^o$ with the plane constituting the atoms in the order C9, C4 and C8. This means that the pyrane oxygen atom is roughly $2.495^o$ out of the benzene ring plane. At the same time the atom C3 is more or less in the same plane of benzene ring. C3 has a dihedral angle of $-0.265^o$ with the plane constituted by the atoms in the order C4, C5 and C9 which is very close to the ideal $0^o$. The angle between the bonds at both sides of the pyrane oxygen atom is $116.194^o$. The oxygen atom, O2, actually is bonded to two types of carbon atoms: the aromatic carbon atom C9 and the $sp^3$ carbon atom, C10. This difference is directly reflected in the bond lengths that O2 makes with both above mentioned atoms. C9-O2 bond length is 1.3797 Å and the C10-O2 bond length is 1.4372 Å. The tetrahedral angle between the atoms O2, C10 and C1 is not exactly ideal with $111.013^o$. The atoms C1 and C3 are in $sp^2$ hybridized state with a double bond of 1.3380 Å length between them. It should be noted that the expected planarity is not strictly maintained around the $sp^2$ hybridized C1 and C3 atoms. For example the dihedral angle that S1 makes with the plane constituting the atoms in the order C3, C4 and C1 is $-2.678^o$. Likewise, the dihedral angle that the S2 makes with the plane constituting the atoms in the order C1, C3 and C10 is $-3.742^o$. The bond lengths that the sulfur atoms form with the double bonded carbon atoms are 1.7391 Å for C3-S1 and 1.7359 Å for C1-S2. The 1,3-dithiole heterocyclic ring is more or less planar. The bond angles around the sulfur atoms are C3-S1-C2 = $95.561^o$ and C1-S2-C2 = $95.438^o$. This deviates by roughly $14^o$ from the ideal tetrahedral angle, governed by multiple facts like repulsion from the sulfur lone pairs and ring constraints.

The compounds $[MO(cdt)_2]^{2-}$, [M= Mo, W] are formed according to the following reaction mechanism (figure 11). The first step involves the cleavage of the bonds that the sulfur atom makes with the ketonic carbon atom of the 1,3-dithiol-2-one ring in compound **3**. This reaction is induced by the use of KOH in wet methanol. KOH cleaves the S-C bond to

**Table 1. Selected dimensions in the crystal structure of compound 3**

| Bond lengths (Å) | | Bond angles (°) | | Torsion angles (°) | |
|---|---|---|---|---|---|
| C1-C3 | 1.3380(47) | C9-O2-C10 | 116.194(242) | C9-C4-C8-O2 | 2.495(334) |
| C3-S1 | 1.7391(37) | O2-C10-C1 | 111.013(291) | C4-C5-C9-C3 | -0.265(332) |
| C1-S2 | 1.7359(33) | C3-S1-C2 | 95.561(165) | | |
| C9-O2 | 1.3797(39) | C1-S2-C2 | 95.438(166) | | |
| C10-O2 | 1.4372(47) | | | | |

yield dissolved potassium 2H-chromene-3,4-bis(thiolate). The byproduct in this reaction is carbonic acid which can then either liberate carbon dioxide and form water or precipitate as potassium carbonate in the basic medium. However, no precipitation was observed and the reaction mixture remained a clear red solution, favouring the possibility of $CO_2$ elimination. Since the reaction is not vigorous, any type of bubbling due to $CO_2$ expulsion was not visible in the stirring solution. All attempts to isolate the potassium 2H-chromene-3,4-bis(thiolate) from the solution were failed. Consequently the metal starting compound, $K_3Na[MO_2(CN)_4].6H_2O$ in water was added directly to the reaction mixture. The four CN groups are replaced by two dianionic 2H-chromene-3,4-bis(thiolate) species and the metal atom switches from the hexacoordinate to a pentacccordinate environment by giving up one of the oxo groups. The byproducts in this reaction are assumed to be potassium cyanide and

KOH or NaOH. The compounds **6** and **7** show the $\nu_{Mo=O}$ and $\nu_{W=O}$ bands at 904.5 and 904.6 $cm^{-1}$ respectively. A comparison of these wave numbers with the corresponding values of the similar earlier reported complexes are given in table 2. The comparison reveals that complex **6** has a similar value of $\nu_{Mo=O}$ (904.5 $cm^{-1}$) with that of the bdt complex (905 $cm^{-1}$ for $(Et_4N)_2[MoO(bdt)_2]$ [19]) but significantly lower than that for the mnt complex (932 $cm^{-1}$ for $(Et_4N)_2[MoO(mnt)_2]$ [28] and the $S_2C_2(CO_2Me_2)_2$ complex (914 $cm^{-1}$ for $(Et_4N)_2[Mo(S_2C_2(CO_2Me_2)_2]$ [23]). This result is straight forward when considering the electronegativity of the groups attached to the dithiolene function. The highly electronegative cyanides make S→Mo electron donation less efficient leading to the highest value for $\nu_{Mo=O}$. The electronegativity of the pyrane oxygen atom is less than that of both cyanide and methylcarboxylic groups resulting in the least stretching frequency value among the three. The same trend is clearly visible when compared to the $\nu_{Mo=O}$ values reported in the case of $S_2C_2Me_2$ and sdt complexes of molybdenum. (889 $cm^{-1}$ for the $S_2C_2Me_2$ $cm^{-1}$ complex, $(Et_4N)_2[MoO(S_2C_2Me_2)_2]$ [42] and 879 for the sdt complex, $(Ph_4P)_2[MoO(sdt)_2]$ [50]). These IR results indicate that compound **6** has a weak Mo=O bond and that its molybdenum center is a Lewis acid. This trend based on the electronegativity values is visible in the case of the tungsten complex too. Complex **7** shows a significantly lower value ($\nu_{W=O}$ = 904.6 $cm^{-1}$) than the mnt complex (935 $cm^{-1}$ for $(Et_4N)_2[WO(mnt)_2]$) [36], and a higher value than the $S_2C_2Me_2$, sdt and $S_2C_2Ph_2$ complexes (897 $cm^{-1}$ for $(Et_4N)_2[WO(S_2C_2Me_2)_2]$,[51] 884 $cm^{-1}$ for $(Ph_4P)_2[WO(sdt)_2]\cdot EtOH$ [52]and 886 for $(Et_4N)_2[WO(S_2C_2Ph_2)_2]$ [51]).

These weakened M=O bonds have bioinorganic importance revealed by the EXAFS studies of the oxidized from of arsenite oxidase. The EXAFS studies suggested that the $Mo^{VI}O_2$ core of arsenite oxidase had one longer $Mo^{VI}O$ bond at 1.83 Å and this undergoes protonation to form $Mo^{VI}O(OH)$ in the catalytic cycle.[53, 54] Most of the earlier reported

$Mo^{VI}O_2$ complexes [55-57] with weaker electron donating ligands had a strong Mo=O bond and protonation rarely occurred. In the present study, molybdenum shows a weakened Mo=O bond character which clearly indicates that the presence of the pyrane ring attached to the dithiolene group in molybdopterin is an intelligent design by nature to fine tune the catalytic activity of the molybdenum centre.

**Table 2. $\nu_{M=O}$ values of M(IV)O and W(IV)O bisdithiolene complexes**

| Mo complex | $\nu_{M=O}$ | W complex | $\nu_{M=O}$ |
|---|---|---|---|
| $(NBu_4)[MoO(cdt)_2]$ | 904.5 | $(NBu4)[WO(cdt)2]$ | 904.6 |
| $(Et_4N)_2[MoO(mnt)_2]$ | 932.0 | $(Et_4N)_2[WO(mnt)_2]$ | 935.0 |
| $(Et_4N)_2[Mo(S_2C_2(CO_2Me_2)_2]$ | 914.0 | $(Et_4N)_2[WO(S_2C_2Me_2)_2]$ | 897.0 |
| $(Et_4N)_2[MoO(bdt)_2]$ | 905.0 | $(Ph_4P)_2[WO(sdt)_2].EtOH$ | 884.0 |
| $(Et_4N)_2[MoO(S_2C_2Me_2)_2]$ | 889.0 | $(Et_4N)_2[WO(S_2C_2Ph_2)_2]$ | 886.0 |
| $(Ph_4P)_2[MoO(sdt)_2]$ | 879.0 | | |
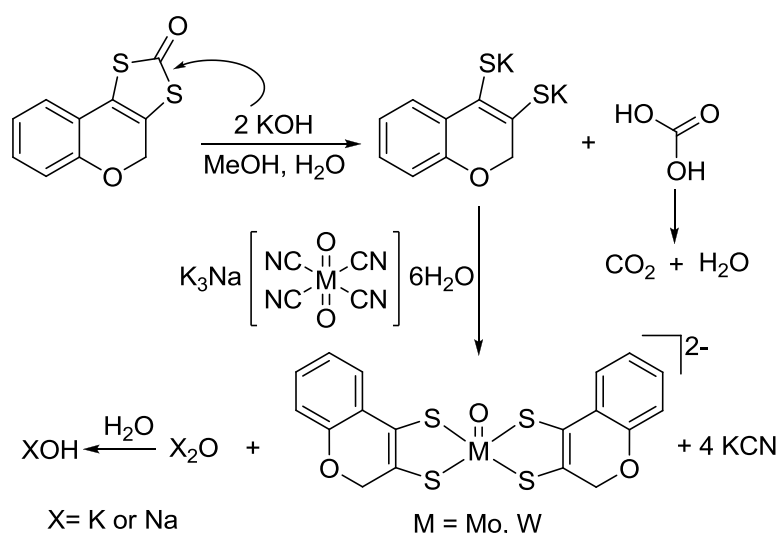


**Fig. 11. Formation of compound 6 and 7**

The crystallization of compound **6** was carried out in a solvent mixture of acetonitrile and hexane (7:3) at -35$^o$C. In fact the crystallization of this compound was very difficult and succeeded only after one year following its preparation. Different cationic groups like [PPh$_4$]$^+$, [NBu$_3$Me]$^+$ and [NEt$_3$(benzyl)]$^+$ were used in the trials to afford crystals. In the case of [NBu$_3$Me]$^+$ and [NEt$_3$(benzyl)]$^+$ both molybdenum and tungsten complexes gave almost oily type semisolids and proved to be very poor for crystallization from any solvent. The only successful combination for the crystallization of the Mo complex was with tetrabutyl ammonium ions, and that too in only one combination of the solvents as mentioned above. Many crystallization attempts were carried out for [WO(cdt)$_2$]$^{2-}$ with different combinations of cationic groups and solvents but unfortunately it seems like one of the most difficult tungsten complexes to produce single crystals suitable for X-ray measurement.

The compound **6** crystallizes in the monoclinic space group Cc with the cell lengths a=15.815(3), b=20.813(4) and c=16.284(3) Å and β=105.03$^o$. The crystal packing structure of compound **6** is shown in figure 12. Figure 13 shows the structure of the anionic part of the molecule. For clarity and for further discussion the tetrabutyl ammonium part is omitted in figure 13. The geometry around the molybdenum centre is square pyramidal (figure 14) with the base of the pyramid constituted of the four sulfur atoms of the two dithiolene groups and the apex being the terminal oxygen atom. The sulfur atoms of individual dithiolenes are separated by the distances S1-S2 = 3.2032 and S3-S4 = 3.1837 Å. The other two sides of the square base are slightly longer: S2-S3 = 3.2548 and S1-S4 = 2.2331 Å. The angles of the square base are S2-S1-S4 = 89.867, S1-S2-S3 = 89.775, S2-S3-S4 = 89.824 and S2-S4-S3 = 90.513$^o$. The diagonal distances of the square are S1-S3 = 4.5577 and S2-S4 = 4.5459 Å. The planarity of the base is very close to the ideal so that the sum of the angles is equal to 359.979, i.e. very close to 360$^o$. However the angular deviation that each corner sulfur atom

has from the plane constituted by the other three sulfur atoms are S1 = 1.083, S2 = 1.083, S3

= 1.100 and S4 = 1.093. The distance each sulfur corner has to the apex oxygen atoms are:

S1-O1 = 3.2869, S2-O1 = 3.3235, S3-O1 = 3.3641 and S4-O1 = 3.3641 Å.
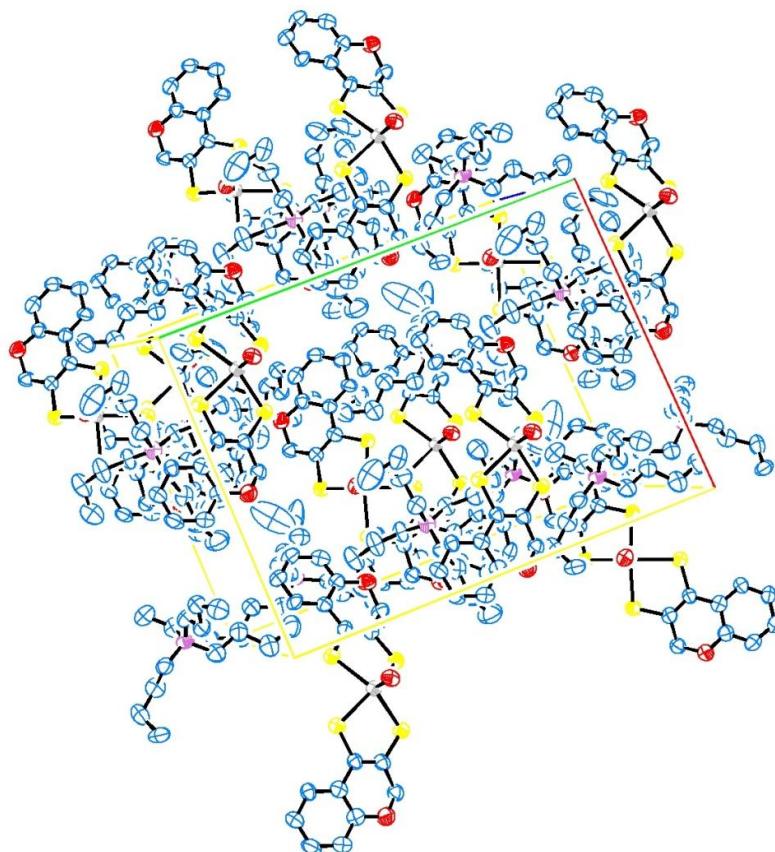


**Fig. 12. Packing of compound 6 molecules in monoclinic Cc space group**
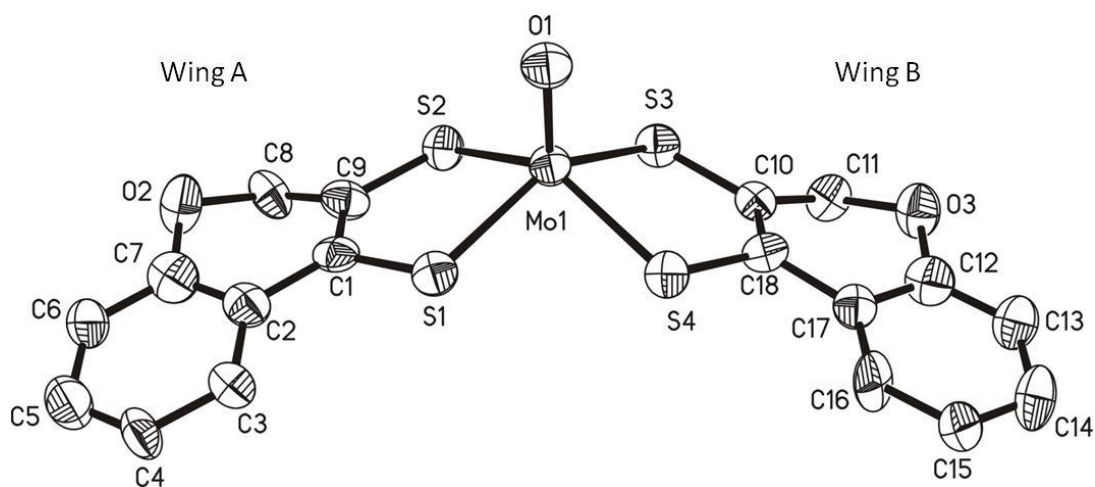


**Fig. 13. Molecular structure of [MoO(cdt)$_2$]$^{2-}$**
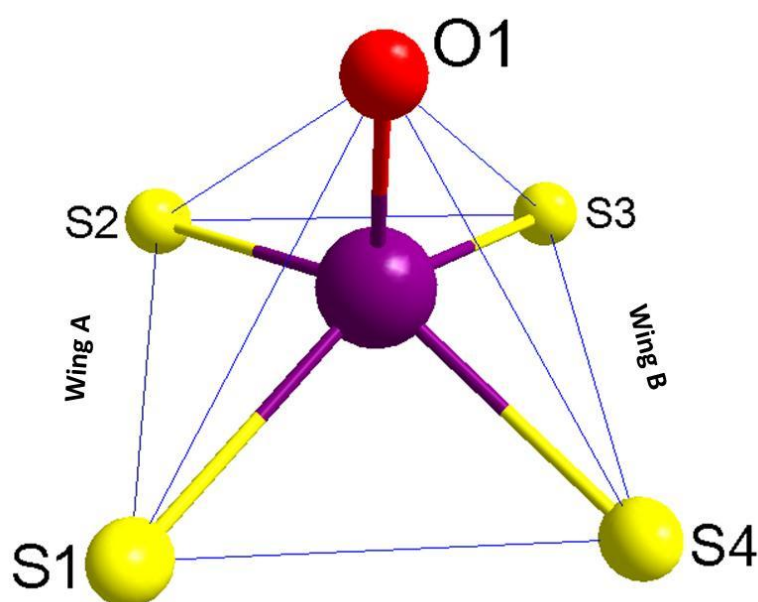
**Fig. 14. Square pyramidal geometry around the molybdenum atom in compound 6**

With respect to the chemical structure of compound **6** based on the crystallographic perspective, it can be seen from figure 13 that the chromandithiolene (cdt) ligands are arranged *cis* to each other. The sulfur-sulfur distances in both dithiolene ligands have been increased compared with the ligand precursor compound **3**. These distances in the case of compound **6** are S1-S2 = 3.2032 Å (wing A) and S3-S4 = 3.1837 Å (wing B) whereas the corresponding value S1-S2 in the case of compound **3** is shorter with 2.9590 Å. This accounts for an average increase of 0.2345 Å in the sulfur-sulfur distance on the formation of the complex.  As in the case of compound **3**, the pyrane oxygen atoms in the complex **6** also have moved away from the plane of the benzene ring. In wing B, the C12-C17-C13-O3 torsion angle is 2.543$^{o}$. The difference is almost negligible compared to the corresponding value of 2.495$^{o}$ in case of compound **3**. But this is different in the wing A dithiolene ligand of compound **6**: the C7-C6-C2-O2 torsion angle is 0.658$^{o}$, the ideal being 0$^{o}$. The angle between the bonds at both sides of the pyrane oxygen atoms are, C7-O2-C8 = 115.321$^{o}$ in wing A and C11-O3-C12 = 115.757$^{o}$ in wing B against the corresponding value of 116.914$^{o}$ in compound

**3**. The tetrahedral angles at C8 and C11 are slightly less ideal than in case of the ligand precursor compound **3**; the values are O2-C8-C9 = 111.287$^o$ and O3-C11-C10 = 111.408$^o$ against the corresponding value of 111.013 in compound **3**. The bonds that the sulfur atoms make with the double bonded carbon atoms are C1-S1 = 1.7901, C9-S2 = 1.7492, C10-S3= 1.7447 and C18-S4 = 1.7622 Å long with an average value of 1.7616 Å, the corresponding average value being 1.7375 in compound **3.** The increase in S-C bond length upon complexation is due to the higher degree of electron sharing between sulfur and molybdenum than between sulfur and carbon. The C=C double bond distances in the dithiolene part of compound **6** are C10-C18 = 1.3246 and C1-C9 = 1.3334 Å. The corresponding distance in compound **3** is C1-C3 = 1.3380 Å which is very close to the ideal C=C distance 1.34 Å. The decrease in C=C bond lengths in the complex is unexpected.

In the compound **3**, the 1,3-dithiole heterocyclic ring is more or less planar. The most important deviation to this in complex **6** is that the S-C=C-S plane has been folded to some angle from the S-Mo-S plane. This angle is defined as the folding angle, **α** (figure 15). As mentioned previously, the dithiolene groups are not ideally planar but show a slight deviation from planarity defined by the torsion angles of the atoms in the order C9-S2-S1-C1 = 1.334$^o$ in wing A and C10-S3-S4-C18 = 0.603$^o$. This means that in wing A, the dithiolene group would attain planarity, if C9 and C1 move closer to each other by an angle of 0.667$^o$ and in wing B the planarity needs the mutual approach of C10 and C18 by 0.3015$^o$. This hypothetical plane is considered as the plane of dithiolene group for simplicity for calculating the folding angle. This can be simply done by calculating the average value of the torsion angles C10-S3-S4-Mo1 (= 169.599) and C18-S3-S4-Mo1 (= 168.997) which is equal to 169.298$^o$ in wing B. This corresponds to the value **β** in figure 15. Therefore the folding angle in wing B is 180-168.997 = 11.003$^o$. A similar calculation by considering the torsion angles

C1-S1-S2-Mo1 (= 168.757) and C9-S1-S2-Mo1 (= 167.423) in wing A gives the value of the folding angle equal to 11.91$^\circ$. The selected bond lengths, bond angles and other crystallographic information are summarized in table 3.
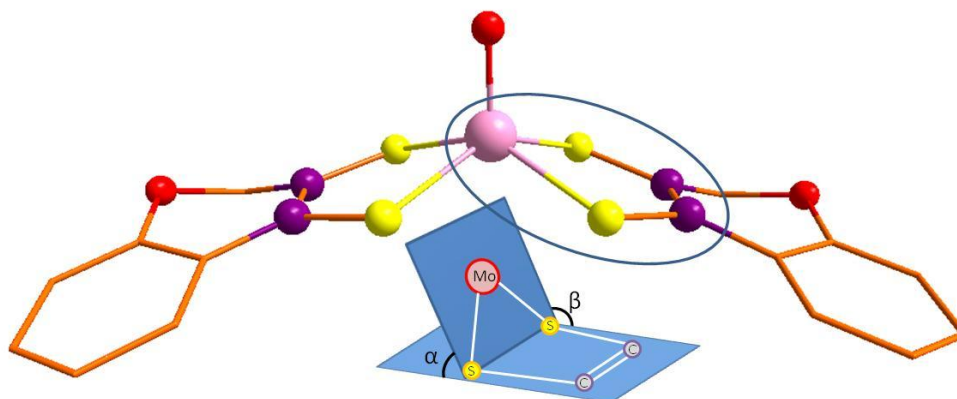


**Fig.15. Folding angle of compound 6**

**Table 3. Selected structural parameters in compound 6**

| Bond lengths (Å) | | Bond angles ($^\circ$) | | Torsion angles ($^\circ$) | |
|---|---|---|---|---|---|
| Mo1-S1 | 2.3843(22) | C7-O2-C8 | 115.321(721) | C12-C17-C13-O3 | 2.543(818) |
| Mo1-S2 | 2.3990(22) | C11-O3-C12 | 115.757(706) | C7-C6-C2-O2 | 0.658(891) |
| Mo1-S3 | 2.3986(24) | O2-C8-C9 | 111.287(746) | C9-S2-S1-C1 | 1.334(441) |
| Mo1-S4 | 2.3916(24) | O3-C11-C10 | 111.408(741) | C10-S3-S4-C18 | 0.603(467) |
| C1-C9 | 1.3334(114) | Mo1-S1-C1 | 105.721(283) | C10-S3-S4-Mo1 | 169.599(335) |
| C10-C18 | 1.3246(125) | Mo1-S2-C9 | 104.747(286) | C18-S3-S4-Mo1 | 168.997(358) |
| Mo1-O1 | 1.6971(50) | Mo1-S3-C10 | 105.437(286) | C1-S1-S2-Mo1 | 168.757(325) |
| C1-S1 | 1.7901(79) | Mo1-S4-C18 | 105.902(288) | C9-S1-S2-Mo1 | 167.423(334) |
| C9-C2 | 1.7492(87) | | | | |
| C10-S3 | 1.7447(87) | | | | |
| C18-S4 | 1.7622(99) | | | | |

Because crystallization attempts for compound **6** failed repeatedly as mentioned earlier it was decided to get structural information of the first coordination shell by X-ray absorption methods. For simulations, the *trans*-molecule was used as this isomer was assumed to be energetically favored (figure 16). The presence of a conjoint plane of the two benzopyran rings was supported by the simulation. All transitions were covered and only the inevitable early decay of the simulation amplitude due to FEFFs inability to consider inelastic losses was noticeable. In the XANES simulations it was found that a fit with 60% *trans* and 40% *cis* isomers of compound **6** shows a better agreement with the experimental spectrum than using only the *trans* isomer and a far better fit than with the *cis* alone. Though this method is not a 100% reliable it really shows that a mixture of *cis* and *trans* are forming in the synthesis of compound **6** and this is the reason for the difficulties in growing suitable crystals. Table 4 provides the bond distances and angles obtained from EXAFS and single crystal X-ray diffraction for compound **6** and its enzyme paragon arsenite oxidase. The data shows that the results obtained from both methods are almost identical. The Mo=O and Mo-S bond lengths of compound **6** taken from EXAFS experiment, though show a better agreement with the corresponding values for AO.

**Table 4. Selected metric parameters in compound 6 and AO**

| Bond length/angle | Compound 6 | | Arsenite oxidase | |
|---|---|---|---|---|
| | XRD | EXAFS | XRD | EXAFS |
| Mo=O (Å) | 1.70 | 1.71 | 1.61 | 1.73 |
| Mo-S (Å) | 2.39 | 2.38 | 2.36 | 2.36 |
| O=Mo-S ($^{o}$) | 108.02 | 110.0 | | |
| S-Mo-S$_{interligand}$ ($^{o}$) | 85.33 | 85.0 | | |
| S-Mo-S$_{intraligand}$ ($^{o}$) | 83.69 | 83.0 | | |
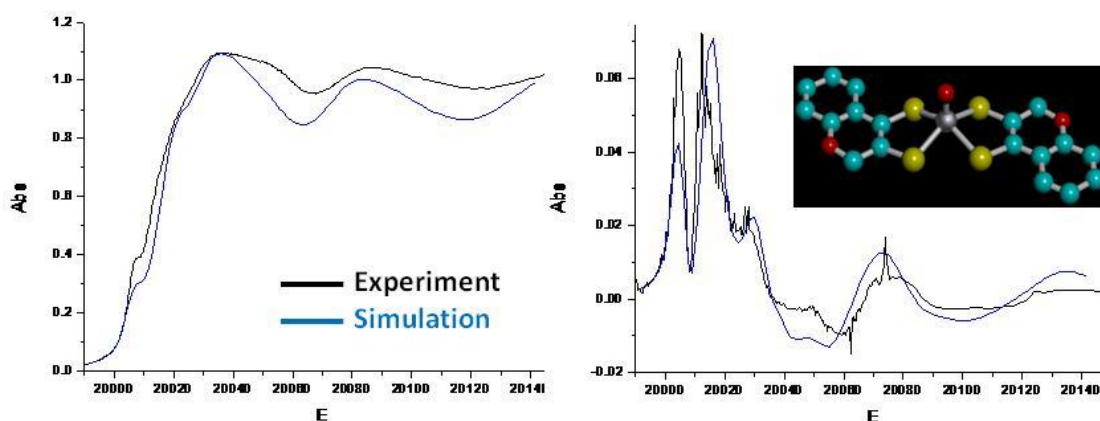
**Fig. 16. The experimental and simulated X-ray absorption spectra (XANES and EXAFS range; (left) and $k^3$ weighted FT-EXAFS spectra with the model structure used (right)**

# References

[1]   Bruce, A.; Corbin, J. L.; Dahlstrom, P. L.; Hyde, R.; Minelli, M.; Stiefel, E. I.; Spence, J. T.; Zubieta, J. *Inorg. Chem.* 21 (1982) 917

[2]   Liebeskind, L. S.; Sharpless, B. K.; Wilson, R. D.; Albers, J. *J. Am. Chem. Soc. 100* (1978) 7061

[3]   Marabella, C. P.; Enemark, J. H.; Newton, W. E.; McDonald, J. W. *Inorg. Chem. 21* (1982) 623

[4]   Bristow, S.; Enemark, J. H.; Garner, C. D.; Minelli, M.; Morris, G. A.; Ortega, R. B. *Inorg. Chem. 24* (1985) 4070

[5]   Mondal, J. U.; Schultz, F. A.; Brennan, T. D.; Scheidt, W. R. *Inorg. Chem. 27* (1988) 3950

[6]   Jalal, L. S.; Mondal, U.; Uhrhammer, D.; Schultz, F. A. *Inorg. Chim. Acta* 278 (1998) 1

[7]   Jalal, L. S.; Mondal, U.; Zamora, J. G.; Kinon, M. D.; Schultz, F. A. *Inorg. Chim. Acta* 309 (2000) 147

[8]   Jalal, L. S.; Mondal, U.; Zamora, J. G.; Siew, S.-C.; Garcia, G.T.; George, E. R.; Kinon M. D.; Schultz, F. A. *Inorg. Chim. Acta* 321 (2001) 83

[9]     Głowiak, T.; Jerzykiewicz, L.; Sobczak, J. M.; Ziółkowski, J. *Inorg. Chim. Acta* 356 (2003) 387

[10]    Jalal, L. S.; Mondal, U.; Almaraz, E.; Bhat, N. G. *Inorg. Chem. Commun.*  7 (2004) 1195

[11]    Hanna, T. A.; Ghosh, A. K.; Ibarra, C.; Zakharov, L. N.; Rheingold, A. L.; Watson, W. H. *Inorg. Chem. 43* (2004) 7567

[12]    Boyd, I. W.; Dance, I. G.; Landers, A. E.; Wedd, A. G. *Inorg. Chem. 18* (1979) 1875

[13]    McNaughton, R. L.; Tipton, A. A.; Rubie, N. D.; Conry, R. R.; Kirk, M. L. *Inorg. Chem.* 39 (2000) 5697

[14]    McMaster, J.; Carducci, M. D.; Yang, Y. -S.; Solomon, E. I.; Enemark, J. H. *Inorg. Chem.* 40 *(2001*) 687

[15]    Bradbury, J. R.; Wedd, A. G.; Bond, A. M. *Chem. Commun.* (1979) 1022

[16]    Wang, X. -B.; Inscore, F .E.; Yang, X.; Cooney, J. J. A.; Enemark, J. H.; Wang, L. -S. *J. Am. Chem. Soc.* 124 (2002) 10182

[17]    Davie, S. R.; Rubie, N. D.; Hammes, B. S.; Carrano, C. J.; Kirk, M. L., Basu, P. *Inorg. Chem.* 40 (2001) 2632

[18]    Nemykin, V. N.; Davie, S. R.; Mondal, S.; Rubie, N.; Kirk, M. L.; Somogyi, A.; Basu, P. *J. Am. Chem. Soc.* 124 (2002) 756

[19]    Boyde, S.; Ellis, S. R.; Garner, C. D.; Clegg, W. *Chem. Commun.* (1986) 1541

[20]    Davies, E. S.; Beddoes, R. L.; Collison, D.; Dinsmore, A.; Docrat, A.; Joule, J. A.; Wilson, C. R.; Garner, C. D. *Dalton Trans.* (1997) 3985

[21]    Oku, H.; Ueyama, N.; Kondo, M.; Nakamura, A. *Inorg. Chem.* 33 (1994) 209

[22]    Ansari, M. A.; Chandrasekaran, J.; Sarkar, S. *Inorg. Chim. Acta* I33 (1987) 133

[23]    Coucouvanis, D.; Hadjikyriacou, A.; Toupadakis, A.; Koo, S. -M.; Ileperuma, O.; Draganjac, M.; Salifoglou, A. *Inorg. Chem. 30* (1991) 754

[24]  Oku, H.; Ueyama, N.; Nakamura, A. *Inorg. Chem. 36* (1997) 1504

[25]  Matsubayashi, G.; Nojo, T.; Tanaka, T. *Inorg. Chim.* Acta 54 (1988) 133

[26]  McCleverty, J. A.; Locke, J.; Ratcliff, B.; Wharton, E. J. *Inorg. Chim. Acta* 3 (1969) 283

[27]  Das, S. K.; Chaudhury, P. K.; Biswas, D.; Sarkar, S. *J. Am. Chem. Soc. 116* (1994) 9061

[28]  Donahue, J. P.; Goldsmith, C. R.; Nadiminti, U.; Holm, R. H. *J. Am. Chem. Soc. 120* (1998) 12869

[29]  Enemark, J. H.; Cooney, J. J. A.; Wang, J. J.; Holm, R. H. *Chem. Rev.* 104 (2004) 1175

[30]  Schulzke, C. *Dalton Trans*. (2005) 713

[31]  Sugimoto, H.; Harihara, M.; Shiro, M.; Sugimoto, K.; Tanaka, K.; Miyake, H.; Tsukube, H. *Inorg. Chem.* 44 (2005) 6386

[32]  Chen, G. J. -J.; McDonald, J. W.; Newton, W. E. Inorg. Chim. Acta 9 (1976) L67

[33]  Cervilla, A.; Llopis, E.; Ribera, A.; Domenech, A.; Sinn, E. *Dalton Trans.* (1994) 3511

[34]  Yu, S. -B.; Holm, R. H. Inorg. Chem. 28 (1989) 4385

[35]  Ueyama, N.; Oku, H.; Nakamura, A. *J. Chem. Am. Soc.* 114 *(*1992) 7310

[36]  Das, S. K.; Biswas, D.; Maiti R.; Sarkar, S. *J. Chem. Am. Soc.* 118 *(*1996) 1387

[37]  Sarkar, S.; Das, S. K. *Proc. Ind. Ac. Sci. Chem. Sci.* 104 (1992) 533

[38]  Lim, B. S.; Sung, K. -M.; Holm, R. H. *J. Am. Chem. Soc.* 122 (2000*)* 7410

[39]  Sugimoto, H.; Sugimoto, K. *Inorg. Chem. Commun.* 11 (2008) 77

[40]  Lorber, C.; Donahue, J. P.; Goddard, C. A.; Nordlander, E.; Holm, R. H. *J. Am. Chem. Soc*. 120 (1998) 8102

[41]  Lim, B. S.; Donahue, J. P.; Holm, R. H. *Inorg. Chem. 39* (2000) 263

[42]  Lim, B. S.; Holm, R. H. *J. Am. Chem. Soc.* 123 (2001) 1920

[43]  Wang, J. J.; Tessier, C.; Holm, R. H. *Inorg. Chem. 45* (2006*)* 2979

[44]  Groysman, S.; Holm, R. H. *Inorg. Chem.* 46 (2007) 4090

[45] Enemark, J. H.; Garner, C. D. *J .Bio. Inorg. Chem.* 2 (1997*)* 817

[46] Collison, D.; Garner, C. D.; Joule, J. A. *Chem. Soc. Rev.* 25 (1996) 25

[47] Bertero, M. G.; Rothery, R. A.; Palak, M.; Hou, C.; Lim, D.; Blasco, F.; Weiner, J. H.; Strynadka, N. C. J. *Nature Struct. Biol.* 10 (2003) 681

[48] Sheldrick, G. M. Acta Crystallogr., Sect. A: Found. Crystallogr. 64 (2008) 112

[49] Smith, J. P.; Purcell, W.; Roodt, A.; Leipoldt, J. G. *Polyhedron*, 12 (1993) 2271

[50] Davis, E. S.; Beddoes, R. L.; Collison, D.; Dinsmore, A.; Docrat, A.; Joule, J. A.; Wilson, C. R.; Garner, C. D. *J. Chem. Soc. Dalton Trans*. (1997) 3985

[51] Goddard, C. A.; Holm, R. H. *Inorg. Chem*. 38 (1999) 5389

[52] Davis, E. S.; Aston, G. M.; Beddoes, R. L.; Collison, D.; Dinsmore, A.; Docrat, A.; Joule, J. A.; Wilson, C. R.; Garner, C. D. *J. Chem. Soc. Dalton Trans.* (1998) 3647

[53] Ellis, P. J.; Conrads, T.; Hille, R.; Kuhn, P. *Structure*, 9 (2001) 125

[54] Conrads, T.; Hemann, C.; George, G. N.; Pickering, I. J.; Prince, R.C.; Hill, R. *J. Am. Chem. Soc.* 124 (2002) 11276

[55] Moore, F. W.; Larson, M. L. *Inorg. Chem*. 6 (1967) 998.

[56] Dowerah, D.; Spence, J. T.; Singh, R.; Wedd, A. G.; Wilson, G. L.; Farchione, F.; Enemark, J. H.; Kristofzski, J.; Bruck, M. *J. Am. Chem. Soc*. 109 (1987) 5655

[57] Berg, J. M.; Holm, R. H. *J. Am. Chem. Soc*. 107 (1985) 917

# ELECTROCHEMISTRY AND OXOTRANSFER ABILITY OF [MO(cdt)₂]²⁻ (M = Mo, W) COMPLEXES

## 3.1. Model oxotransfer catalysis by Mo and W complexes

Chapter 1.2 described in brief the ability of the Mo and W enzymes to catalyze oxygen atom transfer (OAT) reactions in nature. Even prior to the elucidation of the active site structures of MPT bearing enzymes, the oxotransfer catalytic ability of molybdenum and tungsten complexes was thoroughly studied by inorganic chemists.[1] Oxygen atom transfer reactions by molybdenum or tungsten are facilitated by a change of the metal's oxidation state between +IV and +VI. One of the most extensively studied redox couples is $Mo^{IV}O/Mo^{VI}O_2$ as a 'natural choice' due to the high frequency of occurrence of these groups in conventional molybdenum chemistry.[2] A Large number of reactions involving this redox couple have been reported and most of them were originally proposed as relevant for the reactions catalyzed by the DMSO reductase family of enzymes. A widely cited example is the

compound MoO$_2$(*t*-BuL-NS)$_2$ (figure 1) (where *t*-BuL-NS = bis(4-tert-butylphenyl)- 2-pyridylmethanethiolate) prepared by the Holm Group at Harvard, the oxotransfer catalytic ability of which according to equation 1 was extensively studied with a wide variety of substrates.[3,4]
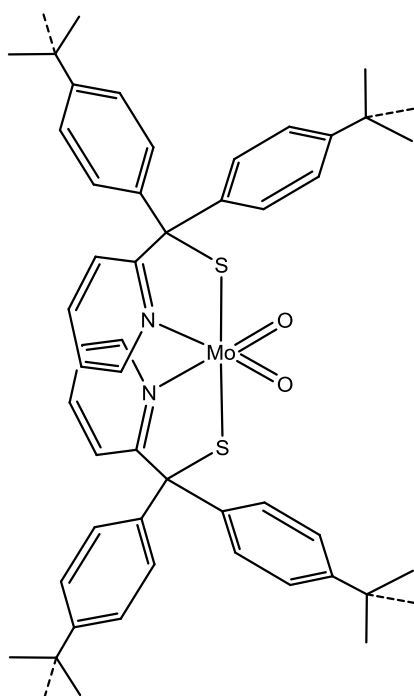


**Figure 16. Chemical structure of MoO$_2$(*t*-BuL-NS)$_2$**

MoO$_2$(*t*-BuL-NS)$_2$ + X $\leftrightarrows$ MoO(*t*-BuL-NS)$_2$ + XO .......................................................(1)
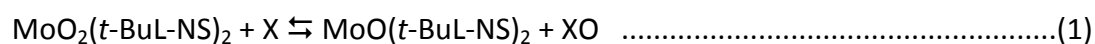
The mechanism of oxotransfer reactions in enzymes as well as in inorganic model complexes had been a challenging area of research for chemists and biologists. However, new insights into the active site structures of oxotransferases continue to demand the timely revision of existing ideas. Holm and co-workers investigated the mechanism of OAT using the isolated enzyme *R. sphaeroides* DMSO reductase as catalyst in the model oxotransfer reaction between Me$_2$S$^{18}$O (labeled oxygen donor) and 1,3,5-Triaza-7-phosphatricyclo[3.3.1.1$^{3,7}$]decane (PTA) (oxo acceptor) by absorption spectroscopy and CI mass spectrometry.[5] In the single turnover experiments anaerobic treatment of DMSO

reductase with a large excess of the oxygen acceptor PTA resulted in replacement of the observed broad band in the UV-Vis spectrum at 720 nm by a less intense broad band at 640 nm over ca. 4 h corresponding to reaction 2. Further addition of $Me_2SO$ oxidizes the already reduced enzyme regenerating the 720 nm signal in the UV-Vis spectrum. Interestingly, in the reaction between $Me_2S^{18}O$ and PTA in the presence of the reduced enzyme, $^{18}O$ isotope transfer from $Me_2SO$ to PTA was detected. Since there was no reaction in the absence of enzyme, it was concluded that the enzyme was a necessary mediator of the oxo transfer from $Me_2SO$ to PTA according the mechanism shown in figure 2.[2]

$$\text{Enz Mo}^{VI}\text{O} + \text{PTA} \rightarrow \text{Enz Mo}^{IV} + \text{PTAO} \quad \dots\dots\dots\dots\dots\dots\dots\dots\dots\dots\dots\dots\dots\dots\dots\dots\dots\dots\dots \quad (2)$$
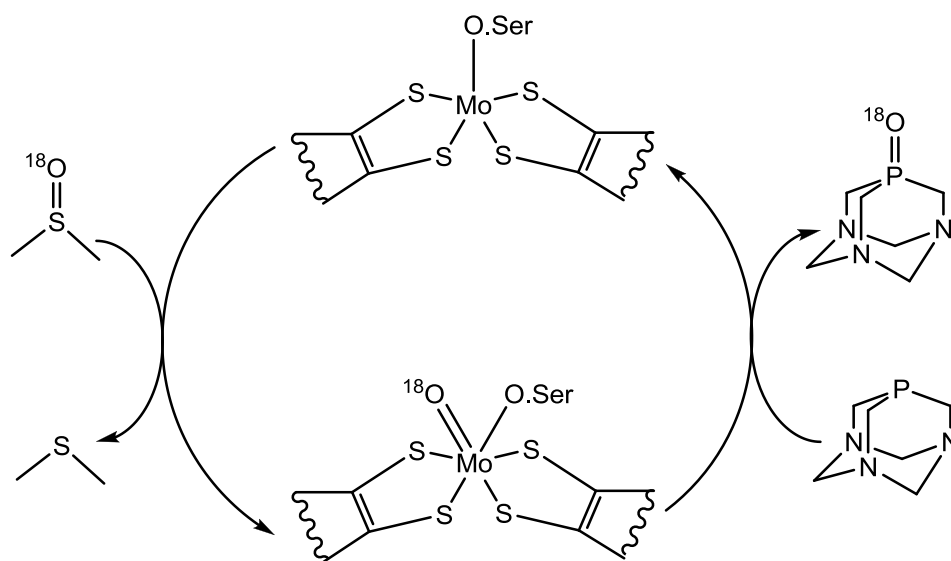


**Fig. 2. Oxotransfer reaction between labeled DMSO and PTA mediated by *R. sphaeroides* DMSO reductase**

The molybdenum mediated oxotransfer catalytic reactions have been well documented throughout the literature even before the importance of dithiolene complexes of $Mo^{IV}O/Mo^{VI}O_2$ in biology was underlined by Rajagoplan's work and subsequent structural

elucidations of enzymes using X-ray crystallography (details in chapter 1.3). $Mo^{IV}O(dithiolene)_2$ type complexes can be oxidized to the corresponding $Mo^{VI}O_2(dithiolene)_2$ complexes upon reaction with strong oxidizing agents as $Me_3NO$ according to equation 3.[6] The reverse transformation follows the reaction 4 and has been reported in the case of $[Mo^{VI}O_2(mnt)_2]^{2-}$ using oxo acceptors as $Et_3P$, $PhEt_2P$, $Ph_2EtP$ and $PPh_3$.

$$Mo^{IV}O(dt)_2]^{2-} + Me_3NO \rightarrow [Mo^{VI}O_2(dt)_2]^{2-} + Me_3N \ldots\ldots\ldots\ldots\ldots\ldots\ldots\ldots\ldots\ldots\ldots\ldots.(3)$$

$$[Mo^{VI}O_2(dt)_2]^{2-} + R_3P \rightarrow [Mo^{IV}O(dt)_2]^{2-} + R_3PO \ldots\ldots\ldots\ldots\ldots\ldots\ldots\ldots\ldots\ldots\ldots\ldots(4)$$
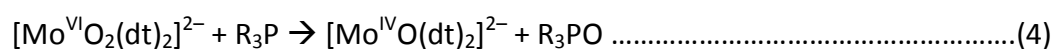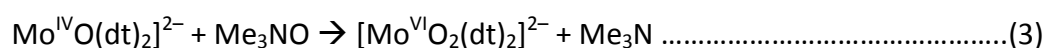
These forward and reverse transformations of molybdenum dithiolene complexes project them as highly viable candidates for oxotransfer catalysis. However, it is well known that the formation of dimeric μ-oxo $Mo^V$ species from the comproportionation of oxidized and reduced species according to reaction 5 often prevents $Mo^{IV}O$ complexes from being effective OAT catalysts.[7,8]

$$Mo^{IV}O + Mo^{VI}O_2 \rightarrow Mo^V_2O_3 \ldots\ldots\ldots\ldots\ldots\ldots\ldots\ldots\ldots\ldots\ldots\ldots\ldots\ldots\ldots\ldots\ldots\ldots\ldots (5)$$

Different approaches have been made to synthesize complexes which will prevent dimerization and thereby act as efficient oxotransfer catalysts. In such an attempt Holm et al. synthesized molybdenum complexes with sterically bulky ligands preventing direct contact between the two metal centers at both ends of a single catalytic turnover.[9,10] The details of this reaction are provided in the next chapter as part of the discussion of model studies of the SO and XO family of enzymes (chapter 4.3). The second strategy is based on reported μ-oxo $Mo^V_2$ complexes showing a *cis*-configuration between terminal and μ-oxo ligands.[11,12] This suggests a possible formation of the dimer by attack of one of the oxo ligands of the $Mo^{VI}O_2$ species to the vacant *trans* position of the $Mo^{IV}O$ species with a

subsequent *trans-cis* rearrangement between the dithiolene and oxo ligands. Nakamura and coworkers studied this property in detail and put forward the idea of prevention of deactivation due to dimerization by an electronic control of the ligands.[6,13,14] For example benzenedithiolene $Mo^{IV}O$ complexes react with $Me_3NO$ to afford the corresponding $Mo^{VI}O_2$ species but do not lead to μ-oxo $Mo^V_2$. This reflects the difficulty of ligand dissociation from the metal caused by the strongly chelating character of this ligand. At the same time the reaction between $(NEt_4)_2[Mo^{IV}O(bdt)_2]$ and $(NEt_4)_2[Mo^{VI}O_2(S_2CNEt_2)_2]$ ($S_2CNEt_2$ = N,N-diethyldithiocarbamato) in acetonitrile proceeds in an interesting and unanticipated way. The only products obtained were $(NEt_4)[Mo^VO(bdt)_2]$ and $[(Mo^VO)_2(μ-O)(S_2CNEt_2)_2]$ while the expected mixed μ-oxo $Mo^V$ species with both ligand types was not detected. This indicates that the stronger binding of the bdt ligand compared to the $S_2CNEt_2$ ligand prevents any isomerization and comproportionation reaction. These results suggest that the reactivity of the $Mo^{IV}O$ or $Mo^{VI}O_2$ species can be controlled not only sterically but also electronically by using strongly chelating dithiolene ligands in order to inhibit the formation of the (μ-oxo)-dimolybdenum(V) center.

In the early days of developing molybdenum mediated oxygen atom transfer catalysis, the $Mo^{IV}O/Mo^{VI}O_2$ couple was considered as relevant for the DMSO reductase family of enzymes. However, the solution of an increasing number of enzymatic active site structures led to the necessity to utilize the chemically much more elusive $Mo^{IV}/Mo^{VI}O$ redox couple for OAT reactions relating to the DMSOR family. A similar chemistry has been established in the case of tungsten too. The relevance of $Mo^{IV}/Mo^{VI}O$ dithiolene complexes has already been explained in chapters 2.1 and 2.2 and the discussion will be continued in chapter 5.3. The oxotransfer ability of desoxo molybdenum complexes was proven in the

reaction of $[Mo^{IV}(OPh)(S_2C_2Me_2)_2]^-$ with oxygen donor compounds XO (X = Me$_3$N, Me$_2$S) to give $[Mo^{VI}O(OPh)(S_2C_2Me_2)_2]^-$ according to reaction 6.[15]

$$[Mo^{IV}(OPh)(S_2C_2Me_2)_2]^- + XO \rightarrow [Mo^{VI}O(OPh)(S_2C_2Me_2)_2]^- + X \text{ ............................... (6)}$$

The reaction system in equation 6 is considered to be the first relevant functional model system for oxygen atom transfer with respect to the DMSO reductase family of enzymes. However, the oxidized species $[Mo^{VI}O(OPh)(S_2C_2Me_2)_2]^-$ is too unstable to be isolated and decays by an internal redox process to a $Mo^V O$ product, liberating an equimolar amount of phenol as per reaction 7.

$$[Mo^{VI}O(OPh)(S_2C_2Me_2)_2]^- \rightarrow [Mo^V O(S_2C_2Me_2)_2]^- + PhO^{\bullet} \text{ ..........................................(7)}$$

As discussed in chapter 1.4. the enzyme arsenite oxidase is considered by Hille as a member of the DMSO reductase family even if it possesses a slightly different core. AO utilizes the widely investigated $Mo^{IV}O/Mo^{VI}O_2$ couple and the literature attributes those reactions also as relevant for DMSOR. The first example of a model complex for arsenite oxidase which participated in both OAT and PCET (proton coupled electron transfer) reactions was reported by the Sugimoto group.[16] The respective $Mo^{IV}O/Mo^{VI}O_2$ redox couple was shown to be able to participate in both OAT and PCET reactions. The $(Bu_4N)_2[Mo^{IV}O(bdtCl_2)_2]$ complex ($bdtCl_2$ = 3,6-dichloro-1,2-benzenedithiolate) is converted to $(Bu_4N)_2[Mo^{VI}O_2(bdtCl_2)_2]$ in aqueous media by a PCET process: $(Bu_4N)_2[Mo^{IV}O(bdtCl_2)_2]$ undergoes chemical oxidation by two equivalents of $K_3[Fe(CN)_6]$ in the presence of two equivalents of $^tBuOK$ in $CH_3CN/H_2O$ (5:7) yielding $(Bu_4N)_2[MoO_2(bdtCl_2)_2]$. When 98% $H_2^{18}O$ was used instead of $H_2O$, the product obtained was $(Bu_4N)_2[Mo^{VI}O^{18}O(bdtCl_2)_2]$ proving water to be the source of oxygen. In the second step $(Bu_4N)_2[MoO_2(bdtCl_2)_2]$ transfers this

oxygen atom to arsenite forming arsenate and regenerating the mono oxo species $(Bu_4N)_2[Mo^{IV}O(bdtCl_2)_2]$. The entire mechanism of the reaction is depicted in figure 3.
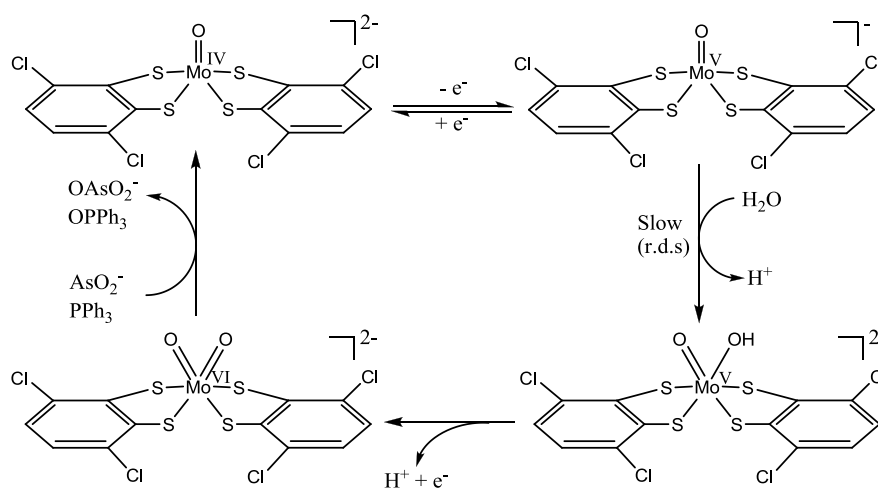


**Figure 3. Proposed catalytic cycle involving the $Mo^{IV}O/Mo^{VI}O_2$ redox couple, participating in both PCET and OAT steps**

A reaction cycle between desoxo $Mo^{IV}$ and $Mo^{VI}O$ centers including both PCET and OAT relevant to the enzymes in the DMSOR family is provided in figure 4.[17] One electron oxidation of $LMo^{V}O(p\text{-}OC_6H_4\text{–}OC_2H_5)_2$ by $(NH_4)_2Ce(NO_3)_6$ leads to the formation of the corresponding mono oxo $Mo^{VI}$ species $[LMo^{VI}O(p\text{-}OC_6H_4\text{–}OC_2H_5)_2]^+$ with $L^- =$ hydrotris(3,5-dimethyl-1-pyrazolyl)borate. Acetonitrile solutions of cationic $[LMo^{VI}O(p\text{-}OC_6H_4\text{–}OC_2H_5)_2]^+$ undergo OAT to yield the cationic desoxo species $[LMo^{IV}(p\text{-}OC_6H_4\text{–}OC_2H_5)_2]^+$ and $OPPh_3$ when treated with $PPh_3$. In presence of water and the oxidizing agent 2,3-dicyano-5,6-dichloro-1,4-benzoquinone (DDQ) the desoxo species is transformed back into the $LMo^{V}O(p\text{-}OC_6H_4\text{–}OC_2H_5)_2$ complex completing the catalytic cycle. When $H_2^{18}O$ was used in the final step $LMo^{V}(^{18}O)(p\text{-}OC_6H_4\text{–}OC_2H_5)_2$ was formed confirming that water acts as the source of oxygen in the entire catalysis.

$$\text{LMo}^{\text{V}}\,{}^{18}\text{OX}_2 \xrightarrow{\text{(NH}_4)_2\text{Ce(NO}_3)_6} [\text{LMo}^{\text{VI}}\,{}^{18}\text{OX}_2]^+(\text{NO}_3)^-$$

i) $H_2{}^{18}O$
ii) DDQ

${}^{18}\text{OPPh}_3$

$PPh_3$

$$[\text{LMo}^{\text{IV}}\text{X}_2]^+(\text{NO}_3)^- \longleftarrow [\text{LMo}^{\text{IV}}({}^{18}\text{OPPh}_3)\text{X}_2]^+(\text{NO}_3)^-$$

$$X = p\text{-O-C}_6\text{H}_4\text{OC}_2\text{H}_5$$
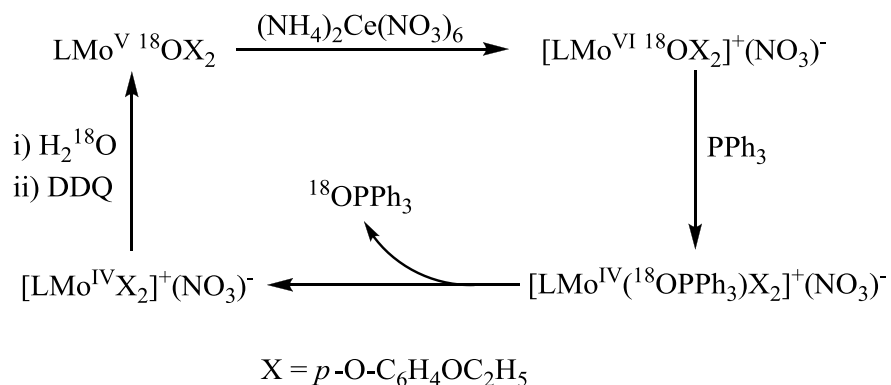
**Fig. 4. The reaction cycle combining PCET and OAT between desoxo Mo$^{\text{IV}}$ and Mo$^{\text{VI}}$O centers**

Even though oxygen atom transfer abilities of Mo$^{\text{IV}}$O/Mo$^{\text{VI}}$O$_2$ and Mo$^{\text{IV}}$/Mo$^{\text{VI}}$O are well documented, such an intensive study has not been carried out in the case of W$^{\text{IV}}$O/W$^{\text{VI}}$O$_2$ and W$^{\text{IV}}$/W$^{\text{VI}}$O redox couples. Still, there are many examples in which tungsten acts as the catalytic center for OAT reactions. For example [W$^{\text{IV}}$O(bdt)$_2$]$^{2-}$ and [W$^{\text{IV}}$O(S$_2$C$_2$Me$_2$)$_2$]$^{2-}$ complexes are readily oxidized by Me$_3$NO yielding the corresponding dioxo W$^{\text{VI}}$ species [W$^{\text{VI}}$O$_2$(bdt)$_2$]$^{2-}$ and [W$^{\text{VI}}$O$_2$(S$_2$C$_2$Me$_2$)$_2$]$^{2-}$ respectively.[18] The oxo transfer ability of tungsten complexes utilizing the W$^{\text{IV}}$/W$^{\text{VI}}$O couple was studied for [W(OSiPh$_2$$^t$Bu)(bdt)$_2$]$^{2-}$ with various substrates as Me$_3$NO, N-morpholine-N-oxide, DMSO, Ph$_3$PO, Ph$_2$SeO and Ph$_3$AsO.[19] The observed reactions were comparatively slow except in the case of Me$_3$NO and N-morpholine-N-oxide presumably due to the bulkiness of the ($^-$OSiPh$_2$$^t$Bu) ligand. As in the case of molybdenum complexes, [W$^{\text{IV}}$(OPh)(S$_2$C$_2$R$_2$)$_2$]$^{2-}$ undergoes oxo transfer with XO (Me$_3$NO, DMSO and Ph$_3$AsO) leading to the corresponding mono-oxo W$^{\text{VI}}$ species [W$^{\text{VI}}$O(OPh)(S$_2$C$_2$R$_2$)$_2$]$^{2-}$.[20-23] Interestingly, the axial ligands were found to have a profound influence on the activity of the complex due to an electronic fine tuning of the central metal. If the axial ligand is *iso*-propoxide for instance, the activity diminishes to a rate which is 200 times slower than that of the phenoxide analogue for the same substrate.

## 3.2. Functional reasons for the choice of active site metal

In chapter 1.1, the evolutionary change of the active sites of MPT bearing enzymes from tungsten to molybdenum was discussed briefly. Investigations are on the way to explore the underlying cause for this transition. Looking at the active sites of enzymes known today, it can be seen that there is a profound dependence of the selection of metal in the active site on the habitat of the organism. In general, tungsten is used only by thermophilic bacteria and archaea and hyperthermophilic archaea. Since these organisms live at high temperatures similar to that prevailed in the early earth, it can be assumed that the ancient organisms used tungsten which was then replaced by molybdenum in the course of the slow cooling of earth's crust. Two reasons have been attributed to this evolutionary change: supply of metal and functional issues. The supply related reasons have already been discussed in chapter 1.1 and the functionality related reasons will be briefed here.[24] There are two important factors governing functional advantages at the active sites of the enzymes: kinetics and thermodynamics. Considering the kinetic factors, molybdenum is presumed to be a better oxidant and tungsten a better reductant.  Since a catalytic cycle is composed of oxidation and reduction half reactions, the above described kinetic properties will be advantageous for both metals in either of the half reactions. Still, the oxidizing power of molybdenum is assumed to be too large at high temperatures and that can be one reason why molybdenum is not used at high temperature habitats. However this argument cannot be related to the evolutionary change from tungsten to molybdenum during the cooling of habitats over the centuries, but thermodynamic factors seem to play a key role. Redox potentials of molybdenum and tungsten which are obviously distinct should be regarded as one of the main deciding factors between the choices of metals in different habitats. In

other words the redox potential of the metal center is assumed to be complimentary to the requirements of the organisms in a given set of conditions provided by the habitats. Interestingly, studies from our laboratory show that the redox potential of tungsten is more temperature sensitive than that of molybdenum.[24] Based on this observation it has been proposed that there was an evolutionary advantage for molybdenum over tungsten because of its more stable redox potential in changing temperature conditions. In addition to the higher temperature sensitivity of its redox potential and directly related to this, tungsten has a larger entropy change for redox processes than molybdenum. A larger entropy change is indicative of a more severe geometric change upon oxidation or reduction. This potentially increases the protein's reorganization energies needed. Besides this a more rigid geometry around molybdenum may also keep the active site in a state which might be closer to an entatic state adapted for function. In short, in addition to the bioavailability, functional reasons like kinetic preferences, redox potential, entropy of redox processes and associated geometrical changes render the use of molybdenum preferentially in organisms to which it is available and drove the evolutionary change away from tungsten. From this point of view, temperature dependent electrochemistry of molybdenum and tungsten with selected variations in the ligand structure can provide useful information on the nature's fine tuning in the cofactor design.

## 3.3. Scope of the present work

The importance of incorporating the pyrane ring in the dithiolene ligands in the model complexes was described in chapter 2.3. It was proposed that the possibility of the pyrane ring opening and closing during the catalytic turn over effects a redox action in the adjacent pterin ring in MPT which is conjugated to the metal dithiolene system. Apart from

this perceptive, the present study is aimed to find out kinetic and thermodynamic effects caused by the pyrane ring adajacent to the dithiolene function. For this reason the electrochemical behavior and catalytic properties of $[MO(cdt)_2](NBu_4)_2$ {M= Mo (**1a**), W(**1b**)} have been compared with those of $[MO(tcdt)_2](NBu_4)_2$ {M= Mo (**2a**), W(**2b**)} and $[MO(tldt)_2](NBu_4)_2$ {M= Mo (**3a**), W(**3b**)}. The three pairs of compounds differ in the identity of atom X in figure 5. Cyclic voltammetry of three pairs of compounds has been carried out and the extent of *non*-innocence of each ligand system has been evaluated. In addition to this the temperature dependent electrochemistry of all six compounds has been explored to find out how sensitive the redox potential of each compound is to the change of temperature. Finally, catalytic properties of the three pairs of compounds have been compared by the model oxotransfer reaction between DMSO and PPh$_3$. Consequently the results of this study lead to certain important points regarding the natural choice of the pyrane ring in the structure of molybdopterin.



X = O; M = Mo (**1a**), W (**1b**)
X = S; M = Mo (**2a**), W (**2b**)
X = C; M =Mo (**3a**), W (**3b**)
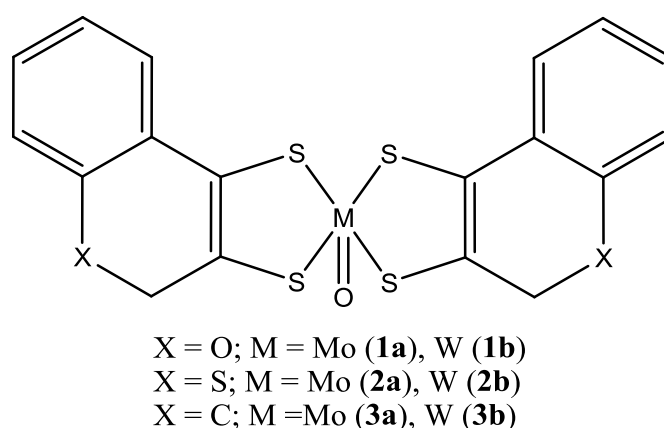
**Fig. 5. Compounds used for comparative studies**

## 3.4. Experimental

### 3.4.1. Synthesis of compounds

The syntheses of compounds **1a** and **1b** are described in chapters 2.4.7 and 2.4.8 respectively. All other compounds were prepared and analyzed by Alexander Döring in collaboration for this work and the synthetic procedures are described elsewhere.[25] Crystalline quality materials were used for the studies.

### 3.4.2. Electrochemistry

Electrochemical measurements were carried out with an AUTOLAB PGSTAT12 potentiostat/galvanostat using glassy carbon or platinum disc electrodes with a reaction surface of 1 mm$^2$ as working electrode. A platinum rod electrode (together with internal referencing *versus* ferrocene/ferrocenium) was used as reference electrode and a platinum knob electrode as auxiliary electrode. All the measured values were corrected by the platinum reference electrode's temperature dependence which was determined using a *non*-isothermal cell. All measurements were carried out inside a glove box under argon atmosphere. Tetrabutylammonium hexafluorophosphate (0.1 M; electrochemical grade from Fluka) was used as electrolyte. The size of each sample was 5 ml of a 0.01 mM to 0.10 mM solution of the respective complex. The temperature of the double walled electrochemical cell was controlled with a Julabo FP50-MV thermostat. Before each recording of the voltammogram, the sample was stirred for at least 15 min after reaching the desired temperature. The electrochemical method used was cyclic voltammetry with a scan rate of 100 mVs$^{-1}$ in all cases. Only the electronic transition between the oxidation states +4 and +5 has been considered in the present study.

### 3.4.3. Oxotransfer catalysis

All compounds were used as catalysts in the oxotransfer reaction between DMSO and PPh$_3$ according to the chemical equation 8.

$$Me_2SO + PPh_3 \rightarrow Me_2S + Ph_3PO \dots\dots\dots\dots\dots\dots\dots\dots\dots\dots\dots\dots\dots\dots (8)$$

The catalyst amount was kept equal to $2.515*10^{-3}$ mmol in all experiments (**1a** = 2.4783 mg, **1b** = 2.6993 mg, **2a** = 2.5591 mg; **2b** = 2.7801 mg; **3a** = 2.4683 mg; **3b** = 2.6894 mg). The catalyst: PPh$_3$ molar ratios were selected as 1:2.5 (PPh$_3$ = 0.0127 molL$^{-1}$), 1:5 (PPh$_3$ = 0.0253 molL$^{-1}$), 1:7.5 (PPh$_3$ = 0.0380 molL$^{-1}$) and 1:10 (PPh$_3$ = 0.0503 molL$^{-1}$). The total volume of the reaction mixture was maintained as 0.5 mL with DMSO-d$^6$. All reaction mixtures were transferred to NMR tubes with air tight screw caps and all manipulations were done using a schlenk line or dry box under nitrogen atmosphere. All NMR tubes were maintained at 60$^o$C using an electronically controlled thermostat. In order to follow the conversion of PPh$_3$ to PPh$_3$O, $^{31}$P-NMR of the reaction mixtures were measured at 81.04 MHz at specific time intervals. The integration of the NMR peaks was carried out using TOPSPIN.

## 3.5. Results and discussion

Figure 6 shows the cyclic voltammograms of compounds **1a** and **1b** recorded at 25$^o$C. The redox potentials M$^{IV}$/M$^V$ of **1a** and **1b** are -0.72 V and -0.89 V respectively. These values have been compared with those obtained for **2a**, **2b**, **3a** and **3b** [25] in table 1.

**Fig.6. Cyclic volatammograms of 1a (A) and 1b (B)**

**Table 1. Electrochemical data of compounds 1 to 3**

| Compound | M | X | $E^0_{1/2}$ vs Fc/Fc$^+$ [V] | Slop of TD graph [mV/K] | $E_{1/2}$(Mo) − $E_{1/2}$(W) [V] |
|---|---|---|---|---|---|
| <br>X = O; M = Mo (**1a**), W (**1b**)<br>X = S; M = Mo (**2a**), W (**2b**)<br>X = C; M =Mo (**3a**), W (**3b**) | Mo | O | −0.72 | −0.31 ± 0.062 | 0.17 |
| | | S | −0.87 | −0.34 ± 0.004 | 0.32 |
| | | C | −0.95 | −0.56 ± 0.033 | 0.26 |
| | W | O | −0.89 | −0.46 ± 0.045 | |
| | | S | −1.19 | −0.66 ± 0. 008 | |
| | | C | −1.21 | −0.98 ± 0.061 | |

For each ligand at 25°C the redox potentials for the molybdenum complexes are more positive than those for the tungsten complexes, but the differences between the pairs vary. The difference in the redox potentials for the molybdenum and the tungsten complexes for a specific ligand depends upon the strength of the *non*-innocent character of that ligand.[26,27] In other words, the more pronounced the *non*-innocence the smaller the difference of the redox potentials.[28] Among the three pairs of molybdenum and tungsten complexes under consideration, the one with the smallest difference (0.17 V) between the redox potentials is the pair **1a** and **1b**. This is the pair with the ligand system in which the dithiolene function is attached to the adjacent pyrane ring (with O as the heteroatom) which closely resembles the natural molybdopterin ligand. Interestingly, when oxygen is replaced by sulfur (**2a** and **2b**) its higher homologue, the *non*-innocence is apparently the smallest with the highest difference (0.32 V) between the redox potentials of both metals. Therefore it is likely that the pyrane subunit plays an important role within the natural molybdopterin with respect to the tuning of the redox properties of the enzymes' active sites.

Figure 7 shows the results of the temperature dependent (TD) electrochemical measurements for compounds **1a** and **1b**. The redox potentials $E_{1/2}$ were plotted against the temperature of the measurement and linear fits are employed to calculate their dependence. The extent of sensitivity of the redox potential to the change in temperature can be taken from the slope of the respective linear fits. The negative sign of the slope shows that with the increase in temperature, the redox potential decreases. The slope of the redox potential for **1b** (slope = −0.98 ± 0.061) is greater than that for **1a** (slope = −0.31 ± 0.062). In other words, the redox potential of the tungsten complex is more temperature sensitive than that of the molybdenum complex. These results have been compared with those obtained for compounds **2a**, **2b**, **3a** and **3b** and are summarized in table 1. The slope of

the temperature dependent redox potential graphs has the least value in the case where X is oxygen. This is true in case of both Mo and W complexes. This means that the temperature sensitivity of the redox potential is the least pronounced when the dithiolene is attached to the pyrane ring as in the case of the natural molybdopterin. Replacing the pyrane ring with the very similar thiopyrane (**2a** and **2b**) or a simple aliphatic six-membered carbon ring (**3a** and **3b**) renders the redox potential of molybdenum or tungsten to be more unstable towards temperature change. In a recent study from our laboratory [24] by investigating temperature dependent redox potentials of a number of molybdenum and tungsten complexes with a variety of dithiolene and non-dithiolene ligands, it has been shown that for each given ligand tungsten's redox potential was more unstable to the temperature change. However, the study focused on those complexes having *non*-innocent dithiolene ligands as well as other strictly inorganic complexes and no attention was paid to investigate the specific role of the pyrane ring present in the natural molybdopterin. In this respect, the comparison of the temperature dependent electrochemical behavior of the three pairs of compounds in the present study is important as it illustrates why nature decided to choose the pyrane ring adjacent to the *non*-innocent dithiolene group. From the above mentioned results it can be concluded that in addition to other functional advantages of the pyrane ring in the catalytic reactions at the molybdenum or tungsten active sites, its presence also contributes: (1) to the fine tuning of the redox potential due to the highly pronounced *non*-innocence and (2) to provide a more stable redox potential of the metal center towards temperature changes prevailing in the gradual development of the living habitats.
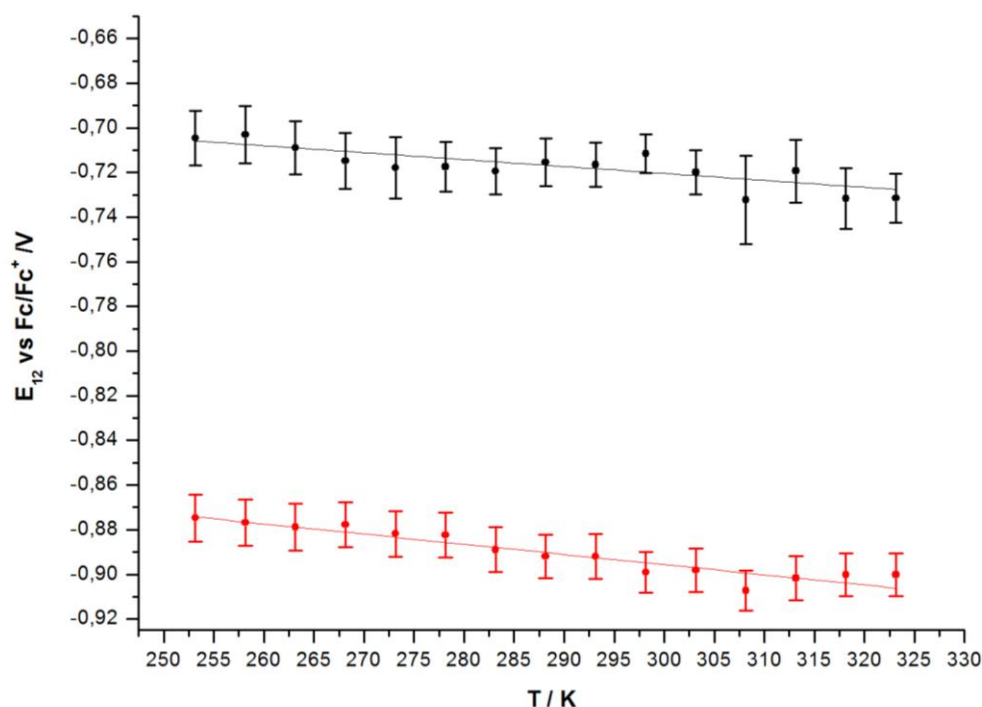
**Fig. 7. Change of redox potential ($E_{1/2}$) with temperature (T) for 1a (upper) and 1b (lower)**

Table 2 summarizes the details of reaction systems used to study the oxotransfer catalytic ability of **1a** and **1b** along with corresponding details from the study by Alexander Döring to investigate similar issues in the case of compounds **2a**, **2b**, **3a** and **3b**. Figure 8 shows the conversion profile of $PPh_3$ to $PPh_3O$ when **1a** and **1b** are used as catalyst as obtained from the integration of $^{31}P$-NMR results. It can be seen that molybdenum catalysts are better, i.e. faster than the tungsten catalyst in all cases. As expected the conversion (entirely different from the term velocity of the reaction) of $PPh_3$ to $PPh_3O$ is fastest in the case of a 1:2.5 molar ratio between the catalyst and $PPh_3$ and slowest in the case of a 1:10 molar ratio. This is because, for a given amount of catalyst, the percentage of substrate molecules colliding with the catalytic centers will be the highest when the total number of the substrate molecules is the smallest. Figure 9 shows the total amount of time needed for a 100% conversion in all of the 24 reactions using catalysts **1a** to **3b**.

**Table 2: Conditions used in the catalytic studies of compounds 1a to 3b**

| Catalyst | Amount of catalyst, mg | Amount of PPh$_3$, molL$^{-1}$ | Cat: PPh3 molar ratio | Total volume of the soln in DMSO, ml | Temperature, °C |
|---|---|---|---|---|---|
| **1a** | 2.4783 | 0.0127 | 1 : 2.5 | | |
| | | 0.0253 | 1 : 5.0 | | |
| | | 0.0380 | 1 : 7.5 | | |
| | | 0.0503 | 1 : 10.0 | | |
| **1b** | 2.6993 | 0.0127 | 1 : 2.5 | | |
| | | 0.0253 | 1 : 5.0 | | |
| | | 0.0380 | 1 : 7.5 | | |
| | | 0.0503 | 1 : 10.0 | | |
| **2a** | 2.5591 | 0.0127 | 1 : 2.5 | | |
| | | 0.0253 | 1 : 5.0 | 0.5 | 60 |
| | | 0.0380 | 1 : 7.5 | | |
| | | 0.0503 | 1 : 10.0 | | |
| **2b** | 2.7801 | 0.0127 | 1 : 2.5 | | |
| | | 0.0253 | 1 : 5.0 | | |
| | | 0.0380 | 1 : 7.5 | | |
| | | 0.0503 | 1 : 10.0 | | |
| **3a** | 2.4683 | 0.0127 | 1 : 2.5 | | |
| | | 0.0253 | 1 : 5.0 | | |
| | | 0.0380 | 1 : 7.5 | | |
| | | 0.0503 | 1 : 10.0 | | |
| **3b** | 2.6894 | 0.0127 | 1 : 2.5 | | |
| | | 0.0253 | 1 : 5.0 | | |
| | | 0.0380 | 1 : 7.5 | | |
| | | 0.0503 | 1 : 10.0 | | |

**Fig. 8. Conversion of PPh₃ against time for: (A) 1a and (B) 1b**
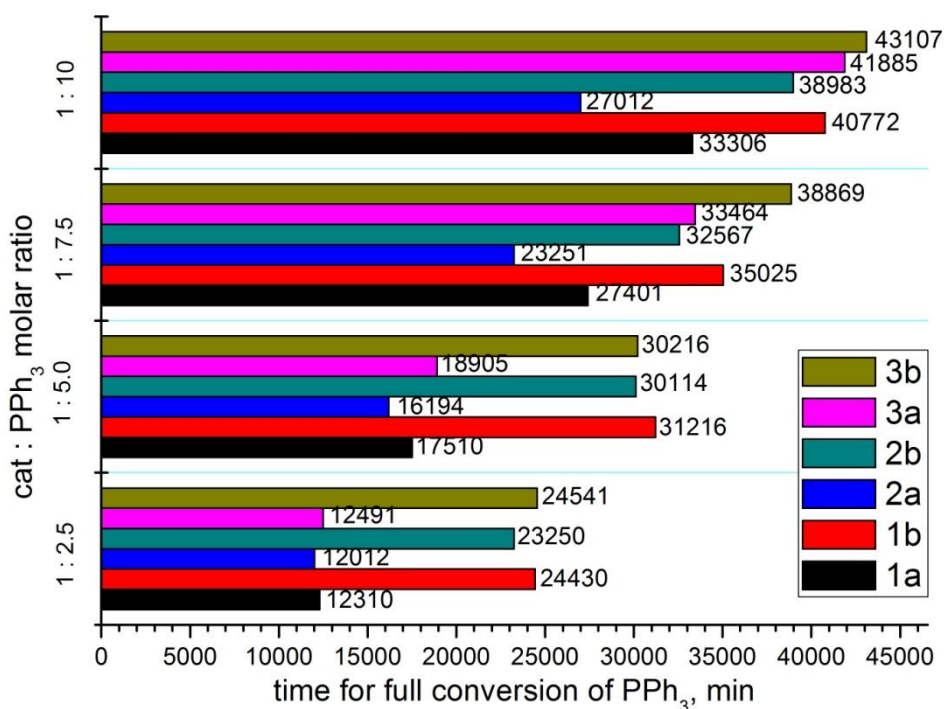


**Fig. 9. Time for full conversion of PPh₃ under different conditions**

For a given amount of catalyst, the faster conversion in the case of lower substrate concentration is a mathematical consequence of placing the initial substrate amount in the

denominator of the equation for calculating the percentage of conversion. However it does not imply a direct proportional relation with the velocity of the reaction. This is because, velocity or rate of the reaction implies how fast the molar concentration of the product develops or how that of the reactant does deplete irrespective of the initial amount. This concept is obvious from figure 10 which shows the plot of the calculated values of the molar concentration of $PPh_3O$ against time in the case of **1a** and **1b**. In case of both catalysts, the highest speed of the reaction was found for a 1:10 molar ratio and the slowest in the case of 1:2.5, exactly opposite to the trend found for the percentage of conversion. The initial rate of the reaction in each case has been calculated from the linear fit of the first five values in the respective graph. The molybdenum catalyst shows a higher initial rate than the tungsten catalyst in each case and the results are summarized in table 3.
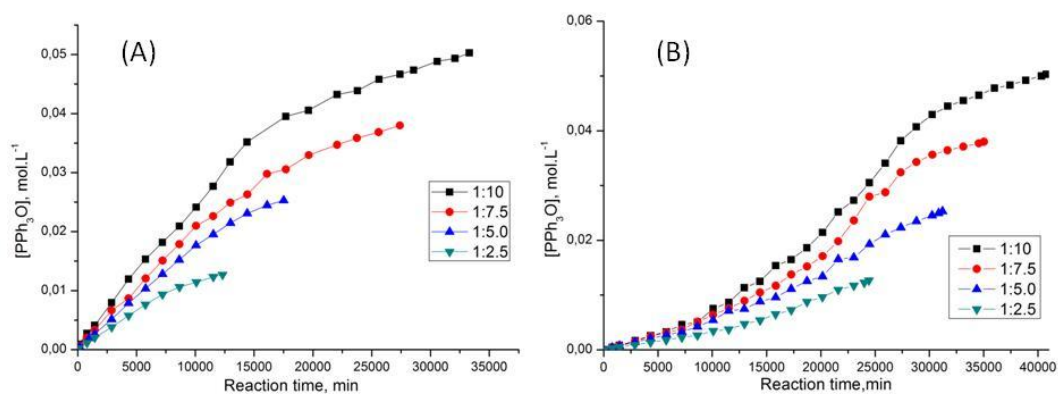


**Fig. 10. Variation of molar concentration of $PPh_3O$ with time**

The amount of DMSO, a second substrate, is in excess and therefore its concentration change during the reaction is negligible. On the basis of this, the reaction is assumed to be first order with respect to the concentration of $PPh_3$. In analogy to the enzymatic reaction kinetics, Michaelis-Menten kinetics has been applied in the present study also. Assuming a quasi-steady-state approximation i.e. the concentration of the substrate bound catalysts

does not change during the reaction and the total catalyst concentration is a constant, the Michaelis-Menton equation for the reactions under study can be set up as:

$$(1/v_0) = (K_M/v_{max})\,(1/[PPh_3]) + (1/v_{max}) \quad\ldots\ldots\ldots\ldots\ldots\ldots\ldots\ldots\ldots\ldots\ldots\ldots\ldots \quad (9)$$

where, $v_0$ is the initial rate, $v_{max}$ is the maximum rate and $K_M$ is the Michaelis constant. $[PPh_3]$ in this case represents the initial concentration of $PPh_3$. For a given amount of catalyst, the value of $v_{max}$ (which is the maximum possible velocity of a reaction with increase in the concentration of the substrate provided the catalyst concentration is kept contstant) is fixed and the only variables in the above equation are $v_0$ and $[PPh_3]$. Obviously, equation 9 is a linear equation with the slope $K_M/v_{max}$ and the y-intercept $1/v_{max}$. The graph for the variables $(1/v_0)$ and $(1/[PPh_3])$ is called a Lineweaver–Burke plot (or double reciprocal plot) [29] and the ratio between its y-intercept and slope will provide the value of $K_M$. In fact, the value of $K_M$ is important in the sense that it is an approximation of the affinity of the catalyst (enzyme analogue) for the substrate and it is numerically equivalent to the substrate concentration at which the rate of conversion reaches half of $v_{max}$. In other words, a small $K_M$ value indicates a high affinity, and a substrate with a smaller $K_M$ will approach $v_{max}$ more quickly. However, the value of $K_M$ as obtained from the Lineweaver–Burke plot is prone to error, as the $y$-axis takes the reciprocal of the rate of reaction in turn increasing any small errors in the measurement. Therefore in the present study, a Hanes–Woolf plot has been used which is obtained by rearranging the equation 9 as follows.

$$([PPh_3]/v_0) = ([PPh_3]/v_{max}) + (K_M/v_{max}) \quad\ldots\ldots\ldots\ldots\ldots\ldots\ldots\ldots\ldots\ldots\ldots \quad (10)$$

A plot of $([PPh_3]/v_0)$ vs. $[PPh_3]$ will give a straight line with the slope equal to $1/v_{max}$ and the y-intercept $(K_M/v_{max})$. The ratio of the y-intercept and slope (which is equal to the x-

intercept) will provide the value of $K_M$. The figure 11 shows the Hanes–Woolf plot for **1a** and

**1b**.
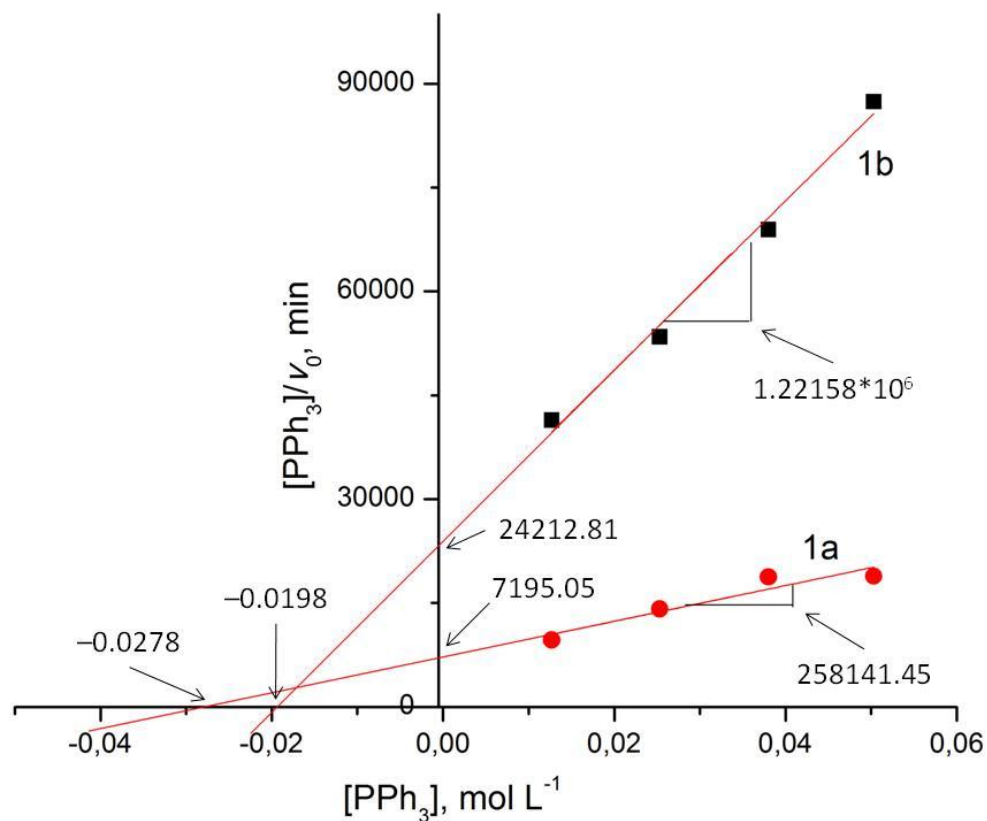


**Fig. 11. Hanes–Woolf plot for 1a and 1b**

The observed kinetic parameters for the reactions catalyzed by **1a** and **1b** are provided in

table 3. These results have been compared with those obtained for **2a**, **2b**, **3a** and **3b**.

**Table 3. Kinetic parameters for the reactions under different conditions.**

| catalyst | [PPh$_3$] (mol L$^{-1}$) | $v_0$ (mol L$^{-1}$ min) | [PPh$_3$]/$v_0$ (min) | $v_{max}$ (mol L$^{-1}$ min) | $K_M$ (mol L$^{-1}$) |
|---|---|---|---|---|---|
| | 0.0127 | $1.31 \cdot 10^{-6}$ | $9.63 \cdot 10^3$ | | |
| | 0.0253 | $1.79 \cdot 10^{-6}$ | $1.41 \cdot 10^4$ | | |
| **1a** | 0.0380 | $2.02 \cdot 10^{-6}$ | $1.87 \cdot 10^4$ | $3.87 \cdot 10^{-6}$ | $2.78 \cdot 10^{-2}$ |

| | 0.0503 | $2.66 \cdot 10^{-6}$ | $1.88 \cdot 10^4$ | | |
|---|---|---|---|---|---|
| **1b** | 0.0127 | $3.06 \cdot 10^{-7}$ | $4.14 \cdot 10^4$ | $8.18 \cdot 10^{-7}$ | $1.98 \cdot 10^{-2}$ |
| | 0.0253 | $4.73 \cdot 10^{-7}$ | $5.34 \cdot 10^4$ | | |
| | 0.0380 | $5.51 \cdot 10^{-7}$ | $6.89 \cdot 10^4$ | | |
| | 0.0503 | $5.75 \cdot 10^{-7}$ | $8.73 \cdot 10^4$ | | |
| **2a** | 0.0127 | $1.37 \cdot 10^{-6}$ | $9.27 \cdot 10^4$ | $5.14 \cdot 10^{-6}$ | $4.0 \cdot 10^{-2}$ |
| | 0.0253 | $1.97 \cdot 10^{-6}$ | $1.28 \cdot 10^4$ | | |
| | 0.0380 | $2.66 \cdot 10^{-6}$ | $1.43 \cdot 10^4$ | | |
| | 0.0503 | $2.97 \cdot 10^{-6}$ | $1.69 \cdot 10^4$ | | |
| **2b** | 0.0127 | $2.31 \cdot 10^{-7}$ | $5.50 \cdot 10^4$ | $8.74 \cdot 10^{-7}$ | $3.5 \cdot 10^{-2}$ |
| | 0.0253 | $3.57 \cdot 10^{-7}$ | $7.09 \cdot 10^4$ | | |
| | 0.0380 | $4.52 \cdot 10^{-7}$ | $8.41 \cdot 10^4$ | | |
| | 0.0503 | $5.11 \cdot 10^{-7}$ | $9.84 \cdot 10^4$ | | |
| **3a** | 0.0127 | $1.16 \cdot 10^{-6}$ | $1.09 \cdot 10^4$ | $3.06 \cdot 10^{-6}$ | $2.3 \cdot 10^{-2}$ |
| | 0.0253 | $1.57 \cdot 10^{-6}$ | $1.61 \cdot 10^4$ | | |
| | 0.0380 | $1.86 \cdot 10^{-6}$ | $2.04 \cdot 10^4$ | | |
| | 0.0503 | $2.17 \cdot 10^{-6}$ | $2.32 \cdot 10^4$ | | |
| **3b** | 0.0127 | $8.60 \cdot 10^{-7}$ | $1.48 \cdot 10^4$ | $1.88 \cdot 10^{-6}$ | $1.8 \cdot 10^{-2}$ |
| | 0.0253 | $1.06 \cdot 10^{-6}$ | $2.39 \cdot 10^4$ | | |
| | 0.0380 | $1.33 \cdot 10^{-6}$ | $2.86 \cdot 10^4$ | | |
| | 0.0503 | $1.42 \cdot 10^{-6}$ | $3.54 \cdot 10^4$ | | |

The table shows that the initial velocity ($v_0$) of the reaction was highest for a 1:10 molar ratio of catalyst and PPh$_3$ and the lowest for 1:2.5 ratios in all cases. Among the molybdenum catalysts, **2a** has the maximum value of $v_{max}$ followed by **1a** and **3a**. Since the maximum velocity is a direct indicator for the activity of the catalyst, the present study shows that the presence of a heteroatom in the adjacent ring of the dithiolene function enhances the catalytic activity. The maximum velocity in the case of **1a** is only 75% of that for **2a**. Interestingly, the thiopyran moiety gives a better activity to the catalyst than the pyrane moiety which is also present in the natural molybdopterin. Now the important question arises: would the natural enzymes catalyze specific reactions with better activity if sulfur was incorporated in place of oxygen in the pyrane ring of molybdopterin? The answer is: perhaps it would! Then why oxygen? The reasons may be diverse. One could be a more facile biosynthesis of the MoCo including molybdopterin with the pyrane ring. Another possibility is the feasibility of a ring opening and closing mechanism of pyrane or thiopyrane moieties. Here the focus is based on the kinetic behavior exhibited by the catalysts with pyrane or thiopyrane. It should be noted that the natural selection of the active sites of enzymes for specific reactions is not purely based on the speed of the reaction. In fact, this is finely tuned to the requirements of the organism. In other words, the reaction rate is an optimized parameter which is neither too low so that the organism cannot survive nor too high which is not required. In this respect, the affinity of the enzyme for the substrate in a given reaction is an important factor. Provided, the maximum velocity is optimized, the enzyme with the highest affinity for the substrate will have the lowest value of $K_M$. Simply said, for a given maximum velocity, a catalyst with the lowest value of $K_M$ will bring the maximum velocity at the lowest concentration of the substrate. Interestingly, the value of $K_M$ for **1a** is only 70% of that for **2a** even though the later shows better activity. A final word on the advantage of the

pyrane ring over the thiopyrane would not be valid based only on the values of $K_M$ as both catalysts have considerable difference in the values of maximum velocity.

It is interesting to note that in the case of tungsten catalysts, **3b** is the best in terms of the values of $v_{max}$ and $K_M$.  The $v_{max}$ value of **3b** ($1.88 \cdot 10^{-6}$ mol.L$^{-1}$.min) is 230 and 215 % of that for **1b** and **2b** respectively. At the same time its $K_M$ value is only 91 % of **1a** and 51% of **1b**. Does this mean that there is no kinetic advantage of the presence of the heterocyclic ring in the tungsten enzymes? The present study supports this, if and only if there is no other internal mechanism altering the chemical structure of the ligand system facilitating the catalytic turn over. The ligand rearrangement mechanisms in the natural molybdopterin still remain a hot area for speculations and imaginations and any such conclusions could not be drawn here. However it should be noticed from the above discussion that in the presence of a heterocyclic ring system, molybdenum catalysts have a special kinetic advantage over the tungsten catalysts. This can be one of the driving forces for the evolutionary incorporation of molybdenum into enzymes with tungsten active sites coordinated by molybdopterin ligands.

The electrochemical and kinetic study of compounds **1**, **2** and **3**, indicates that the presence of the heteroatom in the ring adjacent to the dithiolene function has a great influence. The natural selection of the pyrane seems to be a wise choice as a compromise between advantages and disadvantages. The quest for the optimum reactivity, high substrate affinity, very high *non*-innocence and most stable redox potential renders the pyrane as the best choice in the complicated structure of molybdopterin.

# References

[1]     Holm, R. H. *Coord. Chem. Rev*. 100 (1990) 183

[2]     Enemark, J. H.; Cooney, J. J. A.; Wang, J.J.; Holm, R. H. *Chem. Rev.* 104 (2004) 1175

[3]     Clark, R. J. H.; Turtle, P. C. *Dalton Trans* (1977) 2142

[4]     Schultz, B. E.; Holm, R. H. *Inorg. Chem.* 32 (1993) 4244

[5]     Schultz, B. E.; Hille, R.; Holm, R. H. *J. Am.* Chem. Soc. 117 (1995) 827

[6]     Oku, H.; Ueyama, N.; Kondo, M.; Nakamura, A., *Inorg. Chem.* 33 (1994) 209

[7]     Holm, R.H. *Coord. Chem. Rev*. 100 (1990) 183

[8]     Topich, J.; Lyon, J.T. *Inorg. Chem.* 23 (1984) 3202

[9]     Hille, R. *J. Biol. Inorg. Chem.* 2 (1997) 804

[10]   Fischer, B.; Enemark, J. H.; Basu, P. *J. Inorg. Biochem.* 72 (1998)  13

[11]   Dahlstrom, P. L.; Hyde, J. R.; Vella, P. A.; Zubieta, J. *Inorg. Chem.* 21 (1982)  927

[12]   Craig, J.A.; Harlan, E. W.; Snyder, B. S.; Whitener, M. A.; Holm, R. H. *Inorg. Chem.* 28 (1989) 2082

[13]   Ueyama, N.; Oku, H.; Kondo, M; Okamura, T.; Yoshinaga, N.; Nakamura, A. *Inorg. Chem.* 35 (1996)  643

[14]   Oku, H.; Ueyama, N.; Nakamura, A. *Inorg. Chem.* 34 (1995)  3667

[15]   Lim, B. S.; Holm, R. H. *J. Am. Chem. Soc.* 123 (2001) 1920

[16]   Sugimoto , H.; Tarumizu, M.; Miyake, H.; Tsukube, H. *Eur.J. Inorg. Chem.* (2006) 4494

[17]   Nemykin, V. N.; Davie, S. R.; Mondal, S., Rubie, N.; Kirk, M. L.; Somogyi, A.; Basu, P. *J. Am. Chem. Soc.* 124 (2002) 756

[18]   Ueyama, N.; Oku, H.; Nakamura, A. *J. Chem. Am. Soc.* 114 (1992) 7310

[19]  Lorber, C.; Donahue, J. P.; Goddard, C. A.; Nordlander, E.; Holm, R. H. *J. Am. Chem. Soc*. 120 (1998) 8102

[20]  Lim, B. S.; Sung, K.-M.; Holm, R. H. *J. Am. Chem. Soc.* 122 (2000) 7410

[21]  Sung, K.-M.; Holm, R. H. *Inorg. Chem.* 40 (2001) 4518

[22]  Sung, K.-M.; Holm, R. H. *J. Am. Chem. Soc.* 124 (2002)  4312

[23]  Sung, K.-M.; Holm, R. H. *J. Am. Chem. Soc.* 123 (2001) 1931

[24]  Döring, A. ; Schulzke, C., *Dalton Trans.* 39 (2010) 5623

[25]  Döring, A. Verbindungen von Molybdän und Wolfram in den Oxidationsstufen IV – VI als Modelle für Molybdän- und Wolfram-Cofaktoren, Ph.D Dissertation 2010, University of Göttingen

[26]  Tucci, G. C.; Donahue J. P.;  Holm, R. H. *Inorg. Chem.*, 37 (1998) 1602

[27]  Fomitchev, D. V.; Lim B. S.; Holm, R. H. *Inorg. Chem.*, 40 (2001)  645

[28]  Schulzke, C. *Dalton Trans.*, (2005) 713

[29]  Lineweaver, H.; Burk, D. *J. Am. Chem. Soc*. 56 (1934) 658

# N-HETEROCYCLIC CARBENE COMPLEXES OF MOLYBDENUM AND THEIR DITHIOLENE CHEMISTRY

## 4.1. General Introduction to transition metal carbene complexes

Carbenes are neutral compounds featuring a divalent carbon atom with only six electrons in its valence shell: two in each bond and two nonbonding electrons, which are often represented as $:CR_2$. The notation can be misleading, but $:CR_2$ is a widely used symbol for a carbene. Carbenes are extremely reactive species. For example, they are trapped by alcohols to make ethers, they will react with alkenes to make cyclopropanes, and they will also insert into C–H bonds. Even though most of the carbenes are too reactive to be observed directly, in certain cases electronic and, more importantly, steric effects can make the compounds stable for their isolation and crystallization. Spectroscopic investigations of a number of carbenes of differing structures have shown that they fall broadly into two groups: (1) Triplet carbenes possessing unpaired electrons as demonstrated by ESR spectroscopy with R-C:-R bond angles between 130–150°; and (2) Singlet carbenes, which are EPR silent and thus possessing a lone pair of electrons with the R-C:-R bond angles

between 100–110°. Based on the observed bend structure of the carbenes, the carbon atom seems to possess $sp^2$ hybridization. An $sp^2$ hybridized carbene would have three (lower-energy) $sp^2$ orbitals and one (high-energy) p orbital and all the six electrons are distributed in these four orbitals or less. The two possible ways of distribution of electrons are: (1) all of the electrons can be paired, with each pair occupying one of the $sp^2$ orbitals and (2) two of the electrons can remain unpaired, with one electron in each of the p orbitals and one of the $sp^2$ orbitals. The two observed classes of carbenes are derived from these two possibilities. In the first case where all electrons are paired, the spin multiplicity, $2S+1$, is equal to 1 and thereby known as singlet carbenes. In the second case, there are two unpaired electrons giving rise to $2S+1$ value equal to 3 and thereby known as triplet carbenes. Thus the singlet and triplet in the case of carbenes represent the two possible arrangements of six electrons (spin states) in its orbitals. When it comes to the molecular orbitals that the carbon shares with the other two bonding atoms, the orbitals are the same in both cases but in triplet carbenes we have one electron in each of the two molecular orbitals and in singlet carbenes both electrons go into the $sp^2$ orbital. In short, triplet carbenes have two unpaired electrons, one in each of an $sp^2$ and a p orbital, while singlet carbenes have a pair of electrons in a nonbonding $sp^2$ orbital and have an empty p orbital. As an extreme case, carbenes can possess linear geometry also. In such cases the geometry implies an sp hybridized carbene center with two non-bonding degenerate orbitals, $p_x$ and $p_y$.

Since carbenes have only 6 electrons in their valence shell, they are desperate to complete the octet by making bonds with other atoms. Interestingly, this property of carbenes has been well utilized in inorganic chemistry so that there are numerous examples of inorganic complexes with one or more carbene ligands. Metal carbene complexes are

often classified into two types. The **Fischer carbenes** named after Ernst Otto Fischer and

**Schrock carbenes**, named after Richard R. Schrock.  In Fischer carbenes, the metal is a strong

π-acceptor and the carbene carbon atom is higly electrophilic. In Schrock carbenes, the

carbene carbon center is nucleophilic and they typically prefer higher valent metals. The

Fischer carbenes generally have a singlet carbene center with a heteroatom substituent

unlike Schrock carbenes which usually have alkyl substituents on a triplet carbene center.

(figure 1). Fischer carbenes are typically found on electron-rich, low oxidation state metal

complexes (mid to late transition metals) containing pi-acceptor ligands. The presence of the

heteroatom on the alpha carbon allows us to draw a resonance structure that is not possible

for an unsubstituted Schrock-type carbene (figure 2). From a molecular/atomic orbital

perspective, one lone pair is donated from the singlet carbene to an empty d-orbital on the

metal (red), and a lone pair is back-donated from a filled metal orbital into a vacant $p_z$ orbital

on carbon (blue). There is competition for this vacant orbital by the lone pair(s) on the

heteroatom, consistent with the second resonance structure. Single crystal x-ray diffraction

studies confirm that the second resonance form plays a major role in describing the bonding

in metal carbene complexes. The metal double carbon bonds in these complexes tend to be

longer than typical M=C double bonds, but shorter than M-C single bonds. Likewise, the

carbon-heteroatom bond length is somewhat shorter than a typical M-E bond. Schrock

carbenes, having a triplet carbene center lack back bonding and form formal double bonds

with the metal. N-heterocyclic carbenes(NHCs), where the carbon center is bonded to

nitrogen atoms, were popularized following Arduengo's isolation of a stable free carbene

(compound **A**) (figure 3) in 1991.[1] Being strongly stabilized by pi-donating substituents,

NHCs are good σ-donors but π-bonding with the metal is weak. For this reason, the bond

between the carbon and the metal center is often represented by a single dative bond, whereas Fischer and Schrock carbenes are usually depicted with carbon-metal double bonds.

**Schrock carbene complex**

**Fishcher carbene complex**

$$Ln\ M = C \overset{R}{\underset{H}{\diagdown}}$$

$$Ln\ M = C \overset{ER}{\underset{H}{\diagdown}}$$
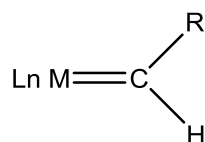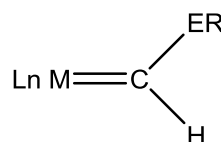
R = H, alkyl, aryl

R = alkyl, aryl, etc.
E = O, S, N

**Fig. 1. Fischer and Schrock type carbene complexes**

$$Ln\ M=C \overset{OR}{\underset{R'}{\diagdown}} \longleftrightarrow Ln\ \overset{\ominus}{M}-\overset{\oplus}{C} \overset{OR}{\underset{R'}{\diagdown}}$$
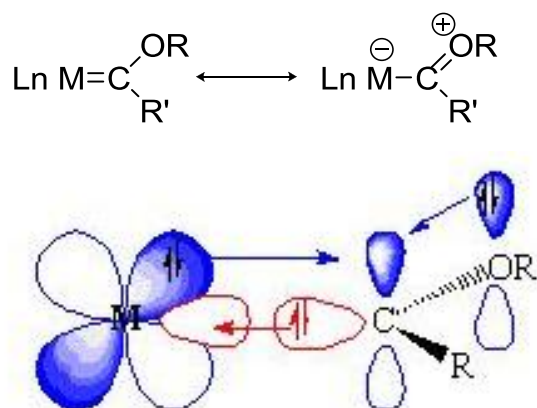


**Fig. 2. Resonance in a Fischer carbene**

In fact the use of NHC's as ligands for transition metal complexes was described four decades ago by Öfele and Wanzlick who prepared compounds **B** and **C.** (figure 3).[2-3] Even though Lappert conducted extensive studies in the chemistry of late transition metal carbene complexes such as **D**,[4-12] little attention was paid to these species until the 1991 report of Arduengo et al. describing the isolation and crystallization of a free carbene.[1] When bound to metals, *N*-heterocyclic carbenes are significantly less reactive than the Schrock and Fischer carbenes. In fact, relative to these two types of ligands, NHC's can be

93

considered to be spectator ligands.[13] In other words, they do not undergo reactions typically attributed to metal carbenes, say for example metathesis reactions, cyclopropanations, or many of the other reactions. This is the main reason why NHC's were not as prominent in organometallic chemistry as their more reactive cousins. However, the pioneering studies by Grubbs,[14-19] Herrmann,[20-27] Nolan,[28-33] Fürstner,[23, 34-41] Hoveyda [42-46] and Lappert [4-12] have clearly demonstrated the utility and uniqueness of these species as ancillary ligands on a variety of transition metals.
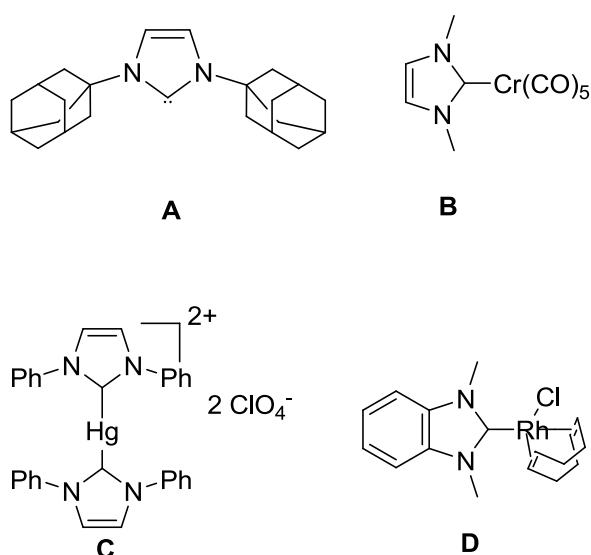


**Fig. 3. Some of the early developed NHC compounds. (1) The first isolated NHC by Arduengo, (2) Öfele's NHC complex, (3) Wanzlick's NHC complex and (4) Lappert's NHC complex**

After Arduengo and coworkers isolated and crystallized the first of the N-heterocyclic carbenes (NHC) in 1991, the following last two decades witnessed their enormous potential for applications in both organic and inorganic chemistry.[1] In addition to this, extensive research has been carried out over the last few years to produce a large number of complexes bearing heterocyclic carbene ligands. Today, carbene related inorganic chemistry has been flourished with not only complexes of all the transition metals [13, 21, 47-49] and adducts with many of the main-group elements,[50] but also the complexes of the

lanthanides,[51-53] and uranium[54-55]. The use of NHC complexes as transition metal catalysts in organic synthesis has contributed significantly to its widely documented development in the last decades.

An overall analysis of the literature shows that the NHC metal complexes reported so far have been prepared mainly by three routes: The first method involves the in situ deprotonation of carbene ligand precursors especially advantageous in the cases where the free NHC is unstable. The deprotonation can be effected by a base function. For example, Brönstedt basic metallate anions deprotonate the azolium cations on heating to form the respective NHC-metal complexes. The first NHC-transition metal complex (NHC)Cr(CO)$_5$ prepared by Öfele utilized this methodology in which [HCr(CO)$_5$]$^-$ acts as the basic metal precursor to deprotonate the imidazolium salt to form imidazolin-2-ylidene complex.[2] However, limited availability of the metal precursors often reduces the utilization of this method in many cases. But there are plenty of examples where the Brönsted basic functions directly associated with either the metal precursor or the azolium salt can deprotonate in situ leading to the NHC- complex. One of the earliest work by Schönherr to prepare the [(NHC)$_2$Hg]$^{2+}$ complex utilized this method.[3] In this work 1,3-diphenylimidazolium perchlorate was treated with mercury(II) acetate in dimethyl sulfoxide (DMSO) to obtain the bis(1,3 -diphenylimidazolio)mercury diperchlorate with the liberation of acetic acid. In the last two decades this method was widely employed for the synthesis of many NHC complexes, especially in the case of palladium(II) and nickel(II). The reaction of diacetates of these metals with imidazolium or triazolium salts yielded the products in most of the cases. [24, 56-59] In addition to this, the same methodology was used in many cases to prepare the methylene bridged bidentate carbene complexes of palladium and nickel.[26, 60-62] Interestingly, through this method of deprotonation by basic anions, the μ-hydroxo or μ-

alkoxo bridged polynuclear complexes of chromium, molybdenum, tungsten and rhenium afford monomeric bis(NHC) complexes.[63-64] In the second popular method for preparing NHC complex, an enetetramine is being attacked by a metal precursor complex to cleave the electron rich olefinic bond. This method has been applied to preparing the NHC complexes of various metals like manganese, iron, cobalt, ruthenium and nickel from their carbonyls.[10, 65-66] In addition to the mononuclear metal carbonyls, dinuclear metal complexes can also cleave the enetetramine olefinic center to afford the corresponding mononuclear NHC complex. For example, $[(\eta^4\text{-cod})RhCl]_2$ reacts with the enetetramine compound to form $[(NHC)(\eta^4\text{-cod})RhCl]$.[12] The third method for the preparation of NHC complexes uses the application of free NHC, having been successfully isolated by Arduengo's procedure.[1] Free NHCs have been found useful in many cases to cleave the dimeric complexes with bridging ligands to form the corresponding NHC-metal complex.[56, 67-69] For example the dimeric complex $[(\eta^4\text{-cod})RhCl]_2$ in which chlorine atoms are bridging the Rh atoms reacts with two equivalents of free NHCs to form mononuclear $[(\eta^4\text{-cod})RhCl(NHC)]$.[68] Another advantage of using free NHCs is that they can substitute weakly bound ligands of a precursor metal complex to form the corresponding NHC complex. Exchange of phosphines by NHCs have been well documented throughout the literature because of the ease with which the exchange proceeds even below room temperature.[20, 22, 28] For instance, the reactions of various NHCs with dichloro-bis(tricyclohexylphosphine)benzylidene ruthenium(II), the olefin metathesis catalyst, have been reported by Herrmann et al.. In these reactions, different NHCs were found to replace both phosphines retaining the benzylidene ligand intact.[20] Not only phosphines, but also many examples of other neutral ligands or coordinated solvent molecules can be substituted by free NHCs. One or two CO ligands in the carbonyl complexes, $W(CO)_6$,[68] $Mo(CO)_6$,

Cr(CO)$_6$ [70-71] or Ni(CO)$_4$ [67] can be replaced by free NHCs. Moreover, amine ligands like TMEDA [71] and coordinated solvents can also be exchanged with NHCs.

## 4.2. Carbene related molybdenum chemistry

Like for other transition metals, carbene related chemistry of molybdenum has been thoroughly studied and documented throughout the literature. Even from the earliest stages of development of carbene related co-ordination chemistry, bis-carbene complexes of molybdenum carbonyls such as (**E**) and (**F**) are known (figure 4).[72-73] Later on, in 1996, Herrmann and coworkers synthesized a tris-carbene complex (**G**) using the same carbene ligand by treating it with MoO$_2$Cl$_2$(THF)$_2$.[74] In an equilibrium reaction of gaining and losing one of the NHCs the compound (**G**) affords compound (**H**), a bis-NHC complex. It should be noted that the bis or tris carbene complexes were simply afforded in these cases due to the sterically non demanding nature of the NHC ligand. In fact, regarding studies of N-heterocyclic carbene complexes of molybdenum, examples involving Mo(VI) are scarce, while most of them concern carbonyl molybdenum(0) complexes. After the above mentioned work of Herrmann, the next example of a NHC–Mo(VI) complex appeared in the literature only after 10 years.[75] In this work, Royo et al. treated MoO$_2$Cl$_2$(THF)$_2$ with two equivalents of 1,3-dialkyl substituted 4,5-dimethylimidazol-2-ylidenes to give the dioxomolybdenum(VI) complexes MoO$_2$Cl$_2$(L$^R$)$_2$ [R = Me (**I**), i-Pr (**J**)]. Treatment of MoO$_2$Cl$_2$(THF)$_2$ with one equivalent of the N-heterocyclic carbenes L$^{Me}$, L$^{i-Pr}$ and $^{Cl}$L$^{n-Bu}$ (L$^{Me}$ = 1,3,4,5-tetramethylimidazol-2-ylidene, L$^{i-Pr}$ = 1,3-diisopropyl-4,5-dimethylimidazol-2-ylidene, and $^{Cl}$L$^{n-Bu}$ = 1,3-dibutyl-4,5-dichloroimidazol-2-ylidene) affords the monocarbene complexes MoO$_2$Cl$_2$(L$^R$) [R = Me (**K**), i-Pr (**L**)] and MoO$_2$Cl$_2$($^{Cl}$L$^{n-Bu}$) (**M**), respectively.  Surprisingly, none of them were structurally characterized. Very recently, Zhao, Hor and coworkers synthesized

cyclopentadienyl molybdenum(VI) N-heterocyclic carbene complexes (**N**) but they were not structurally characterized.[76]
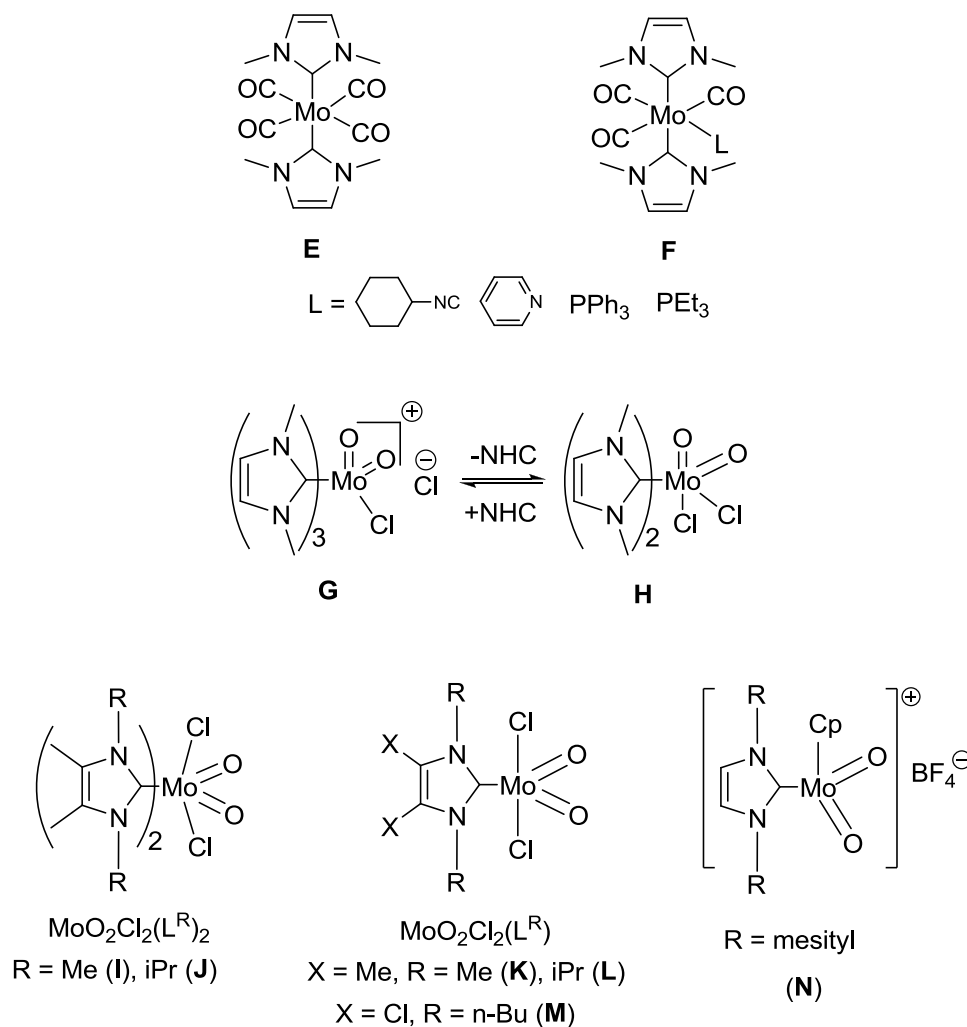


**Fig. 4. Representative examples of NHC complexes of molybdenum**

## 4.3. Modeling studies for SO and XO family enzymes

The common feature of the SO and XO families of enzymes is that both of them carry only one MPT ligand at the molybdenum center. A large number of synthetic analogues has been reported for the SO family of enzymes. Many of them are structurally characterized and screened for their catalytic oxo-transfer properties. Most of the earlier developed model

complexes for the SO family of enzymes were not able to correctly resemble the coordination environment with three thiolate and two terminal oxo groups in their oxidized form. However, the bioinorganic model chemistry in this area was developed with an explicit desire to obtain reactivity analogues. Similar to the catalytic reaction in the enzymes, the oxo-transfer catalysis by analogous complexes included the $Mo^{VI}O_2/Mo^{IV}O$ redox couple. Unfortunately the formation of a $Mo^V_2O_3$ core by reaction of both species with each other inhibits any further activity and obstructs the catalytic cycle. In an attempt to prevent this deactivation by dimerization, Holm et al. synthesized $MoO_2(L-NS_2)$, (compound **O**) (figure 5) where (L-NS$_2$) is a sterically bulky ligand preventing direct contact between the two metal centers at both ends of a single catalytic turn over.[77-78]



| $MoO_2(L-NS_2)$ | $[MoO_2(O_2CC(S)Ph_2)_2]^{2-}$ | $MoO_2(^tBuL-NS)_2$ |
|:---:|:---:|:---:|
| **O** | **P** | **Q** |
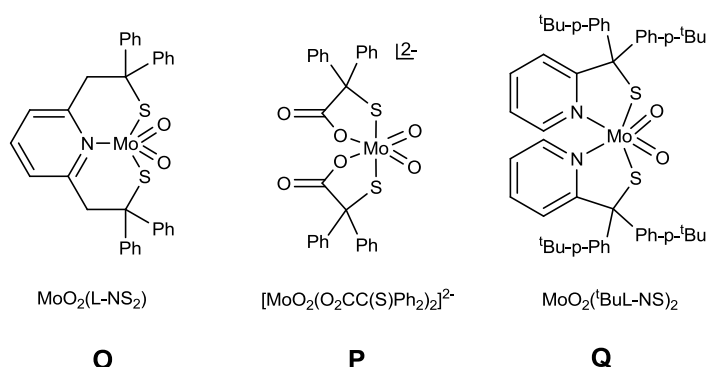
**Fig. 5. Functional model complexes for the sulfite oxidase family of molybdenum enzymes with sterically bulky ligands**

This complex was indeed efficiently catalyzing the oxygen atom transfer from DMSO onto PPh$_3$ to form DMS and PPh$_3$O, but catalytic turnover caused an unforeseen reorientation of the ligand allowing the formation of the Mo$_2$O$_3$ core anyway. After the paramount relevance of these steric factors in ligand systems had been demonstrated by Holm, as a first example of a coordinatively saturated molybdenum complex reacting readily and reversibly with organophosphines at room temperature in water or methanol, the Cervilla group synthesized $[NH_4]_2[MoO_2(O_2CC(S)Ph_2)_2] \cdot 2H_2O$ (compound **P**) (figure 5).[79]

Both terminal oxo ligands at the molybdenum center of this complex are sterically shielded by one phenyl ring from the ligand in the direction of a potential Mo-O-Mo bond preventing dimerization. A similar complex with respect to sterics and catalytic properties, incorporating two terminal oxo groups and two sulfur atoms from a sterically crowded ligand system was the six-fold coordinated $Mo^{VI}O_2(Bu^tL-NS)_2$ (compound **Q**). The reduced form of this complex, $Mo^{IV}O(But-NS)_2$, is a stable five-fold coordinated system.[80-81]

The regeneration of the sulfite oxidase's active center from Mo(IV)O to Mo(VI)O$_2$ is achieved through a Mo(V) transient state as emphasized by EPR studies.[82] The oxygen atom transfer facilitated by the interconversion of Mo(VI)O$_2$ and Mo(IV)O of model compounds has been documented widely throughout the literature. But the first model complex which accomplished the regeneration of Mo(VI)O$_2$ from Mo(IV)O through two distinguished one electron transfer steps, accurately resembling the natural system, was $LMo^VO_2(SPh)$; [L = hydrotris( 3,5 dimethyl- 1- pyrazolyl)borate anion].[83] This complex is another example of the class of compounds which is noted for the presence of sterically highly demanding ligand systems able to minimize or prevent comproportionation of reduced and fully oxidized species. In DMF or MeCN oxygen atom abstraction by PPh$_3$ from $LMoO_2(SPh)$ leads to the formation of $LMo^{IV}O(SPh)$ or weakly solvated $LMo^{IV}O(SPh)(solvent)$. It can be trapped as mononuclear species in pyridine $LMo^{IV}O(SPh)(py)$ or in CH$_2$Cl$_2$ $LMo^VOCl(SPh)$. In contrast, it forms dinuclear $[LMo^VO(SPh)]_2O$ in dry toluene. The reaction takes yet another course in wet THF or toluene: the presence of small amounts of water results in the formation of $LMo^VO(OH)(SPh)$ according to the reaction:

$$LMo^{IV}O(OH_2)(SPh) + LMo^{V1}O_2(SPh) \rightarrow 2 LMo^VO(OH)(SPh)$$
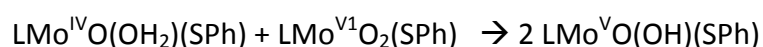
$LMo^VO(OH)(SPh)$ can be oxidized quantitatively to $LMo^{VI}O_2(SPh)$. Consequently, the $LMo^{VI}O_2(SPh)$ complex is a catalyst for the oxidation of PPh$_3$ to PPh$_3$O. Oxygen isotope ($^{18}$O)

tracing using labeled $H_2O$ shows that the oxygen in $PPh_3O$ stems from water. This was the first model system which displayed the full catalytic cycle proposed for oxidizing molybdenum enzymes featuring the $[Mo^{VI}O_2]^{2+}$ resting state in resemblance to SO.[84]

With a more structural than functional focus on the SO enzymes active sites *cis-*, *trans*-$[Mo^VO(L-N_2S_2)(SR)]$ (L-$N_2S_2H_2$ = *N,N'*-dimethyl-*N,N'*bis(mercaptophenyl)ethylenedi-amine; R = $CH_2Ph$, $CH_2CH_3$, and *p*-$C_6H_4$−Y (Y = $CF_3$, Cl, Br, F, H, $CH_3$, $CH_2CH_3$, and $OCH_3$) has been developed. It contains three thiolate donors bound to molybdenum in the equatorial plane (figure 6). It should be noted that these are the first structurally characterized mononuclear molybdenum compounds with three thiolate donors.[85] Even though not exactly reflecting the ligand environment of the active site molybdenum in SO, its coordination geometry places two adjacent S p$\pi$ orbitals parallel to the Mo=O bond, analogous to the orientation of the MPT ligand in sulfite oxidase, with the third S p$\pi$ orbital lying in the equatorial plane.
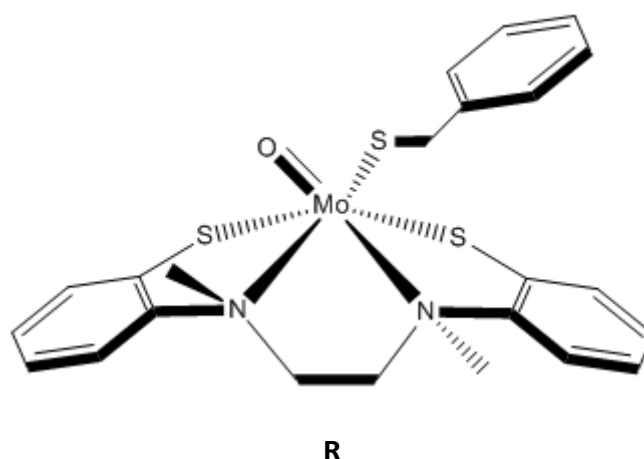


**R**

**Fig. 6. $[Mo^VO(L-N_2S_2)(SCH_2Ph)]$ - three thiolate donors bound to molybdenum in the equatorial plane**

Closer coordination environment mimics of the SO family of enzymes need to bear exactly one dithiolene ligand at the Mo center. Such mono-dithiolene complexes were

regarded as unusual and difficult to synthesize until recently but their relevance was underlined after the cofactor of SO was characterized crystallographically. Two very different synthetic pathways for realizing this type of complexes were described by the Holm group.[86] The first method leads to the formation of monodithiolene Mo(V)complexes analogous to the high pH form of sulfite oxidase by starting with the *bis*-dithiolene complexes. For example, $[Mo^VO(S_2C_2Me_2)_2]^{1-}$ or $[Mo^VO(bdt)_2]^{1-}$ (bdtH$_2$ = 1,2 benzene-dithiol) is reacted with PhSeCl in a way that one of the ene-dithiolate ligands is replaced by two chlorides forming $[Mo^VOCl_2(S_2C_2Me_2)]^{1-}$ or $[Mo^VOCl_2(bdt)]^{1-}$ respectively. Upon treatment with a sterically hindered thiol, these complexes undergo ligand substitution reactions forming other monodithiolene Mo(V) complexes $[MoO(2\text{-}AdS)_2(S_2C_2Me_2)]^{1-}$, $[MoO(SR)_2(bdt)]^{1-}$ (R = 2-Ad or 2,4,6-Pr$^i_3$C$_6$H$_2$ , and $[MoOCl(SC_6H_2\text{-}2,4,6\text{-}Pr^i_3)(bdt)]^{1-}$. The latter complex presents the closest similarity to the active site structure of sulfite oxidase in its high pH form with one oxo, one thiol, one dithiolene and the chloro ligand, which is in place of the hydroxide. The second synthetic and slightly more economic route leads to analogues of the fully oxidized form of SO. Treatment of $[Mo^{VI}O_2(OSiPh_3)_2]$ with Li$_2$(bdt) in THF affords $[Mo^{VI}O_2(OSiPh_3)(bdt)]^{1-}$ which reacts with the bulky thiol 2,4,6-Pr$^i_3$C$_6$H$_2$SH in acetonitrile giving $[Mo^{VI}O_2(SC_6H_2\text{-}2,4,6\text{-}Pr^i_3)(bdt)]^{1-}$. The result is an excellent model for the oxidized form of SO with both of the oxo ligands, a thiolate in place of cysteinate and benzenedithiolene mimicking MPT.

The model chemistry for the XO family of enzymes is still in its infant stage, as the Mo$^{VI}$OS core with additional dithiolene chelation is an uncommon motive in synthetic inorganic chemistry. In the enzymes the Mo$^{VI}$OS center is believed to be converted to a Mo$^{IV}$O(SH) species, following hydride transfer from the substrate to the sulfido group and this presents additional synthetic challenges.[87] After all, the fundamental importance of

understanding the chemical role of bridging or terminal sulfur atoms in the catalytic turnover still challenges bioinorganic chemists working in this field. Early examples of simple synthetic analogues of the xanthine oxidase family of enzymes include oxothiomolybdates, $[MoO_{4-n}S_n]^{2-}$,[88] hydroxylamido complexes, $MoOS(ONR_2)_2$ [89-90] and organometallic derivatives as $Cp*MoOS(CH_2SiMe_3)$.[91] One of the first truly comparative studies of analogue complexes and different species of milk xanthine oxidase was carried out by Wedd and co-workers.[92] Model complexes used in this work include $[MoOXL]^{1-}$ and $[MoO(XH)L]$, where X = O, S and $LH_2$ = N,N'-dimethyl-N,N'-bis(2-mercaptopheny1)- 1,2-diaminoethane. Rapid Type 1, Rapid Type 2, and Slow centers of milk xanthine oxidase (named after characteristic EPR signals upon enzyme reduction by different methods) were compared to the synthetic species $[MoOXL]^{1-}$ and $[MoO(XH)L$ (X=O, S) by definition of the $^{95}Mo$ hyperfine matrices from multifrequency EPR spectra. Similarly, $^{33}S$ hyperfine matrices were extracted for the sulfide ligand of $[MoOSL]^-$ and for the mercapto ligand $SH^-$ of $[MoO(SH)L]$ and compared with the $^{33}S$ coupling observed in a number of EPR signals of xanthine oxidase species. Detailed evaluation revealed $[Mo^VO(SH)]$, $[Mo^VO(SH)(OH)]$, and $[Mo^VO(OH)]$ cores as being responsible for the Rapid Type I , Rapid Type 2, and Slow EPR signals. Strong evidence for $[Mo^VOS]$ as being the source of the very rapid signal was obtained in addition.

Recently synthetic model chemistry was advanced by Young and co-workers, as they were successfully utilizing oxygen atom transfer and sulfur atom transfer reactions in the preparation of mononuclear oxo-sulfido-molydenum(VI) complexes such as $Tp*MoO(S)\{SP(S)Pr^i_2\}$ [Tp* = hydrotris-(3,5-dimethylpyrazol-1-yl)borate], $Tp'MoO(S)\{SP(S)R_2\}$ (compound **S**)[Tp' = hydrobis(3-isopropylpyrazolyl-1-yl)(5-isopropylpyrazolyl-1-yl)borate; R = $Pr^i$, Ph] and $Tp^{iPr}MoOS(OAr)$ [$Tp^{iPr}$ = hydrotris(3-isopropylpyrazol-1-yl)borate; OAr = phenolate] (compound **T**) (figure 7).[93-94] As a notable feature both of the former *cis-*

oxosulfidomolybdenum(VI) complexes are stabilized by a weak, intra-molecular Mo(O)=S∵∵S=P interaction generating five membered rings. The bond order of the weak interaction was calculated to be approximately ⅓ but it still lengthens the Mo=S bond slightly. Interestingly and importantly this weak S∵∵S interaction prevents reduction of molybdenum/oxidation of sulfur and the subsequent dimerization leading to Mo$^V$O(S-S)Mo$^V$O species, which is an unwanted but common feature and one of the major obstacles in the chemistry of Mo$^{VI}$OS. In contrast and as expected in the absence of the stabilizing S∵∵S interaction the otherwise very similar Tp$^{iPr}$MoOS(OAr) dimerizes in solution.



(**S**)                                    (**T**)

Tp*MoO(S){SP(S)R$_2$}          Tp$^{iPr}$MoOS(OAr)
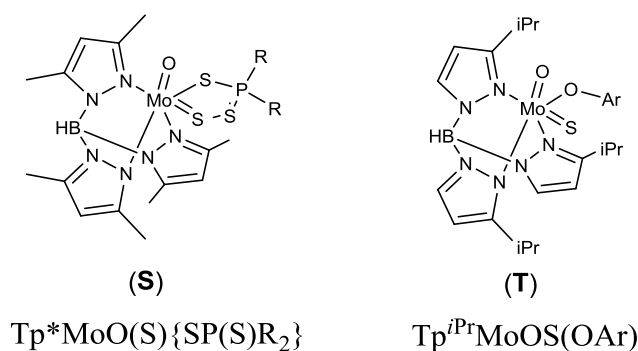
**Fig. 7. Tp*MoO(S){SP(S)PR$_2$ and  and  Tp$^{iPr}$MoOS(OAr)**

## 4.4. A carbene based approach to synthesize monodithiolene complexes of Mo

As indicated earlier under section 4.3, attempts to synthesize the monodithiolene complexes of molybdenum is the least documented area in dithiolene chemistry. The known method based on using bis(dithiolene) complexes as the starting material for monodithiolene complexes is a laborious process and has great disadvantages in terms of requiring strong chlorinating reagents like PhSeCl. In addition this method was not successful in the case of Mo(IV) compounds. This urges inorganic chemists to develop new synthetic routes leading to monodithiolene molybdenum complexes because of their significant

importance in bioinorganic chemistry. The strategy used in this work utilizes the convenient starting material $MoOCl_3$ supported by a carbene center with steric prominence without altering its oxidation state or consuming the chloride groups. A resulting carbene complex is then used for binding the dithiolene group. Such a pentacoordinated Mo(V) monodithiolene complex will serve as an excellent model complex for the intermediate of the catalytic turn over in SO. Any development of synthetic inorganic chemistry in preparing monodithiolene complexes can open the treasure of ideas in the curious minds of chemists towards exploring and extending further possibilities for attaining apt synthetic models for the SO and XO families of enzymes. In the present work, I report the synthesis and characterization of four NHC-molybdenum complxes: (1) $Mo(NHC)(CH_3CN)(CO)_4$, (2) $Mo(NHC)OCl_3$, (3) $Mo(NHC)OCl(tdt)$ and (4) $Mo(NHC)O_2Cl_2$. The first compound is prepared by selective replacement of one of the acetonitrile ligand of $Mo(CH_3CN)_2(CO)_4$ by free NHC. The second compound results from the free coordination of NHC to $MoOCl3$ in THF. The third complex has been prepared by the reaction of the sodium salt of toluene dithiolene (tdt) ligand with the second compound. The fourth compound was prepared by the replacement of chelating ligand dme (1,2-dimethoxyethane) of $MoO_2Cl_2(dme)$ by free NHC.

## 4.5. Experimental

### 4.5.1. Materials and methods

Syntheses of all compounds were done under strict inert atmosphere using Schlenk line techniques or a drybox and all solvents used were perfectly dry and flushed with nitrogen. The commercially obtained solid chemicals were used as received. NMR-spectra were recorded on NMR-spectrometers Bruker Avance DRX 500 or Bruker Avance DPX 300. The residual ^{1}H peak of the deuterated solvent was used as an internal standard and

tetramethysilane as external standard for $^1H$ spectra. Infrared spectra were collected on a Mattson Genesis FT-MIR spectrometer in the range of 4000 - 400 $cm^{-1}$ using KBr pellets. Mass spectra were recorded with a Finnigan MAT System 8200 for FAB spectra ionization was achieved using 3-nitrobenzylalcohol. Elemental analyses were carried out with a 4.1 Varido EL 3 Analyzer from Elementar. Suitable crystals were mounted on a glass fiber and data was collected on an IPDS II Stoe image-plate diffractometer (graphite monochromated Mo $K_\alpha$ radiation, $\lambda$=0.71073 Å at 133(2) K. The data was integrated with X-Area. The structures were solved by Direct Methods (SHELXS-97) and refined by full-matrix leastsquares methods against $F^2$ (SHELXL-97).[95] All non-hydrogen atoms were refined with anisotropic displacement parameters.

**4.5.2. Preparation of Mo(NCCH$_3$)$_2$(CO)$_4$·CH$_3$CN; (1):** Molybdenum hexacarbonyl was suspended in dry acetonitrile and dissolved by heating to 80$^o$C for 8 h. Upon cooling to -20$^o$C a mixture of Mo(CO)$_6$ and Mo(CO)$_4$(NCCH$_3$)$_2$ · CH$_3$CN crystallized. 0.60 g of this mixture was redissolved in 24 ml of acetonitrile. After 20 hours at -20$^o$C a first fraction of Mo(CO)$_6$ crystallized. The remaining solution was transferred to another flask and was evaporated to 15 mL. On cooling to -35$^o$C, Mo(NCCH$_3$)$_2$(CO)$_4$·CH$_3$CN was obtained.[96]

**4.5.3. Preparation of bis(2,6 -diisopropylphenyl)diazabutadiene; (2):** This compound was prepared by the condensation reaction between 2,6-diisopropylaniline and glyoxal.[97] A 500 ml round-bottom flask was charged with 2,6-diisopropylaniline (50 g, 282 mmol), glyoxal (15.74 ml , 140 mmol, 40% in water) and 250 ml of absolute ethanol. A few drops of formic acid were added as catalyst. The color of the reaction mixture turned from colorless to yellow immediately, and a yellow precipitate appeared after three hours. The reaction mixture was stirred for two days and the yellow solid was collected by filtration and washed with cold methanol to afford compound **2.**

Elemental analysis for $C_{26}H_{36}N_2$ (376.58 g/mol), Calcd (%): C: 82.93; H: 9.64; N: 7.44. Expt (%): C: 83.14; H: 9.23; N: 7.86. $^1$H-NMR (CDCl$_3$-[d$_1$], 500 MHz, 25°C, TMS): δ = 1.29-1.27 (d, 24H), 2.98-3.08 (sep, 4H), 7.22-7.29 (m, 6H), 8.19 (s, 2H).

**4.5.4. Preparation of 1,3-bis(2,6-diisopropylphenyl)-1H-imidazol-3-ium chloride; (3):** To a solution of bis (2,6-diisopropylphenyl)diazabutadiene (25 g, 66 mmol) in toluene (500 ml) paraformaldehyde (2 g, 66 mmol) was added in solid form. The reaction mixture was heated to 100°C till most of the paraformaldehyde was dissolved. It was then cooled to 40°C and 16.5 ml of HCl (66 mmol, 4 M in dioxane) was syringed in. The reaction mixture was heated to 70°C for 5 h during which time the color of the reaction mixture turned brown and a white precipitate appeared. It was then allowed to stir at room temperature for 36 h. The off-white precipitate was collected by filtration and washed with THF.[98]

$^1$H-NMR (CD$_2$Cl$_2$-[d$_2$], 500 MHz, 25°C, TMS): δ = 1.23-1.25 (d, 12 H), 1.26-1.28 (d, 12 H), 2.37-2.47 (sep, 4 H), 7.16-7.20 (t, 2 H), 7.36-7.44 (m, 4 H), 7.80 (s, 2 H), 11.00 (s, 1 H).

**4.5.5. Preparartion of 1,3-di(2,6-diisoprpylphenyl)imidazol-2-ylidene; (NHC); (4):** To a mixture of compound **3** (12 g, 27.69 mmol) and KO$^t$Bu (3.29 g, 27.69 mmol) was added THF (60 ml) at room temperature. The color of the resulting solution turned to brown immediately and a white precipitate was formed. The reaction mixture was stirred for 4 h, the solvent was removed in vacuo and the residue was taken up in hot toluene (70°C). The reaction mixture was then filtered through Celite. Evaporation of the volatiles afforded compound **4** as an off brown solid.[98]

Elemental analysis for $C_{27}H_{36}N_2$ (388.59 g/mol), calcd (%): C: 83.45; H: 9.34; N: 7.21. Expt (%): C, 83.09; H, 9.01; N, 7.68, $^1$H-NMR (C$_6$D$_6$-[d$_6$], 500 MHz, 25°C, TMS): δ = 1.12-1.14 (d, 12 H), 1.22-1.24 (d, 12 H), 2.84-2.98 (sep, 4 H), 6.57 (s, 2 H), 7.08-7.15 (m, 4 H), 7.19-7.25 (m, 2 H).

IR (KBr) [cm$^{-1}$]: 445.7 (w), 519.9 (vw), 548.6 (w), 633.0 (w), 660.9 (w), 754.7 (s), 769.7 (m),

801.1 (s), 806.8 (s), 859.5 (vw), 936.7 (s), 979.1 (w), 1028.2 (w), 1060.9 (m), 1095.5 (m), 1106.6 (w),  1163.3 (vw), 1180.0 (w), 1205.1 (vw), 1227.7 (w), 1263.5 (m), 1330.3 (w), 1361.3 (w), 1389.8 (m), 1469.7 (s), 1534.1 (vw), 1590.3 (w), 1669.5 (w), 1804.9 (vw), 1939.3 (vw), 1952.3 (w), 2606.7 (vw), 2753.2 (vw), 2868.4 (m), 2927.2 (m), 2962.5 (m), 3024.0 (w), 3060.9 (w), 3096.3 (vw), 3144.3 (w).

**4.5.6. Preparation of MoOCl$_3$; (5):** To a solution of MoCl$_5$ (5 g, 18 mmol) in 30 ml dichloromethane, a solution of Me$_3$Si-O-SiMe3 (2.98 g, 18 mmol) was slowly added over 15 minutes at room temperature.[99] An immediate reaction gives a brown solid as the product and the stirring was continued for another 2 h. The solid was allowed to settle and the supernatant liquid was decanted. The solid product was washed several times with dichloromethane, filtered and dried.

**4.5.7. Preparation of Mo(NHC)(NCCH$_3$)(CO)$_4$; (6):** This compound was obtained by the reaction of Mo(CH$_3$CN)$_2$(CO)$_4$·CH$_3$CN (0.1g, 0.302 mmol) with one equivalent of 1,3-di(2,6-diisoprpylphenyl)imidazol-2-ylidene (0.117g, 0.302 ) for 6 hours in THF at room temperature. Keeping a saturated solution of the compound in THF at 0$^o$C yielded pale yellow crystal blocks in 24 hours.

IR (KBr) [cm$^{-1}$]: 452.2 (w), 553.3 (w), 578.6 (w), 587.6 (w),  608.8 (m), 633.1 (w), 698.8 (m), 739.1 (w), 755.2 (m), 799.7 (m), 876.8 (vw), 938.9 (w), 959.2 (w), 1025.8 (w), 1041.5 (w), 1060.7 (w), 1071.5 (w), 1102.0 (w), 1118.1 (w), 1179.5 (w), 1200.4 (vw), 1235.1 (vw), 1261.6 (w), 1291.8 (w), 1327.5 (w), 1364.3 (w), 1391.1 (w), 1446.1 (w), 1465.3 (m), 1564.6 (vw), 1593.5 (vw), 1700.8 (vw), 1816.0 (s), 1864.0 (s), 1901.5 (s), 1928.4 (s), 1972.9 (w), 1995.2 (w), 2010.4 (s), 2059.4 (m), 2272.4 (vw), 2357.7 (vw), 2874.0 (w), 2931.2 (w), 2966.7 (m), 3013.6 (vw), 3037.1 (vw), 3073.3 (w), 3144.8 (vw), 3174.9 (vw), 3892.2 (vw).

**4.5.8. Preparation of Mo(NHC)OCl$_3$; (7):** To a solution of MoOCl$_3$ (1 g, 4.58 mmol) in THF (20 ml), NHC (1.78 g, 4.58 mmol) in 15 ml THF was added at -60$^o$C while stirring and allowed to warm to room temperature. The mixture was stirred for 6 h at room temperature to obtain a dark green solution. THF was completely evaporated, the residue was redissolved in toluene and filtered to collect the clear solution. Keeping this solution at -35$^o$C yielded green crystals of Mo(NHC)OCl$_3$.

Elemental analysis for C$_{27}$H$_{36}$Cl$_3$MoN$_2$O (606.89 g/mol), Calcd (%): C: 53.43; H: 5.98; N, 4.62. Expt (%):C: 53.89; H: 6.34; N, 4.47. IR (KBr) [cm$^{-1}$]: 459.3 (vw), 634.5 (vw), 705.1 (w), 757.1 (s), 803.0 (s), 924.0 (w), 947.1 (w), 970.6 (w), 991.3 (w), 1013.1 (s), 1060.1 (w), 1112.1 (w), 1182.9 (w), 1207.7 (w), 1261.4 (w), 1290.6 (vw), 1328.4 (w), 1352.2 (vw), 1364.9 (m), 1386.6 (m), 1404.8 (m), 1442.2 (m), 1465.6 (s), 1559.5 (w), 1595.2 (w), 1653.7 (w), 2345.7 (w), 2362.9 (w), 2870.7 (m), 2929.8 (m), 2966.9 (s), 3032.3 (vw), 3071.3 (vw), 3143.2 (w), 3171.5 (w). EI-MS: 607 [C$_{27}$H$_{36}$Cl$_3$MoN$_2$O]$^+$.

**4.5.9. Preparation of Mo(NHC)OCl(tdt); (8):** To a solution of Mo(NHC)OCl$_3$ (1g, 1.65 mmol) in 20 ml THF cooled in a aceton-dry ice slush bath, was added 0.33 g of sodium 4-methylbenzene-1,2-bis(thiolate), (Na$_2$tdt), suspended in 30 ml THF cooled to -40$^o$C. The solution was stirred and allowed to warm to room temperature slowly. After the solution turned to dark green it was stirred again for 2 h. THF was removed in vacuum and the compound was extracted with toluene.

IR (KBr) [cm$^{-1}$]: 445.5 (w), 483.0 (vw), 545.7 (w), 634.7 (vw), 661.4 (w), 680.2 (w), 701.9 (w), 754.5 (w), 798.5 (s), 865.3 (m), 964.6 (w), 1020.4 (s), 1093.8 (s), 1202.7 (vw), 1262.3 (s), 1327.8 (w), 1365.6 (vw), 1387.4 (w), 1400.1 (w), 1457.4 (w), 1542.4 (vw), 1587.3 (vw), 2345.9 (vw), 2376.1 (vw), 2868.9 (w), 2963.9 (m). EI-MS: 691 [C$_{34}$H$_{42}$ClMoN$_2$OS$_2$]$^+$

**4.5.10. Preparation of Mo(NHC)O$_2$Cl$_2$; (9):** To a solution of MoO$_2$Cl$_2$(dme) (1g, 3.46 mmol) in 15 ml THF cooled to -20$^o$C, NHC (1.34 g, 3.46 mmol) dissolved in 15ml cold THF was added drop wise. A light green color appeared after the addition and the reaction mixture was stirred overnight to complete the reaction. The solution was dried under vacuum and the compound was extracted with toluene. A concentrated solution of the compound in toluene affords light green crystals at room temperature.

## 4.6. Results and discussion

This work presents four NHC supported molybdenum complexes one of which bearing a biologically important dithiolene group. Figure 8 shows the synthetic steps involved in the preparation of compounds described in this chapter. During the formation of compound **6**, one of the two acetonitriles is replaced by the better electron donating ligand, NHC. In sections 4.1 and 4.2, reactions involving the replacement of CO groups by NHCs were described in brief. It was found that more than one CO could be replaced by NHC in certain cases to form dicarbene complexes. Here, the CO groups in compound **1** remain intact and only one acetonitrile group undergoes replacement of carbene, due to the fact that the used carbene is bulky and acetonitrile is more labile than the carbonyl group. Compound **6** carries the formerly free NHC coordinated to the Mo(0) center with one acetonitrile and four carbonyl groups. This compound crystallizes in the monoclinic space group P 21/m with the cell dimensions a=8.8489(18), b=19.551(4), c=9.4000(19) and β=106.64(3). Figure 9 shows the molecular structure of compound **6** obtained by X-ray diffraction method. The co-ordination geometry around the metal center is distorted octahedral (figure 10) with a mirror plane passing through the molybdenum center, the NHC
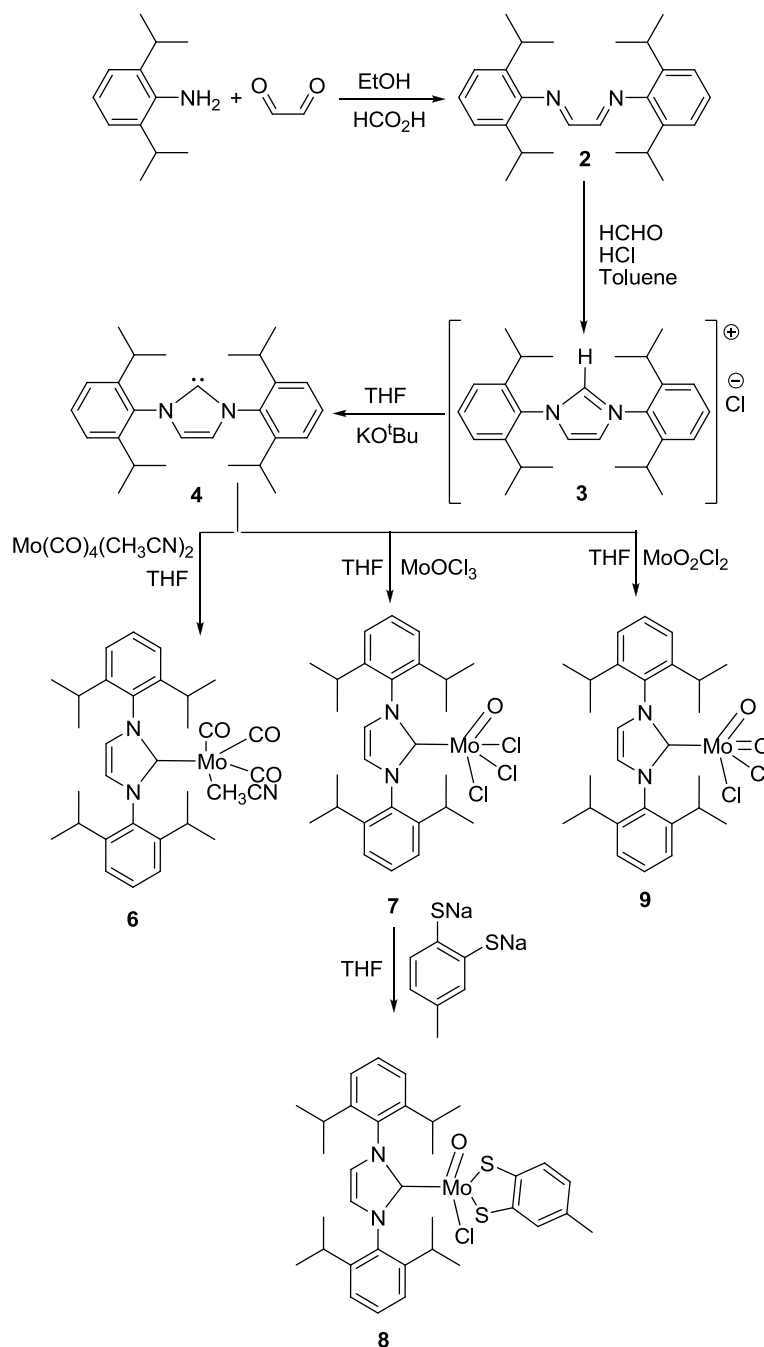
**Fig. 8. Synthetic routes for NHC molybdenum complexes**

and the acetonitrile ligand, dividing the carbene moiety into two equal parts. The Mo-C-O

bond *trans* to the carbene is almost liner (Mo1-C2-O2 =178.838°) as expected since it is the

most exempted from the steric strain induced by the bulkiness of the carbene ligand. The

carbonyl group *trans* to the $CH_3CN$ has also a close to linear geometry with a Mo1-C1-O1

angle of 178.415°. This carbonyl group suffers little stress from the carbene because it lies in

the mirror plane and the bulky 2,6-diisopropylphenyl groups are pointing away from this plane.

Different is the case of the remaining two carbonyl groups which are comparatively close to the 2,6-diisoprpylphenyl groups. The 'would be linear geometry' of the Mo1-C3-O3 moiety has been distorted, giving rise to a bent structure with a Mo1-C3-O3 angle of 172.001$^o$. It can be seen that the oxygen atoms in these two carbonyl groups are pointing away from the carbene side of the molecule. The linear structure around the sp hybridized carbon atom C4 has been slightly distorted so that the C5 atom is leaning towards the carbene side giving rise to a N1-C4-C5 bond angle of 177.174$^o$. It should be noted that while the Mo1-C1 bond is in an angle of 94.840$^o$ with the molybdenum carbene bond Mo1-C7, the Mo1-N1 bond *trans* to it has been found to be leaning towards the carbene part of the molecule with a C7-Mo1-N1 bond angle of 82.416$^o$.
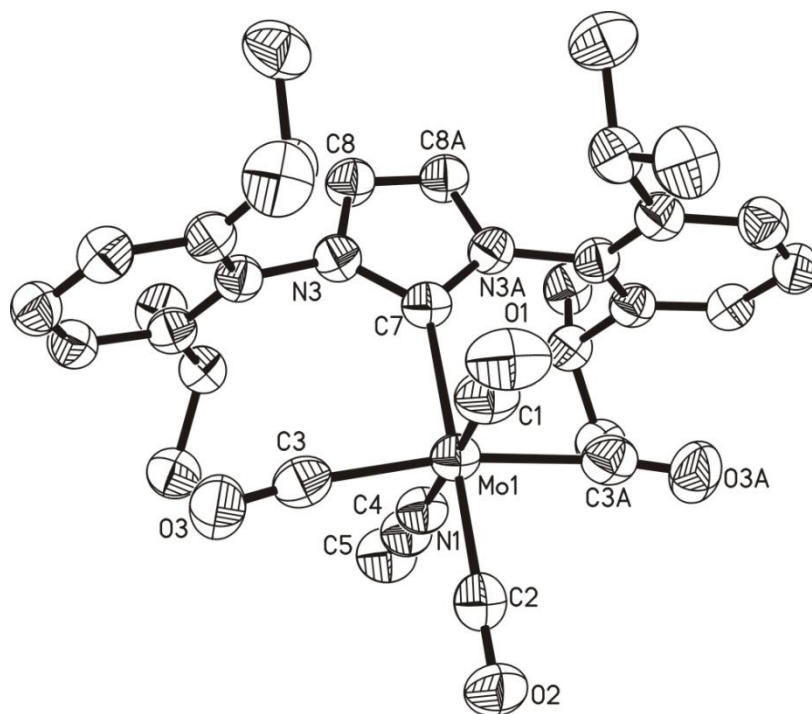


**Fig. 9. Molecular structure of compound 6 (ortep plot with 50 % probability ellipsoids; hydrogen atoms are omitted for clarity)**
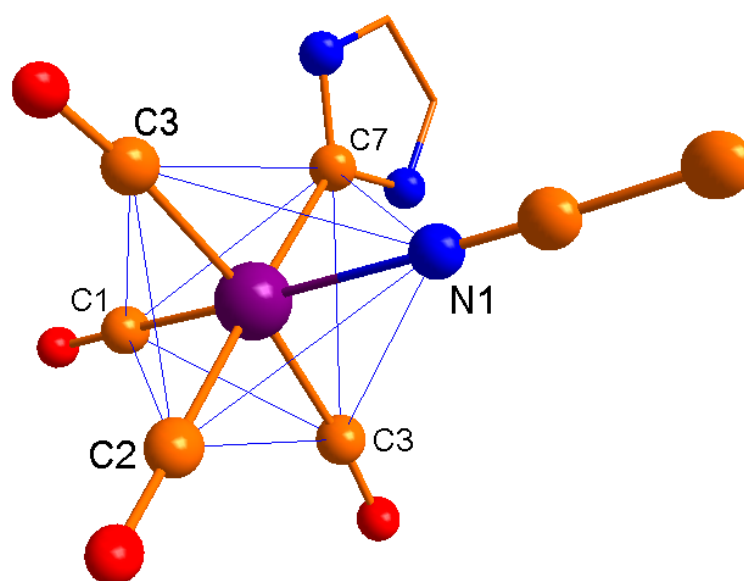
**Fig. 10. Distorted octahedral arrangement of atoms around the molybdenum atom in compound 6**

The relatively large Hirshfeld Test Differences (HTD) [100] around the molybdenum atom are typical for carbonyl complexes.[101] In fact the Hirshfeld test is based on the observation that bond stretching vibrations are small compared to other types of vibration and consequently the bond distance should not be altered too much during stretching vibrations, being the movement of composed atoms at two ends of a bond in synchrony. When it comes to the case of metal carbonyl complexes bearing the M-C-O fraction, the prerequisites of the Hirshfeld postulates is satisfactory only in the case of a C-O bond composed of atoms with equivalent masses connected by a covalent bond. Conversely, the HTD in the cases of atom pairs M-C or M-O neither relate the atoms of similar masses nor does M-O represent a pair of bonded atoms. A detailed analysis of the HTDs , $\Delta_{O-C}$, $\Delta_{C-M}$ and $\Delta_{O-M}$ on different carbonyl complexes by Braga et al.[101] showed that carbon atoms of terminal CO groups slide towards O atom along the M---O vector. The general stretching of the M-C bond is accompanied by an equivalent shortening of the C-O bond so that the M---O

distance remains almost constant. In the structure of compound **6**, the M-C bond distances of the carbonyl carbons are 1.9414 for Mo1-C1, 1.9171 for Mo1-C2 and 2.0452 for Mo1-C3. The relatively large bond lengths for Mo1-C2 and Mo1-C3 are in accordance with their observed HTDs. The bond distance between the carbene carbon atom and the molybdenum center is 2.2782 Å.

Unlike as usual, the structure is free of disorders, even if there are isopropyl groups present in the molecule which are very prone to it due to the relatively easy thermal rotations possible for the end carbon atoms bound to a $sp^3$ carbon. Table 1 provides structural data of compound **6** with details of selected bond angles, bond lengths and other crystallographic parameters. The IR spectroscopic data is in good agreement with the structural information collected. The C≡N stretching band is observable at 2272 cm$^{-1}$. The metal carbonyl absorption bands are seen at 2010, 1928, 1901, 1894 and 1816 cm$^{-1}$ consistent with a *cis*-M(CO)$_4$ core.

**Table 1: Selected bond lengths and bond angles in compound 6**

| Bond lengths (Å) | | Bond angles (°) | |
|---|---|---|---|
| Mo1-C3 | 2.0452(39) | Mo1-C1-O1 | 178.415(517) |
| Mo1-C3A | 2.0452(39) | Mo1-C3-O3 | 172.001(342) |
| Mo1-C1 | 1.9414(52) | Mo1-C3A-O3A | 172.001(342) |
| Mo1-C2 | 1.9771(62) | Mo1-C2-O2 | 178.838(473) |
| Mo1-C7 | 2.2782(57) | Mo1-N1-C4 | 178.239(443) |
| C3-O3 | 1.1470(51) | Mo1-C7-N3 | 128.555(117) |
| C1-O1 | 1.1725(62) | Mo1-C7-N3A | 128.555(117) |
| C2-O2 | 1.1637(22) | N1-C4-C5 | 177.174(595) |

| | | | |
|---|---|---|---|
| C3A-O3A | 1.1470(51) | C7-N3-C8 | 112.015(316) |
| N1-C4 | 1.1394(60) | C7-N3-C8A | 112.015(316) |
| C4-C5 | 1.4630(71) | N3-C8-C8A | 106.815(321) |
| C7-N3 | 1.3722(45) | | |
| C8-C8A | 1.3314(53) | | |
| N3-C8 | 1.3887(50) | | |
| N3A-C8A | 1.3887(50) | | |
| N3-C10 | 1.4433(46) | | |

Compound **7** is the first of its kind to the best of my knowledge with an NHC coordinated to a Mo(V) center. The synthesis of this compound was first attempted using the green coloured starting compound $MoOCl_3(THF)_2$ obtained by treating cold THF with $MoCl_5$. Nevertheless preparing this starting material and purifying it is laborious as the reaction is very vigorous leaving unwanted side products. The isolation of the compound in this case is possible only through crystallization from a concentrated THF solution. The compound is very unstable and the yield is also comparably low. This disadvantage was overcome by the easy preparation of brown colored $MoOCl_3$ from dichloromethane by treating $MoCl_5$ with hexamethyldisiloxane at room temperature. The reaction is neither vigorous nor does it end up with a poor yield. The isolation is free of re-crystallization and purification can be done by dichloromethane extraction. The only byproduct formed is the highly volatile $Me_3SiCl$. The washing followed by drying under extreme vacuum renders pure $MoOCl_3$. Adding this compound to THF leaves a green solution resulting from the coordination of the solvent molecules to the molybdenum center. So in solution, the starting material is assumed to have an octahedral geometry with six atoms around the molybdenum

center. On addition of the free NHC, both solvent molecules which are assumed to be at the molybdenum center are replaced by the sterically demanding carbene ligand. Thus the atomic arrangement around the molybdenum undergoes a transition from octahedral to distorted square pyramidal. Figure 11 shows the molecular structure and atom numbering scheme for compound **7**. Figure 12 shows the molecular packing of compound **7** in the crystal. Table 2 summarizes the selected bond lengths and bond angles of compound **7**.
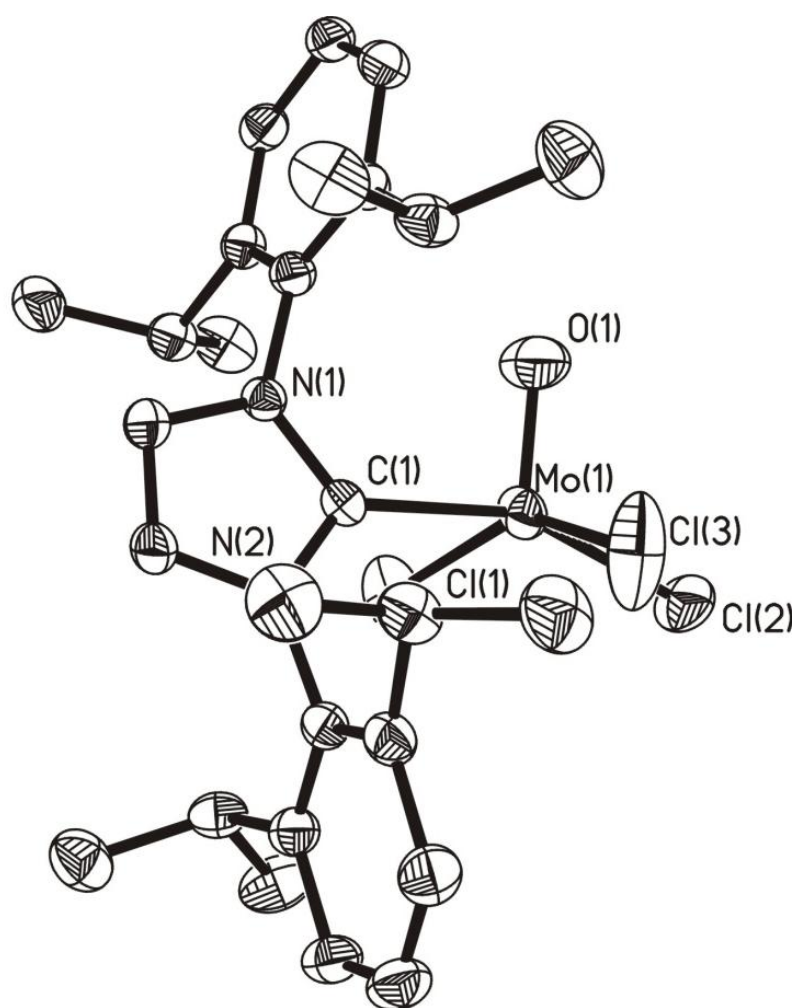


**Fig. 11. Molecular structure of compound 7 (ortep plot with 50 % probability ellipsoids, hydrogen atoms are omitted for clarity)**
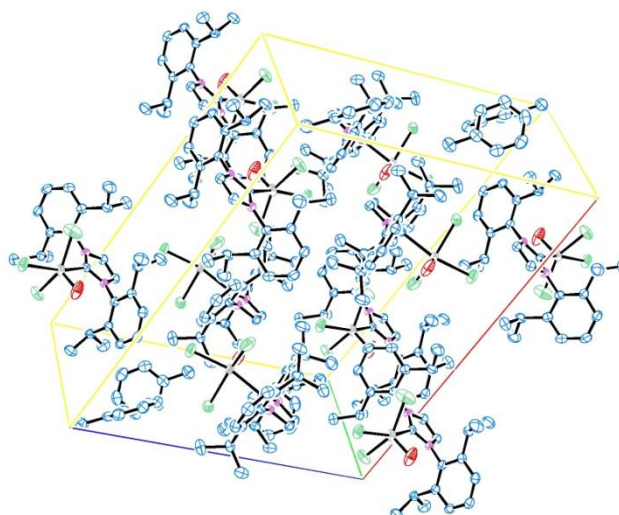
**Fig. 12. Molecular packing in the crystal of compound 7**

As indicated earlier, compound **7** has a molybdenum(V) center in a distorted square pyramidal environment. The three chlorine atoms bound to molybdenum are showing different bond distances to Mo: Mo1-Cl1 = 2.3303, Mo1-Cl2 = 2.3497 and Mo1-Cl3 = 2.2576 Å. The bond length of the carbene carbon atom to molybdenum is 2.2131 Å. It should be noted that this bond distance in comparison with the similar bond in compound **6** is shorter by 0.0651 Å. The difference in bond length can be attributed to the difference in the oxidation state of the molybdenum which will be addressed later in this section.

The distorted square pyramidal geometry around the metal center is depicted in figure 13. The base of the pyramid is constituted by the atoms C1, Cl1, Cl2 and Cl3 while O1 occupies the apex position. The distorted square base has the edge lengths: C1-Cl1 = 3.1090, Cl1-Cl2 = 3.2265, Cl2-Cl3 = 3.2358 and Cl3-C1 = 3.089 Å. The distances of the basal atoms to the apex are: C1-O1 = 2.9375, Cl1-O1 = 3.2208, Cl2-O1 = 3.1830, Cl3-O1 = 3.1695 Å.
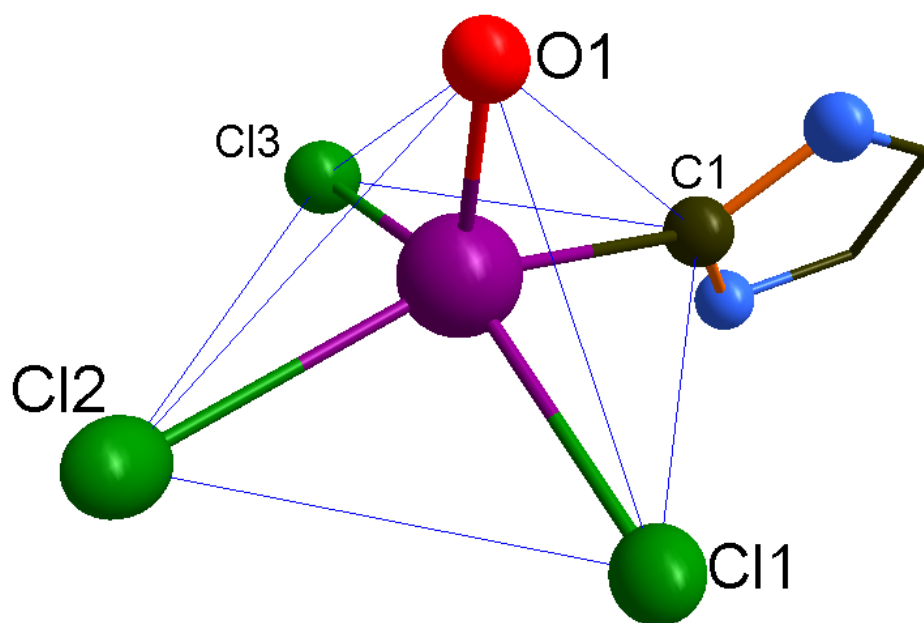
**Fig. 13. Square pyramidal arrangement of atoms around the molybdenum center in compound 7**

**Table. 2: Selected bond lengths and bond angles in compound 7**

| Bond lengths (Å) | | Bond angles (°) | |
|---|---|---|---|
| Mo1-Cl1 | 2.3303(12) | O1-Mo1-Cl1 | 106.791(131) |
| Mo1-Cl2 | 2.3497(11) | O1-Mo1-Cl2 | 104.099(093) |
| Mo1-Cl3 | 2.2576(14) | O1-Mo1-Cl3 | 107.397(128) |
| Mo1-O1 | 1.6498(28) | O1-Mo1-C1 | 97.946(120) |
| Mo1-C1 | 2.2131(29) | N1-C1-N2 | 104.733(229) |
| C1-N1 | 1.3582(36) | | |
| C1-N2 | 1.3565(35) | | |
| C14-C15 | 1.3394(41) | | |

The most important reactivity of the Mo(NHC)OCl$_3$ complex in the context of this work is that with dithiolenes. On reaction with the sodium salt of toluene dithiol, it affords Mo(NHC)OCl(tdt) by the elimination of two molecules of sodium chloride. Monodithiolene molybdenum complexes are particularly important for bioinorganic chemists as they serve as rare model complexes relevant for the sulfite oxidase and xanthine oxidase families of enzymes. As mentioned previously in brief, such mono-dithiolene complexes were regarded as unusual and difficult to synthesize. The first and last and very difficult synthetic pathway for realizing this type of complexes bearing a Mo(V) center with one dithiolene group was described by the Holm group.[102] In this method, *bis*-dithiolene complexes, for example, [Mo$^V$O(S$_2$C$_2$Me$_2$)$_2$]$^{1-}$ or [Mo$^V$O(bdt)$_2$]$^{1-}$ (bdtH$_2$ = 1,2 benzene-dithiol) are reacted with PhSeCl in a way that one of the ene-dithiolate ligands is replaced by two chlorides forming [Mo$^V$OCl$_2$(S$_2$C$_2$Me$_2$)]$^{1-}$ or [Mo$^V$OCl$_2$(bdt)]$^{1-}$ respectively. The synthesis of bis-dithiolene species itself as a starting material for obtaining the monodithiolene species is a laborious job and the overall yield is very low. Moreover, the use of PhSeCl often results in unwanted side products if not carefully controlled. I hereby report the first method to prepare a monodithiolene complex of molybdenum(V) supported on an NHC. The complex not only exhibits a square pyramidal shape but also carries the essential oxo and dithiolene groups. Attempts to obtain single crystals of this compound were not successful though different methods were tested. Figure 14 shows the mass spectrum obtained for this complex and its theoretical spectrum which are in excellent agreement.
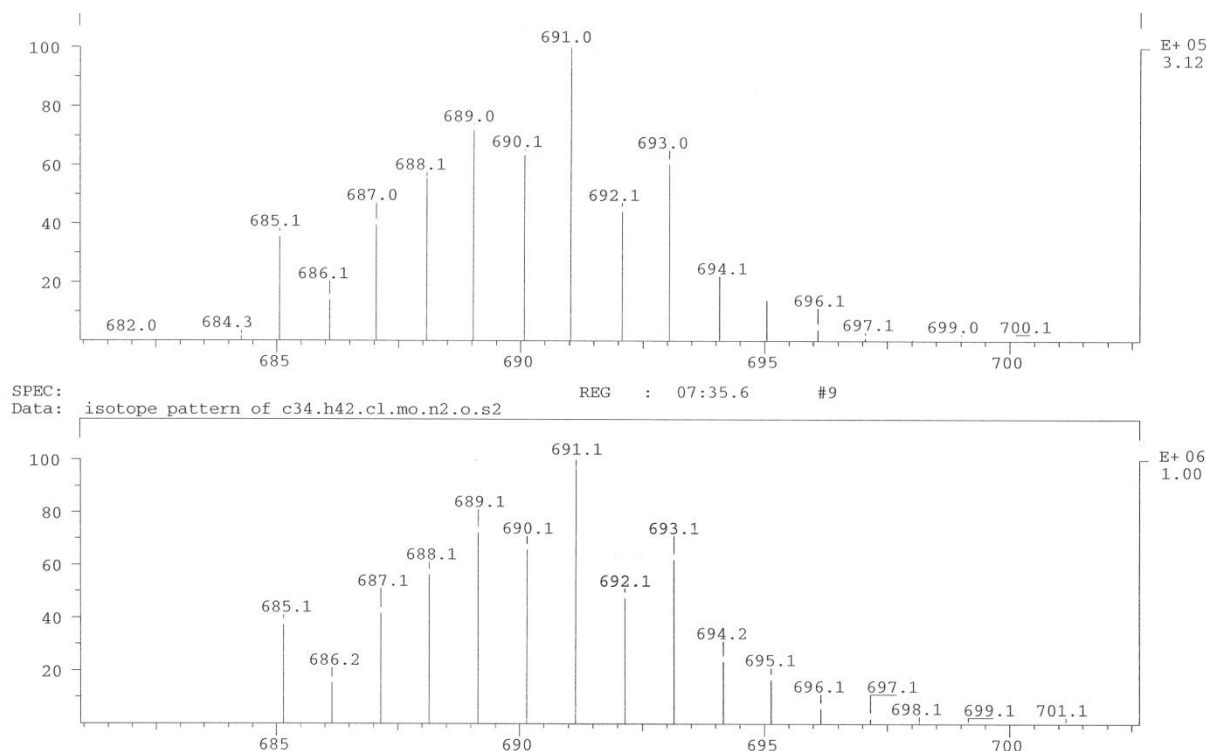
**Fig. 14. MASS spectrum (EI-MS) of compound 8**

The easy and direct synthesis of this type of a compound is especially important because the coordination environment and geometry mimics the proposed Mo(V) intermediate in the catalytic cycle of sulfite oxidase as shown in figure 15. The intermediate compound highlighted red in figure 15 has a Mo(V) center with a square pyramidal geometry. The oxygen atom is in the apical position and the two corners of the square base are occupied by the dithiolene sulfur atoms of MPT. The remaining two basal positions are filled by the sulfur atom of a cysteinate ligand and a hydroxyl group. In a similar manner, compound **8** is proposed to carry the oxygen atom at the apical position of a square pyramid with two dithiolene-sulfur donor atoms at the base and two additional monodentate ligands completing the coordination sphere. Further experiments are in progress to exchange the remaining chlorine atom with a thiolate species analogous to the amino acid ligand present in the natural enzyme centers. Yet another possibility is to introduce a hydroxyl group which will be of highest interest for anyone interested in molybdenum cofactors.
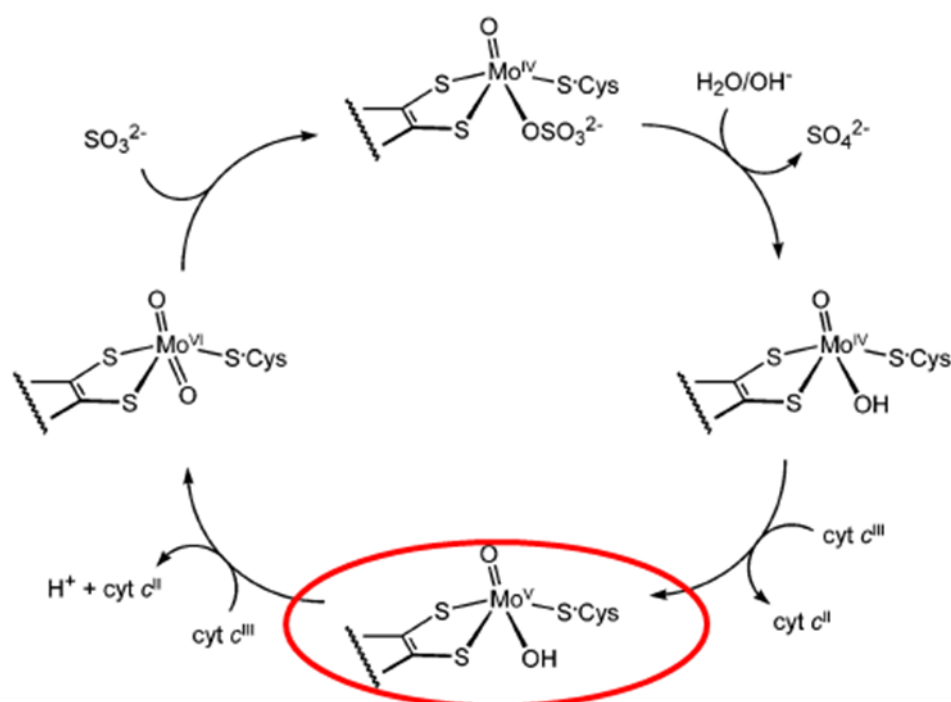
**Fig. 15. Proposed catalytic cycle in sulfite oxidase**

It was stated earlier that there are only a few mono NHC complexes of Mo(VI) reported and none of them were structurally characterized. I hereby report the first crystal structure of a mono-NHC MO(VI) complex, $MoO_2Cl_2(NHC)$ (**9**). Compound **9** was obtained by the replacement of a bidentate ligand dme from a Mo(VI) center by free NHC. $MoO_2Cl_2(dme)$ has octahedral geometry and the molybdenum in this compound is coordinatively saturated. This renders $MoO_2Cl_2(dme)$ relatively stable for long time. Replacement of dme by the monodentate NHC transforms the hexa-coordinate Mo(VI) to an air and moisture sensitive penta-coordinated complex. As described in section 4.2 previous attempts to synthesize NHC complexes of $MoO_2Cl_2$ afforded bis or tris carbene compounds of Mo(VI) in most cases. This was concluded as a direct result of selecting non-sterically demanding NHCs. In the present study, this difficulty to obtain mono-NHC complexes of $MoO_2Cl_2$ has been overcome by using the sterically demanding NHC compound **4**.

Compound **9** crystallizes in the monoclinic space group P 21/c with the cell dimensions a = 21.428(4), b = 9.839(2) and c = 17.043(3) Å and β = 108.52°. Figure 16 shows the molecular structure of this compound. The structure shows distorted trigonal bipyramidal geometry around the molybdenum center (figure 17). The equatorial positions are occupied by O1, O2 and Cl2 and the axial positions by C1 and Cl1. Both axial atoms are leaning towards Cl2. The distorted trigonal bipyramid has the edge lengths: Cl1-Cl2 = 3.1738, Cl1-O1 = 3.1130, Cl1-O2 = 3.0795, Cl2-Cl1 = 2.9432, O1-Cl1 = 2.8341, O2-Cl1 = 2.8005, Cl2-O1 = 3.5816, O1-O2 = 2.6927 and Cl2-O2 = 3.6535 Å. The important bond lengths and bond angles in compound **9** are summarized in table 3.
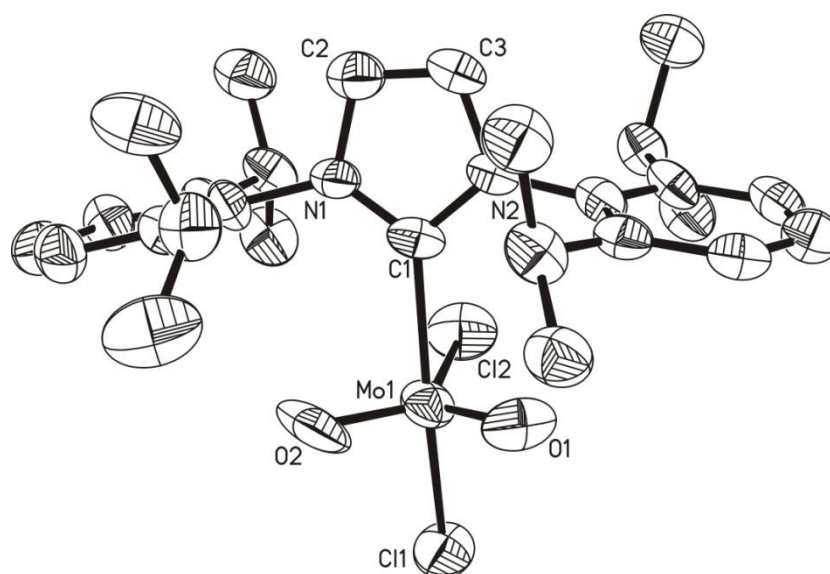


**Fig. 16. Molecular structure of compound 9 (ortep plot with 50 % probability ellipsoids; hydrogen atoms are omitted for clarity)**
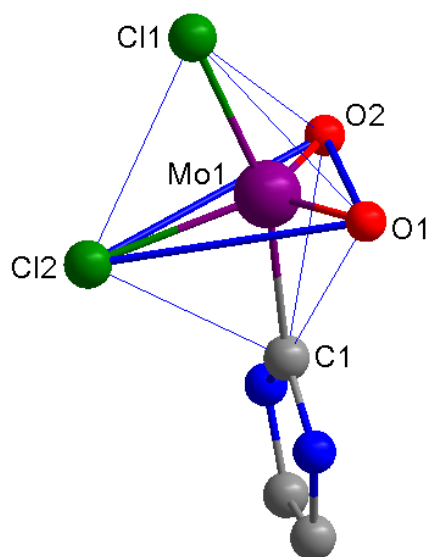
**Fig. 17. Trigonal bipyramidal geometry in compound 9**

**Table 3: Selected bond lengths and angles in compound 9**

| Bond lengths (Å) | | Bond angles (°) | |
|---|---|---|---|
| Mo1-Cl1 | 2.3605(35) | O1-Mo1-Cl1 | 99.510(302) |
| Mo1-Cl2 | 2.3853(43) | O2-Mo1-Cl1 | 98.560(334) |
| Mo1-O1 | 1.6766(98) | Cl2-Mo1-Cl1 | 83.943(139) |
| Mo1-O2 | 1.6574(105) | O1-Mo1-C1 | 91.503(406) |
| Mo1-C1 | 2.2414(103) | O2-Mo1-C1 | 90.560(418) |
| C3-N2 | 1.4005(147) | Cl2-Mo1-C1 | 78.944(298) |
| C2-N1 | 1.3983(140) | Cl1-Mo1-C1 | 162.767(274) |
| C2-C3 | 1.3419(176) | | |

The two Mo-Cl bonds in compound **9** have slightly different lengths: Mo1-Cl1 = 2.3605 and Mo1-Cl2 = 2.3853 Å. The lengths of the Mo-O bonds vary too: Mo1-O1 = 1.6766 and Mo1-O2 = 1.6574. The bond distance between the carbene carbon atom and Mo is Mo1-

C1 = 2.2414, which is less than the corresponding bond length in **6** (2.2782 Å; octahedral Mo(0)) but greater than that in **7** (2.2131 Å; square pyramidal Mo(V)). However the Mo-C bond length reported here for compound **9** is not strictly reliable because of the relatively high R vale (R =12.26, wR2 = 29.51 %) for the crystal of this compound. Since there are no other structures of carbene complexes reported for molybdenum (V and VI), a comparison to similar compounds is not possible at this stage. However, a careful survey of the Mo-C bond length of the reported carbene complexes of Mo(0 & II) could still be helpful. An Mo(0)-C bond distance of 2.26 Å was found in the Mo(NHC)(CO)$_5$ complex (**U**) (figure 13) prepared by Liu et al., where NHC is the simple imidazol-2-ylidene.[103] Even though this value is close to the observed value in the Mo(0) complex, there are exceptions too. In the *cis*- and *trans*-Mo(NHC)$_2$(CO)$_4$ (**V** and **W**) complexes (where NHC is 1,3-dimethylimidazol-2-ylidene) prepared by Lappert et al.[104-105] the Mo-C bond distances observed are 2.293 and 2.232 for *cis* and *trans* isomers respectively. The value seen in the *cis* isomer is close to the observed bond distance in our Mo(0) complex while that in the *trans* isomer is closer to the observed value in our Mo(V) complex. Nevertheless, all values mentioned above for the bond distance between the carbene carbon atom and Mo(0) are greater than that in the Mo(V)-NHC complex reported here. At the same time equivalent bond distances reported in some of the Mo(II) NHC complexes show a medium value in between that observed in Mo(0) and the new Mo(V) complexes. For example, in cyclopentadienyl molybdenum(II) N-heterocyclic carbene complexes **X(i-v) and Y** prepared by Zhao and coworkers [76] very recently, the M(II)-C bond distances observed are 2.224 (**X-i**), 2.241 (**X-ii**), 2.441 (**X-iii**), 2.221(**X-iv**), 2.224 (**X-v**) and 2.249 Å (**X**). All these bond distances are larger than Mo(V)-C and smaller than Mo(0)-C. So, it can be concluded that there is a trend in the bond distance between the carbene carbon atom and the molybdenum in NHC complexes which heavily

depends on the oxidation state of the metal. However, the observed Mo-C bond length in compound **9** (despite its greater R values) is not fitting with this trend and a further structural analysis of this compound with better quality crystals is necessary to continue this discussion more confidently. Table 4 lists the above discussed bond lengths in the mono NHC molybdenum complexes with the metal oxidation states, 0, II, V and VI.

**Table 4: Metal-carbene bond lengths Mo-NHC compounds**

| Oxidation state | Compound ID | Mo-C bond length (Å) |
|---|---|---|
| 0 | U | 2.26 |
| | V | 2.293 |
| | W | 2.232 |
| | 6 | 2.278 |
| II | X-i | 2.224 |
| | X-ii | 2.241 |
| | X-iii | 2.441 |
| | X-iv | 2.221 |
| | X-v | 2.224 |
| V | 7 | 2.213 |
| VI | 9 | 2.241 |

Before interpreting the above observed trend in carbene-metal bond distances, it should be admitted that our understanding of the bonding of NHC ligands to transition metals is still limited, and constitutes a topic of ongoing research activity. After Arduengo's NHC was reported, in the first few years, the wide spread use of NHC all over the scientific community resulted in a number of complexes, but with the notion that the NHC to transition metal bond only constitutes a simple σ donation. This concept was further affirmed by theoretical calculations on transition metal complexes of the type NHC→MCl, where M = Cu, Ag, Au.[106] However, in the early 2000s on the basis of structural and electronic data of group 11 NHC complexes, a significant amount of π-interaction between the metal and carbene was proposed by Tulloch et al [107] and Hu et al.[108] A further theoretical investigation by Hu et al. supported this proposal.[109] In a recent computational

study by Jacobsen et al. [110] on the $\pi$-Acidity and $\pi$-basicity of N-heterocyclic carbene ligands, it was concluded that besides $\sigma$ donation, there are two other significant types of $\pi$-interactions, namely $\pi$ donation as well as $\pi$ back donation work. While $\sigma$ donation and $\pi$ donation is from ligand to transition metal, the $\pi$ back donation is from metal to ligand. Jacobsen's studies revealed that even the $d^0$ systems show a significant amount of $\pi$-backdonation around 65% of the total $\pi$-bonding contribution. This amount increases with increasing d-electron count and takes on values around 90% for $d^{10}$ complexes. Whereas for systems with a low d electron count both $\pi$ donation as well as $\pi$-backdonation constitute important contributions to the orbital interaction term, the NHC ligand in systems with a high d electron count is best described as a $\pi$-acid. In another computational approach by Frenking and co-workers [111] on NHC$\rightarrow$ MCl type complexes it was found that the orbital interaction part of the carbene-metal bonding has about 20% $\pi$ back-bonding. They concluded that metal–carbene bonds are mainly held together by classical electrostatic attraction, which contributes at least to 65% of the binding interactions. On the wake of all these findings, the metal to carbene bond seems to have a complex nature. It is assumed that ligands that deplete electron density at the transition metal center due to $\pi$-acceptance lead to a decrease in attractive orbital interaction and at the same time to a decrease in Pauli repulsion. Also, Ligands that enhance electron density at the transition metal center due to secondary $\pi$-interaction lead to an increase in attractive orbital interaction and at the same time to an increase in Pauli repulsion. Based on all these assumptions, it is now possible to explain why the metal carbene bond is shorter in the case of Mo(V) than in the case of Mo(0). The electrostatic interaction between Mo(V) and the carbene center is supposed to be greater than in the case of Mo(0). This will lead to a shorter bond in the case of Mo(V). However, there may not be a linear relation between this interaction and the bond

length as the π interaction is governed by many factors. Mo(0) having a high d electron count is assumed to contribute greater to the π back donation as stated earlier. In addition to this, other groups like chlorine and CO are also supposed to have a significant influence on the metal carbene-interaction as the carbonyl ligands are π accepting and the chloride ligands are π donating. A proper assignment of the factors governing the bond energy and length demands sophisticated computational and spectroscopic approaches.



**U**                    **V**                    **W**

**X**                                         **Y**

(i) X =Br, $R_1$ =$R_2$ = Me                   R = 2,4,6-trimethylphenyl
(ii) X = Br, $R_1$= $R_2$ = $^nPr$
(iii) X = Br, $R_1$ = $R_2$ = Mes
(iv) X = Cl, $R_1$ = $R_2$ = Bz
(v) X = Br , $R_1$ = Me, $R_2$ = $^nPr$
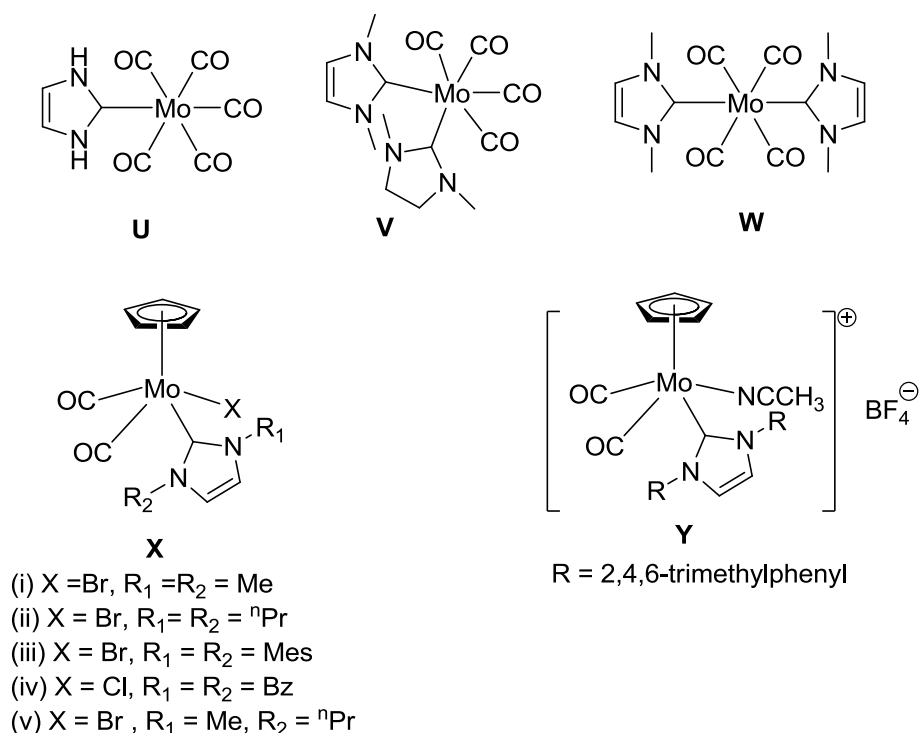
**Fig. 18. Liu, Lappert and Zhao NHC complexes of molybdenum in different oxidation states**

**References**

[1]    Arduengo, A. J.; Harlow, R. L.; Kline, M. *J. Am. Chem. Soc.* 113 (1991) 361

[2]    Öfele, K. *J. Organomet. Chem*. 12 (1968) 42

[3]    Wanzlick, H. -W.; Schönherr, H. -J. *Angew. Chem. Int. Ed. Engl.* 7 (1968) 141

[4]    Cardin, D. J.; Cetinkaya, B.; Lappert, M. F. *Chem. Rev.* 72 (1972) 545

[5]    Doyle, M. J.; Lappert, M. F. *J. Chem. Soc., Chem. Commun*. (1974) 679

[6]    Doyle, M. J.; Lappert, M. F.; McLaughlin, G. M.; McMeeking, J. *J. Chem. Soc., Dalton Trans.* (1974) 1494

[7]    Hitchchock, P. B.; Lappert, M. F.; Pye, P. L. *J. Chem. Soc., Dalton Trans.* (1977) 2160

[8]    Doyle, M. J.; Lappert, M. F.; Pye, P. L.; Terreros, P. *J. Chem. Soc., Dalton Trans.* (1984) 2355

[9]    Coleman, A. W.; Hitchcock, P. B.; Lappert, M. F.; Maskell, R.K.; Muller, J. H. *J. Organomet. Chem.* 296 (1985) 173

[10]   Lappert, M. F. *J. Organomet. Chem.* 358 (1988) 185

[11]   Cetinkaya, B.; Hitchcock, P. B.; Lappert, M. F.; Shaw, D. B.; Spyropoulos, K.; Warhurst, N. J. W. *J. Organomet. Chem.* 459 (1993) 311

[12]   Çetinkaya, B.; Hitchcock, P. B.; Küçükbay, H.; Lappert, M. F.; Al-Juaid, S. *J. Organomet. Chem.* 481 (1994) 89

[13]   Crudden, C. M.; Allen, D. P. *Coord.Chem. Rev.* 248 (2004) 2247

[14]   Scholl, M.; Trnka, T. M.; Morgan, J. P.; Grubbs, R. H. *Tetrahedron Lett.* 40 (1999) 2247

[15]   Scholl, M.; Ding, S.; Lee, C. W.; Grubbs, R. H. *Org. Lett.* 1 (1999) 953

[16]   Sanford, M. S.; Love, J. A.; Grubbs, R. H. *J. Am. Chem. Soc.* 123 (2001) 6543

[17]   Trnka, T. M.; Morgan, J. P. ; Sanford, M. S. ; Wilhelm, T. E. ; Scholl, M. ; Choi, T.; Ding, S.; Day, M. W.; Grubbs, R. H. *J. Am. Chem. Soc.* 125 (2003) 2546

[18]   Love, J. A. ; Sanford, M. S.; Day, M. W.; Grubbs, R. H. *J. Am. Chem. Soc.* 125 (2003) 10103

[19]   Seiders, T. J.; Williams, D. W. ; Grubbs, R.H. *Org. Lett.* 3 (2001) 3225

[20]   Weskamp, T.; Schattenmann, W. C.; Spiegler, M.; Herrmann, W. A. *Angew. Chem. Int. Ed.* 37 (1998) 2490

[21]    Herrmann, W. A. *Angew. Chem. Int. Ed.*  41 (2002) 1290

[22]    Weskamp, T.; Kohl, F. J.; Hieringer, W.; Gleich, D., Herrmann, W. A. *Angew. Chem. Int. Ed. Engl.* 38 (1999) 2416

[23]    Ackermann, L.; Furstner, A.; Weskamp, T.; Kohl, F. J.; Herrmann, W. A. *Tetrahedron Lett.* 40 (1999) 4787

[24]    Herrmann, W. A.; Elison, M.; Fischer, J.; Köcher, C.;  Artus, G. R. J. *Angew. Chem. Int. Ed. Engl.* 34 (1995) 2371

[25]    Herrmann, W. A.; Öfele, K.; Preysing, D. V.; Schneider, S. K. *J. Organomet. Chem.* 687 (2003) 229

[26]    Herrmann, W. A.; Reisinger, C. -P.; Spiegler, M. *J. Organomet. Chem.* 557 (1998) 93

[27]    Gstöttmayr, C. W. K.; Böhm, V. P. W.; Herdtweck, E.; Grosche, M.; Herrmann, W. A. *Angew. Chem. Int. Ed.* 41 (2002) 1363

[28]    Huang, J.; Stevens, E. D.; Nolan, S. P.; Petersen, J. L. *J. Am. Chem. Soc.* 121 (1999) 2674-2678

[29]    Viciu, M. S.; Germaneau, R. F.; Nolan, S. P. *Org. Lett.* 4 (2002) 4053

[30]    Viciu, M. S; Germaneau, R.F.; Navarro-Fernandez, O. ; Stevens, E. D.; Nolan, S. P. *Organometallics* 21 (2002) 5470

[31]    Huang, J.; Schanz, H. J.; Stevens, E. D.; Nolan, S. P. *Organometallics* 18 (1999) 2370

[32]    Hillier, A. C.; Sommer, W. J.; Yong, B. S.; Petersen, J. L.; Cavallo, L.; Nolan, S. P. *Organometallics* 19 (2003) 4327

[33]    Navarro, O.; Kaur, H.; Mahjoor, P.; Nolan, S. P. *J. Org. Chem.* 69 (2004) 3173

[34]    Fürstner, A.; Ackermann, L.; Gabor, B.; Goddard, R.; Lehmann, C. W.; Mynott, R.; Stelzer, F.; Thiel, O. R. *Chem. Eur. J.* 7 (2001) 3236

[35]    Pruehs, S.; Lehmann, C. W.; Fürstner, A. *Organometallics* 23 (2004) 280

[36]    Fürstner, A.; Thiel, O. R.; Lehmann, C. W. *Organometallics* 21 (2002) 331

[37]    Fürstner, A.; Thiel, O. R.; Ackermann, L.; Schanz, H. J.; Nolan, S. P. *J. Org. Chem.* 65 (2000) 2204

[38]    Fürstner, A.; Thiel, O. R.; Ackermann, L. *Org. Lett.* 3 (2001) 449

[39]    Fürstner, A.; Thiel, O. R.; Blanda, G. *Org. Lett.* 2 (2000) 3731

[40]    Fürstner, A.; Radkowski, K.; Wirtz, C.; Goddard, R.; Lehmann, C. W.; Mynott, R. *J. Am. Chem. Soc.* 124 (2002) 7061

[41]    Aıssa, Riveiros, R.; Ragot, J.; Fürstner, A. *J. Am. Chem. Soc*. 125 (2003) 15512

[42]    Van Veldhuizen, J. J.; Gillingham, D. G.; Garber, S. B.; Kataoka, O. ; Hoveyda, A. H. *J. Am. Chem. Soc.* 125 (2003) 12502

[43]    Van Veldhuizen, J. J.; Garber, S. B.; Kingsbury, J. S.; Hoveyda, A. H. *J. Am. Chem. Soc.* 124 (2002) 4954

[44]    Kingsbury, J. S.; Harrity, J. P. A.; Bonitatebus, P. J.; Hoveyda, A. H. *J. Am. Chem. Soc.* 121 (1999) 791

[45]    Hoveyda, A. H.; Gillingham, D. G.; Van Veldhuizen, J. J.; Kataoka, O.; Garber, S. B.; Kingsbury, J. S.; Harrity, J. P. A. *Org. Biol. Chem*. 2 (2004) 8

[46]    Garber, S. B.; Kingsbury, J. S.; Gray, B. L.; Hoveyda, A. H. *J. Am. Chem. Soc.* 122 (2000) 8168

[47]    Herrmann, W. A.; Köcher, C. *Angew. Chem. Int. Ed.* 36 (1997) 2162

[48]    Weskamp, T.;Böhm, V. P.W.; Herrmann, W. A. *J. Organomet. Chem*. 600 (2000) 12

[49]    Glorius, F. A. *Top. Organomet. Chem.* 21 (2007) 1

[50]    Kuhn, N.; Al-Sheikh, A. *Coord. Chem. Rev.* 249 (2005) 829

[51]    Schumann, H.; Glanz, M.; Winterfeld, J.; Hemling, H.; Kuhn, N.; Kratz, T. *Angew. Chem. Int. Ed.*  33 (1994) 1733

[52]    Arduengo III, A. J.; Tamm, M.; McLain, S. J.; Calabrese, J. C.; Davidson, F.; Marshall, W. J. *J. Am. Chem. Soc.* 116 (1994) 7927

[53]    Arnold, P. L.; Liddle, S. T. *Chem. Commun.* (2006) 3959

[54]    Oldham, W. J.; Jr., Oldham, S. M.; Scott, B. L.; Abney, K. D.; Smith, W. H.; Costa, D. A. *Chem. Commun.* (2001) 1348

[55]    Mehdoui, T.; Berthet, J. -C.; Thury, P.; Ephritikhine, M. *Chem. Commun.* (2005) 2860

[56]    Herrmann, W. A.; Elison, M.; Fischer, J. ;Köcher, C.; Artus, G. R. J. *Chem. Eur. J.* 2 (1996) 772

[57]    Herrmann, W. A.; Gerstberger, G.; Spiegler, M. *Organometallics* 16 (1997) 2209

[58]    Herrmann, W. A.; Schwarz, J.; Gardiner, M. G.; Spiegler, M. *J. Organomet. Chem.* 575 (1999) 80

[59]    Herrmann, W. A.; Schwarz, J.; Gardiner, M. G. *Organometallics* 18 (1999) 4082

[60]    Gardiner, M. G.; Herrmann, W. A.; Reisinger, C. -P.; Schwarz, I.; Spiegler, M. *J. Organomet. Chem.* 572 (1999) 239

[61]    Herrmann, W. A.; Bohm, V. P. W.; Reisinger, C. -P. *J. Organomet. Chem.* 576 (1999) 23

[62]    Bertrand, G.; Diez-Barra, E.; Fernandez-Baeza, J.; Gornitzka, H.; Moreno, A.; Otero, A.; Rodriguez-Curiel, R. I.; Tejeda, J. *Eur. J. Inorg. Chem.* (1999) 1965

[63]    Herrmann, W. A.; Mihalios, D.; Öfele, K.; Kiprof, P.; Belmedjahed, F. *Chem. Ber.* 125 (1992) 1795

[64]    Öfele, K.; Herrmann, W. A.; Mihalios, D.; Elison, M.; Herdtweck, E.; Priermeier, T.; Kiprof, P. *J. Organomet. Chem.* 498 (1995) 1

[65]    Lappert, M. F.; Pye, P. L.; *J. Chem. Soc. Dalton Trans.* (1977) 2172

[66]    Hitchcock, P. B.; Lappert, M. F.; Pye, P. L. *J. Chem. Soc. Dalton Trans.* (1978) 826

[67]     Herrmann, W. A.; Gooβen, L. J.; Köcher, C.; Artus, G. R. J. *Angew. Chem. Int. Ed. Engl.*

35 (1996) 2805

[68]     Herrmann, W. A.; Köcher, C.; Gooβen, L. J.; Artus, G. R. J. *Chem. Eur. J.* 2 (1996) 1627

[69]     Herrmann, W. A.; Gooβen, L. J.; Artus, G. R. J.; Köcher, C. *Organometallics* 16 (1997)

2472

[70]     Kuhn, N.; Kratz, T.; Boese, R.; Bläser, D. *J. Organomet. Chem.* 470 (1994) C8

[71]     Öfele, K.;Herrmann, W. A.; Mihalios, D.; Elison, M.; Herdtweck, E.; Scherer, W.; Mink,

J. *J. Organomet. Chem.* 459 (1993) 177

[72]     Manriquez, J. M.; McAlister, D. R.; Sanner, R. D.; Bercaw, J. E. *J. Am. Chem. Soc.* 98

(1976) 6735

[73]     Rieke, V. R. D.; Kojima, H.; Öfele, K. *Angew. Chem.* 92 (1980) 550

[74]     Herrmann, W. A.; Lobmaier, G. M.; Elison, M. *J. Organomet. Chem.* 520 (1996) 231

[75]     Elena Mas-Marzá, Patrícia M. Reis, Eduardo Peris, Beatriz Royo, *J. Organomet. Chem*.

691 (2006) 2708

[76]     Li, S.; Kee, C. W.; Huang, K. -W. ; Hor, T. S. A.; Zhao, J. *Organometallics*  29 (2010)

1924

[77]     Hille, R. *J. Biol. Inorg. Chem.* 2 (1997) 804

[78]     Fischer, B.; Enemark, J. H.; Basu, P. *J. Inorg. Biochem.* 72 (1998) 13

[79]     Berg, J. M.; Holm, R. H. *J. Am. Chem. Soc.* 107 (1985) 917

[80]     Berg, J. M.; Holm, R. H. *J. Am. Chem. Soc.* 107 (1985) 925

[81]     Palanca, P.; Picher, T.; Sanz, V., Romero, P.G.; Llopis, E.; Domenech, A.; Cervilla, A.,

Chem. Commun. **(**1990) 531

[82]     Gheller, S. F., Schultz, B. E.; Scott, M. J.; Holm, R. H. *J. Am. Chem. Soc.* 114 (1992)

6934

[83]    Schultz, B. E., Gheller, S. F.; Muetterties, M. C.; Scott, M. J.; Holm, R. H.; *J. Am. Chem. Soc.* 115 (1993) 2714

[84]    Bray, R.C. *Rev. Biophys.* 21 (1988) 299

[85]    Xiao, Z.; Young, C. G.; Enemark, J. H.; Weddt, A. G., *J. Am. Chem. Soc.* 114 (1992) 9194

[86]    Mader, M. L.; Carducci, M. D.; Enemark, J. H. *Inorg. Chem.* 39 (2000)  525

[87]    Bonin, I.; Martins, B. M.; Purvanov, V.; Fetzner, S.; Huber, R. Dobbek, H. *Structure* 12 (2004) 1425

[88]    Mueller, A.; Diemann, E.; Rainer, J.; Boegge H. *Angew. Chem., Int. Ed.* 20 (1981)  934

[89]    Wieghardt, K.; Hahn, M.; Weiss, J.; Swiridoff, W. *Z. Anorg. Allg. Chem* 492 (1982) 164

[90]    Bristow, S.; Collison, D.; Garner, C.D.; Clegg, W. *Dalton Trans* (1983) 2495

[91]    Faller, J.W.; Ma, Y. *Organometallics* 8 (1989) 609

[92]    Wilson, G.L.; Greenwood, R.J.; Pilbrow, J.R.; Spence, J.T.; Wedd, A.G. *J. Am. Chem. Soc.* 113 (1991)6803

[93]    Laughlin, L. J.; Aston A. E.; Graham N. G.; Edward R. T. T.; Young, C. G. *Inorg. Chem.* 46 (2007)  939

[94]    Doonan, C. J.; Nielsen, D. J; Smith, P. D.; White, J. W.; George, G. N; Young, C. G. *J. Am. Chem. Soc.* 128 (2006)  305

[95]    Sheldrick, G. M. *Acta Crystallogr., Sect. A: Found. Crystallogr.* 64 (2008) 112

[96]    Biesemeier, F.;  Harms, K.; Müller, U.  *Z. Kristallogr. NCS* 218 (2003) 419

[97]    Yang, K.; Lachicotte, R.J.; Eisenberg, R. *Organometallics* 16 (1997) 5234

[98]    Jafarpour, L.; Stevens, E. D; Nolan, S. P. *J. Organomet. Chem.* 606 (2000) 49

[99]    Gibson, V. C.; Kee, T. P.; Shaw A., *Polyhedron* 9 (1990) 2293-2298

[100]   Hirshfeld, F. L.; *Acta. Cryst.* A32 (1976) 239

[101]   Braga, D.; Koetzle T.F., *Acta Cryst.* B44 (1988)151

[102]    Xiao, Z.; Bruck, M. A.; Enemark, J. H.; Young,C. G.; Wedd, A. G. *Inorg. Chem.* 35 (1996) 7508

[103]    Liu, C. -Y.; Chen, D. -Y.; Lee, G. -H.; Peng, S.-M.; Liu. S. -T. *Organomet.* 15 (1996) 1055

[104]    Lappert, M. F.; Pye, P. L.; McLaughlin, G. M. *J. Chem. Soc., Dalton Trans.* (1977) 1272

[105]    Lappert, M. F.; Pye, P. L. ; Rogers, A. J.; McLaughlin, G. M. *J. Chem. Soc., Dalton Trans.* (1981) 701

[106]    Boehme C.;Frenking, G. *Organometallics*  17 (1998) 5801

[107]    Tulloch, A. A. D.; Danopoulos, A. A.; Kleinhenz, S.;Light, M. E; Hursthouse, M. B.; Easthamon, G. *Organometallics* 20 (2001) 2027

[108]    Hu, X.; Tang, Y. ; Gantzel, P.; Meyer, K. *Organometallics*  22 (2003) 612

[109]    Hu, X.; Castro-Rodriguez, I.; Olsen, K.; Meyer, K. *Organometallics* 23 (2004) 755

[110]    Jacobsen, H.; Correa, A.; Costabile, C.; Cavallo, L. *J. Organomet. Chem.* 691 (2006) 4350

[111]    Nemcsok, D.; Wichmann, K.; Frenking, G. *Organometallics* 23 (2004) 3640

# MOLYBDENUM COMPLEXES OF BIPYRIDINE DERIVATIVES AND β-DIKETIMINATE AND THEIR DITHIOLENE CHEMISTRY

## 5.1. Molybdenum bipyridine complexes- General overview

Which is the most widely used category of ligands in the fundamental chemistry of transition elements? Such a question can provoke a number of answers, perhaps limited only by the subjectivity of the respondent! Highly viable candidates include Schiff bases, carbenes, ethylene diamines, bipyridines etc. Yet I would argue for bipyridine, based on the compelling number of examples possessing a common substructure including a 2,2'-bipyridine coordinated to any transition element. The chemistry of bipyridine supported molybdenum compounds has a long history stretching over decades. Chemists and spectroscopists took advantage of this type of compounds as it paves the way for generating soluble molybdenum complexes without altering their oxidation state. In addition to this, bipyridine has proven to make coordination complexes with molybdenum in different oxidation sates. Throughout the literature different bipyridine derivatives given in figure 1 have been used as chelating ligands for molybdenum in various oxidation states and in the

second half of the last century, attempts to understand the physical and chemical characteristics of this type of complexes were enormously advanced. However since the scope of this thesis is essentially dithiolene chemistry, and bpy- ligands are only used as co- or spectator ligands, bpy-transition metal chemistry will not be discussed in detail. Still, some representative examples showing the diversity in structure and synthesis of bpy chemistry that was reported within the past few decades will be described.

The bipyridine ligand has been used extensively in the complexation of metal ions since its discovery at the end of the nineteenth century.[1] There are symmetrical (2,2', 3,3', and 4,4') and asymmetrical (2,3', 2,4', and 3,4'), isomers of bipyridine. Out of these the 2,3'- and the 3,3'-bipyridines are found to be naturally abundant in certain varieties of tobacco.[2-3] The 2,2'-bipyridine ligand has been extensively used as a metal chelating ligand due to its robust redox stability and ease of functionalization. In contrast to other commonly used ligands, such as catechol, which is dianionic, and derivatives of the acetylacetonate ion, which are monoanionic, 2,2'-bipyridine is a neutral ligand. It thus forms both charged and neutral complexes with metals depending on their oxidation states and the nature of the other coordinated ligands. This property has been exploited in the design and synthesis of metal-bipyridine complexes for a variety of applications. This chapter focuses on molybdenum complexes of bipyridine derivatives with a few examples representing each category.

The synthesis and crystal structures of bipyridine complexes of molybdenum carbonyls are well documented. The facile reaction of $Mo(CO)_6$ with 2,2'-bipyridine in toluene affords $Mo(CO)_4(bpy)$. (bpy = 2,2'-bipyridine).[4] Oxidative decarbonylation of $Mo(CO)_6$ with $Me_3NO$ in the presence of bipyridine affords the same tetracarbonyl product in a better yield. Further, a stoichiometric replacement of carbonyl from $Mo(CO)_4(bpy)$ with
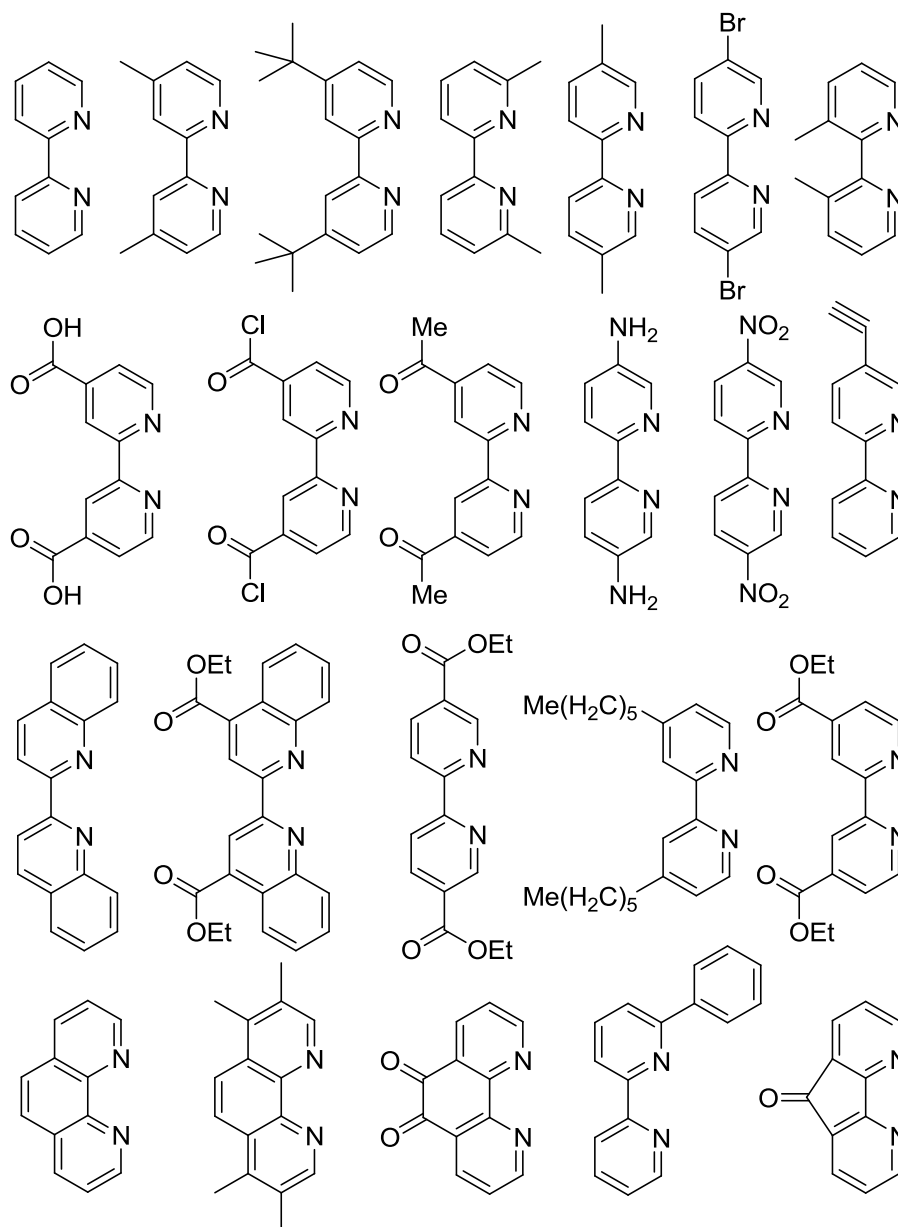
**Fig. 1. Common bipyridine ligands known to make complexes with molybdenum**

a unidentate bis(diphenylphosphino)methane results in the formation of Mo(CO)3(bipy)(dppm), (dppm= bis(diphenylphosphino)methane).[5] Reaction of the compounds Mo(CO)$_4$(bipy) with excess of chlorine and bromine leads to derivatives of the metals in oxidation states 4, 5, and 6.[6] Reaction in pure dichloromethane yields the derivatives M(bipy)X$_4$, while similar reactions in the presence of small amounts of ethanol lead to the oxo-trihalides MoO(bipy)X$_3$ [X=Cl,Br]. Reaction of bromine with the compound

Mo(CO)$_4$(bipy) in a 1:1 ethanol-dichloromethane solution yields MoO$_2$(bipy)Br$_2$ and the corresponding dichloride can be prepared by a metathesis reaction in boiling acetone. In addition to this molybdenum pentachloride can act as a starting material to form different bipyridine complexes. For example, MoCl$_5$ on treating with bipyridine yields Mo(bipy)Cl$_4$ in ether [7] and MoO(bipy)Cl$_3$ in moist CCl$_4$ [8].

[Mo(CO)$_4$L], [L= (bipy), 1,10-phenanthroline (phen), or 2,2′-dipyridylamine (dpa)] on reactions of triphenylcyclopropenyl bromide yield the two series of products [MoBr(CO)$_2$($\eta^3$-C$_3$Ph$_3$)L] and [MoBr(CO)$_2$($\eta^3$-C$_4$Ph$_3$O)L]. The cyclopropenyl complexes can be prepared from [MoBr(CO)$_2$($\eta^3$-C$_3$Ph$_3$)(NCMe)$_2$] by reaction with L in acetonitrile. Another example for bipyridine supported Mo(II) carbonyl is (isothiocyanato)dicarbonyl-2,2′-bipyridine-π-allylmolybdenum, NCS(CO)$_2$(C$_{10}$H$_8$N$_2$)(π-C$_3$H$_5$)Mo, reported by Graham et al..[9] The complex has essentially an octahedral arrangement of ligands. If it is viewed such that the 2,2′-bipyridine and dicarbonyl ligands lie in equatorial positions, the allyl and isothiocyanato ligands lie in the axial positions, one on each side of the equatorial plane. The equatorial ligands are each planar and dip away from the plane of the allylic carbon atoms. Another type of Mo(0) complexes involves only the three bypiridine ligands arranged in the octahedral fashion.

Marzilli and Buckingham reported the synthesis of bipyridine and 1,10-phenanthroline chelates of molybdenum(III) , [Mo(bipy)$_3$]Cl$_3$ and [Mo(phen)$_3$]Cl$_3$ respectively in a good yield.[10] The reaction of the ligands with MoCl$_3$ results in occupation of all six coordination sites around molybdenum pushing out the chloride ions to the outer sphere. They prepared [MoCl$_2$ (bipy)$_2$][MoCl$_4$(bipy)] by the direct reaction of K$_3$MoCl$_6$ with bipyridine. [MoCl$_3$(py)(phen)] and [MoCl$_3$(py)(bipy)] were obtained from the reaction of [MoCl$_3$(py)$_3$] with the respective ligands with the formation of [MoCl$_2$(phen)$_2$][MoCl$_4$(phen)] and [MoCl$_2$

(bipy)$_2$][MoCl$_4$(bipy)]. In 1968 Bois and coworkers extensively studied the electrochemistry of bipyridine complexes of molybdenum(III) chloride.[11] They synthesized trichloropyridinebipyridinemolybdenum(III), [Mo(py)(bipy)Cl$_3$] and Trichloropyridinephen-anthrolinemolybdenum(III), [Mo(py)(phen)Cl$_3$] by treating MoCl$_3$(py)$_3$ with bipyridine or phenanthroline with an excess of the Mo starting compound as a modification of the procedure by Marzilli and Buckingham to avoid the formation of Mo(II)-Mo(IV) binuclear complexes. Electrochemistry of the above molybdenum(III) complexes in acetonitrile, showed that the tendency for reduction of the metal is dependent on the nature of the aromatic $\pi$ system of the coordinated bipyridine. Increase in the electron acceptor character of the aromatic $\pi$ system causes a marked positive shift of the potential at which reduction occurs.

The reaction of donor ligands like diphenyl thiourea (dptu) with [Mo(CO)4(bipy)] yields [Mo(CO)$_3$(bipy)(dptu)].[12] The halogen oxidation of this complex results in the formation of different compounds heavily depending on which halogen is being used. For example, reaction of [Mo(CO)$_3$(bipy)(dptu)] with bromine or iodine will afford the heptacoordinated products [Mo(CO)$_3$(bipy)X$_2$] (X= Br, I), whereas the chlorine can replace both dptu and CO groups to give [MoCl$_4$(bpy)], the hexacoordinated Mo(IV)complex.[13] In addition to halides the bipyridine complexes of molybdenum oxyhalides in oxidation states V and VI have been documented in the literature. Dehydrohalogenation reaction of (bpyH$_2$)MoOCl$_5$ forms the Mo(V) complex, MoOCl$_3$(bipy), (figure 2).[14] This complex has been extensively studied for its electron paramagnetic resonance,[15] electrochemical behavior [16] and for chemical reactivity.[17-19] A similar product MoOCl$_3$(Me$_2$bipy), (Me$_2$bipy = 4,4'-dimethyl-2,2'-bipyridine) has also been reported.[20-21]
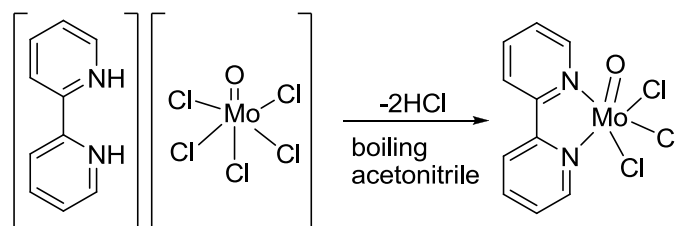
**Fig. 2. Formation of Mo(bpy)OCl₃ by dehydrohalogenation method**

As well as mono and bis bipyridine complexes, there are examples for tris bipyridine complexes. One of such complexes is Tris(2,2'-bipyridine)molybdenum(0) prepared from bis(benzene)molybdenum(0) and 2,2'-bipyridine under drastic conditions.[22] The reaction takes place in oxygen-free xylene in a Pyrex tube sealed under nitrogen atmosphere at 250 °C. In the present study, I have successfully synthesized molybdenum oxotrichlorides supported by different bipyridine derivatives and used them as starting materials in order to make dithiolene complexes of bioinorganic importance. Even though the compounds **2** and **3** reported in this chapter have been known for several years, no crystal structures were published. Also a different synthetic approach has been developed compared to the earlier reported method by Saha.[14] The main disadvantage of compounds **2** and **3** is their poor solubility in most of the commonly used solvents like THF, toluene, dichloromethane etc..

## 5.2. β-Diketiminate complexes - General overview

The β–diketiminate ligands generally known as "nacnac", have a chemical composition in the form of [{RNC(R')}₂CH]⁻ (where R = aryl, alkyl, H, SiMe₃ etc. and R = Me or another organic group) (Figure 3). In recent years this type of ligands has emerged as popular among other ancillary supports, in view of their strong binding to metals, their tunable steric and electronic effects and their diversity in bonding modes.[23-29] The nacnac ligand skeleton is analogous to the "acac" (acetyl acetonate) ligand with the difference that

oxygen atoms are replaced by nitrogen-based moieties such as NR (Figure 3). This leads to the most interesting and highly advantageous feature of nacnac by introducing steric protection around the metal center provided by bulky substituents at the nitrogen donor atoms.
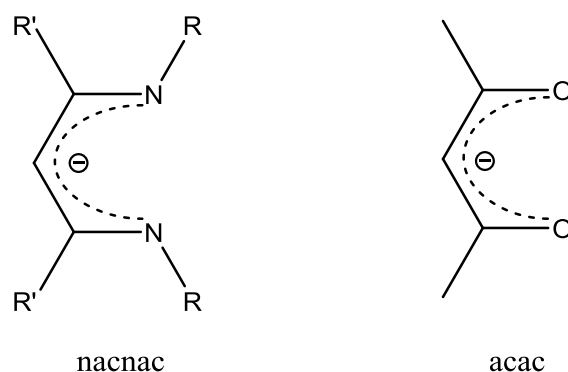


**Fig. 3. Chemical structure of nacnac and acac ligands**

The first complexes with $\beta$−diketiminate ligands were prepared in the mid to late 1960's as homoleptic complexes of Co, Ni, Cu, and Zn.[30-42] The bulkiness of group R at the nitrogen atoms is a deciding factor in the multiplicity of the compound unit.  For example, when R is a small moiety such as H, Me and SiMe$_3$, the compound is easily formed as a dimer (homonuclear bimetallic complexes in which metal atoms are bridged by two or more ligands) leading to the higher coordination number at the metal center, whereas a bulky aryl group on the nitrogens usually leads to the isolation of monomeric species with low coordination numbers at the metal center. To date, various $\beta$−diketiminate complexes containing main group,[43-44] transition [45-47] and lanthanide elements [48-52] have been synthesized and structurally characterized. Some of them have found application in catalysis like polymerization of ethylene and styrene [53-54] and lactides and related cyclic esters [55-57]. Besides these, $\beta$-diketiminate complexes were found to act as models for the active sites of enzymes. For example Holland and Tolman synthesized and extensively studied the

complex LCuSCPh3 (L = nacnac) as the structural analogue of the unusual trigonal nearly planar copper sites for instance found in ceruloplasmin, that, though lacking the fourth ligand, are still being considered as Type 1 copper due to their cysteine coordination and spectroscopic properties.[58-59]

Surprisingly, the chemistry of β-diketiminate complexes of group VI elements is not well established. The first complex of this category was chromium(III) β-diketiminate prepared by Richeson in 1989 [60] followed by tungsten(III) β-diketiminates reported by Flippou in 1993.[61] The first report of a molybdenum β-diketiminate appeared in 2006 in which the reaction of $Mo(NAr)(CHCMe_2Ph)(OTf)_2(dme)$ (Ar = 2,6-i-$Pr_2C_6H_3$, Tf = $CF_3SO_2$) with the lithium salt of various β-diketiminates leading to complexes of the type Mo(NAr)-($CHCMe_2Ph)(L)(OTf)$ (L = β-diketiminate) is described (Figure 4).[62] Treatment of these compounds with $NaB[3,5-(CF_3)_2C_6H_3]_4$ in dichloromethane affords rare examples of cationic imido alkylidene complexes. Following this first report, several complexes of the same kind $Mo(NR)(CHCMe_2R')(Ar-nacnac)(OTf)$ (R = 2,6-diisopropylphenyl, 2,6-dimethylphenyl, 1-adamantyl, 2,6-dichlorophenyl, or 2-tert-butylphenyl; Ar = 2,6-dichlorophenyl, 2,6-dimethylphenyl, 3,5-dimethylphenyl, or 2,6-difluorophenyl; R' = Me or Ph; Ar-nacnac = $[ArNC(Me)]_2CH$; OTf = trifluoromethanesulfonate) were prepared from $Mo(NR)(CHCMe_2RO(OTf)_2(dme)$ by metathesis with the corresponding Li{Ar-nacnac} salt.[63] Recently a dimeric nacnac compound of molybdenum was reported by Lyashenko et al..[64] Treatment of $[MoO_2(\eta^2-Pz)_2]$ (Pz = 3,5-di-*tert*-butylpyrazolate) with nacnacH at 55$^o$C affords the reduced dimeric molybdenum(V) compound $[\{MoO_2(nacnac)\}_2]$. This dimer consists of a $[Mo_2O_4]^{2+}$ core with a short Mo–Mo bond (2.5591(5) Å) and one coordinated diketiminate ligand on each metal atom. The reaction of $[MoO_2(\eta^2-Pz)_2]$ with nacnacH in benzene at room temperature leads to a mixture of the dimeric molybdenum(V) compound and the

monomeric molybdenum(VI) compound [MoO$_2$(nacnac)($\eta^2$-Pz)]. Further high oxidation state molybdenum compounds containing the nacnac ligand can be obtained by the reaction of [Mo(NAr)$_2$Cl$_2$(dme)] (Ar = 2,6-Me$_2$C$_6$H$_3$) and [Mo(N-*t*-Bu)$_2$Cl$_2$(dme) with one equivalent of the potassium salt of nacnac forming [Mo(NAr)$_2$Cl(nacnac)] and [Mo(N-*t*-Bu)$_2$Cl(nacnac)] respectively.
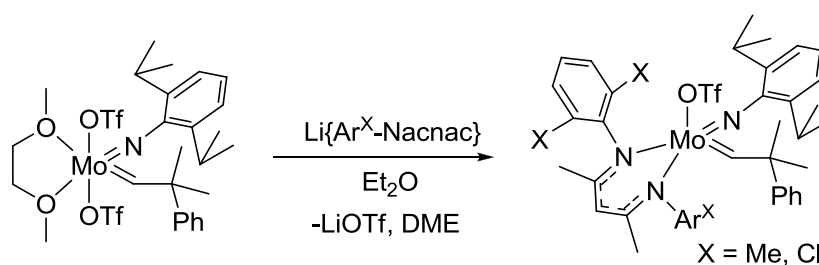


**Fig. 4. Synthesis and chemical structure of Mo(NAr)-(CHCMe$_2$Ph)(L)(OTf)**

## 5.3 Desoxo complexes of molybdenum: Structural analogues of DMSOR

As mentioned in chapter 2, the Mo$^{IV}$O(dt)$_2$/Mo$^{VI}$O$_2$(dt)$_2$ (dt = dithiolene) couple was extensively utilized for bioinorganic modeling studies because of the frequent occurrence of this redox couple in conventional molybdenum chemistry. Even though these complexes do resemble the active site structure of AO, for a detailed understanding of structure function relationships in the majority of enzymes in the DMSOR family Mo$^{IV}$(dt)$_2$/Mo$^{VI}$O(dt)$_2$ couples need to be developed and studied carefully. This type of complexes, however, was not known to inorganic chemists until 1998 when Donahue et al. described the reactions 1 and 2 affording [Mo$^{IV}$(bdt)$_2$(OSi$^t$BuPh$_2$)]$^-$ and [Mo$^{VI}$O(bdt)$_2$(OSi$^t$BuPh$_2$)]$^-$.[65]

$$[\text{Mo}^{IV}\text{O(bdt)}_2]^{2-} + \text{Ph}_2{}^t\text{BuSiCl} \rightarrow [\text{Mo}^{IV}\text{(bdt)}_2\text{(OSi}^t\text{BuPh}_2\text{)}]^- + \text{Cl}^- \dots\dots\dots\dots\dots (1)$$

$$[\text{Mo}^{VI}\text{O}_2\text{(bdt)}_2]^{2-} + \text{Ph}_2{}^t\text{BuSiCl} \rightarrow [\text{Mo}^{VI}\text{O(bdt)}_2\text{(OSi}^t\text{BuPh}_2\text{)}]^- + \text{Cl}^- \dots\dots\dots\dots (2)$$
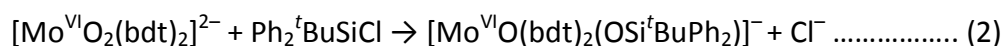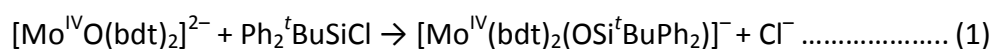
This approach was refined even further by the same group with respect to the modeling characteristics of the products by inclusion of alcoholate, thiolate and selenolate functions (reactions 3 and 4) giving compounds of the formula $[Mo(S_2C_2R_2)_2L(CO)_{2-n}]^-$ (n = 1 or 2; R= Me, Ph; L = $^-OR$, $^-SR$, $^-SeR$).[66]

$$[M(CO)_3(MeCN)_3] + 2[Ni(S_2C_2R_2)_2] \rightarrow [M(S_2C_2R_2)_2(CO)_2] + [Ni^{II}_2(S_2C_2R_2)_2] + 3MeCN + CO \ldots\ldots(3)$$

$$[M(S_2C_2R_2)_2(CO)_2] + L^- \rightarrow [M(S_2C_2R_2)_2L(CO)_{2-n}]^- + n\ CO \ldots\ldots (4)$$
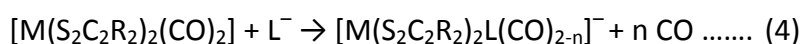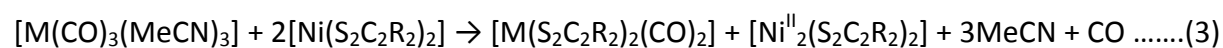
One or two labile carbonyl ligands in $[Mo(S_2C_2R_2)_2(CO)_2]$ are replaced by one mono-anionic ligand $L^-$ (LH= PhOH, PhSH, PhSeH, 2,5,6-$^iPr_3$PhOH, 2,5,6-$^iPr_3$PhSH, 2,5,6-$^iPr_3$PhSeH, AdOH, AdSH, AdSeH). The nature of the anionic ligand (steric demand depending on ligand size and length of the metal donor bond) dictates the number of CO ligands that are leaving the complex. For instance, in the case of anionic oxygen ligands $PhO^-$, 2,5,6-$^iPr_3PhO^-$ and $AdO^-$, both carbonyl groups are replaced to afford complexes of the type $[M(S_2C_2R_2)_2L]^-$. $PhS^-$ gives a monocarbonyl species $[M(S_2C_2R_2)_2L(CO)]^-$ but other bulkier thiolates replace both carbonyls leading to $[M(S_2C_2R_2)_2L]^-$. In case of selenolate the metal selenium bond is even longer and consequently $PhSe^-$ and 2,5,6-$^iPr_3PhSe^-$ produce monocarbonyl species $[M(S_2C_2R_2)_2L(CO)]^-$ whereas the sufficiently bulkier $AdSe^-$ replaces both carbonyls. The carbonyl displacing ability of the ligands are in the order: alcoholate > thiolate > selenolate, exactly opposed to the order in M-L bond length: M-O < M-S < M-Se. Thus, the mode of reactions described above is governed by both steric restrictions and the metal-ligand bond length. This may play a role in the enzymatic reactions as well. Similar reactions were carried out with other alcoholates like $^iPrO^-$ and $C_6F_5O^-$ to obtain $[M(S_2C_2R_2)_2L]^-$ complexes of square pyramidal geometry.[67] In order to synthesize an oxidized analogue to these $Mo^{IV}$

complexes, [$Mo^{IV}(OPh)(S_2C_2Me_2)_2$]$^-$ was reacted with N-oxides and S-oxides to yield [$Mo^{VI}O(OPh)(S_2C_2Me_2)_2$]$^-$ in solution, but this species could not be isolated.

## 5.4. Bipyridine and nacnac based molybdenum dithiolene chemistry

Chapter 5.3. describes how important the desoxobis(dithiolene) molybdenum complexes are as they are rare models for the DMSOR family of enzymes. Another important aspect of model chemistry was already described in chapter 4 where carbene stabilized molybdenum oxotrichloride was used as a template to synthesize a monodithiolene complex of molybdenum. Such complexes were shown to mimic the pentacoordinate Mo center in SO and XO. A similar approach has been made using bipyridine and nacnac supported molybdenum (V) compounds to afford both monooxomonodithiolene and desoxobisdithiolene complexes of molybdenum. In short, this chapter describes two important classes of dithiolene compounds: 1) desoxobis(dithiolene)Mo(IV) as in the case of reduced form of DMSO reductase and 2) monooxomono(dithiolene) complexes of molybdenum (V) as in the case of SO and XO. Both types of compounds are included in the same chapter because they share the feature that two valencies in both types of compounds are occupied by nitrogen atoms provided by either the neutral bipyridine or the monoanionic nacnac.

## 5.5. Experimental

### 5.5.1. Materials and methods

Syntheses of all compounds were done under strict inert gas atmosphere using Schlenk line techniques and drybox and all solvents used were perfectly dry and flushed with nitrogen. The commercially obtained solid chemicals were used as received. NMR-spectra

were recorded on NMR-spectrometers Bruker Avance DRX 500 or Bruker Avance DPX 300. The residual ^{1}H peak of the deuterated solvent was used as an internal standard and tetramethysilane as external standard for ^{1}H spectra. Infrared spectra were collected on a Mattson Genesis FT-MIR spectrometer in the range of 4000 - 400 $cm^{-1}$ using KBr pellets. Mass spectra were recorded with a Finnigan MAT System 8200. Elemental analyses were carried out with a 4.1 Varido EL 3 Analyzer from Elementar. Suitable crystals were mounted on a glass fiber and data was collected on an IPDS II Stoe image-plate diffractometer (graphite monochromated Mo $K_\alpha$ radiation, $\lambda$=0.71073 Å at 133(2) K. The data was integrated with X-Area. The structures were solved by Direct Methods (SHELXS-97) and refined by full-matrix leastsquares methods against $F^2$ (SHELXL-97).[68] All non-hydrogen atoms were refined with anisotropic displacement parameters.

**5.5.2. Preparation of Mo(t-Bu-bpy)OCl₃; (1):** To a schlenk flask containing $MoOCl_3$ (1 g, 4.57 mmol), 20 ml THF cooled to -20$^o$C was added and stirred for 5 minutes to obtain a green solution. To this, a solution of 4,4'-di-tert-butyl-2,2'-bipyridine (1.23 g, 4.57 mmol) in 20 ml THF was added slowly at -20$^o$C. An immediate reaction leads to the partial precipitation of a pink colored material which was stirred for further 2 hrs to afford a pale brown solid. The solution was concentrated and filtered. The brown solid was washed with pentane and dried under vacuum. Cooling (-35$^o$C) a concentrated solution of this compound in dichloromethane affords green crystals suitable for XRD measurement.

Elemental analysis for $C_{18}H_{24}Cl_3MoN_2O$ (486.69 g/mol), calcd (%): C: 44.42; H: 4.97; N: 5.76. expt (%): C: 43.89; H: 4.27; N: 5.95. IR (KBr) [$cm^{-1}$]: 485.8 (vw), 550.7 (w), 606.2 (m), 703.7 (vw), 719.6 (vw), 801.4 (s), 859.7 (m), 891.8 (w), 902.4 (w), 927.1 (vw), 972.8 (s), 1022.3 (s), 1096.7 (s), 1157.9 (vw), 1202.6 (w), 1262.1 (s), 1306.3 (w), 1364.6 (w), 1413.0 (m), 1458.6

(w), 1465.6 (w), 1481.7 (w), 1485.1 (w), 1546.0 (w), 1613.3 (m), 2471.5 (w), 2869.3 (vw), 2965.2 (m). EI-MS: *m/z* 487 $[C_{18}H_{24}Cl_3MoN_2O]^+$

**5.5.3. Preparation of Mo(Me-bpy)OCl₃; (2):** To a schlenk flask containing $MoOCl_3$ (1g, 4.57 mmol), 20 ml THF cooled to -20$^o$C was added and stirred for 5 minutes to obtain a green solution. To this, a solution of 5,5'-di-methyl-2,2'-bipyridine (0.84 g, 4.57 mmol) in 20 ml THF was added slowly at -20$^o$C. An immediate reaction leads to the precipitation of a pink colored material which was stirred for further 2 hrs. The solution was concentrated and filtered. The brownish solid was washed with pentane and dried under vacuum. Cooling (-4$^o$C) a concentrated solution of this compound in acetone affords green crystalline blocks suitable for XRD measurement.

Elemental analysis for $C_{12}H_{12}Cl_3MoN_2O$ (402.91 g/mol), calcd (%): C: 35.81; H: 3.00; N: 6.96; expt (%): C: 36.37; H: 3.44; N: 6.49; IR (KBr) [cm$^{-1}$]: 424.3 (w), 458.0 (vw), 492.8 (w), 657.5 (w), 693.2 (w), 726.5 (m), 795.9 (w), 822.7 (w), 840.7 (s), 904.3 (vw), 926.8 (vw), 936.9 (vw), 970.0 (s), 1004.2 (vw), 1055.7 (m), 1069.7 (vw), 1097.6 (vw), 1165.3 (w), 1242.3 (m), 1319.8 (m), 1388.1 (m), 1448.4 (w), 1482.8 (s), 1506.7 (w), 1570.0 (vw), 1585.2 (vw), 1601.7 (m), 1967.6 (vw), 2312.7 (vw), 2345.1 (vw), 2357.3 (vw), 2743.0 (vw), 2867.0 (vw), 2924.4 (vw), 2961.0 (vw), 3050.2 (w).  EI-MS: *m/z* 403 $[C_{12}H_{12}Cl_3MoN_2O]^+$

**5.5.4. Preparation of Mo(bpy)OCl₃; (3):** To a schlenk flask containing $MoOCl_3$ (1 g, 4.57 mmol), 20 ml THF cooled to -20$^o$C was added and stirred for 5 minutes to obtain a green solution. To this, a solution of 2,2'-bipyridine (0.72 g, 4.57 mmol) in 20 ml THF was added slowly at -20$^o$C. An immediate reaction leads to the precipitation of a pink colored material which was stirred for further 2 hrs to afford a pale brown solid. The solution was concentrated and filtered. The pale brown solid was washed with pentane and dried under vacuum.

147

Elemental analysis for $C_{10}H_8Cl_3MoN_2O$ (374.48 g/mol), calcd. (%): C: 32.07; H: 2.15; N, 7.48. exp. (%): C: 31.46; H: 2.02; N, 7.87. IR (KBr) [cm$^{-1}$]: 417.4 (m), 443.7 (w), 465.9 (vw), 524,7 (vw), 618.3 (vw), 637.8 (m), 650.7 (w), 658.5 (m), 728.4 (s), 766.4 (s), 802.9 (vw), 908.2 (vw), 971.8 (s), 1017.9 (m), 1030.5 (m), 1044,8 (vw), 1063.9 (w), 1076.0 (w), 1107.3 (w), 1122.0 (vw), 1159.2 (w), 1178.7 (vw), 1218.1 (vw), 1246.3 (w), 1280.2 (vw), 1318.8 (s), 1368.9 (vw), 1443.9 (s), 1475.2 (s), 1496.8 (m), 1516.9 (vw), 1564.1 (w), 1571.7 (w), 1600.4 (s), 1861.8 (vw), 1899.7 (vw), 1974.1 (vw), 2345.1 (vw), 2360.5 (vw), 3037.1 (vw), 3063.9 (w), 3116.7 (vw), 3200.0 (vw). EI-MS: $m/z$ 375 $[C_{10}H_8Cl_3MoN_2O]^+$

**5.5.5. Preparation of Mo(t-Bu-bpy)(bdt)$_2$; (4):** To a solution of Mo(t-Bu-bpy)OCl$_3$ (0.5 g, 1.03 mmol) in 20 ml THF, benzene-1,2-dithiol (0.15 g, 1.03 mmol) in 15 ml THF was added slowly at -20$^o$C. After stirring for 2min, a solution of triethylamine (0.207 g, 2.06 mmol) in 15 ml THF was added and stirred again for 5 hrs until the deposition of triethylammonium chloride was clearly visible on the walls of the schlenk flask. The solution was evaporated to dryness and extracted with toluene to obtain a green solution. The solution was filtered and kept at room temperature to afford dark green crystals.

IR (KBr) [cm$^{-1}$]: 434.0 (vw), 465.8 (vw), 483.6 (vw), 549.0 (vw), 603.1 (w), 662.5 (w), 696.7 (w), 731.7 (m), 746.8 (m), 756.5 (m), 801.9 (s), 835.5 (m), 849.0 (w), 879.1 (w), 899.6 (w), 931.8 (m), 1017.8 (s), 1098.4 (s), 1201.5 (vw), 1262.0 (s), 1289.4 (vw), 1302.8 (w), 1363.9 (w), 1410.4 (m), 1443.2 (w), 1458.6 (w), 1479.7 (w), 1544.7 (w), 1614.3 (m), 2385.0 (vw), 2868.9 (w), 2906.3 (w), 2963.6 (m). $^1$H-NMR (toluene-[d$_8$], 500 MHz, 25°C, TMS): δ = 1.185 (s, 18 H), 6.666-6.678 (m, 2H), 6.685-6.721 (m, 2H), 7.218-7.237 (m, 2H), 7.426-7.444 (m, 2H), 8.553-8.562 (d, 2H). EI-MS: 646 $[C_{30}H_{32}MoN_2S_4]^+$

**5.5.6. Preparation of (nacnac)Li(Et$_2$O); (5):** 12 M HCl (5 ml) was added to a solution of pentan-2,4-dione (4.45 g, 44.4 mmol) and 2,6-diisopropylaniline (19.1 g, 107 mmol) in

148

ethanol (200 ml). The solution was refluxed for 3 days and the solvent was removed to afford a dark pink solid residue. This solid was then refluxed with 300 mL of hexane for 1 h. The slurry was filtered, and the obtained solid hydrochloride salt was stirred with 200 ml saturated aqueous $Na_2CO_3$ solution and 300 ml dichloromethane in a 1 L flask until the solid dissolved. The organic layer was separated, dried over $MgSO_4$ and filtered. The solvent was then removed to leave a white solid residue which was then washed with cold (ca. $0^{o}C$) methanol (50 ml). The solid compound was dried under reduced pressure to remove any residual methanol. A part of the product (10 g, 23.9 mmol) was dissolved in diethyl ether (90 ml) with vigorous stirring, and treated drop wise with 15.0 ml of a 1.6 M $n$-BuLi solution in hexane. The solution was allowed to come to room temperature and stirred again for 12 h. On removing $Et_2O$ under reduced pressure the product precipitated as an off-white solid. It was redissolved under gentle heating and cooled in $-35^{o}C$ to afford the final product.[69]

$^{1}$H NMR (benzene [$d_6$], 500 MHz, 25°C, TMS): δ : 0.46-0.51 (t, 6 H), 1.16-1.18 (d, 12 H), 1.21-1.24 (d, 12 H), 1.88 (s, 6 H), 2.70-2.82 (q, 4 H), 3.22-3.45 (sept, 4 H), 4.98 (s, 1 H), 7.00-7.10 (m, 6 H)

**5.5.7. Preparation of Mo(nacnac)OCl$_2$; (6):** To a schlenk flask containing $MoOCl_3$ (1 g, 4.57 mmol), 20 ml THF cooled to $-20^{o}C$ was added and stirred for 5 minutes to obtain a green solution. To this, a solution of (Dipp$_2$nacnac)Li(Et$_2$O) (2.28 g, 4.57 mmol) in 30 ml THF was added slowly at $-20^{o}C$. The reaction was allowed to reach room temperature and stirred again for 6 hours to afford a dark green solution with the deposition of lithium chloride particles on the walls of the flask. The THF was completely evaporated and the compound was extracted with toluene. A portion of this toluene solution was kept at $-35^{o}C$ to afford

dark green crystals for X-ray analysis. The other portion was concentrated and mixed with a large volume of pentane to precipitate the fine quality green powder.

Elemental analysis for $C_{29}H_{41}Cl_2MoN_2O$ (600.49 g/mol), Calcd. (%), C: 58.00; H: 6.88; N: 4.67. Expt (%): C: 58.19, H: 7.04; N: 4.79. IR (KBr) [cm$^{-1}$]: 461.1 (w), 531.4 (w), 592.1 (vw), 704.8 (w), 760.6 (m), 797.2 (s), 846.8 (w), 860.3 (m), 936.0 (w), 990.2 (m), 1023.4 (s), 1057.1 (w), 1098.3 (m), 1164.0 (vw), 1178.9 (w), 1228.3 (vw), 1248.5 (w), 1260.8 (w), 1283.2 (w), 1315.5 (m), 1354.9 (m), 1384.5 (m), 1440.2 (w), 1458.5 (w), 1466.2 (w), 1521.6 (m), 1541.7 (s), 1590.7 (w), 1935.8 (vw), 2251.8 (vw), 2395.6 (vw), 2868.3 (w), 2927.4 (w), 2962.6 (m), 3060.2(vw). EI-MS: $m/z$ 601 $[C_{29}H_{41}Cl_2MoN_2O]^+$

**5.5.8. Preparation of Mo(nacnac)O(tdt); (7):** A suspension of sodium 4-methylbenzene-1,2-bis(thiolate), (Na$_2$tdt), (0.33 g, 1.67 mmol) in 20 ml THF was added to Mo(nacnac)OCl$_2$ (1 g, 1.67 mmol) previously dissolved in 25 ml THF at -30$^o$C under vigorous stirring. The reaction mixture was allowed to reach room temperature slowly and stirred again for another 6 hrs. After evaporating the solvent the green compound was extracted with toluene and dried under vacuum.

Elemental analysis for $C_{36}H_{47}MoN_2OS_2$ (683.84 g/mol), calcd (%): C: 63.23; H: 6.93; N: 4.10; S: 9.38. expt. (%): C: 63.37; H: 6.82; N: 4.22; S: 9.26.  IR (KBr) [cm$^{-1}$]: 464.4 (vw), 521.3 (vw), 661.1 (w), 687.7 (w), 702.9 (w), 728.6 (w),798.5 (s), 865.0 (w), 932.2 (w), 1018.0 (s), 1093.6 (s), 1262.1 (m), 1363.7 (vw), 1383.5 (vw), 1413.7 (w), 1456.9 (w), 1517.7 (vw), 1545.8 (w), 1590.4 (vw), 2963.1(w).  EI-MS: $m/z$ 685 $[C_{36}H_{47}MoN_2OS_2]^+$

## 5.6. Results and Discussion

The compounds **1** to **3** stem from the reaction of MoOCl$_3$ with different bipyridine derivatives in a 1:1 molar ratio in THF solution. Figure 5 illustrates the formation of these

compounds with MoOCl₃ as the common starting material. As mentioned in the previous chapter the solution of MoOCl₃ is green due to the coordination of THF, and this color changes upon the slow addition of the bipyridine derivative from green to brown or pink depending upon which bipyridine is used. Both MoOCl₃ and bipyridines are efficiently soluble in THF but the resulting complexes show very poor solubility. This makes the purification and isolation of these complexes easier but also presents serious problems with regard to the selection of solvents for crystallization and reactivity studies. Out of the three compounds, **1** has the best solubility in common solvents and **3** has the least.
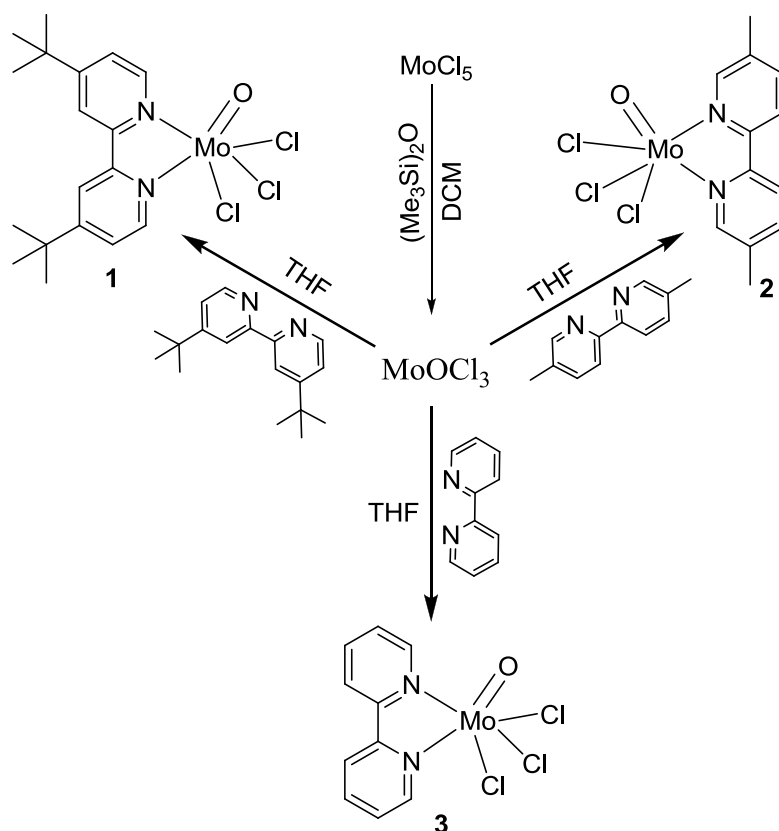


**Fig. 5. Synthesis of bipyridine complexes of MoOCl₃**

The crystallization of compound **1** was carried out from a saturated solution (but not very concentrated due to poor solubility) in dichloromethane at -35°C. Compound **1** crystallizes in the monoclinic space group C2/c with the cell dimensions: a = 14.476(3), b = 17.406(4), c = 25.055(5) and β = 92.80(3). Figure 6 shows the molecular structure of

compound **1** as obtained from the single crystal XRD method. There are two molecules in the asymmetric unit one of which sits at a specific position (Figure 7). That is, Mo2 is at the center where mirror planes and a twofold rotational axis meet. This causes some disorder (O and Cl on both sides of a mirror occupying essentially the same position) whereas the other molecule comprising Mo1 shows no disorder at all.



**Fig. 6. Molecular structure of compound 1 (ortep plot with 50% probability ellipsoids, hydrogen atoms are omitted for clarity)**



**Fig. 7. Asymmetric unit consisting of two molecules of compound 1**

The molybdenum center in compound **1** has a distorted octahedral coordination environment, the six corners of which are occupied by two nitrogen atoms from bipyridine, three chlorine atoms and one oxygen atom. Molybdenum is in the +V oxidation state (figure 8). The distances of the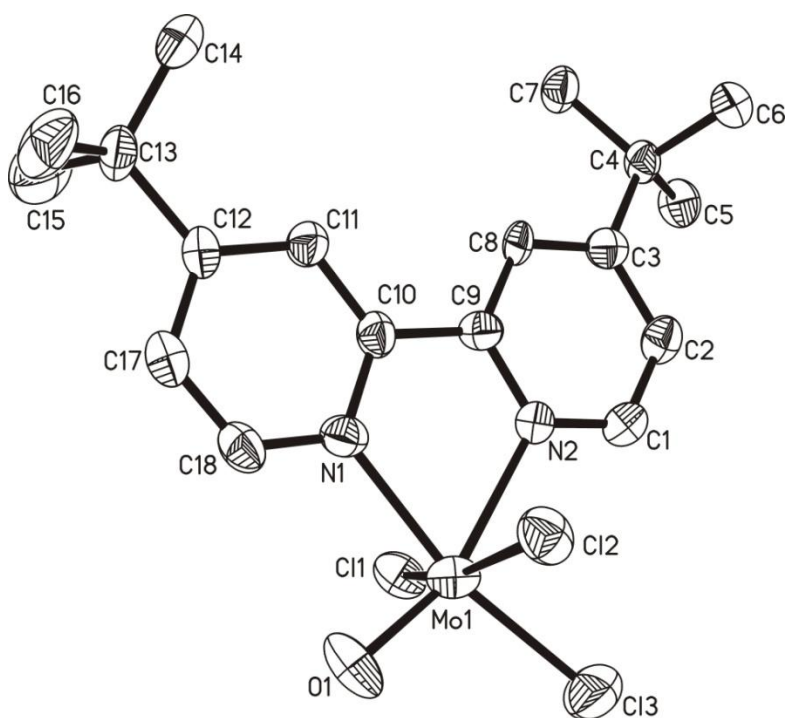se five atoms to the central molybdenum atom are Mo1-N1 = 2.1927, Mo1-N2 = 2.2990, Mo1-Cl1 = 2.3734, Mo1-Cl2 = 2.3684, Mo1-Cl3 = 2.3085, and Mo1-O1 = 1.6984 Å. The distorted octahedron has the edge lengths: N1-N2 = 2.6000, N2-Cl3 = 3.4276, Cl3-O1 = 3.1704, O1-N1 = 2.7649, N1-Cl1 = 3.2090, O1-Cl1 = 3.0969, Cl3-Cl1 = 3.2890, N2-Cl1 = 3.0250, N1-Cl2 = 3.1502, N2-Cl2 = 3.1285, Cl3-Cl2 = 3.3306 and O1-Cl2 = 3.0815.
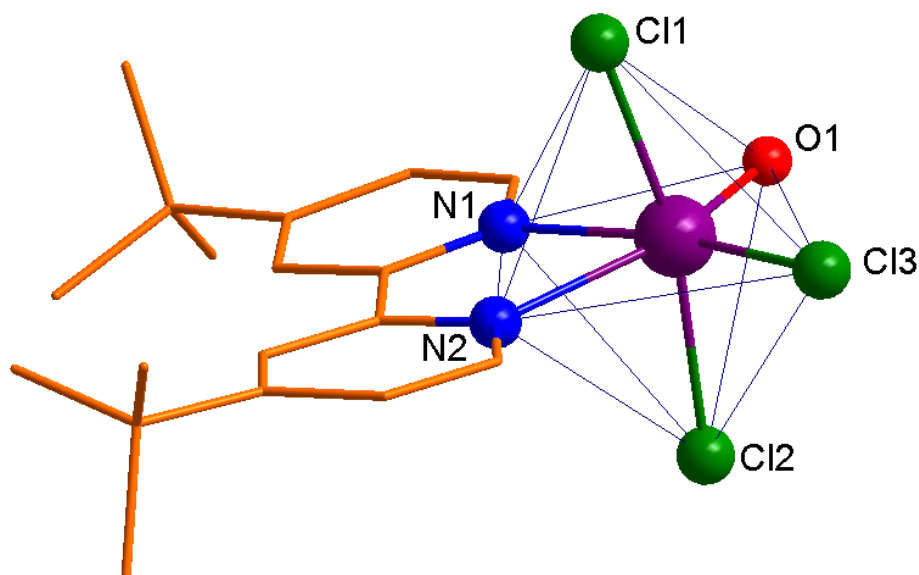


**Fig. 8. Distorted Octahedral arrangement of atoms around the Mo center in compound 1**

The 2,2' bond in the t-Bu-bpy, i.e. C9-C10, has the bond length 1.4541 Å, which is very close to the ideal $^{sp2}C$-$C^{sp2}$ single bond length, (1.47 Å).[70] This indicates that both aromatic rings are not giving rise to a more delocalized π-system, which has been observed for other complexes. In this case molybdenum(V) obviously does not mediate such a delocalization. It can be seen from the structure that the two nitrogen atoms of the bipyridine in compound **1** are tilted by an angle of 4.141° from the C9-C10 bond defined by the torsion angle N1-C9-

C10-N2. The bond lengths that the tertiary carbon atoms make with the pyridine rings are C12-C13 = 1.5367 and C3-C4 = 1.5277. Cl1 and Cl2 which are *trans* to each other, have a similar bond angle with the oxygen atom as O1-Mo1-Cl1 = 97.649$^o$ and O1-Mo1-Cl2 = 97.153$^o$. At the same time the chlorine atom *trans* to N1 is in a quite different bond angle O1-Mo1-Cl3 = 103.556$^o$. The selected bond lengths and bond angles in compound 1 are summarized in table 1.

**Table 1: Selected bond lengths and angles in compound 1**

| Bond length(Å) | | Bond angles ($^o$) | |
|---|---|---|---|
| Mo1-N1 | 2.1927(75) | O1-Mo1-Cl1 | 97.649(191) |
| Mo1-N2 | 2.299(6) | O1-Mo1-Cl2 | 97.153(188) |
| Mo1-Cl1 | 2.3734(21) | O1-Mo1-Cl3 | 103.556(250) |
| Mo1-Cl2 | 2.3684(23) | Cl1-Mo1-Cl2 | 164.758(77) |
| Mo1-Cl3 | 2.3085(27) | Cl1-Mo1-Cl3 | 89.244(93) |
| Mo1-O1 | 1.6984(59) | Cl2-Mo1-Cl3 | 90.809(94) |
| C12-C13 | 1.5367(107) | N1-Mo1-N2 | 70.694(244) |
| C3-C4 | 1.5277(101) | | |
| C9-C10 | 1.4541(106) | | |

Compound **2** was crystallized from a saturated solution in acetone at -4$^o$C. It crystallizes in the triclinic space group P-1 with the cell dimensions: a = 7.7609(16), b = 8.9375(18), c = 13.810(3), α = 96.80(3), β = 92.23(3) and γ = 93.40(3). Figure 9 shows the molecular structure of compound **1** as obtained from the single crystal XRD method.
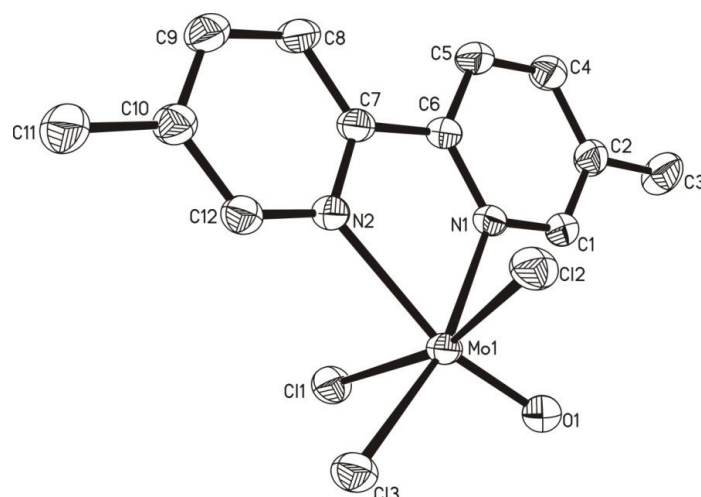
**Fig. 9. Molecular structure of compound 2 (ortep plot with 50% probability ellipsoids, hydrogen atoms are omitted for clarity)**
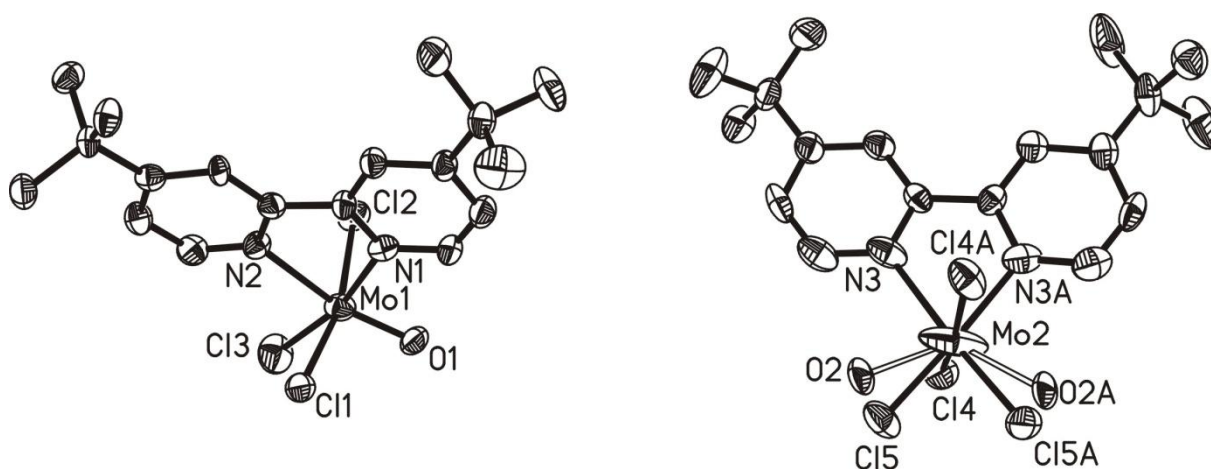
As in the case of compound **1** the molybdenum center in compound **2** also has a distorted octahedral coordination environment. The six corners of the octahedral are occupied by two nitrogen atoms from the bipyridine, three chlorine atoms and one oxygen atom and the molybdenum is in the +V oxidation state. The bond lengths of these five atoms from the central molybdenum atom are Mo1-O1 = 1.6728, Mo1-Cl1 = 2.3469, Mo1-Cl2 = 2.3532, Mo1-Cl3 = 2.3538, Mo1-N1 = 2.1978 and Mo1-N2 = 2.3176 Å. The distorted octahedron has the edge lengths: N1-N2 = 2.6435, N2-Cl2 = 3.4097, Cl3-O1 = 3.2175, O1-N1 = 2.7574, N1-Cl2 = 3.1562, N2-Cl2 = 3.0060, Cl3-Cl2 = 3.3105, O1-Cl2 = 3.0738, N1-Cl1 = 3.2013, N2-Cl1 = 3.085, Cl3-Cl1 = 3.2941, O1-Cl1 = 3.0867. Figure 10 shows the octahedral coordination in compound **2**.

The pyridine rings are separated by a distance defined by the bond length, C6-C7 = 1.4675 Å. C6-C7 is a single bond between two sp2 hybridized carbon atoms and its bond length 1.4675 Å, is very close to the ideal value 1.47 Å. The torsion angle N1-C7-C6-N2 is only $0.596^o$ in contrast to the higher value of $4.141^o$ in case of compound **1**. The C-C bond lengths that the two methyl groups make with the pyridine rings are C2-C3 = 1.4985 and C10-C11 =

1.5020 Å. Similar to the case in compound **1** Cl1 and Cl2 which are *trans* to each other, have similar bond angles with the molybdenum-oxygen bond as O1-Mo1-Cl1 = 98.948$^{o}$ and O1-Mo1-Cl2 = 98.122$^{o}$. The chlorine atom *trans* to N1 shows a different value of the corresponding bond angle as O1-Mo1-Cl3 = 104.814$^{o}$. Table 2 provides selected bond lengths and bond angles in compound **2**.
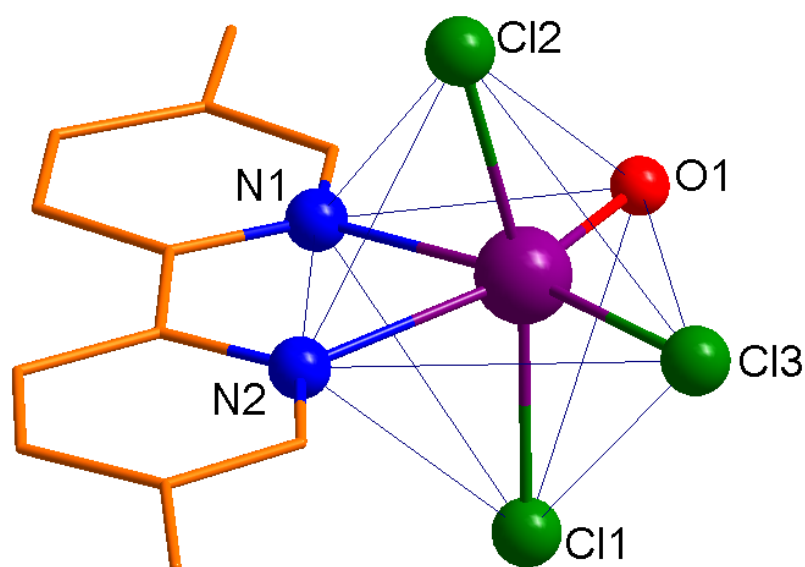


**Fig. 10. Distorted Octahedral arrangement of atoms around the Mo center in compound 2**

One of the significant observations in the structural features of compounds **1** and **2** is the stretching of the Mo-N bond *trans* to the oxo ligand. In both cases, the Mo1-N2 bond length is significantly greater than the Mo1-N1 bond length. This discrepancy arises from the structural *trans* influence (STI) of the O$^{2-}$ ligand in these octahedral complexes. The large STIs of oxo ligands were first noted by F. A. Cotton in 1964 [71] and since then many cases have been documented. Some of the examples of the complexes showing the *trans* influence of O$^{2-}$ together with that observed in the case of compounds **1** and **2** reported here are summarized in table 3.

**Table 2: Selected bond lengths and angles in compound 2**

| Bond lengths (Å) | | Bond angles (°) | |
|---|---|---|---|
| Mo1-O1 | 1.6728(17) [1.6984(59)]* | O1-Mo1-Cl1 | 98.948(59) [97.153(188)]* |
| Mo1-Cl1 | 2.3469(7) [2.3684(23)]* | O1-Mo1-Cl2 | 98.122(59) [97.649(191)]* |
| Mo1-Cl2 | 2.3532(8) [2.3734(21)]* | O1-Mo1-Cl3 | 104.814(60) [103.556(25)]* |
| Mo1-Cl3 | 2.3538(9) [2.3085(27)]* | Cl1-Mo1-Cl2 | 162.698(25) |
| Mo1-N1 | 2.1978(17) [2.1927(75)]* | N1-Mo1-N2 | 71.612(64) |
| Mo1-N2 | 2.3176(18) [2.299(6)]* | Cl2-Mo1-Cl3 | 89.385(23) |
| C6-C7 | 1.4675(30) | Cl1-Mo1-Cl3 | 88.978(23) |
| C2-C3 | 1.4985(36) | | |
| C10-C11 | 1.5020(35) | | |

*Corresponding values found in compound 1 are given in square brackets for comparison. Since Cl1 of compound 1 occupies the similar position of Cl2 in compound 2 and vice versa, a cross reference to the values given in table 1 is to be done with caution.

**Table 3: STI of oxo ligands in octahedral complexes**

| ID. | Compound | L | Bond distances (Å) | | Δ (Å) | Ref. |
|---|---|---|---|---|---|---|
| | | | M-L$_{trans}$ | M-L$_{cis}$ | | |
| **1** | Mo$^V$OCl$_3$(t-Bu-bpy) | N-(t-Bu-bpy) | 2.299(6) | 2.1927(75) | 0.11 | |
| **2** | Mo$^V$OCl$_3$(Me-bpy) | N-(Me-bpy) | 2.3176(18) | 2.1978(17) | 0.12 | |
| i | *cis*-V$^{IV}$O(SO$_4$) (H$_2$O)$_4$·H$_2$O | H$_2$O | 2.223(5) | 2.040(9) | 0.18 | [72] |
| ii | (AsPh$_4$)2[NbVO(*N*CS)5] | NCS$^-$ | 2.27(4) | 2.09(8) | 0.18 | [73] |
| iii | (PPh$_4$)$_3$[Mo$^{IV}$O(CN)$_5$].7H$_2$O | CN$^-$ | 2.373(6) | 2.18(1) | 0.19 | [74] |
| iv | K$_2$[Mo$^V$OCl$_5$] | Cl$^-$ | 2.63 | 2.40 | 0.23 | [75] |
| v | K$_2$[Re$^V$OCl$_5$] | Cl$^-$ | 2.47 | 2.39 | 0.08 | [76] |
| vi | *mer,cis*-Nb$^V$OCl$_3$(hmpa)$_2$ | hmpa | 2.243(4) | 2.048(5) | 0.20 | [77] |
| vii | (C$_4$Ph$_4$Cl)$_2$[Nb$_2^V$OCl$_9$]$_2$ | Cl$^-$ | 2.697(2) | 2.483(2) | 0.21 | [78] |
| viii | *cis,mer*-Mo$^{IV}$OCl$_2$(PMe$_2$Ph)$_3$ | Cl$^-$ | 2.551(3) | 2.464(3) | 0.09 | [79] |
| ix | *cis*-Mo$^{VI}$O$_2$(dedtc)$_2$ | dedtc | 2.639(1) | 2.450(1) | 0.19 | [80] |
| x | Tc$^V$OCl$_2$Tp | Tp | 2.259(4) | 2.087(4) | 0.17 | [81] |
| xi | *cis*-NEt$_4$[Re$^{VII}$O$_2$(*O*TeF$_5$)$_4$] | *O*TeF$_5^-$ | 2.05(1) | 1.94(1) | 0.11 | [82] |
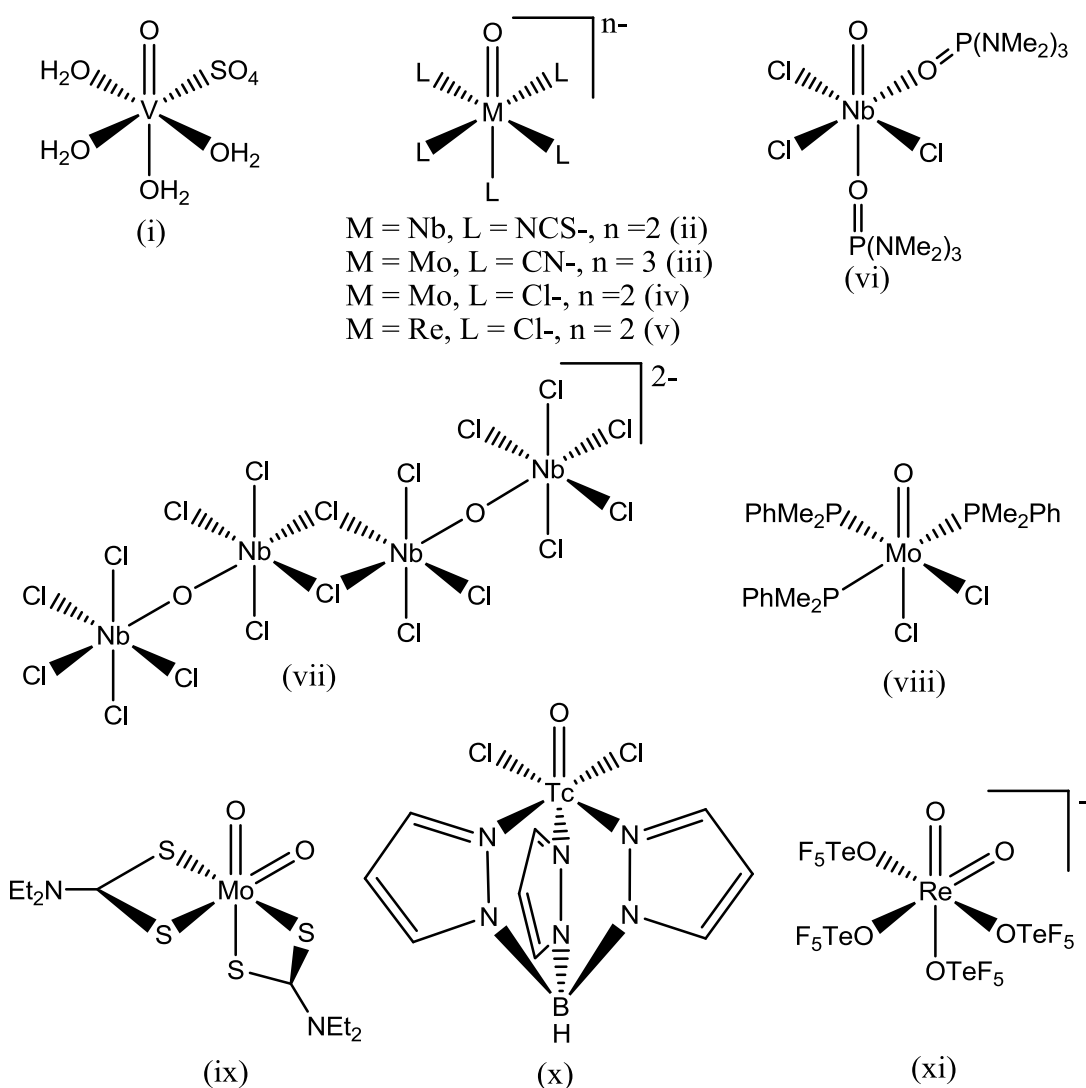
**Fig. 11. Compounds exhibiting STE by $O^{2-}$ ligand**

Compound **3** was least soluble in common solvents and the attempts to obtain crystals suitable for X-ray analysis were not successful. The IR spectra of compounds **1** to **3** show the Mo=O stretching frequencies with slight differences. The $v_{Mo=o}$ values for compounds **1**, **2** and **3** are 972.8, 970.0 and 971.8 $cm^{-1}$ respectively. There is a considerable decrease in the Mo=O stretching frequency values of these compounds compared to the observed $v_{Mo=o}$ value in the starting material $MoOCl_3$ which is 1007 $cm^{-1}$. This decrease indicates the weakening of the Mo=O bond strength which presumably arises from a reduction in the $O(2p\pi) \rightarrow Mo(4d\pi)$ donation which in turn is due to the electron donation

from the highly nucleophilic bipyridine to molybdenum. However the IR results do not show any significant effect on the Mo=O bond character by the substitution of alkyl groups in the bipyridine ring.

Compound **4** was unexpectedly formed in place of the expected Mo(t-Bu-bpy)OCl(bdt). Two equivalents triethyl amine were used in the reaction to facilitate the intermolecular hydrogen chloride elimination from compound **1** and bdt and thereby forming Mo(t-Bu-bpy)OCl(bdt). $Mo^V$(t-Bu-bpy)OCl(bdt) then undergoes disproportionation to produce $Mo^{IV}$(t-Bu-bpy)(bdt)$_2$ (compound **4**) and $Mo^{VI}$(t-Bu-bpy)O$_2$Cl$_2$ (figure 12). All these three compounds were observed in the EI-MS spectrum of the crude reaction mixture. Compound **4** is very well soluble in toluene and it can be easily separated from $Mo^{VI}$(t-Bu-bpy)O$_2$Cl$_2$. Keeping this green solution in toluene at room temperature afforded big dark green crystalline blocks suitable for XRD analysis. Unfortunately, the crystals were twinned with more than three different domains the separation of which was not possible with X-area software. The crystallization of compound **4** was again attempted in different solvents like dichloromethane and THF alone and also in combination with ether or pentane. None of these attempts were successful but crystals were formed again from a mixture of toluene and pentane in a 6:4 ratio. A complete solution of the twin crystal was not possible due to the very poor data quality and so the crystallographic metric parameters presented in this description are to be taken with caution.
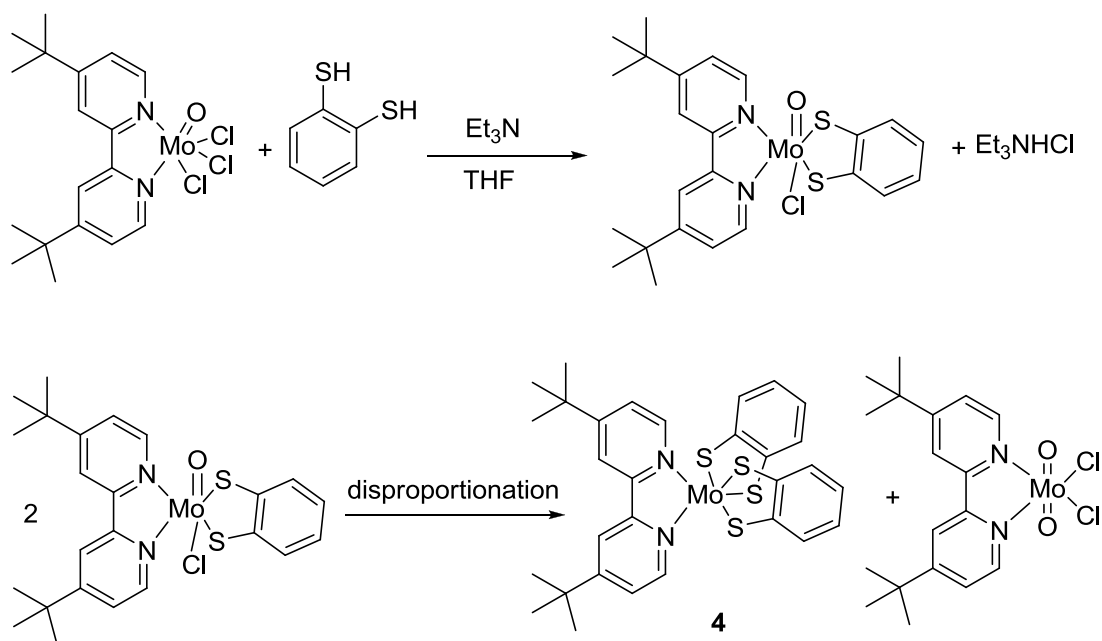
**Fig. 12. Proposed disproportionation mechanism for formation of compound 4**

Figure 13 shows the molecular structure of compound **4** as derived from the crystallographic data obtained. It is a desoxo bisdithiolene structure and such complexes deserve high attention in bioinorganic chemistry and in general molybdenum coordination chemistry. This is due to their rare occurrence in synthetic chemist's laboratories despite the sheer abundance in the micro world as in the case of the active site of DMSO reductase. The coordination geometry around the metal center is trigonal prismatic as shown in figure 14. In addition this is the rarest example of a trigonal prismatic bisdithiolene complex of molybdenum (IV) amidst many other trisdithiolene Mo(IV & VI) complexes with the same geometry. The distance that each corner of the prism has with the molybdenum center are: Mo1-S1 = 2.3438, Mo1-S2 = 2.3551, Mo1-S3 = 2.3233, Mo1-S4 = 2.3324, Mo1-N1 = 2.0946 and Mo1-N2 = 2.2324 Å. The square base of the trigonal prism is made up of four sulfur atoms from two dithiolene ligands and the two apex corners are occupied by nitrogen atoms of the bipyridine.
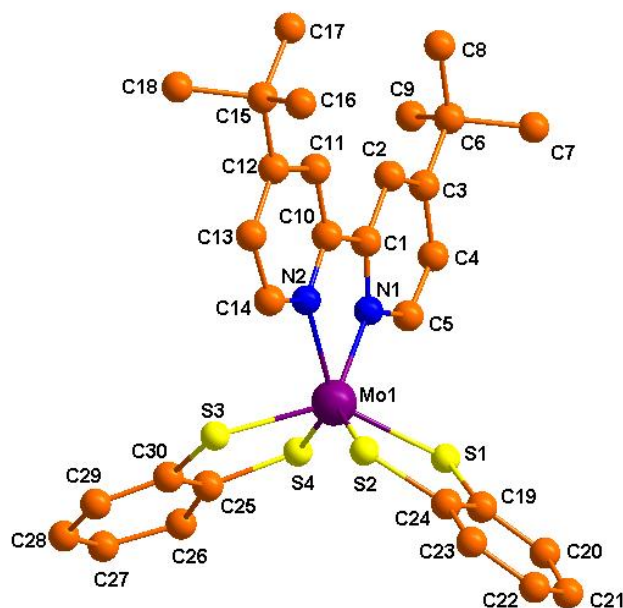
**Fig. 13. Molecular structure of compound 4**
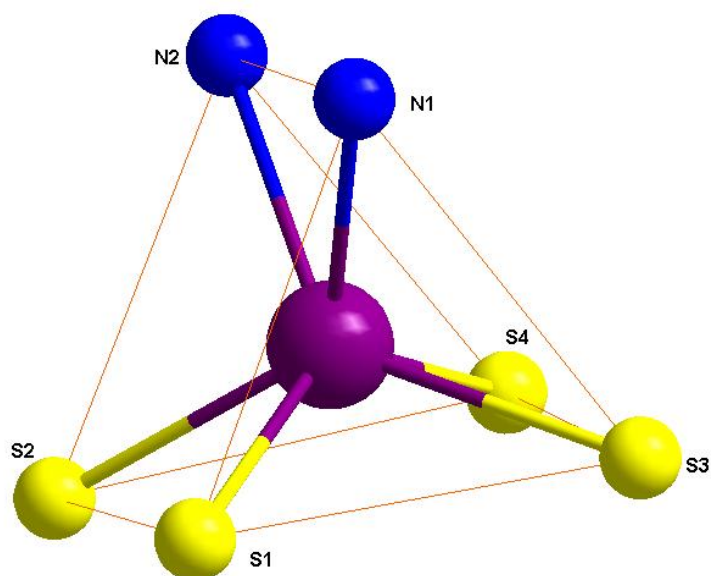


**Fig. 14. Trigonal prismatic arrangement of atoms around the molybdenum center in compound 4**

Bisdithiolene complexes of molybdenum(IV) generally have square pyramidal geometry and the examples of TP geometry are very rare. The Mo(IV) complexes known to have TP geometry possess cores like $MoS_4C_2$ (eg. $[Mo(CO)_2(S_2C_2Me_2)_2]$) and $MoS_4CX$ (X = S, Se) (eg. $[Mo(CO)XPh(S_2C_2Me_2)_2]$). In addition, in all these cases monodentate ligands like CO, SR or SeR (R = alkyl or aryl) were occupying two coordination sites. To the best of my

knowledge, compound **4** is the first bis(dithiolene)molybdenum(IV) complex with TP geometry in which the additional coordination sites other than dithiolene are occupied by a chelating ligand. Investigations on tris(dithiolene) molybdenum (IV & VI) remained a fascinating topic over decades after the preparation of Mo(bdt)$_3$ by Bennet et al. in 1975.[66, 83-94] The combination of three non-innocent dithiole ligands in these complexes was capable of bringing unique chemical and physical properties to these compounds. In this sense the compound **4** is promising with the combination of two types of ligands known to exhibit non-innocence character: dithiolene and bipyridine. Proper structural information can perhaps lead to interesting observations in the future.

Yet another important starting material for making monodithiolene complexes of molybdenum (V) is attained through the preparation of compound **6.** This compound also has two nitrogen atoms coordinated as in the case of compounds **1** to **3** with the difference that it is a monoanionic bidentate ligand. The compound is formed by the intermolecular elimination of one equivalent of LiCl from compound **5** and MoOCl$_3$, as shown in figure 15. The same compound was independently prepared by Alexander Döring [95] in a different but similar synthetic approach simultaneously with me. The molecular structure of the compound **6** as obtained from the single crystal X-ray diffraction method is shown in figure 16. The coordination geometry around the metal center is a distorted square based pyramid in which the molybdenum center is surrounded by two nitrogen atoms from the nacnac ligand, two chlorines and one oxygen atom. Figure 17 depicts the square pyramidal coordination geometry in compound **6**. The square base contains the two nitrogen atoms and the two chlorine atoms. The square base has the edges, N1-N2 = 2.8645, N2-Cl2 = 3.0478, Cl1-Cl2 = 3.1046 and N1-Cl1 = 3.0691 Å. The distances that each corner of the square

base has with the apex oxygen atom are, N1-O1 = 2.9100, N2-O1 = 2.9056, Cl2-O1 = 3.2772
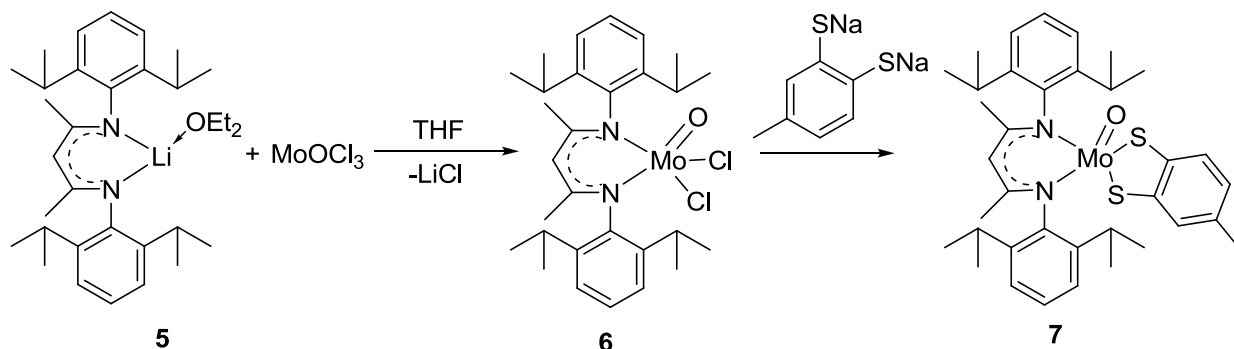
and Cl1-O1 = 3.2173 Å.



**Fig. 15. Formation of compounds 6 and 7**
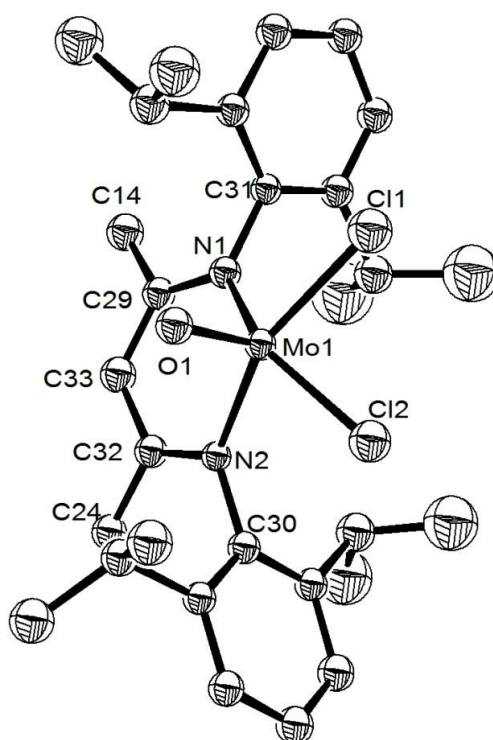


**Fig.16. Molecular structure of compound 6 (ortep plot with 50% probability ellipsoids, hydrogen atoms are omitted for clarity)**
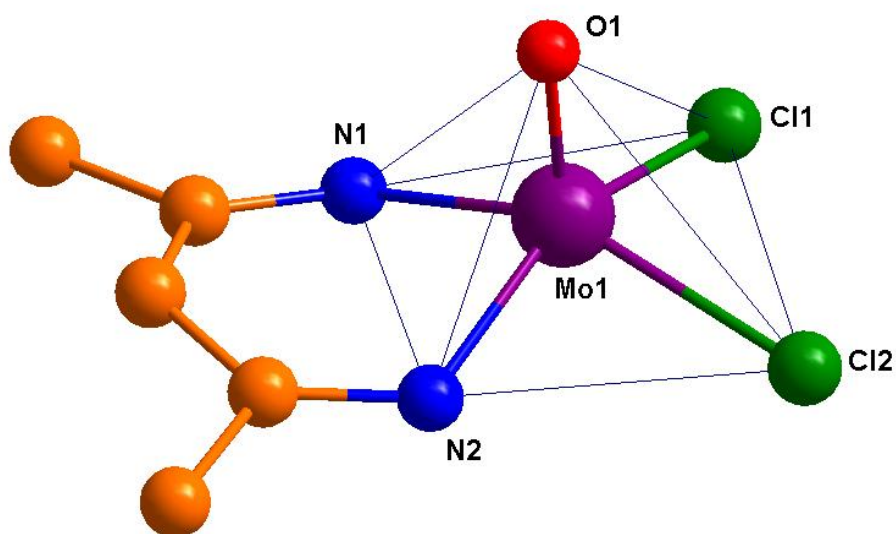
**Fig. 17. Square pyramidal coordination geometry in compound 6**

The bond lengths around the molybdenum atom with other atoms are Mo1-O1 = 1.6417, Mo1-Cl1 = 2.3526, Mo1-Cl2 = 2.3371, Mo1-N1 = 2.0661 and Mo1-N2 = 2.0872 Å. The base of the square pyramid is not ideally planar as indicated by the torsion angle Cl2-N1-N2-Cl1 = 3.385°. The bond angles that the molybdenum-oxygen bond is in with all other atoms in the square pyramid are: O1-Mo1-N1 = 102.811, O1-Mo1-N2 = 101.712, O1-Mo1-Cl2 = 109.674 and O1-Mo1-Cl1 = 105.938°. Other important bond angles inside the square pyramid are: N1-Mo1-N2 = 87.208, Cl1-Mo1-Cl2 = 82.908, N2-Mo1-Cl2 = 86.896 and N1-Mo1-Cl1 = 87.736°. An important feature in the geometry of compound **6** is a noticeable folding of the structure on both sides of the line connecting N1 and N2. Figure 18 is a view along the c axis clearly showing this folding. In the graphic the red atom label indicates the atom in rear view and the green label indicates the atom in front of the red labeled one. Thus N1 is exactly behind N2 and C29 behind C32. The folding angle is represented by α. As discussed in chapter 2.5 the folding angle can be calculated by measuring some important torsion angles. Interestingly, the structure shows a very high degree of planarity of the four

atoms N1, N2, C32 and C29. This is obvious from the very low torsion angle value C29-N1-N2-C32 = 0.055°. This means that a rotation of C29 and C32 by an angle of 0.0275° without changing the N1-N2-C32 and N2-N1-C29 angles will lead to ideal planarity. If this hypothetical plane is considered as the plane of the atoms C29, C32, N1 and N2, its angular deviation from the plane constituting the atoms N1, N2 and Mo1 is the folding angle α in this case. The obtuse angle between the above mentioned hypothetical plane and the N1,N2,Mo1 plane is the average of the torsion angle values Mo1-N1-N2-C29 (=153.027°) and Mo1-N1-N2-C32 (= 153.081) which is equal to 153.054°. So the folding angle α = 180-153.054 = 26.946°.
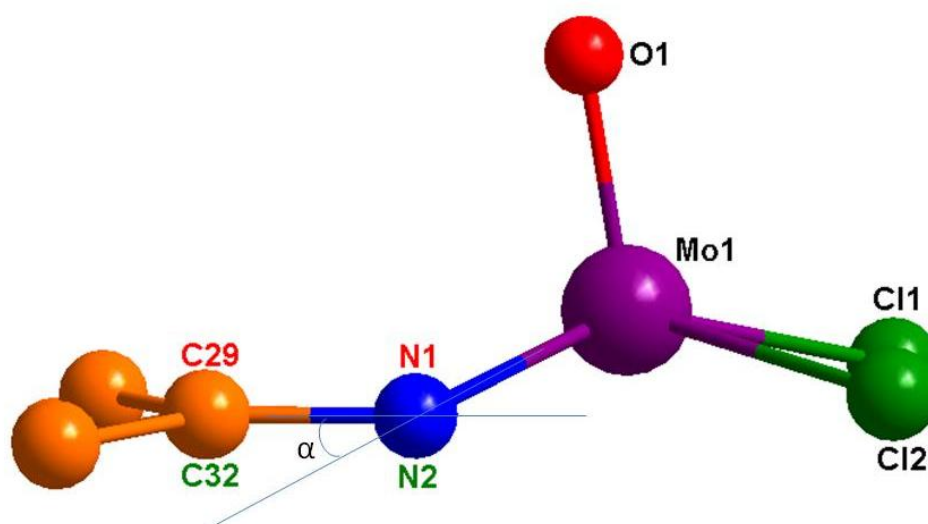


**Fig. 18. Folding along N1-N2 line in compound 6**

As stated previously, the nacnac ligand is monoanionic and it has resonance structures as shown in figure 19. Because of the delocalization of the negative change between N1 and N2 through the electronic current in the N1-C29-C33-C24-N2 backbone, the bonds C29-C33 and C33-C32 are expected to have lengths in a range in between C-C and C=C bond distances. The observed bond lengths are in good agreement with this theory as C29-C33 = 1.4160 and C33-C32 = 1.4195 Å (with localized double and single bonds the values are supposed to be C-C = 1.54 and C=C = 1.34 Å). Likewise, the carbon–nitrogen bonds are also

observed with a bond length in between the single and double bond distances as C29-N1 = 1.3521 and C32-N2 = 1.3456 Å. (values for the localized bonds should be C-N = 1.47 and C=N = 1.29). This charge delocalization based on the observed resonance demands the planarity of the N1-C29-C33-C32-N2 connectivity, but in reality this is not observed. In other words, C33 does not lie in the plane constituting the other four atoms and its position is defined in this case by the measured torsion angles, N2-C29-C32-C33 = 169.265 and N1-C29-C32-C33 = 169.328$^o$. The average of these torsion angles when subtracted from 180$^o$ gives the angular deviation of C33 from the plane of the other four atoms under discussion and it equals 10.7035$^o$. From the above discussion it is clear that, the six membered ring constituted by Mo1, N1, C29, C33, C32 and N2 has a boat shape with Mo1 at the head, C33 at the tail and with N1-N2-C32-C29 being the base of the boat. The head and tail are 26.946$^o$ and 10.7035$^o$ above the base respectively. Figure 20 represents the boat shaped ring in compound **6.** Table 4 provides important bond angles and bond lengths of compound **6.**
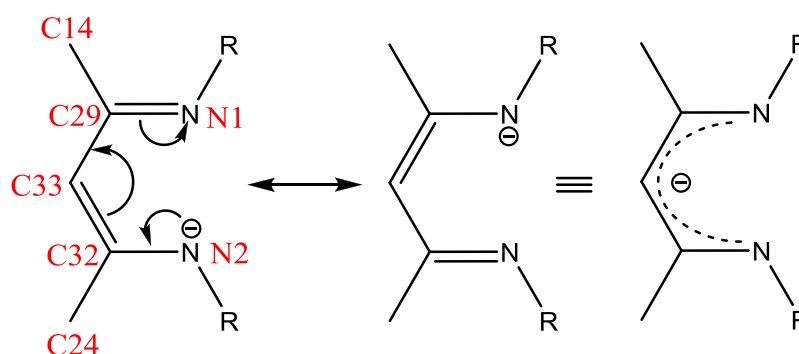


**Fig. 19. Resonance structures of the nacnac anion**

Compound **6** acts as an excellent starting material for preparing the monodithiolene compound **7** ([Mo(nacnac)O(tdt)]). Its reaction with one equivalent of Na$_2$(tdt) results in the elimination of two equivalents of NaCl affording compound **7** which was characterized by elemental analysis, IR and MASS spectroscopy. It can be seen from the IR spectrum that the $v_{M=O}$ value 1023 cm$^{-1}$ in compound **6** shifts to 1018 cm$^{-1}$ in compound 7 indicating a little

reduction in the Mo=O bond strength. Compound **7** is a dark green colored material and the reaction is comparatively fast with deposition of sodium chloride particles on the walls of the reaction flask. However, crystallization of this compound was not efficient to give good quality crystals for X-ray analysis but based on chemical reasoning it is expected to have a square pyramidal structure around the molybdenum atom with an apex oxygen atom. This possibility renders the dithiolene sulfur atoms at the *cis* positions of the square base. In fact such a coordination is very important in bioinorganic chemistry as it mimics the active site structure of the intermediate form of SO in its catalytic turn over. Moreover such coordination environment is seen in the active site of unique CO dehydrogenase also. Figure 21 shows the EI-MS spectrum of compound **7** which is in excellent agreement with the theoretical spectrum.
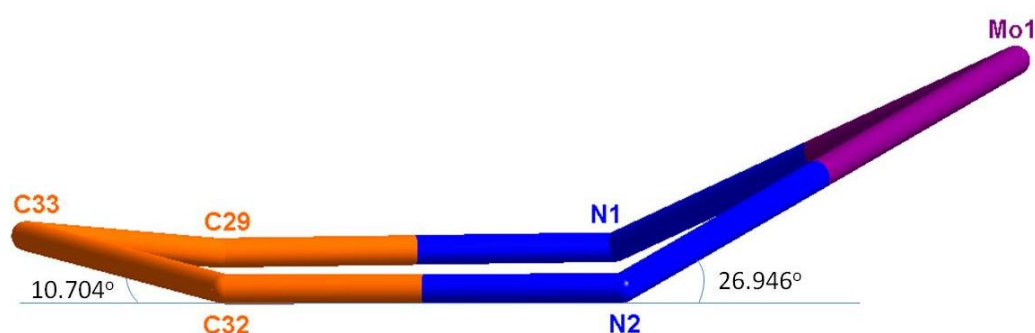


**Fig. 20. Boat structure formed by the nacnac coordination to Mo in compound 6**

**Table 4. Selected bond lengths and angles in compound 6**

| Bond lengths (Å) | | Bond angles (°) | |
|---|---|---|---|
| Mo1-O1 | 1.6417 | O1-Mo1-N1 | 102.811 |
| Mo1-Cl1 | 2.3526 | O1-Mo1-N2 | 101.712 |

| | | | |
|---|---|---|---|
| Mo1-Cl2 | 2.3371 | O1-Mo1-Cl2 | 109.674 |
| Mo1-N1 | 2.0661 | O1-Mo1-Cl1 | 105.938 |
| Mo1-N2 | 2.0872 | N1-Mo1-N2 | 87.208 |
| C29-C33 | 1.4160 | Cl1-Mo1-Cl2 | 82.908 |
| C33-C32 | 1.4195 | N2-Mo1-Cl2 | 86.896 |
| C29-N1 | 1.3521 | N1-Mo1-Cl1 | 87.736 |
| C32-N2 | 1.3456 | Mo1-N1-C29 | 123.862 |
| C29-C14 | 1.5153 | N1-C29-C33 | 124.472 |
| C32-C24 | 1.5226 | C29-C33-C32 | 124.031 |
| N1-C31 | 1.4683 | C33-C32-N2 | 125.724 |
| N2-C30 | 1.4653 | Mo1-N2-C32 | 122.530 |
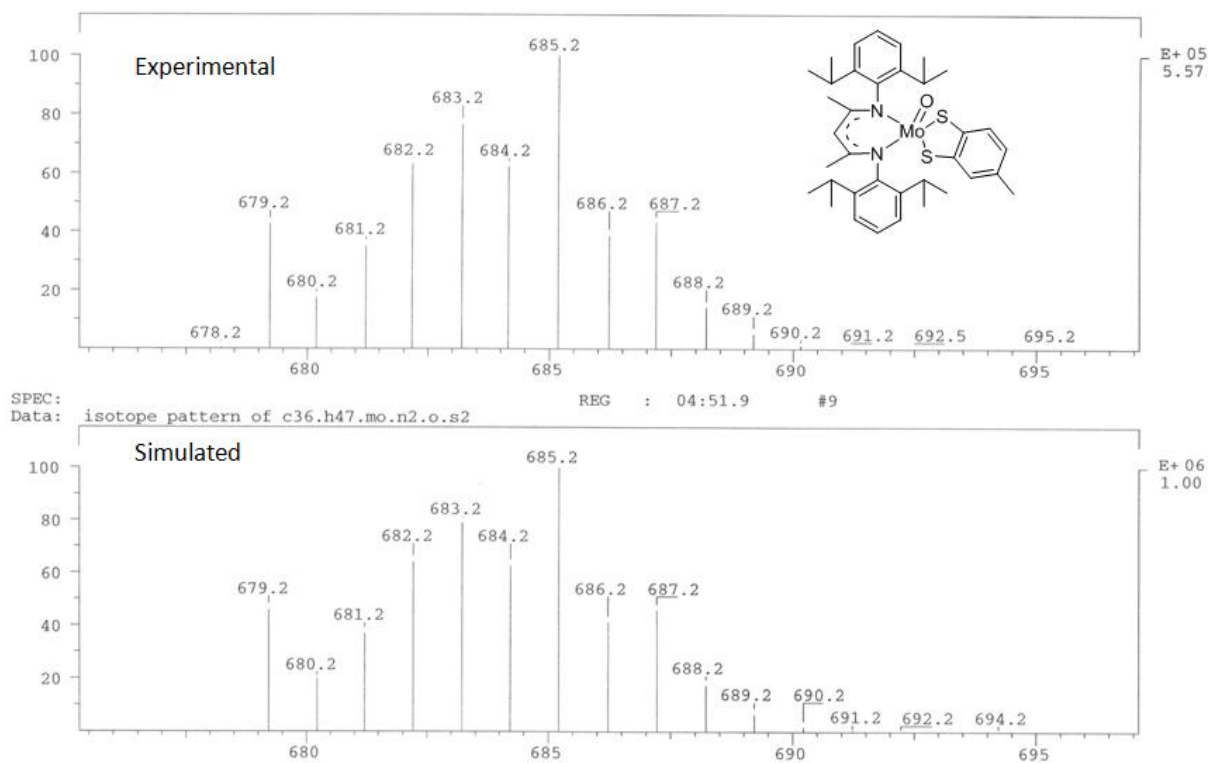


**Fig. 21. EI-MS spectrum of compound 7**

168

### References

[1]     Blau, F. *Monatsh. Chem.* 10 (1889) 375

[2]     Schumacher, J. N.; Green, C. R.; Best, F. W.; Newell, M. P. *J. Agric. Food Chem.* 25 (1977) 310

[3]     Jacob, P.; Benowitz, N.; Yu, L.; Duan, M. J.; Liang, G. *Addiction* 92 (1997) 626

[4]     Stiddard, M. H. B. *J. Chem. Soc.* (1962) 4712

[5]     Andy Hor, T. S.; Chee S-M. *J. of Organometal. Chem.* 331 (1987) 23

[6]     Hull C. G.; Stiddard, M. H. B. *J. Chem. Soc. A* (1966) 1633

[7]     Carmichael, W. M.; Edwards, D. A.; Walton, R. A. *J Chem. Soc.* ( A ) (1966) 97

[8]     Mitchell, P. C. H. *J. Inorg. Nuclear Chem.* 25 (1963) 963

[9]     Graham A. J.; Fenn, R. H. *J. Organomet. Chem.*  17 (1969) 405

[10]    Marzilli P. A.**;** Buckingham, D. A. *Australian J. Chem.* 19 (1966) 2259

[11]    Bois, D. W. D.; Iwamoto, R. T.; Kleinberg, J. *Inorg. Chem.* 8 (4) (1969) 815

[12]    Tripathi, S. C.; Srivastava, S. C.; Pandey, R. D.; Mani R. P. *J. Organomet. Chem.* 110 (1976) 67

[13]    Shrimal, A. K.; Nath, A.; Srivastava, A. *Indian J. Chem.* 43 A (2004) 511

[14]    Saha, H. K; Haldar, M. C.; Brown, T. M.; Wiley, R. *Inorganic Syntheses* 19 (1979) 134

[15]    Scullane, M. I.; Taylor, R. D.; Minelli, M.; Spence, J. T.; Yamanouchi, K.; Enemark, J. H.; Chasteen, N. D. *Inorg. Chem.* 18 (1979) 3213

[16]    Taylor, R. D.; Street, J. P.; Minelli, M.; Spence, J. T. *Inorg. Chem.* 17 (1978) 3207

[17]    Spence, J. T.; Taylor, R. D. *J. Less-Common Metal.*  54 (1977) 449

[18]    Saha, H. K.; Chaudhuri, T. K. Ray, *J. Inorg. Nucl. Chem.* 41 (1979) 417

[19]    Saha, H. K.; Bagchi, Manjusree; Chakravorty, Susmita, *J. Inorg. Nucl. Chem.* 36 (1974) 455

[20]     Saha, H. K.; Mandal, S. S.; Ghorai, P. C. *J. Ind. Chem. Soc.* 59(10) (1982) 1124

[21]     Saha, H. K.; Chaudhuri, T. K. Ray; Mandal, S. S. *J. Ind. Chem. Soc.* 53 (1976) 1086

[22]     Dubois, D. W.; Iwamoto, R.T.; Kleinberg, J.  *Inorg. Chem.* 9 (1970)  968

[23]     Bourget-Merle, L.; Lappert, M. F.; Severn, J. R. *Chem. Rev*. 102 (2002) 3031

[24]     Rahim, M.; Taylor, N. J.; Xin, S.; Collins, S. *Organometallics* 17 (1998) 1315

[25]     Piers, W. E.; Emslie, D. J. H. *Coord. Chem. Rev.* 233-234 (2002) 131

[26]     Roesky, H. W.; Singh, S.; Jancik, V.; Chandrasekhar, V. *Acc. Chem. Res*. 37 (2004) 969

[27]     Mindiola, D. J. *Acc. Chem. Res*. 39 (2006) 813

[28]     Cramer, C. J.; Tolman, W. B. *Acc. Chem. Res*. 40 (2007) 601

[29]     Holland, P. L. *Acc. Chem. Res*. 41 (2008) 905

[30]     Holm, R. H.; Everett Jr., G. W.; Chakravorty, A. *Prog. Inorg. Chem*. 7 (1966) 83

[31]     McGeachin, S. G. *Can. J. Chem.* 46 (1968) 1903

[32]     Dorman, L. C. *Tetrahedron Lett.* 4 (1966) 459

[33]     Barry, W. J.; Finar, I. L.; Mooney, E. F. *Spectrochim. Acta* 21 (1965) 1095

[34]     Bonnett, R.; Bradley, D. C.; Fisher, K. J. *J. Chem. Soc. Chem. Commun.* (1968) 886

[35]     Bonnett, R.; Bradley, D. C.; Fisher, K. J.; Rendall, I. F. *J. Chem. Soc.* (A) (1971) 1622

[36]     Parks, J. E.; Holm, R. H. *Inorg. Chem*. 7 (1968) 1408

[37]     Richards, C. P.; Webb, G. A. *J. Inorg. Nucl. Chem.* 31 (*1969) 3459

[38]     Cotton, F. A.; DeBoer, B. G.; Pipal, J. R. *Inorg. Chem.* 9 (1970) 783

[39]     Elder, M.; Penfold, B. R. *J. Chem. Soc.* (A) (1969) 2556

[40]     Honeybourne, C. L.; Webb, G. A. *Mol. Phys.* 17 (1969) 17

[41]     Honeybourne, C. L.; Webb, G. A. *Chem. Phys. Lett.* 2 (1968) 426

[42]     Hitchcock, P. B.; Lappert, M. F.; Liu, D. -S. *J. Chem. Soc. Chem. Commun*. (1994) 1699

[43]     Nagendran, S.; Roesky, H. W. *Organometallics* 27 (2008) 457

[44]    Roesky, H. W. *Inorg. Chem.* 43 (2004) 7284

[45]    Chai, J.; Zhu, H.; Roesky, H. W.; He, C.; Schmidt, H. -G.; Noltemeyer, M. *Organometallics* 23 (2004) 3284

[46]    Chai, J.; Zhu, H.; Most, K.; Roesky, H. W.; Vidovic, D.; Schmidt, H. -G.; Noltemeyer, M. *Eur. J. Inorg. Chem.* (2003) 4332

[47]    Yao, S.; Milsmann, C.; Bill, E.; Wieghardt, K.; Driess, M. *J. Am. Chem. Soc.* 130 (2008) 13536

[48]    Lee, L. W. M.; Piers, W. E.; Elsegood, M. R. J. ; Clegg, W.; Parvez, M. *Organometallics* 18 (1999) 2947

[49]    Drees, D.; Magull, J. *Z. Anorg. Allg. Chem.* 621 (1995) 948

[50]    Hitchcock, P. B.; Lappert, M. F.; Tian, S. *J. Chem. Soc. Dalton Trans.* (1997) 1945

[51]    Drees, D.; Magull, J. *Z. Anorg. Allg. Chem*. 620 (1994) 814

[52]    Ruspic, C.; Spielmann, J.; Harder, S. *Inorg. Chem.* 46 (2007) 5320

[53]    Bai, G.; Singh, S.; Roesky, H. W.; Noltemeyer, M.; Schmidt, H. -G. *J. Am. Chem. Soc.* 127 (2005) 3449

[54]    Gurubasavaraj, P. M.; Mandal, S. K.; Roesky, H. W.; Oswald, R. B.; Pal, A.; Noltemeyer, M. *Inorg. Chem*. 46 (2007) 1056

[55]    O'Keefe, B. J.; Hillmyer, M. A.; Tolman, W. B. *J. Chem. Soc. Dalton Trans.* (2001) 2215

[56]    Chisholm, M. H.; Gallucci, J.; Phomphrai, K. *Chem. Comm.* (2003) 48

[57]    Chisholm, M. H.; Gallucci, J. C.; Phomphrai, K. *Inorg. Chem.* 43 (2004) 6717

[58]    Holland, P. L.; Tolman, W. B. *J. Am. Chem. Soc.* 121 (1999) 7270

[59]    Randall, D. W.; George, S. D.; Holland, P. L.; Hedman, B.; Hodgson, K. O; Tolman, W. B.; Solomon, E. I. *J. Am. Chem. Soc.* 122 (2000) 11632

[60]    Richeson, D. S.; Mitchell, J. F.; Theopold, K. H. *Organometallics* 8 (1989) 2570

[61]    Filippou A. C.; Völkl C.; Rogers, R. D. *J. Organometal*. *Chem.* 463 (1993) 135

[62]    Tonzetich, Z. J.; Jiang, A. J.; Schrock, R. R.; Müller, P.  *Organometallics* 25 (2006) 4725

[63]    Tonzetich, Z. J.; Jiang, A. J.; Schrock, R. R.; Müller, P. *Organometallics* 26 (2007) 3771

[64]    Lyashenko, G.; Herbst-Irmer, R.; Jancik, V.; Pal, A.; Mösch-Zanetti, N. C. *Inorg. Chem.* 47 (2008) 113

[65]    Donahue, J. P.; Goldsmith, C. R.; Nadiminti, U.; Holm, R. H. *J. Am. Chem. Soc.* 1998, 120, 12869

[66]    Lim, B. S.; Donahue, J. P. Holm, R. H. *Inorg. Chem.* 2000, 39, 263

[67]    Lim, B. S.; Holm, R. H. *J. Am. Chem. Soc.* 2001, 123, 1920

[68]    Sheldrick, G. M. *Acta Crystallogr., Sect. A: Found. Crystallogr.* 64 (2008) 112

[69]    Stender, M.; Wright, R. J.; Eichler, B. E.; Prust, J.; Olmstead, M. M.; Roesky,  H. W.; Power, P. P., *J. Chem. Soc.*, *Dalton Trans*., (2001) 3465

[70]    Müller, P., Ed. *Crystal structure refinement: A crystallographer's guide to SHELXL*, Oxford University Press. (2006)

[71]    Blake, A. B.; Cotton, F. A.; Wood, J. S. *J. Am. Chem. Soc.* 86 (1964) 3024

[72]    Ballhausen, C. J.; Djurinskij, B. F.; Watson, K. J. *J. Am. Chem. Soc.* 90 (1968) 3305

[73]    Kamenar, R.; Prout, C. K. *J. Chem. Soc.* A (1970) 2379

[74]    Wieghardt, K.; Backes-Dahmann, G.; Holzbach, W.; Swiridoff, W. J.; Weiss, J.  *Z. Anorg. Allgem. Chem.* 499 (1983) 44

[75]    Tkachev, V. V.; Krasochka, O. N.; Atovmyan, L. O. *Zh. Struct. Khim.* 17 (1976) 940

[76]    Shustorovich, E.M.; Porai-Koshits, M.A.; Buslaev, Y.A. *Coord. Chem. Rev*. 17 (1975) 1

[77]    Hubert-Pfalzgraf, L. G.; Pinkerton, A. A. *Inorg. Chem.* 16 (1977) 1895

[78]    Hey, E.; Weller, F.; Dehnicke, K. *Z. Anorg. Allgem. Chem*. 502 (1983) 45

[79]    Manojlovic-Muir, L. *J. Chem. Soc.* A (1971) 2796

[80] Berg, J. M.; Hodgson, K. O. *Inorg. Chem.* 19 (1980) 2180

[81] Thomas, R. W.; Estes, G. W.; Elder, R. C.; Deutsch, E. *J. Am. Chem. Soc.* 101 (1979) 4581

[82] Casteel Jr. W.J.; MacLeod D.M.; Mercier, H.P.A.; Schrobilgen, G.J. *Inorg. Chem.* 35 (1996) 7279

[83] Cowie M.; Bennett, M.J. *Inorg. Chem.* 15 (1975) 1584

[84] Wang, K.; McConnachie J.M.; Stiefel, E.I. *Inorg. Chem.* 38 (1999) 4334

[85] Friedle, S.; Partyka, D.V.; Bennett M.V.; Holm, R.H. *Inorg. Chim. Acta* 359 (2006) 1427.

[86] Kapre, R.R.; Bothe, E.; Weyhermüller, T.; George S.D; Wieghardt, K. *Inorg. Chem.* 46 (2007) 5642. ;

[87] Boyde, S.; Garner, C.D.; Enemark, J.H.; Bruck M.A.; Kristofzski, J.G. *J. Chem. Soc., Dalton Trans.* (1987) 2267.

[88] Cervilla, A.; Lopis, E.; Marco D.; Perez, F. *Inorg. Chem.* 40 (2001) 6525

[89] Isfort, C.S.; Pape T.; Hahn, F.E. *Eur. J. Inorg. Chem.* (2005) 2607

[90] Formitchev, D.; Lim B.S.; Holm, R.H. *Inorg. Chem.* 40 (2001) 645

[91] Sugimoto, H.; Furukawa, Y.; Tarumizu, M.; Miyake, H.; Tanaka K.; Tsukube, H. *Eur. J. Inorg. Chem.* (2005) 3088

[92] Boyde, S.; Garner, C.D.; Enemark J.H.; Bruck, M.A. *J. Chem. Soc., Dalton Trans.* (1987) 297

[93] Draganjac M.; Coucouvanis, D. *J. Am. Chem. Soc.* 105 (1983) 139

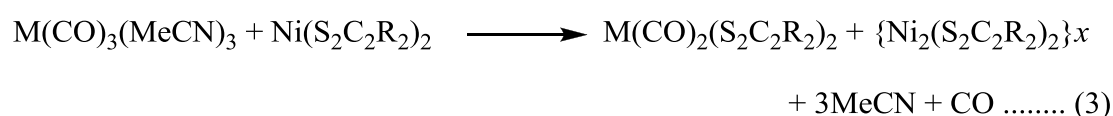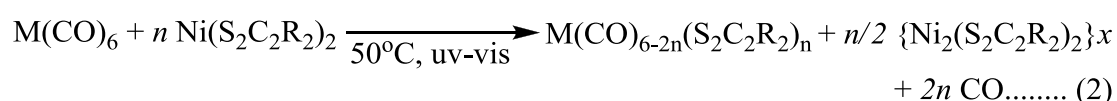[94] Matsubayashi, G.; Douki, K.; Tamura, H.; Nakano M.; Mori, W. *Inorg. Chem.* 32 (1993) 5990

[95]     Döring A. Verbindungen von Molybdän und Wolfram in den Oxidationsstufen IV – VI

als Modelle für Molybdän- und Wolfram-Cofaktoren, Ph.D Dissertation 2010,

University of Göttingen

# DITHIOLENE LIGAND TRANSER FROM TUNGSTEN TO STRONTIUM: AN UNPRECEDENTED CHEMISTRY

## 6.1. Introduction to metal to metal dithiolene transfer

Dithiolenes - are they just noninnocent? Not only noninnocent but these remarkable ligands have been known to change their loyalty from metal to metal depending on the (chemical) circumstances. However, this is one of the least documented areas in the scientific literature. Dithiolene ligand transfers so far have been known to take place only between transition metals. Such reactions can be mainly classified into two types: (1) redox reactions which involve the change in oxidation state of the metal atoms included and (2) non-redox reactions in which the oxidation states remain unaltered during the reaction. In all redox reactions reported so far nickel was the only donor of the dithiolene ligands. The first report of dithiolene transfer from nickel to a transition metal was by Schrauzer et al. in 1966.[1] In this remarkable work, $Ni(S_2C_2R_2)_2$, (R = alkyl or aryl) was refluxed with $M(CO)_6$, (M= Cr, Mo, W) to afford the tris(dithiolene) compound $M(S_2C_2R_2)_3$ according to equation 1. When the same reaction was carried out at milder conditions in the presence of UV-Vis light,

the carbon monoxide bearing molybdenum and tungsten dithiolates were obtained according to equation 2. Later on, the Holm group modified the second reaction by replacing $M(CO)_6$ by $M(CO)_3(CH_3CN)_3$, (M =Mo, W).[2-3] This reaction took place in dichloromethane in the absence of irradiation resulting in a better yield according to equation 3. The bis(dithiolene)Mo/W compound was isolated by silica gel column chromatography. In all three cases one $S_2C_2R_2$ ligand was transferred to the group VI metal; the other ligand remained attached to the nickel, forming the insoluble and probably polymeric nickel dithiolate, $(Ni^{II}_2S_4C_4R_4)x$.

$$M(CO)_6 + Ni(S_2C_2R_2)_2 \xrightarrow[120^oC]{} M(S_2C_2R_2)_3 + 1.5\ \{Ni_2(S_2C_2R_2)_2\}x + 6CO \cdots\cdots (1)$$

$$M(CO)_6 + n\ Ni(S_2C_2R_2)_2 \xrightarrow[50^oC,\ uv\text{-}vis]{} M(CO)_{6\text{-}2n}(S_2C_2R_2)_n + n/2\ \{Ni_2(S_2C_2R_2)_2\}x$$
$$+ 2n\ CO \ldots\ldots (2)$$

$$M(CO)_3(MeCN)_3 + Ni(S_2C_2R_2)_2 \longrightarrow M(CO)_2(S_2C_2R_2)_2 + \{Ni_2(S_2C_2R_2)_2\}x$$
$$+ 3MeCN + CO \ldots\ldots (3)$$
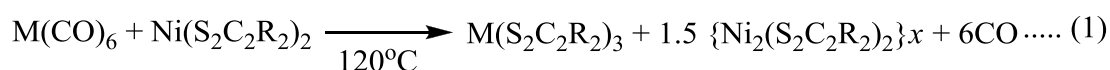
In a very similar synthetic route, Holm et al. synthesized $[W(CO)_2(S_2C_2(C_6H_4\text{-}p\text{-}X)_2)_2]$, (x = Br, F, Me, OMe), by the dithiolene ligand transfer between $[Ni(S_2C_2(C_6H_4\text{-}p\text{-}X)_2)_2]$ and $W(CO)_3(MeCN)_3$ (Figure 1-A).[4] Recently, Donahue modified Holm's procedure by varying the separation methods and found that in a reaction between $Ni(S_2C_2Me_2)_2$ and $W(CO)_3(MeCN)_3$ in dichloromethane, the dithiolene transfer from Ni to W results in the formation of three products: the mono(dithiolene), $W(S_2C_2Me_2)CO_4$, the bis(dithiolene), $W(S_2C_2Me_2)_2(CO)_2$ and the tris(dithiolene), $W(S_2C_2Me_2)_3$.[5] All these three products were isolated and systematically characterized. Other examples of dithiolene transfer from nickel to $M(CO)_3(MeCN)_3$, (M = Mo, W) were described in a report by Sugimoto and are illustrated in figure 1-B.[6-7] This reaction occurs in the exact same way as described in equation 3 with

(A)

X = Br, F, Me, OMe

(B)

X = C, O, S

M = Mo, W
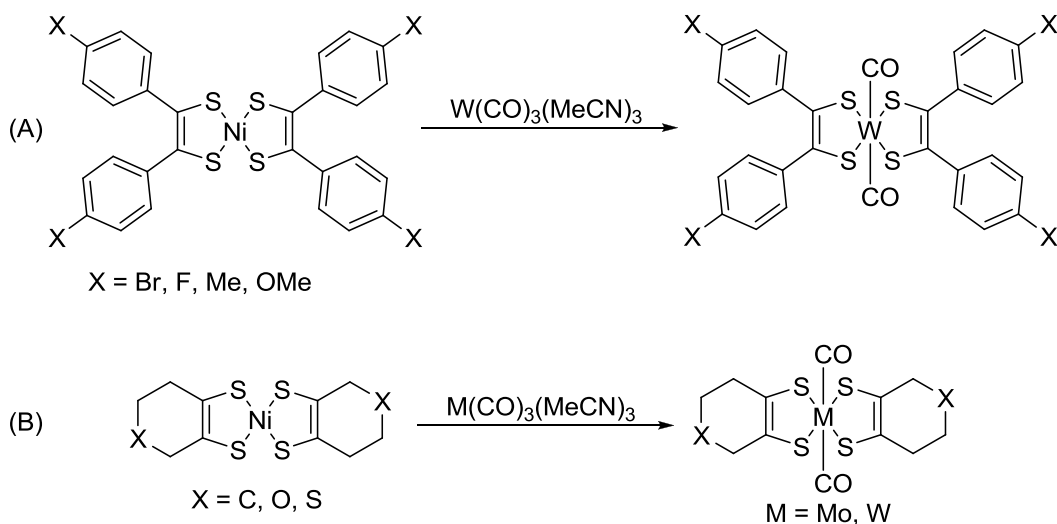
**Fig. 1. Representative examples of dithiolene ligand transfer from Ni to M(CO)$_3$(MeCN)$_3$**

(The byproducts of the reactions are similar to that given in equation 3)
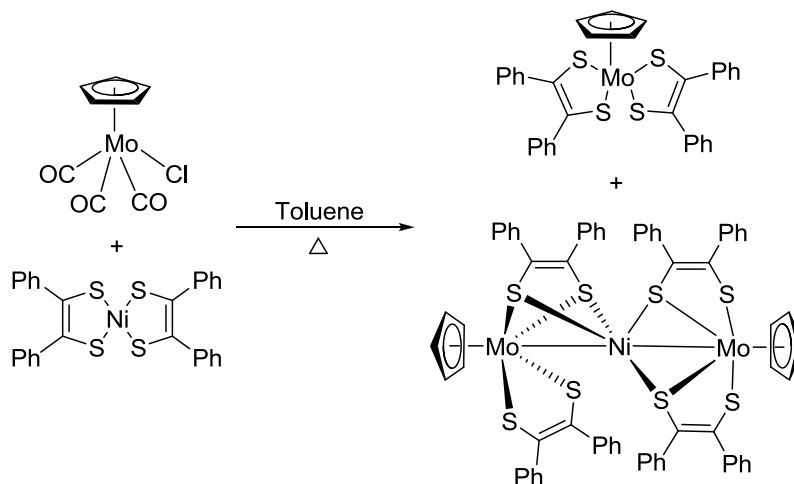


**Fig. 2. Dithiolene ligand transfer from Ni to CpMo(CO)$_3$Cl**

two of the CO groups being retained at the molybdenum atom after the dithiolene

substitution. But the retention of the CO groups largely depends on the steric factor based

on other ligands. For example, the dithiolene ligand transfer reaction between [Ni(S$_2$C$_2$Ph$_2$)$_2$]

and [CpMo(CO)$_3$Cl], (Cp = η-C$_5$H$_5$) affords the neutral paramagnetic molybdenum

bis(dithiolene) complex [CpMo(S$_2$C$_2$Ph$_2$)$_2$] in which all CO groups have been displaced from

the molybdenum center due to the presence of the sterically demanding Cp group.[8] In

contrast to the above mentioned reactions of this kind, the second product of this reaction is

the unusual trinuclear species Ni[Mo(S$_2$C$_2$Ph$_2$)$_2$Cp]$_2$ with three different dithiolene bonding

modes - terminal, bridging, and semi-bridging - in the same molecule. (Figure 2)

Nickel to iron dithiolene transfer was reported in 1972 by Schrauzer who investigated

the reaction between a nickel dithiolene complex with Fe(CO)$_5$ as illustrated in figure 3.[9]

However, further examples of the Ni to Fe dithiolene transfer are limited in the literature.

Another metal which has been shown to accept dithiolene from nickel is ruthenium. In the

reaction between [Ni(SCR=CPhS)$_2$] (R = Ph, H) and [RuCl$_2$(PPh$_3$)$_3$] one dithiolene is rapidly

transferred to yield [RuCl$_2$(SCR=CPhS)(PPh$_3$)$_2$] at room temperature whereas in refluxing

toluene two dithiolene ligands are incorporated to give [Ru(SCR=CPhS)$_2$(PPh$_3$)] (figure 4).[10]
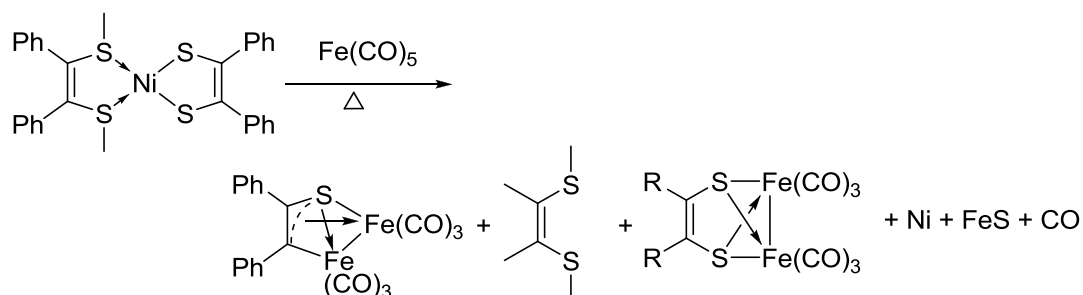
**Fig. 3. Ni to Fe dithiolene transfer**
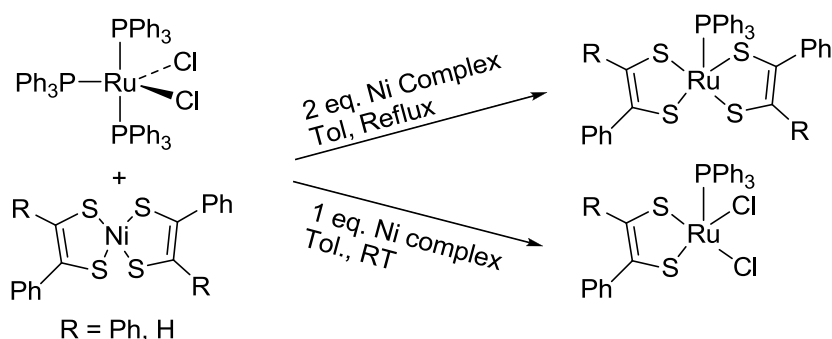
**Fig. 4. Dithiolene transfer from Ni to Ru**

The non-redox dithiolene transfer chemistry has not been intensively studied so far and examples in the literature are rare. Non-redox reactions usually involve the use of Zn(II) or $Cp_2Ti(IV)$ based complexes as dithiolene donors. Dithiolenes of Ti(IV) and Zn(II) transfer the alkenedithiolate to softer metals. For example, $[Cp_2Ti(S_2C_2R_2)]$ (R = $CO_2Me$, $CF_3$), reacts with $[RhCl_2(CO)_2]^-$ or $NiCl_2(PR_3)_2$, to give the corresponding late metal dithiolene.[11] Likewise $[Zn(S_2C_2(CO_2Me)_2)(tmeda)]$, (tmeda = tetramethylethylenediamine) also displays dithiolene transfer reactivity with $PdCl_2(MeCN)_2$ to form the palladium hexamer compound $[PdS_2C_2(CO_2Me)_2]_6$ as shown in figure 5.[12] Organic salts of $[Zn(dmit)_2]^{2-}$ (dmit = 4,5-dimercapto-1,3-dithiole-2-thione) readily undergo dithiolene transfer reactions with metal chlorides. For example, this dianion reacts with $[Cp_2TiCl_2]$, $VCl_3$, $NbCl_5$ and $[AuCl(PPh_3)]$ to afford $[Cp_2Ti(dmit)]$,[13] $[V(dmit)_3]^{2-}$,[14] $[Nb_2S_4(dmit)_4]^{2-}$ [15] and $[\{Au(PPh_3)\}_2(dmit)]$ [16] respectively.
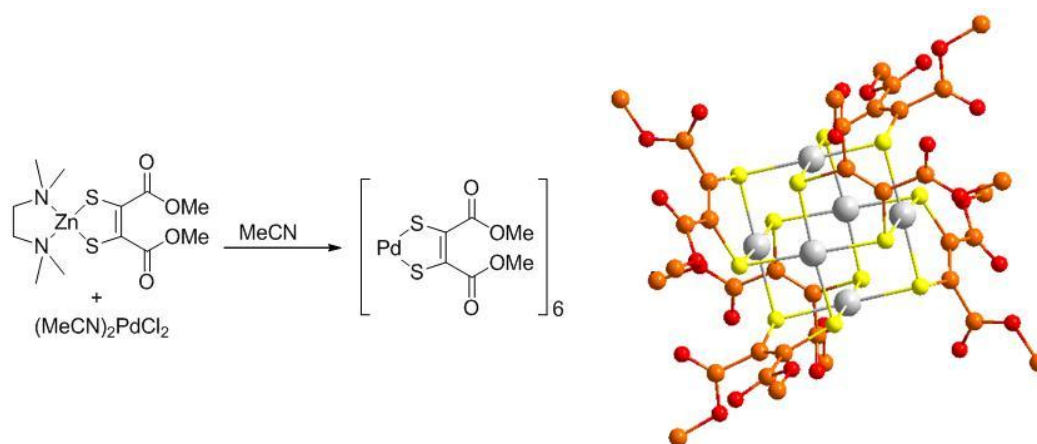


**Fig. 5. Dithiolene transfer from Zn to Pd**

## 6.2. Dithiolene complexes of main group elements

Several main group dithiolene complexes are known today. They include monodithiolene, homoleptic bis(dithiolene) and homoleptic tris(dithiolene) complexes.

Carbon,[17-18] silicon,[19] germanium,[20] antimony,[21-23] thallium,[24] lead,[25] bismuth [26-27] and tellurium [28-29] are known to make bis(dithiolene) complexes as illustrated in figure 6. Most of these complexes have a distorted tetrahedral geometry around the metal center. C, Si, Ge, and Tl complexes have a nearly identical tetrahedral geometry with dihedral angles between the dithiolene ligands of nearly $90^{\circ}$. At the same time both tellurium complexes given in figure 6 have a square planar geometry. The main group elements which are known to form homoleptic tris(dithiolene) complexes are tin,[30-31] indium [32] and antimony [33-35] and the chemical structures of these compounds are given in figure 7. Monodithiolene complexes are rare and the examples include $[Sr(C_4S_4)]\cdot 2H_2O$,[36] $Ba_4K_2(C_4S_4)_5\cdot 16\ H_2O$,[36] $[Mg(C_4S_4)]\cdot 6H_2O$ [37] and $[Ca(C_4S_4)]\cdot 4H_2O$ [37] (figure 8).



**Fig.6. Homoleptic bis(dithiolene) complexes of main group elements**

M = Sn, Sb; X =S
M = Sn; X = O



M= Sn, n = -2
M= In, n = -3

X = H, Me
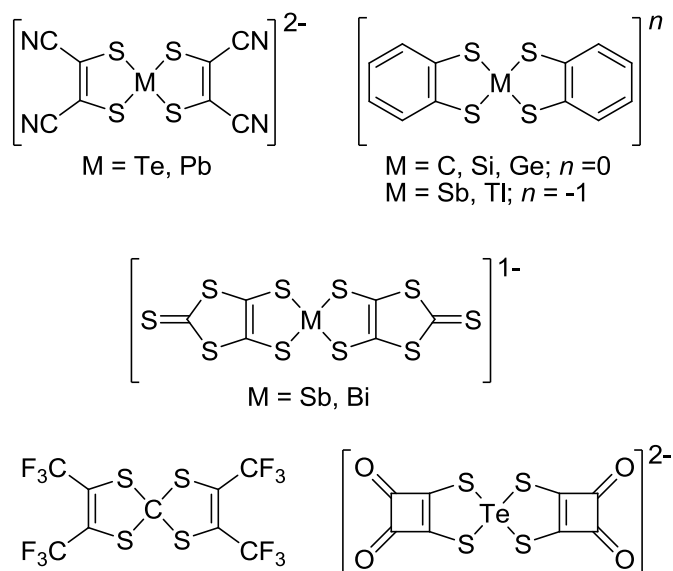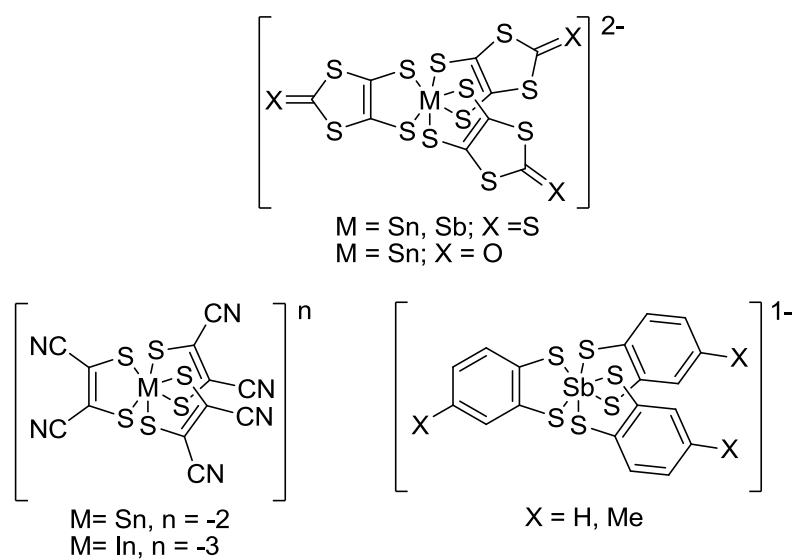
**Fig. 7. Homoleptic tris(dithiolene) complexes of main group elements**
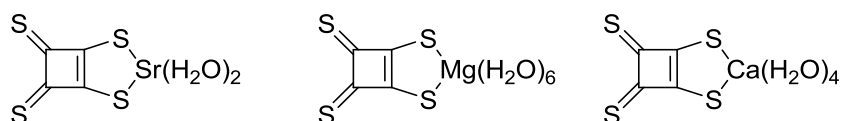


**Fig. 8 Mono(dithiolene) complexes of main group elements**

## 6.3. Scope of the present study

The above discussion shows that the metal to metal dithiolene transfer chemistry is not as thoroughly studied as possible and only a few metals like nickel, zinc and titanium are known to act as dithiolene donors in the published studies. In many cases the group VI metals, especially Mo and W, act as the ligand accepters. However, in this respect exceptional behavior of tungsten was observed in the course of my own studies. I hereby report the first dithiolene transfer reaction in which the donor metal is tungsten. In a reaction between the bis(dithiolene) complex of tungsten and nacnac supported strontium iodide, tungsten transfers its dithiolene ligand to strontium. In fact, this result is a serendipity and the original intention was to synthesize the compound

[WO(cdt)$_2$][Sr(nacnac)]$_2$. The idea originated after several methods to crystallize [WO(cdt)$_2$]$^{2-}$ failed (details in chapter 2.5). The nacnac moiety (which is well known for giving good crystals) was chosen to support the crystallization of the crucial anionic part of the complex as illustrated in figure 9. But the isolated product formed was a strontium hexamer bridged by sulfur atoms of the cdt ligand in a truly unique way.
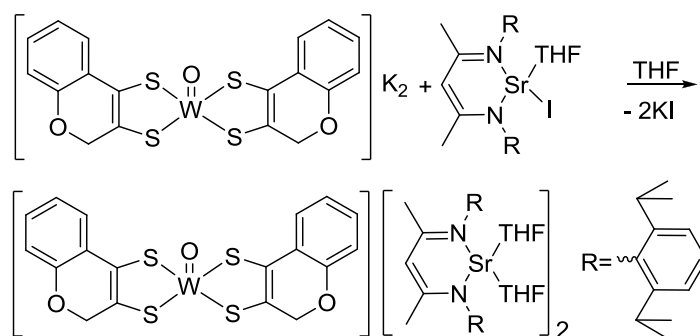


**Fig. 9. Original idea behind the formation of [Sr(cdt)(THF)$_2$]$_6$**

## 6.4. Experimental

**6.4.1. Preparation of [Sr(cdt)(THF)$_2$]$_6$; (1):** To a solution of K$_2$[WO(cdt)$_2$] (200 mg, 0.3 mmol) in THF (20 ml), [LSr($\mu$-I)(THF)]$_2$ (422mg, 0.3 mmol) (L = $\beta$-diketiminate) [38] previously dissolved in 10 ml THF was added at -20$^o$C slowly under nitrogen atmosphere. The reaction was allowed to reach room temperature in 1 hour and stirred again for 15 hrs. The solution was concentrated to 10 ml and filtered to collect the brownish red solution. On cooling to -35$^o$C, tiny crystals of [Sr(cdt)(THF)$_2$]$_6$ were obtained. The crystals were removed from the pasty brownish byproduct (which was not characterized) by hand picking under a microscope and a suitable crystal was mounted on a glass fiber and data was collected on an IPDS II STOE image-plate diffractometer (graphite monochromated Mo K$_\alpha$ radiation,

$\lambda$=0.71073 Å at 133(2) K. The data was integrated with X-Area. The structure was solved and refined by SHELXS-97.[39]

## 6.5. Results and Discussion

As stated previously, the chromandithiolene (cdt) ligand in $K_2[WO(cdt)_2]$ is transferred to the strontium center (Figure 10). The byproducts in this reaction were not characterized. Compound **1** crystallizes in a trigonal space group R-3 with the cell dimensions a = 40.425(6), b = 40.425(6) and c = 27.550(11) Å. By stoichiometry, each strontium atom is attached to one cdt ligand and two molecules of THF. The coordinatively unsaturated strontium atoms are then bridged through the sulfur atoms of cdt to form the hexamer. A monomer unit of compound 1 is shown in figure 11. In the given unit, the dithiolene plane defined by S1-C1-C2-S2 has a dihedral angle with the S1-S2-Sr1 plane of 75°. The C1-C2 bond length is 1.3591 Å which is slightly more than the ideal C=C double bond length (1.34 Å). The lengths of the Sr-S bonds are: Sr1-S1 = 3.0546, Sr1-S2 = 2.9829 (both from the monomeric unit), Sr2-S1 = 3.134, Sr6-S1 = 3.080 and Sr6-S2 = 2.954 Å (all three from the bridging to the neighboring monomeric units). Figure 12 shows the hexamer molecule in which the strontium atoms are connected through the sulfur atoms.
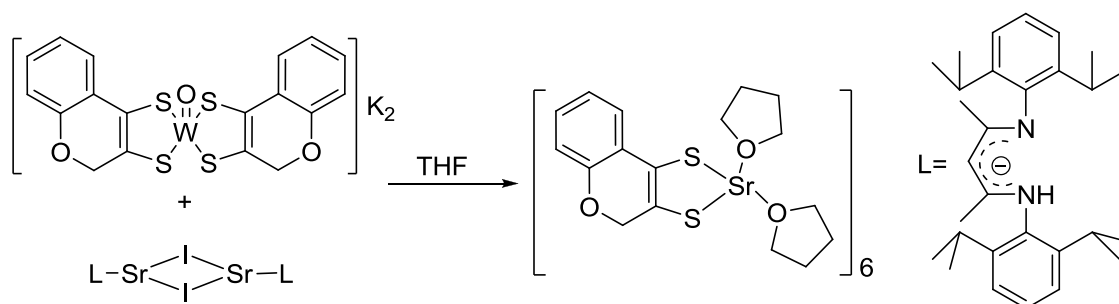


**Fig. 10. Formation of compound 6 by dithiolene transfer**
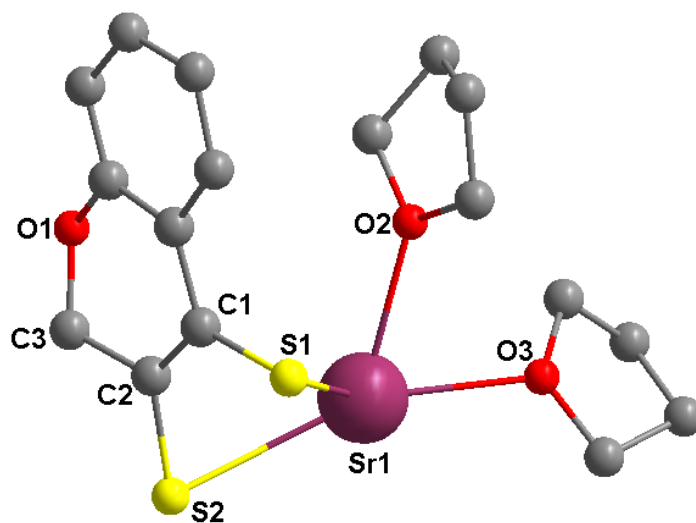
**Fig. 11. The monomer unit of compound 1**
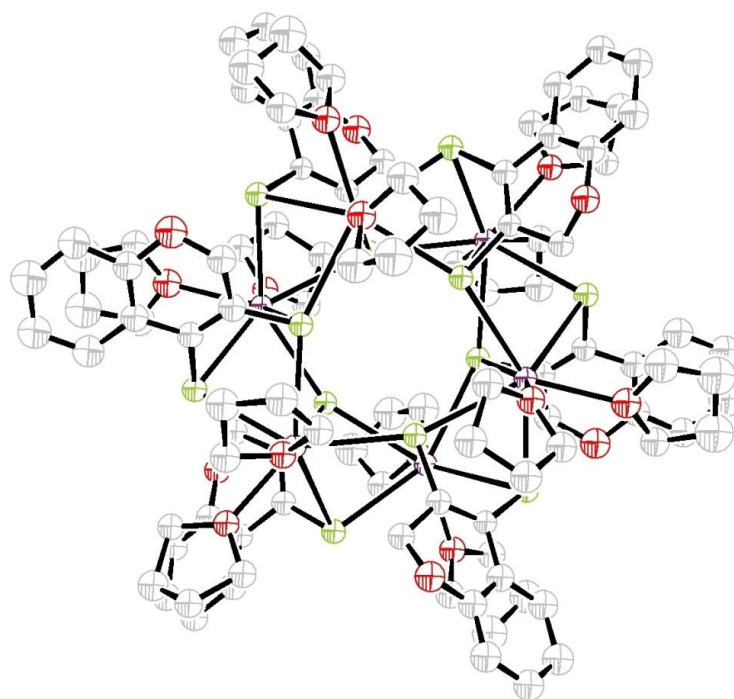


**Fig. 12. Hexameric structure of compound 1**

For simplicity, the coordinated THF molecules are eliminated in figure 13. It can be seen that there are two types of bridging sulfur atoms: six $\mu^2$ sulfur atoms (S2, S4, S6, S8, S10 and S12) which bridge two strontium atoms each and six $\mu^3$ sulfur atoms (S1, S3, S5, S7, S9 and S11) which bridge three strontium atoms. For each cdt ligand, one sulfur atom acts as $\mu^2$ and the other one as $\mu^3$. For example S1 is a $\mu^3$ sulfur atom which bridges, Sr1, Sr2 and Sr6

and S2 is a $\mu^2$ sulfur which bridges Sr1 and Sr6. This different bridging nature of the sulfur atoms is also reflected in the corresponding C-S bond length. The $\mu^2$ sulfur atoms have an average C-S bong length equal to 1.76 Å while the average C-S bong length for $\mu^3$ sulfur atoms is 1.77 Å.  The selected geometric parameters of compound **1** are provided in table 1. All metric values are to be taken with caution due to the twinning and consequent high R-value. (A crystal of this compound has been measured on a Bruker Smart 6000 CCD diffractometer equipped with a rotating anode generator and Incoatec Helios optics using Cu Kα radiation (λ=1.54178 Å) by Kevin Pröper and the data is in the publishable range. However, the metrical data of the better measurement has not been used here because the complete data necessary for an in depth discussion was not made available at the time of writing this thesis. Therefore the metrical values given in this chapter will be changed according to the new data in future publication. For details, see appendix 4)
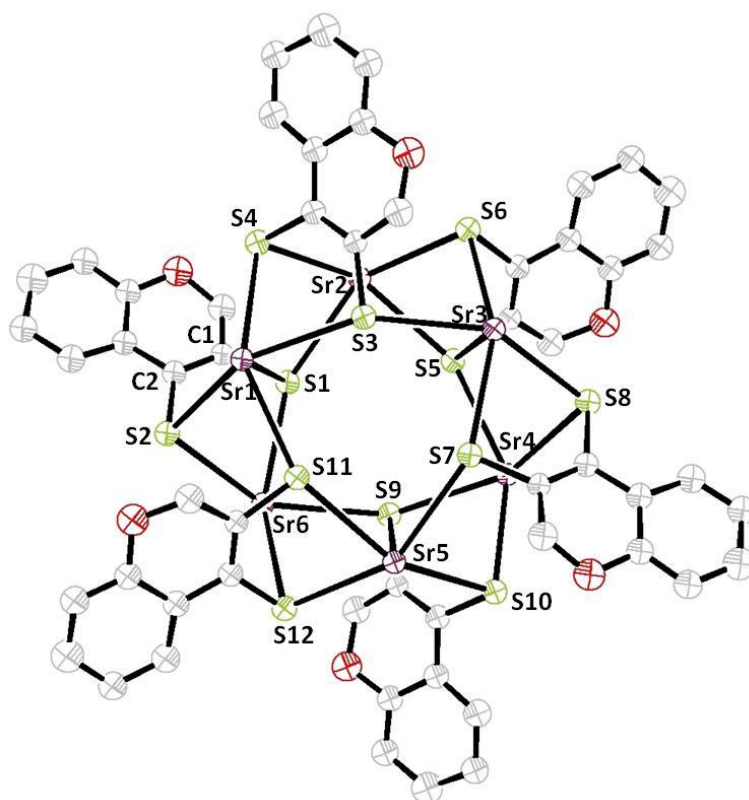


**Fig. 13. Structure of [Sr(cdt)(THF)₂]₆ (THF molecules are omitted for clarity)**

**Table 1: Selected bond lengths and angles in compound 1**

| Bond lengths (Å) | | Bond angles (°) | |
|---|---|---|---|
| Sr1-S1 | 3.055 | S11-Sr1-S3 | 82.50 |
| Sr1-S2 | 2.983 | Sr6-S1-Sr2 | 149.51 |
| Sr1-S3 | 3.080 | S2-Sr1-S11 | 80.14 |
| Sr1-S4 | 2.954 | S2-S6-S11 | 81.91 |
| Sr1-S11 | 3.134 | S4-Sr1-S3 | 68.34 |
| Sr2-S1 | 3.134 | S4-Sr2-S3 | 68.31 |
| Sr6-S1 | 3.080 | C2-S2-Sr1 | 75.07 |
| Sr6-S2 | 2.954 | C1-S1-Sr1 | 74.80 |
| C2-S2 | 1.760 | | |
| C1-S1 | 1.770 | | |
| C1-C2 | 1.359 | | |

Figure 14 shows the Sr-S core in compound 1. The adjacent strontium atoms are separated by a distance of 4.176 Å. In fact the entire core is a stacking of six equilateral triangles with parallel planes: S3-S7-S11 (edge length = 4.097 Å), S1-S5-S9 (edge length = 4.097Å), S4-S8-S12 (edge length = 8.769 Å), S2-S6-S10 (edge length = 8.769 Å), Sr1-Sr3-Sr5 (edge length = 5.995 Å) and Sr2-Sr4-Sr6 (edge length = 5.995 Å). The positions of six strontium atoms resemble a chair structure with a dihedral angle of 91.63°. There are other reports of hexameric compounds of strontium already in the literature. $[Sr_6\{O_2CN(PPh_2)_2\}_6\{N(CO_2)_3\}](THF)_7$ is a strontium hexameric compound prepared by the Kemp group in which strontium atoms are bridged through μ-O-C-O-μ groups provided by

$O_2CN(PPh_2)_2$ moieties.[40] Another example is an $Sr_{12}$ aggregate synthesized by the Fromm group in which two oxocentered $Sr_6$-octahedra $[\{Sr_6(O)(\mu^3\text{-}I)(I)_2(O^tBu)_7(THF)_3\}_2(\mu\text{-}I)]^-$ are bridged via iodide along a Sr-I-Sr bond.[41] In this context my work presents a strontium hexamer, in which six strontium atoms are trapped inside an organic matrix that is novel with respect to three features. Firstly the strontium centers are bridged by sulfur atoms without any involvement of oxygen (or iodine) in the structure coherence. Secondly the inside of the cluster contains a cavity and no coordinating atoms as in the other two known structures. And thirdly, in this beautiful cluster the dithiolene ligands act as bridging ligands in an unprecedented $\mu^2$ and $\mu^3$ type of way in which one sulfur donor is even bound to three different metal centers.
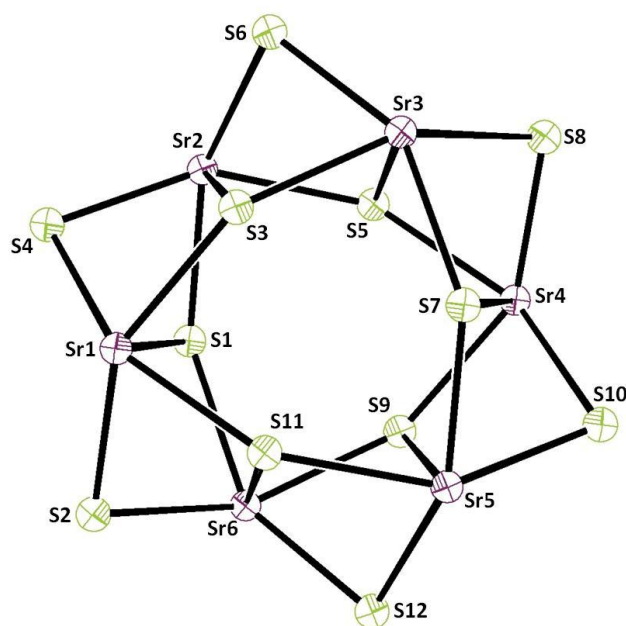


**Fig. 14. Strontium-sulfur core in [Sr(cdt)(THF)$_2$]$_6$**

## References

[1]    Schrauzer, G. N.; Mayweg, V. P.; Heinrich, W. *J. Am. Chem. Soc.* 88 (1966) 5174

[2]    Lim, B. S.; Donahue, J. P.; Holm, R. H. *Inorg. Chem.* 39 (2000) 263

[3]     Goddard, C. A.; Holm, R. H. *Inorg. Chem.* 38 (1999) 5389

[4]     Sung, K. -M.; Holm, R. H. *J. Am. Chem. Soc.* 124 (2002) 4312

[5]     Chandrasekaran, P.; Arumugam, K.; Jayarathne, U.; Perez, L. M.; Mague, J. T.; Donahue, J. P. *Inorg. Chem.* 48 (2009) 2103

[6]     Sugimoto, H.; Harihara, M.; Shiro, M.; Sugimoto, K.; Tanaka, K.; Miyake, H.; Tsukube, H. *Inorg. Chem*. 44 (2005) 6386

[7]     Sugimoto, H.; Sugimoto, K. *Inorg. Chem. Commun.* 11 (2008) 77

[8]     Adams, H.; Gardner, H. C.; McRoy, R. A.; Morris, M. J.; Motley, J. C.; Torker, S. *Inorg. Chem.* 45 (2006) 10967

[9]     Schrauzer, G. N.; Kisch*, H. *J. Am. Chem. Soc.* 95 (1973) 2501

[10]    Adams, H.; Coffey, A. M.; Morris, M. J.; Morris, S. A. *Inorg. Chem.* 48 (2009) 11945

[11]    Bolinger, C. M.; Rauchfuss, T. B. *Inorg. Chem.* 21 (1982) 3947

[12]    Beswick, C. L.; Terroba, R.; Greaney, M. A.; Stiefel, E. I. *J. Am. Chem. Soc.* 124 (2002) 9664

[13]    Fourmigue´, M. *Coord. Chem. Rev*. 178–180 (1998)  823

[14]    Matsubayashi, G.; Akiba, K.; Tanaka, T. *Inorg. Chem.* 27 (1988) 4744

[15]    Matsubayashi, G.; Natsuaki, K.; Nakano, M.; Tamura, H.; Arakawa, R. *Inorg. Chim. Acta* 262 (1997) 103

[16]    Cerrada, E.; Laguna, A.; Laguna, M.; Jones, P. G. *J. Chem. Soc., Dalton Trans.* (1994) 1325

[17]    Udea, K.; Iwamatsu, M.; Sugimoto, T.; Tada, T.; Nishimura, K. -I. *Acta Crystallogr. Sect. C (Cr. Str. Comm.)* 56 (2000) e160

[18]    Reimann-Andersen, S.; Pritzkow, H.; Sundemeyer, W. *Chem. Ber.* 127 (1994) 533

[19]    Herzog, U.; Bohme, U.; Rheinwald, G. *J. Organomet. Chem.* 612 (2000) 133

[20]   Pfeiffer, J.; Noltemeyer, M.; Meller, A. *Z. Anorg. Allg. Chem.* 572 (1989) 145

[21]   Wegener, J.; Kirschbaum, K.; Giolando, D. M. *J. Chem. Soc., Dalton Trans.* (1994) 1213

[22]   Ganis, P.; Marton, D.; Spencer, G. M.; Wardell, J. L.; Wardell, S. M. S. V. *Inorg. Chim. Acta* 308 (2000) 139

[23]   Doidge-Harrison, S. M. S. V.; Irvine, J. T. S.; Spencer, G. M.; Wardell, J. L.; Wei, M.; Ganis, P.; Valle, G. *Inorg. Chem.* 34 (1995) 4581

[24]   Bosch, B. E.; Eisenhawer, M.; Kersting, B.; Kirschbaum, K.; Krebs, B.; Giolando, D. M. *Inorg. Chem.* 35 (1996) 6599

[25]   Hummel, H. -U.; Meske, H. *Z. Naturforsch. Teil B* 44 (1989) 1531

[26]   Comerlato, N. M.; Costa, L. A. S.; Howie, R. A.; Pereira, R. P.; Rocco, A. M.; Silvino, A. C.; Wardell, J. L.; Wardell, S. M. S. V. *Polyhedron* 20 (2001) 415

[27]   Comerlato, N. M.; Harrison, W. T. A.; Howie, R. A.; Silvino, A. C.; Wardell, J. L.; Wardell, S. M. S. V. *Inorg. Chem. Commun.* 3 (2000) 572

[28]   Golic, L.; Dietzsch, W.; Kohler, K.; Stach, J.; Kirmse, R. *J. Chem. Soc., Dalton Trans.* (1988) 97

[29]   Drutkowski, U.; Strauch, P. *Inorg. Chem. Commun*. 4 (2001) 342

[30]   Day, R. O.; Holmes, J. M.; Shafieezad, S.; Chandrasekhar, V.; Holmes, R. R. *J. Am. Chem. Soc.* 110 (1988) 5377

[31]   Assis, F. de; Chohan, Z. H.; Howie, R. A.; Khan, A.; Low, J. N.; Spencer, G. M.; Wardell, J. L.; Wardell, S. M. S. V. *Polyhedron* 18 (1999) 3533

[32]   Einstein, F. W. B.; Jones, R. D. G. *J. Chem. Soc.* A (1971) 2762

[33]   Wegener, J.; Kirschbaum, K.; Giolando, D. M. *J. Chem. Soc., Dalton Trans.* (1994) 1213

[34]   Kisenyl, J. M.; Willey, G. R.; Drew, M. G. B.; Wandiga, S. O. *J. Chem. Soc., Dalton Trans.* (1985) 69

[35]   Spencer, G. M.; Wardell, J. L.; Aupers, J. H. *Polyhedron* 15 (1996) 2701

[36]   Beck, J.; Ben-Amer, Y. *Z. Anorg. Allg. Chem.* 634 (2008) 1522

[37]   Beck, J.; Ben-Amer, Y. *Z. Anorg. Allg. Chem.* 633 (2007) 435

[38]   Sarish, S.P.; Jana, A.; Roesky, H.W.; Schulz, T.; John, M.; Stalke, D. *Inorg. Chem*. 49 (2010) 3816

[39]   Sheldrick, G. M. *Acta Crystallogr., Sect. A: Found. Crystallogr.* 64 (2008) 112

[40]   Dickie, D. A.; Parkes, M. V.; Kemp, R. A. *Angew. Chem. Int. Ed*. 47 (2008) 9955

[41]   Maudez, W.; Vig-Slenters, T.; Mirolo, L.; Fleury, A; Fromm, K.M. *Main Group Chem*. 5 (2006) 41

# SUMMARY AND OUTLOOK

## 7.1. Summary

Molybdenum is crucially important for almost all organisms ranging from ancient single cell microorganisms to modern human being. This is somehow unusual since molybdenum is the only second row transition element known to have a role in vital enzymatic processes. Its higher homologue tungsten is the only third row transition element of biological importance and it is used in similar enzymes for analogous reactions especially if molybdenum is not available in a specific habitat. The reactions catalyzed by molybdenum and tungsten cofactors involve two electron oxidation or reduction usually accompanied by an oxygen atom transfer from water to substrate or vice versa as part of the carbon, nitrogen and sulfur metabolism. All molybdenum and tungsten enzymes (except nitrogenase) have one or two of a unique ligand called molybdopterin in their active site and this ligand establishes the coordination to the metal through a dithiolene function. The remaining coordination sites in the metal are filled by a varying combination of oxo, sulfido, hydroxo, water and/or amino acid residue ligands. Since the discovery of the molybdenum

and tungsten cofactors it has been the aim of several bioinorganic chemistry groups to understand their structure and functionality by model chemistry. Bioinorganic chemists' attempts in this respect have afforded so far quite a number of molybdenum and tungsten complexes being structural or functional models or both. Most of them were developed using the conventional dithiolene ligands even though the role of the complicated and unique structure of molybdopterin in the function of the enzyme is beyond doubt. In order to address this issue, the first focus of this thesis has been devoted to the detailed study of molybdenum and tungsten compounds with pyrane dithiolene derivatives. This type of compounds is important because, the structure of the natural molybdopterin also has a pyrane ring adjacent to the dithiolene function.

The second chapter of this thesis presents two important bisdithiolene complexes: $[MoO(cdt)_2]^{2-}$ and $[WO(cdt)_2]^{2-}$. The former one is a very close mimic for the active site of arsenite oxidase in the reduced state as shown in figure 1. Both compounds show a weakened M=O bond character. This weakened M=O bonds have bioinorganic importance revealed from the EXAFS studies of the oxidized form of arsenite oxidase. The EXAFS studies suggested that the $Mo^{VI}O_2$ core of arsenite oxidase had one longer $Mo^{VI}O$ bond at 1.83 Å and this undergoes protonation to form $Mo^{VI}O(OH)$ in the catalytic cycle. Most of the earlier reported $Mo^{VI}O_2$ complexes with weaker electron donating ligands had strong Mo=O bonds and protonation rarely occurred. The weakened M=O bond character of complexes synthesized in the present study indicate the importance of incorporating pyrane in the model complexes of molybdopterin based enzymes.

**Figure 1**

The temperature dependent electrochemistry and catalytic properties of both $[MoO(cdt)_2]^{2-}$ and $[WO(cdt)_2]^{2-}$ were studied in comparison with other model complexes (figure 2) and the results are described in chapter 3 of this thesis. The atom X in figure 2 has been chosen to be carbon, sulfur or oxygen. The electrochemical studies indicated that for X = O (as in the case of natural molybdopterin) the non-innocence of the ligand was more pronounced than if X = C or S. This is an important observation, because the noninnocence of the molybdopterin ligand is believed to have a prime role in fine tuning the metal's oxidation state and thereby optimizing the catalytic activity. The temperature dependent electrochemical analysis showed that for each ligand, the temperature sensitivity of the redox potential was greater for the tungsten compound than for its molybdenum counterpart. In addition, the temperature sensitivity of redox potential is least pronounced when X= O. On the basis of these studies it can be concluded that the presence of a pyrane ring in molybdopterin contributes to the fine tuning of the redox potential and to providing a more stable redox potential of the metal center towards temperature changes prevailing in the gradual development of living habitats. It is argued that this more stable redox potential

of molybdenum was one of the driving forces for the evolutionary development of molybdenum enzymes from an era of tungsten enzymes of the early earth.



M = Mo, W
X = O, S, C
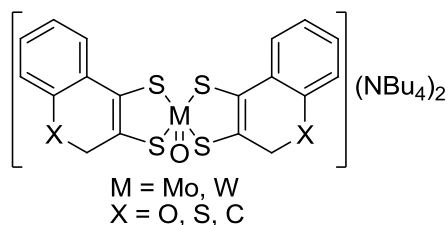
**Figure 2**

Chapter 3 continues with discussing the catalytic properties of all three pairs of compounds described above. It was found that in an oxotransfer reaction between DMSO and $PPh_3$, the molybdenum catalysts act better than the tungsten catalysts. But the identity of atom X has been shown to have a strong influence on the catalytic ability of the compounds. In the case of molybdenum the presence of a heteroatom (X = S, O) enhances the catalytic activity but no such apparent influence was seen in the case of tungsten. More over the value of the maximum velocity ($v_{max}$) is higher for the complex with a thiopyrane than with a pyrane moiety. At the same time, the substrate affinity of the catalyst is better when pyrane is present instead of thiopyrane. Coining all these observations together, it can be concluded that the natural selection of pyrane seems to be a wise choice between advantages and disadvantages. The quest for optimum reactivity, high substrate affinity, very high non-innocence and the most stable redox potential renders pyran as the best choice in the complicated structure of molybdopterin.

The second focus of the thesis is to develop novel and economic synthetic strategies to develop monodithiolene complexes of molybdenum as such complexes represent the models for XO and SO enzyme families. The strategy used in general is to support molybdenum oxohalides by N-heterocyclic carbene (NHC), bipyridine derivatives or β-

diketiminate and further replacing the chlorides with dithiolene ligands. As a part of this, NHC complexes of molybdenum in different oxidation states have been synthesized and structurally characterized (figure 3). Compounds **3B** and **3C** are the first structurally characterized NHC complexes of Mo(V and VI). Comparison of these complexes with other reported NHC complexes of molybdenum indicate that the metal oxidation state has a significant influence on the M-C: bond length. Compound **3D** is a monodithiolene complex of Mo(V) supported by NHC. This compound has a similar coordination environment as an intermediate in the catalytic cycle of SO.
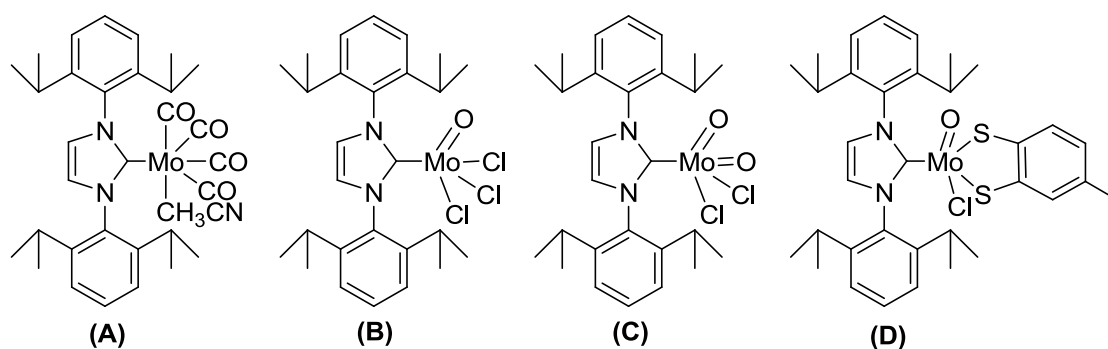


**Figure 3**

In chapter 5, utilization of bipyridine and β-diketiminate supported molybdenum oxochlorides in the synthesis of monodithiolene complexes are described. Figure 4 shows some of the complexes synthesized or structurally characterized in this study. The crystal structure of compounds **4A** and **4B** shows a Mo-N bond stretching due to the trans influence of the oxo group. The reaction of **4A** with bdt in the presence of triethylamine first produces a mono dithiolene complex **4C** which then undergoes disproportionation reaction to give a rare example of a bisdithiolene complex (**4D**) with trigonal prismatic geometry. The Mo chemistry of β-diketiminates is still in its infant stage and compound **4E** is one among very few such complexes known. It reacts with the sodium salt of tdt to produce the monodithiolene complex **4F**.
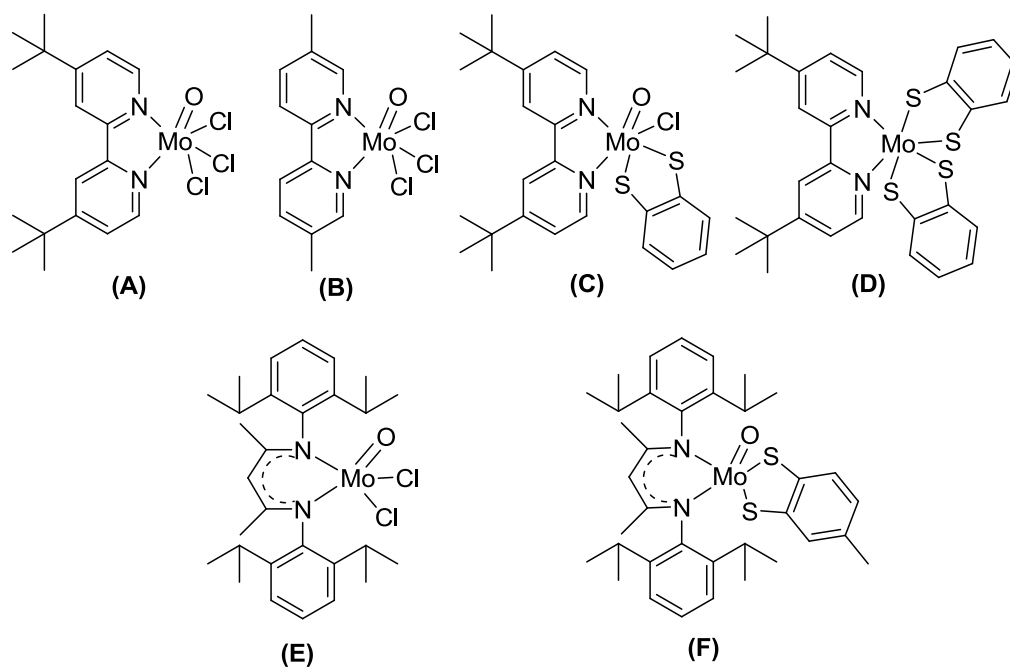
**Figure 4**

Chapter 6 presents a serendipity in an attempt to produce crystals of $[WO(cdt)_2]^{2-}$ by introducing $[Sr(nacnac)]^+$ ions to its outer sphere. The reaction resulted in the unprecedented dithiolene exchange from tungsten to strontium to produce a beautiful strontium hexamer in which strontium atoms are connected by the $\mu^2$ and $\mu^3$ bridging sulfur donors from the dithiolene groups (figure 5). This type of bridging character is unique for dithiolenes and the obtained hexameric strontium compound is the first example of this kind.
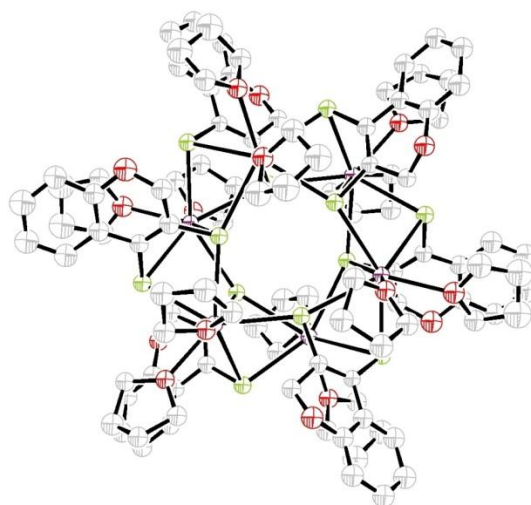


**Figure 5**

## 7.2. Outlook

The results reported in this thesis clearly indicate the importance of using more biomimetic ligands than the conventional dithiolene ligands for future model studies in this field. In this respect incorporating a pyrazine ring adjacent to the pyrane ring (as seen in molybdopterin) will be an interesting task. A part of my research work had been devoted to this topic but the project was unsuccessful due to many synthetic difficulties. It should be noted though, this had been a challenging task for inorganic chemists for more than one decade.

The transformation of the bisdithiolene complexes reported in this thesis to the corresponding monodithiolene complexes was attempted by treating them with PhSeCl but the reaction resulted in the decomposition of the material or polymerization of molybdenum-oxo species. Modified synthetic methods are still to be developed to achieve this goal.

Synthesis and structural characterization of NHC complexes of Mo(V and VI) were one among the main achievements in the course of this work. Such complexes are highly promising for bioinorganic chemists as they allow, subject to proper synthetic procedures, the design of demanding and unusual coordination environment around molybdenum. One such possibility is to synthesize a molybdenum hydroxide with dithiolene ligands as depicted in figure 6, which would be a so far elusive and highly sought after model of the sulfite oxidase intermediate.
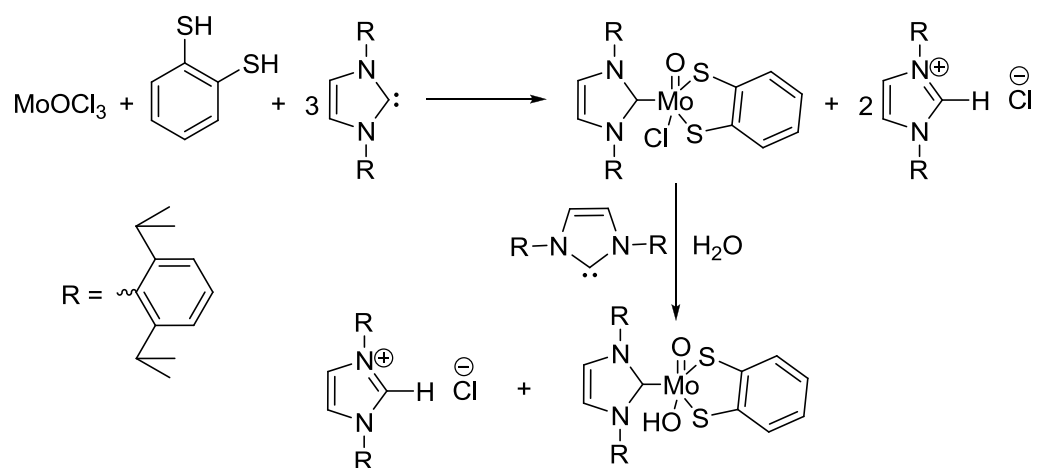
**Figure 6**

# ABBREVIATIONS

acac            Acetyl acetonate

Ad              Adamantyl

AH              Acetylene hydratase

AN              Acetonitrile

AO              Arsenite oxidase

AOR             Aldehyde oxido reductase

Ar              Aryl

Asp             Aspartate

bdt             Benzenedithiolate

bpy             2,2'-Bipyridine

$^t$Bu          *tert*-Butyl

$^t$Bu-bpy      4,4'-ditertiarybutyl-2,2'-bipyridine

cat             catecholate

cdt             2H-chromene-3,4-dithiolate

Cys             Cysteine

dme             Ethyleneglycol dimethylther

DMSO            Dimethylsulfoxide

DMSOR           DMSO reducase

DTBcat          3,5-di-tertiarybutylcatecholate

dtc             Dithiocarbamate

dtp             Dithiophosphinate

| | |
|---|---|
| E. coli | Escherichia coli |
| edt | Ethene-1,2-dithiolate |
| EXAFS | Extended X-ray absorption fine structure |
| FDH | Formate dehydrogenase |
| fdt | Flavano-ene-dithiolate |
| FOR | Formaldehyde ferredoxin oxidoreductase |
| $^i$Pr | *iso*-Propyl |
| Me | Methyl |
| Me-bpy | 5,5'-dimethyl-2,2'-bipyridine |
| MGD | Molybdopterin guanine dinucliotide |
| mnt | 2,3-Dimercaptomaleonitrile (maleonitriledithiolene) |
| MPT | Molybdopterin |
| nacnac | (E)-N-((Z)-4-(2,6-diisopropylphenylamino)pent-3-en-2-ylidene)-2,6-diisopropylaniline |
| NR | Nitrate reductase |
| NHC | N-heterocyclic carbene |
| OAT | Oxygen atom transfer |
| ppb | Parts per billion |
| ppm | Parts per million |
| PCET | Proton coupled electron transfer |
| pdt | Pyrane-ene-dithiolate |
| Ph | Phenyl |
| PTA | 1,3,5-Triaza-7-phosphatricyclo[3.3.1.1$^{3,7}$]decane |
| PymS | Pyrimidinthiol |

PyS            Pyridine-2-thionate

PySe           Pyridine-2-selenolato

rds            Rate determining step

SECIS          Selenocysteine insertion sequence

Se-Cys         Selenocysteine

Ser            Serine

SO             Sulfite oxidase

ssp            2-(Salicylideneamino)benzenethiolate)

tdt            benzene-1,2-dithiolate

TMAOR          Trimethylamine *N*-oxide reductase

Tp*            Hydrotris-(3,5-dimethylpyrazol-1-yl)borate

XO             Xanthine oxidase

# Appendix 1

## Crystallographic data for the structural analysis of compounds in chapter 2

| Compound ID | 3 | 6 |
|---|---|---|
| Empirical formula | $C_{10}H_6O_2S_2$ | $C_{50}H_{84}MoN_2O_3S_4$ |
| Formula weight | 222.27 | 985.37 |
| Wavelength [Å] | 0.71073 | 0.71073 |
| T [K] | 133(2) | 133(2) |
| Crystal system | monoclinic | monoclinic |
| Space group | P21/c | Cc |
| $a$ [Å] | 3.9405(8) | 15.815(3) |
| $b$ [Å] | 11.454(2) | 20.813(4) |
| $c$ [Å] | 20.200(4) | 16.284(3) |
| $\alpha$ [°] | 90 | 90 |
| $\beta$ [°] | 91.01(3) | 105.03(3) |
| $\gamma$ [°] | 90 | 90 |
| $V$ [Å$^3$] | 911.6(3) | 5176.7(18) |
| $Z$ | 4 | 4 |
| $D_{calcd}$ [g cm$^{-3}$] | 1.620 | 1.264 |
| $\mu$[mm$^{-1}$] | 0.548 | 0.455 |
| $F$(000) | 456 | 2112.0 |
| $\vartheta$ range [°] | 2.02 – 25.83 | 1.65 - 27.16 |
| Reflections collected | 4179 | 24985 |
| Independent reflections | 1694 [$R_{int}$ = 0.0561] | 10506 [$R_{int}$ = 0.1130] |
| Data/restraints/parameters | 1664 / 0 / 151 | 10506 / 2 / 550 |
| $R1$, $wR2$ [$I > 2\sigma(I)$][a] | 0.0548, 0.0738 | 0.0811, 0.1333 |
| $R1$, $wR2$ (all data) [a] | 0.0947, 0.0814 | 0.1378, 0.1531 |
| GoF | 1.049 | 1.050 |
| $\Delta\rho$(max), $\Delta\rho$(min) [e Å$^{-3}$] | 0.206, -0.236 | 0.736, -0.450 |

[a]$R1 = \Sigma||F_o|-|F_c||/\Sigma|F_o|$; $wR2 = [\Sigma w(F_o^2-F_c^2)^2/\Sigma w(F_o^2)^2]^{0.5}$

# Appendix 2

## Crystallographic data for the structural analysis of compounds in chapter 4

| Compound ID | 6 | 7 | 9 |
|---|---|---|---|
| Empirical formula | $C_{33}H_{39}MoN_3O_4$ | $C_{34}H_{44}Cl_3MoN_2O$ | $C_{34}H_{44}Cl_2MoN_2O_2$ |
| Formula weight | 637.61 | 699.00 | 679.55 |
| Wavelength [Å] | 0.71073 | 0.71073 | 0.71073 |
| T [K] | 133(2) | 133(2) | 133(2) |
| Crystal system | monoclinic | monoclinic | monoclinic |
| Space group | P21/m | P21/c | P21/c |
| $a$ [Å] | 8.8489(18) | 21.400 | 21.428(4) |
| $b$ [Å] | 19.551(4) | 9.5239 | 9.839(2) |
| $c$ [Å] | 9.4000(19) | 17.450 | 17.043(3) |
| $\alpha$ [°] | 90 | 90 | 90 |
| $\beta$ [°] | 106.64(3) | 103.89(3) | 108.52 |
| $\gamma$ [°] | 90 | 90 | 90 |
| $V$ [Å$^3$] | 1558.1(5) | 3452.6(12) | 3407.1(12) |
| $Z$ | 2 | 4 | 4 |
| $D_{calcd}$ [g cm$^{-3}$] | 1.359 | 1.345 | 1.325 |
| $\mu$[mm$^{-1}$] | 0.461 | 0.640 | 0.573 |
| $F(000)$ | 664 | 1452 | 1416 |
| $\vartheta$ range [°] | 2.08 - 27.12 | 2.35 - 25.86 | 2.30 - 25.98 |
| Reflections collected | 14621 | 26797 | 13719 |
| Independent reflections | 3496 [$R_{int}$ = 0.0633] | 6437 [$R_{int}$ = 0.0377] | 6248 [$R_{int}$ = 0.1060] |
| Data/restraints/parameters | 3496 / 0 / 204 | 6437 / 0 / 379 | 6248 / 0 / 379 |
| $R1$, $wR2$ [$I > 2\sigma(I)$][a] | 0.0575, 0.1060 | 0.0453, 0.1028 | 0.1226, 0.2554 |
| $R1$, $wR2$ (all data) [a] | 0.0744, 0.1111 | 0.0543, 0.1069 | 0.1886, 0.2951 |
| GoF | 1.139 | 1.075 | 1.074 |
| $\Delta\rho$(max), $\Delta\rho$(min) [e Å$^{-3}$] | 0.572, -0.811 | 1.295, -1.289 | 1.971, -1.241 |

[a]$R1 = \Sigma||F_o|-|F_c||/\Sigma|F_o|$; $wR2 = [\Sigma w(F_o^2-F_c^2)^2/\Sigma w(F_o^2)^2]^{0.5}$

# Appendix 3

## Crystallographic data for the structural analysis of compounds in chapter 5

| Compound ID | 1 | 2 | 6 |
|---|---|---|---|
| Empirical formula | $C_{18}H_{24}Cl_3MoN_2O$ | $C_{15}H_{18}Cl_3MoN_2O_2$ | $C_{36}H_{49}Cl_2MoN_2O$ |
| Formula weight | 486.68 | 460.60 | 692.61 |
| Wavelength [Å] | 0.71073 | 0.71073 | 0.71073 |
| T [K] | 133(2) | 133(2) | 133(2) |
| Crystal system | monoclinic | triclinic | orthorhombic |
| Space group | C2/c | P-1 | Pbca |
| $a$ [Å] | 14.476(3) | 7.7609 | 19.382(4) |
| $b$ [Å] | 17.406(4) | 8.9375 | 18.065(4) |
| $c$ [Å] | 25.055(5) | 13.810 | 20.419(4) |
| $\alpha$ [°] | 90 | 96.80(3) | 90.00 |
| $\beta$ [°] | 92.80 | 92.23(3) | 90.00 |
| $\gamma$ [°] | 90 | 93.40(3) | 90.00 |
| $V$ [Å$^3$] | 6306(2) | 948.5(3) | 7149(2) |
| $Z$ | 12 | 2 | 8 |
| $D_{calcd}$ [g cm$^{-3}$] | 1.538 | 1.613 | 1.287 |
| $\mu$[mm$^{-1}$] | 1.014 | 1.122 | 0.545 |
| $F(000)$ | 2964 | 462 | 2904 |
| $\vartheta$ range [°] | 1.83 - 25.96 | 2.58 - 26.95 | 1.84 - 25.86 |
| Reflections collected | 26834 | 8257 | 57436 |
| Independent reflections | 6095 [$R_{int}$ = 0.0636] | 4064 [$R_{int}$ = 0.0304] | 6584 [$R_{int}$ = 0.0322] |
| Data/restraints/parameters | 6095 / 0 / 358 | 4064 / 0 / 212 | 6659 / 6 / 395 |
| $R1$, $wR2$ [$I > 2\sigma(I)$][a] | 0.0852, 0.1553 | 0.0271, 0.0711 | 0.0273, 0.0657 |
| $R1$, $wR2$ (all data) [a] | 0.1107, 0.1662 | 0.0291, 0.0721 | 0.0346. 0.0682 |
| GoF | 1.069 | 1.048 | 1.037 |
| $\Delta\rho$(max), $\Delta\rho$(min) [e Å$^{-3}$] | 2.995, -2.241 | 0.579, -0.781 | 0.565 / -0.326 |

[a]$R1 = \Sigma||F_o|-|F_c||/\Sigma|F_o|$; $wR2 = [\Sigma w(F_o^2-F_c^2)^2/\Sigma w(F_o^2)^2]^{0.5}$

# Appendix 4

## Crystallographic data for the structural analysis of compounds in chapter 6

| Compound ID | 1 | 1* |
|---|---|---|
| Empirical formula | $C_{1368}H_0O_{216}S_{144}Sr_{72}$ | $C_{246}H_{321}O_{39}S_{24}Sr_{12}$ |
| Formula weight | 30810.96 | 5722.91 |
| Wavelength [Å] | 0.71073 | 1.54178 |
| T [K] | 133(2) | 100(2) |
| Crystal system | trigonal | trigonal |
| Space group | $R-3$ | R -3 |
| $a$ [Å] | 40.425(6) | 40.3380(11) |
| $b$ [Å] | 40.425(6) | 40.3380(11) |
| $c$ [Å] | 27.550(11) | 27.5701(9) |
| $\alpha$ [°] | 90 | 90 |
| $\beta$ [°] | 90 | 90 |
| $\gamma$ [°] | 120 | 120 |
| $V$ [Å$^3$] | 38990(18) | 38851(2) |
| $Z$ | 18 | 6 |
| $D_{calcd}$ [g cm$^{-3}$] | 1.312 | 1.468 |
| $\mu$[mm$^{-1}$] | 2.692 | 5.428 |
| $F(000)$ | 14973 | 17694 |
| $\vartheta$ range [°] | 1.38 - 26.01 | 2.04 -71.71 |
| Reflections collected | 100204 | 191123 |
| Independent reflections | 16797 [$R_{int}$ = 0.2049] | 16706 [$R_{int}$ = 0.0701] |
| Data/restraints/parameters | 16797 / 0 / 397 | 16706 / 5478 / 1048 |
| $R1$, $wR2$ [$I > 2\sigma(I)$][a] | 0.1546, 0.3148 | 0.0957, 0.2569 |
| $R1$, $wR2$ (all data) [a] | 0.2097, 0.3439 | 0.1130, 0.2844 |
| GoF | 1.211 | 1.127 |
| $\Delta\rho$(max), $\Delta\rho$(min) [e Å$^{-3}$] | 1.845, -1.157 | 5.865, -0.930 |

$$[a]R1 = \Sigma||F_o|-|F_c||/\Sigma|F_o|; \; wR2 = [\Sigma w(F_o^2-F_c^2)^2/\Sigma w(F_o^2)^2]^{0.5}$$

*Newly available data for [Sr(cdt)(THF)$_2$]$_6$ in the publishable range. The metric values given in this thesis will be changed according to the new data in future publication.

# Scientific contributions

**Reviews**

1. Molybdenum and tungsten cofactor model chemistry: Past, present and future. **P. P. Samuel**, C. Schulzke, *Handbook of Inorganic Chemistry Research.* Ch. 3. Nova Sci. Publ. NY. 2010.
2. Periodic mesoporous organosilicas: An overview towards catalysis. S. Shylesh, **P.P. Samuel**, S. Sisodiya, A.P. Singh, *Catal. Surv. Asia*. 12 (2008) 266

**Articles/communications**

3. A crystallographic and Mo-K-edge XAS study of molybdenum oxo bis-, mono- and non-dithiolene complexes and DMSOR: evaluation of geometrical first coordination shell and electronic properties. **P. P. Samuel**, S. Horn, A. Döring, K. G. V. Havelius, S. Reschke, S. Leimkühler, M. Haumann, C. Schulzke. *Eur. J. Inorg. Chem.* (2011) 4387
4. Pyrane as a wise choice by nature in the molybdopterin structure: From the electrochemical and kinetic perspective. **P. P. Samuel**, A. Döring, C. Schulzke. (under preparation)
5. N-heterocyclic carbene complexes of molybdenum (0,V,VI): Synthesis, structure and reactivity with dithiolenes. **P. P. Samuel**, C. Schulzke. (under preparation)
6. Monooxo molybdenum trichloride supported on bipyridine derivatives: Structural trans influence and reactivity to dithiolenes. **P. P. Samuel**, C. Schulzke. (Under preparation)
7. An unusual hexameric strontium complex bridged by unique $\mu^2$ and $\mu^3$ sulfur atoms of a dithiolene ligand. **P. P. Samuel**, K. Pröper, C. Schulzke. (under preparation)
8. β-Diketiminate complexes of molybdenum and their dithiolene complexes: Structural and electronic properties. A. Döring, **P. P. Samuel**, C. Stückl, C. Schulzke. (under preparation)
9. Selective Aromatic C−F and C−H Bond Activation with Silylenes of Different Coordinate Silicon. A. Jana, **P. P. Samuel**, G. Tavcar, H.W. Roesky, C. Schulzke., *J. Am. Chem. Soc*. 132 (2010) 10164
10. Synthesis of phosphine substituted β-diketiminate based isomeric Ge(II) complexes. N. D. Reddy, A. Jana, H. W. Roesky, **P. P. Samuel**, C. Schulzke, *Dalton Trans.*, 39 (2010) 234
11. Preparation of iron carbonylcomplexes of Ge(II) and Sn(II) each with a terminal fluorine atom. A.Jana, **P. P. Samuel**, H.W. Roesky, C. Schulzke, *J. Flur. Chem.* 131 (2010) 1096
12. Insertion Reaction of a Silylene into a N−H Bond of Hydrazine and a [1+4] Cycloaddition with Diphenyl Hydrazone. A. Jana, H. W. Roesky, C. Schulzke, **P. P. Samuel**, *Organometallics*, 28 (2009) 6574
13. A rational design for an efficient synthesis of a monomeric hydroxide. A. Jana, S. P. Sarish, H. W. Roesky, C. Schulzke, **P. P. Samuel**. *Chem. Commun.*, 46 (2010) 707
14. Synthesis and Characterization of N-heterocyclic Carbene Complexes of Titanium(IV) and Titanium(III). J. Li, C. Schulzke, S. Merkel, H. W. Roesky, **P. P. Samuel**, A. Döring, D. Stalke. *Z. Anorg. Allg. Chem.* 636 (2009) 511
15. Synthesis and Reaction of Monomeric Germanium(II) and Lead(II) Dimethylamide and the Synthesis of Germanium(II) Hydrazide by Clevage of one N−H bond of Hydrazine. A. jana, H.W. Roesky, C. Schulzke, **P. P. Samuel**, A. Döring, *Inorg. Chem.* 49 (2010) 5554
16. An Efficient Route for the Synthesis of a Tin(II) Substituted Carbodiimide from a Diazo Compound. A. Jana, H. W. Roesky, C. Schulzke, P. P. Samuel, *Inorg. Chem.* 49 (2010) 3461
17. Reaction of Tin(II) Hydride with Compounds Containing Aromatic C−F Bonds. A. Jana, H.W. Roesky, C. Schulzke, **P.P. Samuel**, *Organometallics* 29 (2010) 4837
18. Synthesis of a Lewis Base Stabilized Dimer of N-Substituted Hydrosila Hydrazone and a Silaaziridine. S. P. Sarish, A. Jana, H. W. Roesky, **P. P. Samuel**, C. E. A. Andrade, B. Dittrich, C. Schulzke, *Organometallics* (2010) ASAP

19. Catalytic properties of tin-containing mesoporous molecular sieves in the selective reduction of carbonyl compounds (Meerwein-Ponndorf-Verley (MPV) reaction. **P.P. Samuel**, S. Shylesh, A.P. Singh, *J. Mol. Catal. A. Chem*. 266 (2007) 11

20. Cyclooctene epoxidation over mesoporous organo vanadosilicates having –CH2-CH2- groups in the frame wall positions. S. Shylesh, **P.P. Samuel**, A.P. Singh, *Catal. Commun*. 8 (2007) 894

21. Chromium containing small pore mesoporous silicas: Synthesis, characterization and catalytic behavior in the liquid phase oxidation of cyclohexane. S. Shylesh, **P.P. Samuel**, A.P. Singh, *Appl. Catal. A. Gen*. 318 (2007) 128

22. Synthesis of hydrothermally stable aluminium-containing ethane-silica hybrid mesoporous materials using different aluminium sources. S. Shylesh, **P.P. Samuel**, A.P. Singh, *Micropor. Mesopor. Mater.* 100 (2007) 250

23. Sulfonic acid functionalized mesoporous silicas and organosilicas: Synthesis, characterization and catalytic applications S. Shylesh, **P.P. Samuel**, Ch. Srilakshmi, R. Parischa, A.P. Singh, *J. Mol. Catal. A. Chemical*, 274 (2007) 153

24. Catalytic Meerwein-Ponndorf-Verley reductions over mesoporous silica supports: Rational design of hydrophobic mesoporous silica for enhanced stability of aluminum doped mesoporous catalysts. S. Shylesh, M.P. Kapur, L.R. Juneja, **P.P. Samuel**, Ch. Srilakshmi, A.P. Singh, *J. Mol. Catal. A. Chem*., 301 (2009) 118

25. Ethane bridged hybrid mesoporous silsesquioxanes with sulfonic acid functionalities: synthesis, characterization and catalytic applications. S. Shylesh, **P.P. Samuel**, R. Parischa, A.P. Singh, *Stud. Surf. Sci. Catal* 170 B (2007) 1899

26. Synthesis, characterization and catalytic applications of vanadium containing ethene-bridged hybrid periodic mesoporous organosilicas. A.P. Singh, S. Shylesh, **P.P. Samuel**, *Stud. Surf. Sci. Catal.* 172 (2007) 357

**Book**

27. Molybdenum and Tungsten Cofactor Model Chemistry.
    C. Schulzke, **P.P. Samuel**.
    Nova Science Publ. NY.$^{©}$2010
    ISBN: 978-1-61668-750-2
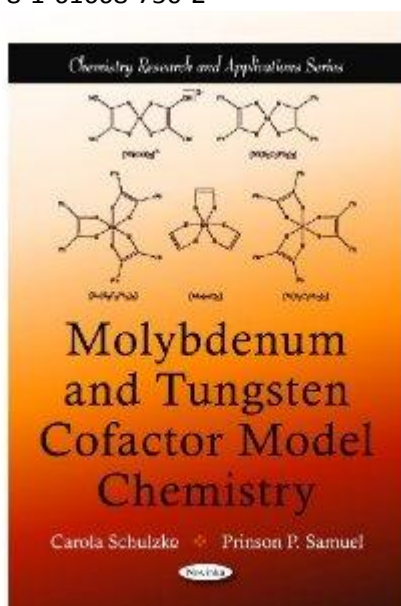
## Conferences/Workshops

1. 10th European Biological Inorganic Conference (EUROBIC 10), Thessaloniki, Greece, June 2010
   Mo and W cofactor model chemistry of pyrane dithiolene derivatives: synthetic analogues of arsenite oxidase (Poster)
   **P. P. Samuel**, C.Schulzke, A. Döring

2. 9th European Biological Inorganic Conference (EUROBIC 10), Wroclaw, Poland, Sept. 2008
   Mo and W complexes of pyrane dithiolene derivatives as the synthetic analogues of the cofactors in oxotransferases(Poster)
   **P. P. Samuel**, C.Schulzke, A. Döring

3. Joint Workshop on Biological Inorganic Chemistry (Uni Potsdam and Tech. Uni. Berlin) Berlin, June 2009
   Mimicking the pyranopterin bearing Mo and W active centers in oxotransferases. (Talk)
   **P. P. Samuel**, C. Schulzke

4. IRTG Workshop 2009, Copenhagen, Denmark, Feb. 2009
   Mo and W complexes of pyrane dithiolene derivatives as the synthetic analogues of the cofactors in oxotransferases (Poster)
   **P.P. Samuel**, A. Döring, C. Schulzke

5. IRTG Workshop 2010, Goslar, Germany, Feb. 2010
   Synthetic analogues of arsenite oxidase (Poster)
   **P.P. Samuel**, A. Döring, C. Schulzke

6. International Conference on the Materials for the Millennium, MATCON, Cochin, India, March 2007
   Hydrothermally stable aluminium-containing smart channel mesoporous materials: Synthesis and Characterization. (Poster)
   **P.P. Samuel**, S. Shylesh, A.P. Singh.

7. 5th Tokyo Conference on Advanced catalytic Science and Technology, TOCAT-5, Japan, 2006
   Synthesis, characterization and catalytic applications of vanadium containing ethene-bridged hybrid periodic mesoporous organosilicas. (Talk).
   A.P. Singh, S. Shylesh, **P.P. Samuel**

8. 15th International Zeolite Conference, IZC-15, Beijing, China, Aug. 2007
   Ethane bridged hybrid mesoporous silsesquioxanes with sulphonic acid functionalities: synthesis, characterization and catalytic applications (Poster)
   S. Shylesh, **P.P. Samuel**, R. Parischa, A.P. Singh

9. National Science Day 2006, National chemical laboratory, India, Feb 2007
   Periodic mesoporous silica vs periodic mesoporous organo-silica (Poster)
   S. Shylesh, **P.P. Samuel**, A.P. Singh

10. 18th National Symposium and Indo-US seminar on Catalysis, Indian Institute of Petroleum, India, April 2007.
    Oxidation of ethyl benzene over M-MCM-41 (M=Sn, Cr and V): Synthesis, characterization and catalytic activity (poster)
    **P.P. Samuel**, S. Shylesh, K.R. Kamble, A.P. Singh

# Curriculum Vita

**Personal Information:**

| | |
|---|---|
| Name | Prinson Poikayil Samuel |
| Nationality | Indian |
| Date of birth: | 21 April 1981 |
| Place of birth | Vilangara, Kerala |

**Educational Qualifications:**

2007 Nov-2008 Oct, **Equivalency of German Diploma**, Faculty of Chemistry, Georg-August University of Göttingen

2007 Nov-2011 Jan, **Completing Ph.D thesis** under the supervision of Prof. Dr. Carola Schulzke, Institute for Inorganic Chemistry, Georg-August University of Göttingen

2004-2006, **Master of Technology (M.Tech)** in Industrial Catalysis, Cochin University of Science and Technology (CUSAT), India.

2001-2003, **Master of Science (M.Sc.)** in Chemistry, University of Kerala, India.

1998-2001, **Bachelor of Science (B.Sc.)** in Chemistry, University of Kerala, India.

1996-1998, **Pre-Degree** in Science, University of Kerala, Kerala, India.

1996, **Secondary School Leaving Certificate (SSLC)**, Board of Public Examinations, Government of Kerala, India.

Schooling:

1994-1996: St. John's Higher Secondary School, Ummannoor

1990-1994: Sreekrishna Vilasam High School, Thrikkannamangal

1986-1990: Govt. Welfare L.P. School, Vilangara